BIOLOGICALLY-INSPIRED
DOUBLE SKIN FACADES
FOR HOT CLIMATES

A Parametric Approach for Performative Design

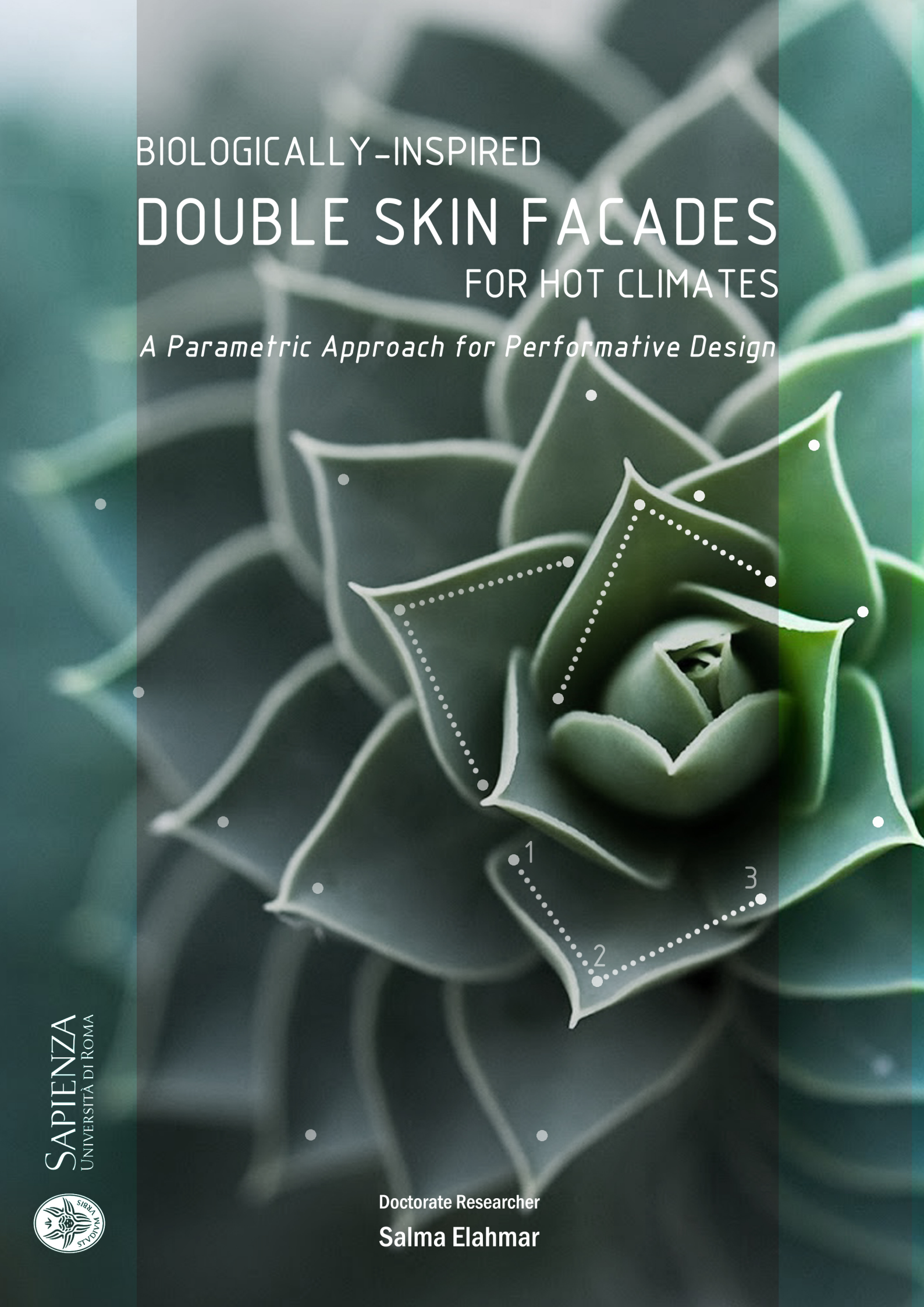

SAPIENZA
UNIVERSITÀ DI ROMA

Doctorate Researcher

Salma Elahmar

Cover Photo:
Wide Screen Wallpapers, 2016. *Succulent Plant Wallpaper.* [Online]
Available at: http://wide-wallpapers.net/succulent-plant-wide-wallpaper/
[Accessed May 2016]. Edited by the author.

SAPIENZA University of Rome
Faculty of Civil and Industrial Engineering
Department of Civil, Building and Environmental Engineering-DICEA
PhD in Architectural Engineering and Urban Planning (28th cycle)

Egypt-Lebanon-EU Mobility Exchange NeTwork

Doctoratal dissertation

Biologically-Inspired Double Skin Facades for Hot Climates
A Parametric Approach for Performative Design

Facciata a Doppia Pelle Ispirati dalla Natura per Regioni Aride
Un approccio parametrico per la progettazione performativa

by
Salma El Ahmar

Supervisor
Prof. Antonio Fioravanti

Tutor
Dr. Francesco Battista

November 2016

This project has been funded with support of the European Commission. This publication reflects the view only of the author, and the Commission cannot be held responsible for any use which may be made of the information contained therein.

To my late father..

Who has always encouraged me to do what I love
and supported me all the way.
May he rest in peace.

ACKNOWLEDGEMENTS

Firstly, I would like to express my sincere gratitude to my supervisor Prof. Antonio Fioravanti for the continuous support of my Ph.D. study and related research activities, for his patience, motivation, and his continuous positive energy from the very first day. His guidance and observations always helped me throughout the research and writing of this thesis. I would like to extend my gratitude to the Doctorate Committee for their insightful comments, encouragement and understanding.

My sincere thanks also go to Prof. Renzo Piva and Prof. Carlo Casciola at the Department of Mechanics as they provided me with the opportunity to have access to their research facilities. They also introduced me to Dr. Francesco Battista, who spent a lot of time and effort in teaching me about Computational Fluid Dynamics and OpenFOAM software. Without his assistance and patience the final verification phase of this research would not have been possible.

I would also like to thank my fellow colleagues in the 28^{th} doctorate cycle, and Silvia Gargaro and Mohammed El Edeissy in the 27^{th} cycle for their friendship and support especially during my first year when I just arrived to Italy and was struggling with the Italian language. I am also grateful to the rest of my colleagues whom I see and work with every day for their friendship and making working times much more enjoyable.

Finally, my deepest gratitude goes to my colleague and long-time friend Sara Hassan for her support and my loving family who endured my absence and always encouraged me to do my best. I can never thank my husband Kareem Elsayed enough for his endless support and encouragement especially in difficult times. His assistance, both professional and personal, along with his continuous motivation kept me going.

ABSTRACT

La Biomimicry è una scienza applicata che studia le forme, i materiali, i sistemi e i processi naturali per individuare soluzioni applicabili anche a problemi umani. Tale scienza trova applicazione in molti campi, quali l'agricoltura, la medicina, l'ingegneria e l'architettura. Grazie ai progressi compiuti nella modellazione parametrica, ad oggi sono disponibili potenti strumenti che, oltre alla simulazione energetica, consentono di esplorare le potenzialità delle soluzioni tratte dal mondo naturale nella progettazione architettonica, superando i limiti della semplice imitazione della forma. Una delle maggiori sfide per gli architetti negli ultimi anni è la riduzione della domanda energetica del costruito. Per i climi caldi, le esigenze di ventilazione e raffrescamento sono pertanto fattori cruciali per migliorarne la prestazione energetica.

La tesi di ricerca affronta il problema della progettazione e dell'efficienza energetica dell'involucro edilizio in contesti climatici caldi, quale l'Egitto. A tal fine, è stato definito e applicato un approccio progettuale biomimetico-computazionale, per studiare e analizzare i comportamenti adattivi di termoregolazione di vari organismi naturali. In particolare, il lavoro di ricerca esplora possibili soluzioni architettoniche, ispirate a caratteristiche biologiche, per l'involucro di un edificio per uffici, con l'obiettivo di ridurre la domanda energetica per il raffrescamento. L'involucro dell'edificio è stato modellato parametricamente utilizzando Grasshopper Visual Programming Language per Rhino 3D Modeller, applicando inoltre alcuni algoritmi evolutivi multi-obiettivo per ottimizzare la soluzione architettonica rispetto al duplice obiettivo di diminuire i carichi di raffrescamento e mantenere un buon livello di illuminazione naturale. In tal modo, la riduzione dei carichi di raffreddamento non comporta un incremento dei consumi elettrici per l'illuminazione artificiale. Le prestazioni termiche dell'edificio sono state valutate con il software EnergyPlus.

La soluzione architettonica esplorata è una facciata a doppia pelle ispirata a vari principi della natura. Le prestazioni della soluzione proposta sono state confrontate con quelle di un edificio per uffici esistente a Il Cairo. Il modello dell'edificio è stato ricostruito sulla base di planimetrie e specifiche sui materiali presenti; inoltre la disponibilità di dati sui consumi energetici per il raffrescamento dell'edificio ha permesso di valutare l'accuratezza della prestazione energetica calcolata con il software di modellazione. La soluzione progettuale è stata comparate anche rispetto alle prestazioni di una tipica facciata a doppia pelle. Inoltre le prestazioni termiche calcolate con EnergyPlus sono state confrontate con quelle ottenute con software di simulazione fluidodinamica computazionale (CFD), più accurati nel calcolo delle facciate a doppia pelle. Tale comparazione ha permesso di identificare il grado di errore e l'appropriatezza dell'uso di EnergyPlus nelle fasi iniziali della progettazione.

La facciata a doppia pelle proposta consente una diminuzione della domanda di raffrescamento fino al 13,4%, migliorando al tempo stesso il livello di illuminazione naturale, che spesso costituisce uno dei maggiori limiti per l'applicazione di tale sistema. La ricerca termina con una sintesi dei risultati ottenuti e una valutazione complessiva del processo di progettazione presentato, degli strumenti di progettazione/simulazione utilizzati e delle prestazioni dell'involucro proposto, discutendone vantaggi e limiti. Sulla base delle sperimentazioni e dei risultati conseguiti, sono state individuate linee guida e raccomandazioni per la progettazione delle facciate a doppia pelle nei climi caldi. Inoltre viene fornita una matrice che raccoglie tutte le idee biomimetiche esplorate e analizzate, che rappresenta una mini-banca dati per architetti o designer interessati a questo approccio progettuale nell'affrontare i problemi di termoregolazione del costruito. Infine, la differenza di accuratezza tra i risultati di EnergyPlus e quelli dello strumento CFD è risultata trascurabile.

.

ABSTRACT

Biomimicry is an applied science that derives inspiration for solutions to human problems through the study of natural designs, materials, structures and processes. Many fields of study benefit from biomimetic inspirations, such as agriculture, medicine, engineering, and architecture. Technological advances in parametric and computational design software in addition to environmental simulation means offer very useful tools in order to explore the potential of nature's inspirations in architectural designs that does not just mimic shapes and forms. Energy efficiency is one of the major and growing concerns facing architects. Cooling and ventilation needs are critical factors that affect energy efficiency especially in hot climates.

This thesis addresses the problem of designing building skins that are energy efficient in the context of hot climates such as that in Egypt. The research attempts to define and apply a biomimetic-computational design approach to study and analyse natural organisms in terms of their behaviour regarding thermoregulation. Aiming to decrease cooling loads, the research explores possible architectural solutions for a biologically inspired skin system for office buildings. The building's skin is parametrically designed using Grasshopper Visual Programming Language for Rhino 3D Modeller, and it is optimised using multi-objective evolutionary algorithms which are particularly important in the attempt of finding a range of solutions that reduce cooling loads while maintaining daylight needs. Consequently, the reduction in cooling loads should not be at the expense of increased energy consumption in artificial lighting. Simulations regarding the thermal performance were performed using EnergyPlus.

A Double-Skin Façade (DSF) is proposed based on inspirations from nature. In order to evaluate the performance of the proposal, it is compared to the performance of the skin of an existing office building in Cairo acting as a reference case. Data regarding the reference case such as the building drawings, material specifications and annual cooling consumption were obtained in order to build its digital model and assess its accuracy. The proposed design is also evaluated by comparing it to a typical flat DSF. The obtained results regarding the thermal performance of the proposed building skin are verified by comparing them to results of more accurate simulations performed using Computational Fluid Dynamics (CFD). The aim is to know the degree of error as well as the appropriateness of using EnergyPlus for geometrically-complex DSFs in early design phases when CFD is not practical.

The proposed DSF was able to decrease cooling loads by up to 13.4% while improving daylight performance at the same time which is often one of the main challenges of using DSFs. The research criticises the presented design approach as a whole, the design/simulation tools used and the performance of the proposed skin discussing their benefits and limitations. Based on the design experimentation and results, general guidelines and recommendations for DSF design in hot climates are presented. Additionally, the research presents a compiled matrix of the biomimetic ideas explored and analysed in order to serve as a mini-data bank for architects or designers interested in this design approach in addressing thermoregulation problems. Finally, the comparison between EnergyPlus and CFD software results showed minor differences.

THESIS STRUCTURE

PART 1 Introduction & literature review

Chapter 1: Introduction
Research aim, scope and methodology

Chapter 2: Biomimicry and Computation
State of the art

Chapter 3: Design and Simulation of Double Facades in Hot Climates
Case studies and tools used

PART 2 Biomimetic design & computation

Chapter 4: Biomimetic Inspirations & Analyses
Strategies in nature and corresponding building skin features

Chapter 5: Biomimetic Design & Computation
Translation of ideas to architecture

Chapter 6: Application and Evaluation of the Proposal
Comparison with existing building and with flat double façade

PART 3 Verification & conclusion

Chapter 7: CFD verification
Detailed simulations to verify the reliability of EnergyPlus results

Chapter 8: Conclusion
Summary, research contributions and future insights

TABLE OF CONTENTS

Chapter 1
Introduction

The elevating problems of climate change throughout the world in addition to increasing use of non-renewable energy sources are creating a sense of urgency for fundamental changes in many industries, and the building sector is no exception. According to the Unites States Energy Information Administration (EIA), almost 40 per cent of total energy consumption in 2012 was by the residential and commercial sectors. These two sectors account for nearly all building-related energy consumption in the U.S. (EIA, 2013). This situation is not very different than that occurring in Egypt, where residential and commercial sectors accounted for almost 48 per cent of total energy consumption in 2010. Egypt's electricity consumption increased by 95 per cent in the period from 2001/02 to 2010/11 to reach a total of 127 billion kilowatts per hour, according to figures released by the Cabinet's Information and Decision Support Centre (IDSC) in 2012. This growth of electricity consumption in Egypt is more than three times the international averages, which only increased by 31 per cent from 2001 till 2009 (Megahed, 2012).

One of the key considerations in designing energy-efficient buildings is their skin. This element -along with others- has the capability of improving the building's performance in natural ventilation, managing heat transfer, redirecting and filtering daylight and enhancing occupant well-being among other functions. In Egypt there is a great increase in the use of ventilation devices such as air conditioners and fans within the past decade. The number of air conditioning units rose from 196,000 in 1999 to three million in 2009 which then doubled to six million in 2012 (Attia, et al., 2012).

This is can be attributed to many reasons such as the hot climate, dense urban population, urban heat island effect, lack of use of passive design strategies, and availability of affordable air conditioning units in the market. All these factors led to greater dependence on mechanical cooling in buildings all over the country, which in turn contributes to the increasing urban heat island effect. Currently, air conditioners account for approximately 20 per cent of energy consumption in buildings (Attia, et al., 2012). Peak demand patterns are observed in the summer, when cooling and ventilation are most needed. This caused the occurrence of multiple power cuts observed in the summers of 2012 and 2013, which in some extreme cases lasted 18 hours per day. Many reports and studies issued by the Egyptian National Institute of Planning (ENIP) warned that by 2015 primary energy supply will not be able to meet demands (Attia, 2012). Solutions to these problems would be related to either the improvement of existing buildings and cities, or the design of new ones. The latter is the focus of this study.

These problems emphasise the critical role of the building skin, and the potential it offers in improving indoor environmental conditions and decreasing cooling loads. The motivation arose to investigate new design ideas for building skins that could help solve these kinds of problems. Turning to nature and biology was chosen for this investigation, since nature possesses a '3.8 billion-year' history of experience, where much of the problems we face today have already been addressed and solved in more effective ways by natural organisms.

Why turn to nature?

> *"…it is biology, of all sciences, which first confronted the central problem of design in nature; and it is very natural that of all sciences it should for this reason attract the special interest of designers."* (Steadman, 2008, p.4)

There are aspects of designed artefacts such as buildings and aspects of the design and construction processes that fit quite well to biological analogies. The ideas of 'survival', 'wholeness', 'coherence', 'symmetry' and 'integration', and others that describe the complex relationships existing in a biological organism, could be used to describe similar relationships in designed objects. The adaptation and/or modification of the organism to its environment, its fitness, can be compared to the harmonious relation of a building to its context. More abstractly, it can be compared to the appropriateness of any designed object for the various purposes for which it is intended as well as its flexibility to change if these purposes change.

An interesting historical fact is that it has been biology out of all the sciences to which architectural and design theorists have most frequently turned to in the past. Indeed it is surprising, in view of the presence of biological references and ideas in the writings of the architectural theorists of the last hundred years, that no work of book length (to the author's knowledge) has so far been devoted to the history and theory of biological analogy. The history is to some point fragmented, leading into many remote corners of the architectural literature. Nevertheless analogy with nature is a constant and recurring theme as it appears in the works of many architects such as Frank Lloyd Write, Louis Sullivan, and Le Corbusier (Steadman, 2008).

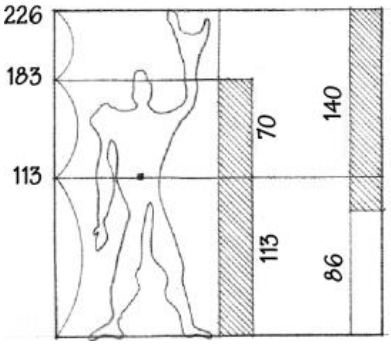

Figure 1.1: The Modulor by Le Corbusier, measured to the human scale and universally applicable to architecture and mechanics (Ching, 2007).

> *"There is a duality between engineering and nature, which is based on minimum use of energy. This is because animals and plants, in order to survive in competition with each other, have evolved ways of living and reproducing using the least amount of resource. This involves efficiency both in metabolism and optimal apportionment of energy between the various functions of life. A similar situation obtains with engineering, where cost is usually the most significant parameter. It seems likely, then, that ideas from nature, suitably interpreted and implemented, could improve the energy efficiency of our engineering at many levels".*
>
> (Julient Vincent cited in Gruber, 2011, p.108)

Digital modelling and simulation tools together with computational design processes are facilitating the realisation of complex forms and materials of many contemporary buildings. They also represent an opportunity to fully explore the potential benefits of biological principles found in nature through deeper understanding of nature's systems and processes.

A truly biomimetic approach (one that does not only mimic shape or form) to architectural design requires the development of novel design methods that integrate environmental factors and influences as well as the modelling of behaviour and the constraints of materialisation process. This requires an understanding of form, material and structure not as separate elements, but rather as complex interrelations that are embedded in and explored through an integral computational design process. Correlating and combining computational form generation methods and natural principles, suggests a new approach developed for architectural design that is strongly related with biology. This approach aims for a more integral design method to correlate object, environment and subject into a synergetic relationship (Hensel et al, 2010).

1.1 Research questions

The primary question of this research is 'What can we learn from natural systems to help us develop building envelopes that decrease cooling loads?' Other key questions to be addressed:

- How could the application of biomimetic design strategies benefit from new software tools for computational design and environmental simulations?
- In the case of geometrically-complex facades, what is the reliability of the software used for environmental simulations and are they appropriate for use in early design phases?

1.2 Aim and objectives

Attempting to answer these questions, the main aim of this research is the proposal, application and criticism of a 'Biomimetic-Computational' design approach for the design of a building skin in a hot climatic area to decrease cooling loads. The research looks into biology with an open mind-set for new ideas and seeks to make use of current technology and software in producing a more sustainable and performative architecture. More detailed objectives are:

- To explore and define the 'Biomimetic-Computational' design approach that will be applied.
- To find and categorise a list of ideas from biology-related literature and present a miniature data-bank for interested designers.
- To select one or more biomimetic ideas to be applied, and employ computational design software for the design, optimisation and environmental analysis of the proposal.
- To evaluate the proposal by comparing it to a reference case.
- To verify the reliability of obtained results by performing detailed simulations using Computational Fluid Dynamics (CFD).
- To assess the design process as a whole and the tools used.

Each objective is addressed in one or more chapters of this thesis.

1.3 Scope

The scope of this thesis falls within the realm of multi-disciplinary research as it attempts to link façade design (or more generally; building skins), sustainability, biomimicry, and Computer-Aided Architectural Design (CAAD) as shown in Figure 1.2. It addresses the problem of envelope energy efficiency in sustainable design, focusing on a specific architectural element which is the building skin in the context of hot climates such as in

Egypt. The chosen building typology is office buildings. The research attempts to study and analyse natural organisms in terms of their behaviour regarding thermal regulation. This is to explore possible architectural solutions for a biologically inspired skin which is parametrically designed. The proposed design will be evaluated with environmental simulation software to compare and highlight its benefits over a traditional façade system represented in the reference case.

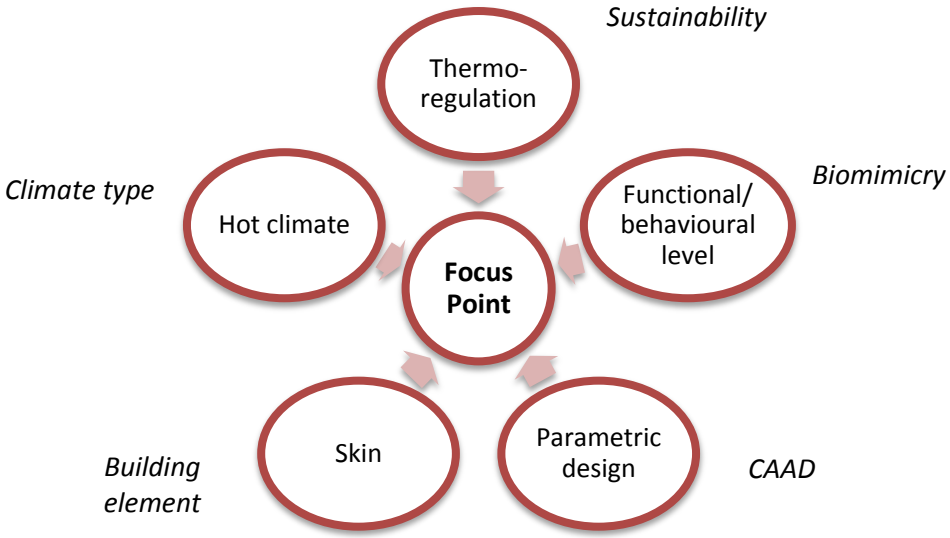

Figure 1.2: Research focus point: an intersection between different fields of study. Source: author.

1.4 Methodology

Different research methodologies are applied in this thesis, (as seen in Figure 1.3) primarily '*research by design and exploration*'. Since the research attempts to propose and apply a biomimetic-computational design approach, therefore there was a critical need for an architectural design exercise that is qualitative by its nature. It is through the actual application of the design process that the author gains insights and deep understanding of it, and discovers its benefits and limitations. The design approach itself will be explained in the following chapter. Additionally, comparative analyses are performed in order to evaluate its outcomes.

The research starts by asking how could we minimise heat gain and/or maximise heat loss through the design of the building skin. The four basic means of heat transfer (radiation, conduction, convection and phase-change) are studied as they will act as the link or common ground between architecture and nature.

A search for biological equivalents is performed by asking the same question: how would nature minimise heat gain and/or maximise heat loss? A number of possible organisms that fulfil this requirement are studied. The means by which they achieve this requirement are analysed and categorised according to the heat transfer method in order to link it to its possible corresponding architectural feature. A list of ideas is compiled, from which one or more are chosen for the design task at hand.

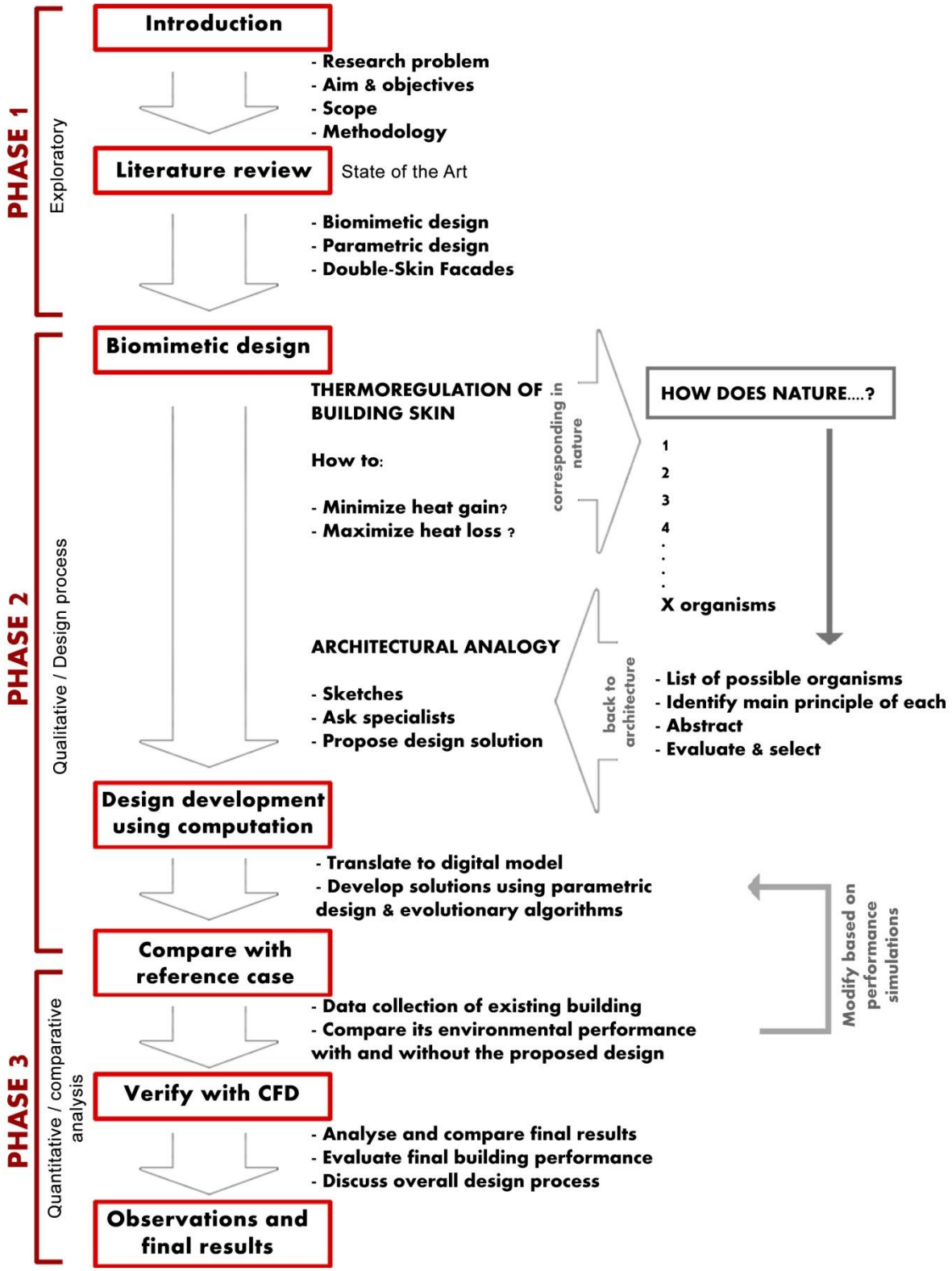

Figure 1.3: Research phases and their applied methodology. Source: author.

After choosing these ideas, it was decided to apply them in the design of a Double-Skin Façade (DSF). Therefore an investigation into similar and/or relevant architectural research of DSFs in hot climates is performed to gain a better understanding of the design proposal and learn from preceding studies. Then the researcher attempted to *quantify* the proposed design solutions, using parametric modelling and testing of the results. The design ideas are translated into mathematical relationships to build up the digital parametric model. A Visual Programming Language is used to model the design solutions (Grasshopper for Rhino 3D modeller) and to optimise the digital model using Evolutionary Optimisation algorithms.

Then a comparative analysis took place as the environmental performance of the skin of an existing office building in Cairo (reference case) is analysed before and after the new proposed skin. Additionally, the proposed skin is compared with a typical flat DSF. The results of the comparisons serve as a means to assess the degree of improvement that has occurred. A final comparative analysis is performed between the obtained results and results from more accurate Computational Fluid Dynamics simulations to verify the reliability and appropriateness of the software used in the early design phase.

1.5 Thesis Outline

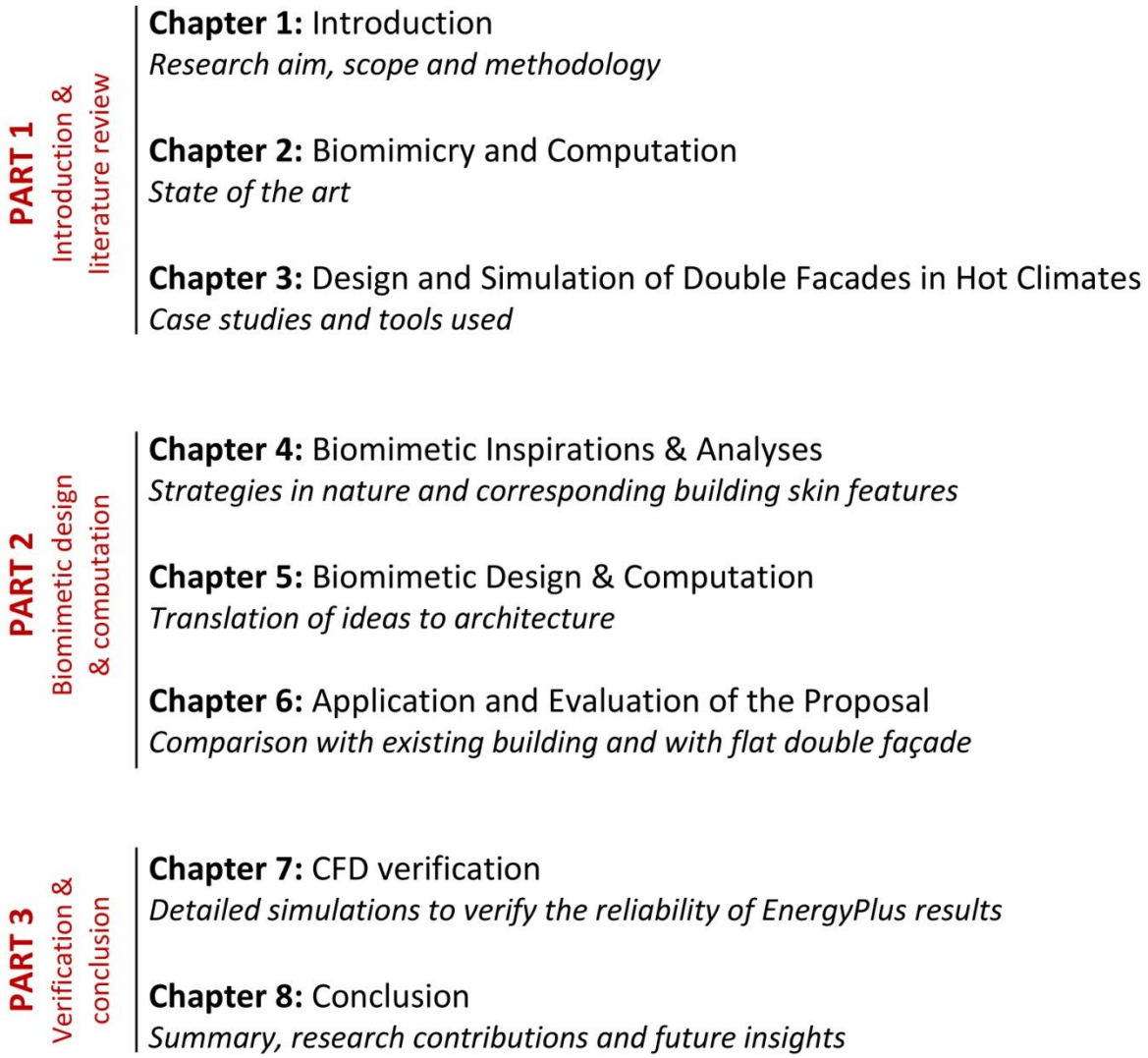

Figure 1.4: General outline of the thesis. Source: author.

The thesis is divided into three main parts as seen in Figure 1.4, indicating the three phases that will take part in this research. The first part is an introductory phase and includes three chapters. The first chapter starts with the research aim and objectives, the addressed problem, the scope of work, and the proposed methodology in order to achieve the stated objectives. The second chapter demonstrates the historical background as well as state of the art of biologically inspired design, in addition to important terms and definitions and their relation to computational design methods. It also includes an introduction to Nature's general principles, highlighting the main design approach and focus point of the research. The third chapter represents a brief overview of the chosen skin typology which is Double-Skin Facades (DSF). Although the choice of DSFs came at a later stage in the research, its overview was placed in Part One of this thesis for the sake of not interrupting the explanation of the design proposal in Part Two, and also because it more appropriately aligns with the nature of Part One as a literature review section.

The second part starts with chapter four, including biomimetic exploration, where certain design functions of the building skin are specified and the search for parallels in nature begins. Ideas from nature are categorised according to the main heat transfer method by which thermoregulation occurs, then they are abstracted to see possible applications in architecture. The chapter ends with two chosen biomimetic ideas to be applied in the design of the building skin.

An investigation into similar building skins was required in addition to the common simulation methods used in simulating their thermal performance. Reviewing previous research on DSFs in hot climates resulted in a set of guidelines, recommendations and limitations. This was particularly important as it resulted in a new added design objective for the proposed building skin, which is to reduce cooling loads *while maintaining daylighting needs.* Hence the reduction in cooling energy consumption would not be associated with increased energy consumption for artificial lighting.

Chapter five includes brainstorming and sketching based on the ideas selected to propose architectural analogies. It also explores possible combinations of several ideas into one coherent proposal for the building skin. It investigates the mathematical translation of the proposed design into a parametric digital model using Grasshopper for Rhino modelling software. Evolutionary optimisation is utilised to reach a solution that achieves a balance between required skin functions which are conflicting (natural lighting vs. solar gain).

In chapter six the proposed design idea is applied to an existing building and evaluated in terms of its environmental performance using digital simulation software such as DIVA and Archsim plug-ins for Rhino and Grasshopper that run on EnergyPlus for energy simulations and Radiance for daylighting simulations. The evaluation takes place by comparing both cooling loads and daylighting of the existing building with and without the proposed building skin. It is also evaluated by comparing it to a typical flat DSF.

The third part presents the verification phase. In chapter seven, the thermal performance of the proposed skin is simulated using the Computational Fluid Dynamics (CFD) Software OpenFOAM. They are compared to results obtained by EnergyPlus in the previous chapter. While differences among the results are expected the aim is to know the degree of error as well as the appropriateness of using EnergyPlus in early design phases when CFD is not yet practical.

The thesis concludes with chapter eight that summarises the results obtained, research contributions, and limitations. It also discusses the advantages and limitations of the proposed skin, the tools used and most importantly criticises the design approach as a whole.

Chapter 2

Biomimicry and Computation
Background and State of the Art

2.1 Introduction

In this chapter the approach of Biomimicry in design is introduced. It represents a literature reviewing phase that addresses the origins of design inspired by nature, the relationship between nature and architecture, and the different biomimetic design methods. It also discusses the main biological principles followed by nature in order to understand how such principles can relate to architectural design. Then a particular focus is made on different biomimetic design strategies. The principle of adaptation is discussed, highlighting how organisms and buildings can adapt to their environment, in addition to the role of the building skin which is the main building element addressed in this thesis.

A brief overview of biomimicry in computational design is presented, since computational tools are intended to be used in the application of biomimetic design. Examples of how such a biomimetic-computational approach can be applied are also demonstrated. Based on this literature review, the chapter ends with defining the design approach and focus points that will be addressed in the rest of the thesis.

2.2 Biomimicry background

2.2.1 Origins of the term

The term ‘bio-technique’ or ‘biotechnics’ appeared in the late 1920s and 1930s. It argues that nature has already a wide range of ingenious ‘inventions’ that have developed throughout the evolution of plants and animals. These inventions solved different kinds of problems faced by engineers, such as structural, chemical and mechanical problems. What was needed therefore is the thorough study of the engineering of nature so that man would find the solutions needed for his technical problems by copying natural models in the design of structures and machines. This would save time and resources which are usually spent in the evolution and development (trial and error) of technology, as it instead ‘borrows’ the time already spent in natural evolution (Steadman, 2008).

The term bionics (Bionik) is literally a combination of two terms: Biology which is the science of life; and technology which is the constructive creation of products, devices and processes by using the materials and forces of nature, taking into account the laws of nature (Gruber, 2011). In 1958 the term ‘bionics’ was mentioned by military doctor Jack Steele who studied natural organisms for the development of medical prostheses such as artificial limbs, heart pacemakers, cochlear implants, etc. The term ‘biomimetics’ was used by Otto Schmitt in the 1950s, but it had a wider meaning and an application that extended beyond the focus on medical and robotic devices studied by Steele (Steadman, 2008). The following definition of the term "bionik" was agreed in 1993 at a meeting of The Association of German Engineers (VDI), and extended by Werner Nachtigall in 1998 (Gruber, 2011, p.14):

> *"As a scientific discipline, bionics deals systematically with the technical execution and implementation of constructions, processes and developmental principles of biological systems. This also includes various forms of interaction between living and non-living elements and systems."*

The term 'biomimicry' was popularised by author and scientist Janine Benyus in her book 'Biomimicry: Innovation Inspired by Nature' in 1997. She defines biomimicry as a:

> *'new science that studies nature's models and then imitates or takes inspiration from these designs and processes to solve human problems'.*

She proposes looking at nature as a model, measure and mentor. Sustainability is addressed as a main objective in her approach.

2.2.2 Pioneers throughout history

Turning to nature for inspiration has occurred since the ancient Greeks. They saw that natural models offered a harmonious balance and proportion between the parts of a design, which are consistent with the classical ideal of beauty. Aristotle studied concepts such as the characteristics of wholeness, integrity, the unity of a structure, how the parts contribute to the aims of the whole, and how no part could be removed without damaging the whole. All these are concepts present in nature. Taking nature as an inspiration is also evident in the works of Vitruvius who believed that architecture is an imitation of nature in attempt to study its proportions, especially that of the human body. This led him to define his famous Vitruvian man which was later drawn by Da Vinci inscribed in the circle and the square (the fundamental geometric patterns of the cosmic order) (Steadman, 2008).

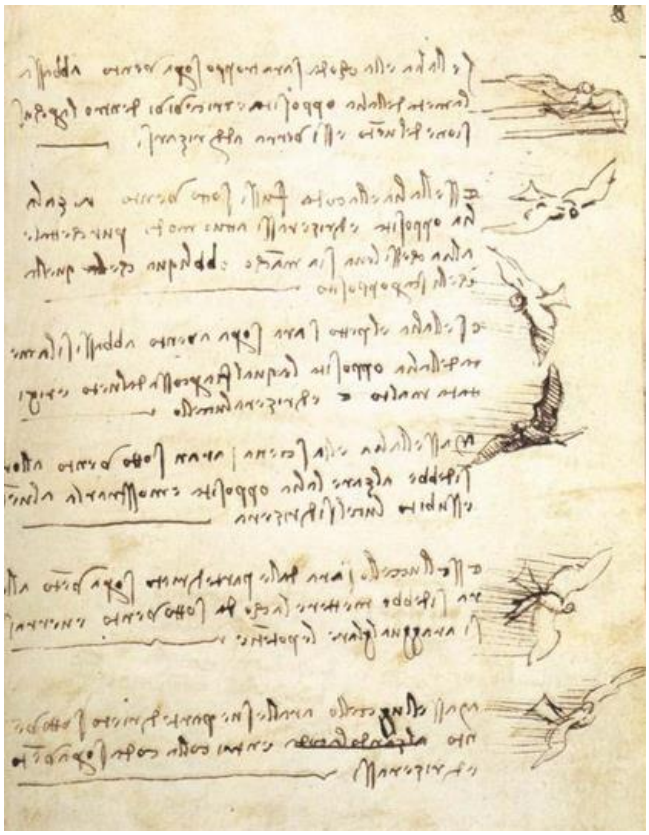

Figure 2.1: Leonardo Da Vinci's Codex on the flight of birds. Source: http://www.leonardodavinci.net/codex-on-the-flight-of-birds.jsp.

Plants are another good example for natural inspiration throughout history. Much of the evidence emphasising the importance of the golden section for example and its relationship with natural form came from detailed botanical observations of the arrangements of leaves and stems in plants, and the patterns of petals in flowers (Steadman, 2008). In the 19th century, the Swiss botanist Simon Schwendener investigated plants and stated that:

> *"Without any doubt plants construct using the same principles as engineers, but their technology is much finer and more perfect."* (Gruber, 2011, p.21).

In the following paragraphs examples of some pioneers of 'design inspired by nature' are presented. It is by no means a comprehensive list but rather a general overview.

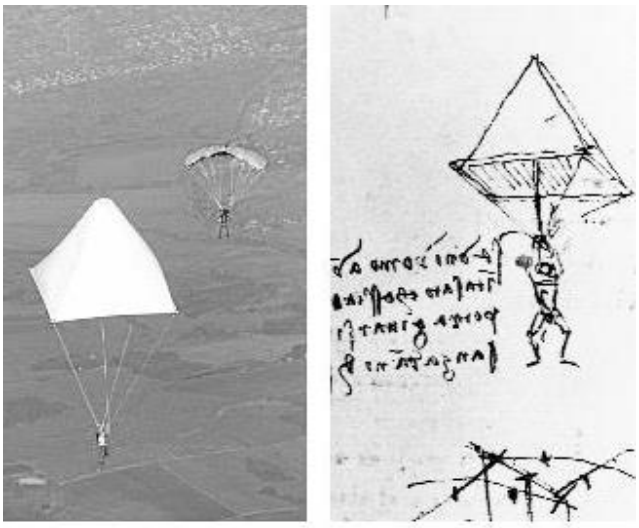

Figure 2.2: July 25, 2000, Adrian Nicholas jumped from 3000 meters altitude over Mpumalanga, South Africa, using a parachute built from a design suggested by Leonardo da Vinci in the 1480s.
Source: http://skydiving-encyclopedia.com/wiki/skydiving/10-fears-of-falling-risks-safety/10-2-risk-death/parachuting-and-skydiving-risk/

Leonardo Da Vinci (1452-1519)

The historical development of flight for example was a challenge that had kept researchers and inventors busy for centuries, where various models from nature were considered and studied. Leonardo Da Vinci in 1505 wrote a book on the flight of birds named 'Codex on The Flight of Birds' where he examined the flight behaviour of birds (as shown in Figure 2.1) and proposed mechanisms for flight of machines. Although his machines were not successful, his ideas inspired many inventors ever since (Nachtigall & Wisser, 2015). In fact, he could be considered the first biomimetic designer as he is the first known researcher to go beyond the investigation of nature's creations, and actually transfer his observations into sketches and design concepts (Mazzoleni & Price, 2013).

He drew many other designs and ideas inspired by nature which despite not being appreciated in his time, influenced and inspired numerous inventors later on. An example could be the parachute design that was tested in 2013 by Adrian Nichols (as seen in Figure 2.2). He used materials available in da Vinci's time and was able to descend to earth from a height of 3000 meters. However the assistance of a modern parachute was required to avoid being hurt by da Vinici's invention that weighs 85 kg (Encyclopædia Britannica, 2015).

Joseph Monier (1823-1906)

Plants have always been sources of inspiration and role models ever since humans started to use technology. Regarding architecture in particular, plants are quite important as they share similarities with buildings such as staying in one place, depending on local environmental conditions, trees can be of the same size of some buildings and experience similar natural forces. Joseph Monier was a gardener who made plant pots from wire mesh and concrete. He observed the fibrous structure of the decaying parts of the Opuntia plant which inspired him to invent reinforced concrete as a solution to prevent the breaking of garden pots. Monier is considered the inventor of reinforced concrete. He patented his idea in 1867 (Nachtigall & Wisser, 2015).

D'Arcy Thompson (1860-1948)

Thompson's book 'On Growth and Form' that was published in 1942 is regarded as a bible describing the development of form and structure of living organisms. It is a main reference

to these kinds of studies as many later works refer to Thompson's findings. It addresses questions of form development, its magnitude, growth and scale. Thompson also investigated natural shapes in terms of geometry and mathematics. In the field of mathematical biology, his works are still an inspiration and are taken forward (Thompson, 1945).

Frei Otto (1925-2015)

Frei Otto has always been concerned throughout his career with the design and construction of large roof structures, combining strength and lightness. This has caused him to turn to natural structures with these characteristics for inspiration. For example, his pavilions for the 1972 Munich Olympic Games which are basically cable-net roofs with clear parallels in spiders' webs (Figure 2.3). The webs are very strong for their weight and so thin that they are almost invisible. The supporting threads of the web hang in catenary curves which interested Otto very much due to their efficiency as pure tensile structures in addition to giving efficient forms for domes and vaults when inverted.

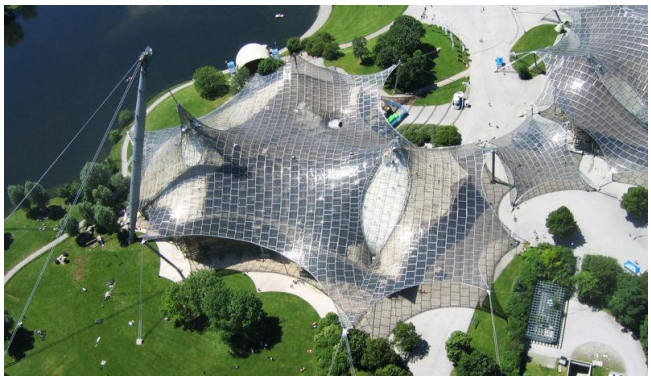

Figure 2.3: Munich Olympic Stadium in Munich, Germany, by Frei Otto and Gunther Behnisch, 1972. Source: http://www.archdaily.com/109136/ad-classics-munich-olympic-stadium-frei-otto-gunther-behnisch.

The huge difference in scale between the web and the building does not change the fact that the shape or form of these structures is based on the same principles. He was also interested in another line of biologically-inspired engineering research which is structures stiffened by the pressure of gases or fluids. He collaborated with Johann-Gerhard Helmcke, a biologist and anthropologist interested in the work of structural engineers, and established the Biology and Building research group in Stuttgart. The flow of knowledge was not one way (from biologist to engineer) as he was also consulted by biologist on how to interpret and translate concepts from plants and animal structures in an engineering context (Steadman, 2008).

Steven Vogel (1940-2015)

Steven Vogel played a critical role in establishing the discipline of biomechanics, and was a prolific author of numerous famous works addressing the intersection between physics and biology. His research covered a wide range of fields such as studies of ventilation currents in prairie dog burrows, flight in tiny insects, leaf streamlining, how air passes through feathery moth antennae, and the mechanics of jet propulsion in squid and scallops. One of his most famous books is "Cats' Paws and Catapults" which is classic in the topic of mechanics particularly highlighting a comparison between how mechanical challenges are addressed in both nature and technology (McKeag, 2010).

2.2.3 Relationship between nature and architecture in modern history

Gruber (2011) presents an interesting overview regarding the relationship between nature and architecture. Throughout the modern history of architecture, certain movements have

their own approaches and position towards nature as will be discussed in the following paragraphs.

One of main factors driving the development in architecture is technology. Pioneers of the futurist movement at the turn of the 19th century were quite enthusiastic about emerging technological developments, and their designs were far from natural interpretations. Steel and glass for example were explored and used in excess around 1900 with the development of the Art Nouveau.

Figure 2.4: Hôtel Tassel (Main entrance & Staircase) is an example of the Art Nouveau movement illustrating Victor Horta's irregularly shaped rooms open freely onto one another at different levels; the natural design of an iron balustrade is echoed in the curving decorative motifs of the mosaic floors or plaster walls.
Source: https://www.pinterest.com/jessicaherreria/victor-horta.

In contrast, the Organic movement for example -with Imre Makovecz as one of its representatives- tried to interpret biological aspects to technical functional elements. The Art Nouveau movement that began in the late 19th century till the early 20th century had the main objective of modernising design, and escaping the historical styles that had been popular earlier. Nature was a main source of inspiration for the designs that emerged in this movement that were characterised by their flowing, curvilinear forms like stems of plants. Victor Horta was one of the most influential figures of this movement. His works tended towards unity and fluidity of the materials used as seen in Figure 2.4. This movement along with Organic movement later influenced Bauhaus architects such as Frank Lloyd Wright who took organic architecture to another level.

Figure 2.5: Oscar Niemeyer's Metropolitan Cathedral of Brasília. It is an example of the revival of the organic movement after the Second World War and developments in concrete construction which opened up new possibilities to architects and designers.
Source:
https://americasouthandnorth.wordpress.com/2012/11/11/get-to-know-a-brazilian-oscar-niemeyer/

However the functionalism movement which highlighted that the building's design should mainly be driven by its function, opposed the use and designs of organic forms. Then the organic movement was revived after the Second World War around the 1950s due to developments in concrete construction techniques. This can be seen in the works of Pier Luigi Nervi, Oscar Niemeyer and Eero Saarinen for example who explored the structural potential of concrete.

Frei Otto's group aimed at understanding structures and processes in nature as mentioned earlier in the previous section. They made use of the physical laws that were established and experimented with minimum energy surfaces such as soap film models. This led to innovative designs regarding the development of membrane constructions. Antonio Gaudi used a similar method much earlier and is still applied by Heinz Isler who developed methods for form-finding by the use of hanging models made of numerous materials to build shell structures.

The ecological design movement came later in the 1970s, which was mainly concerned with nature and problems of energy efficiency and the effect of building construction on the environment. Currently this approach is still applied under many names such as sustainable design, ecological design, bio-architecture or green architecture.

Gruber argues that biomimetics in architecture presents innovation and more importantly a design method that helps us transform ideas from nature to architecture. It is important to note that it is not suitable to define 'Biomimetic Architecture' as a new style or movement, since architectural projects are determined by so many parameters. Furthermore, it is quite difficult to determine whether a certain architectural project is biomimetic or not, since these biomimetic intentions are often not obvious. Biomimetics can influence an architectural project in certain aspects but certainly not all. Therefore it is better expressed as the design methodology itself behind the architectural project:

> *'Biomimetics in architecture is a discipline to gain innovation in architecture by using natural role models, and the comparison between animate nature and built environment creates new insights.'* (Gruber, 2011, p.109)

It is worth noting that sometimes biological analogies in the past have been on a superficial level, where pictures or forms of natural organisms would be simply adjoined and copied to buildings or products of industrial design. What is needed is an analogy at a deeper level to fully explore the potential and benefit of what nature has to offer to produce sustainable solutions to our problems. Nevertheless, even if some biological analogy attempts were not of real benefit, the fact that the biological theme has been continuously repeated throughout history in itself suggests its importance (Steadman, 2008). This implies that there are several possible *levels or* scales of nature-inspired design as will be discussed in the following section.

2.2.4 Levels and scales of biomimetic design

In 2007 the Biomimicry Guild[1] defined three levels of biomimicry, which are the form, process and ecosystem. These levels have been further developed by Zari (2007) to clarify the potential of biomimicry in sustainable design as shown in Figure 2.6, and they include the organism, behaviour and the ecosystem. The organism level refers to a specific animal or plant, and includes mimicking the organism as a whole or just a part of it. The second level refers to mimicking an organism's behaviour, and could include how an organism relates to or interacts with its context. The third level is the mimicking of ecosystems as a whole and the general principles that enable them to function successfully.

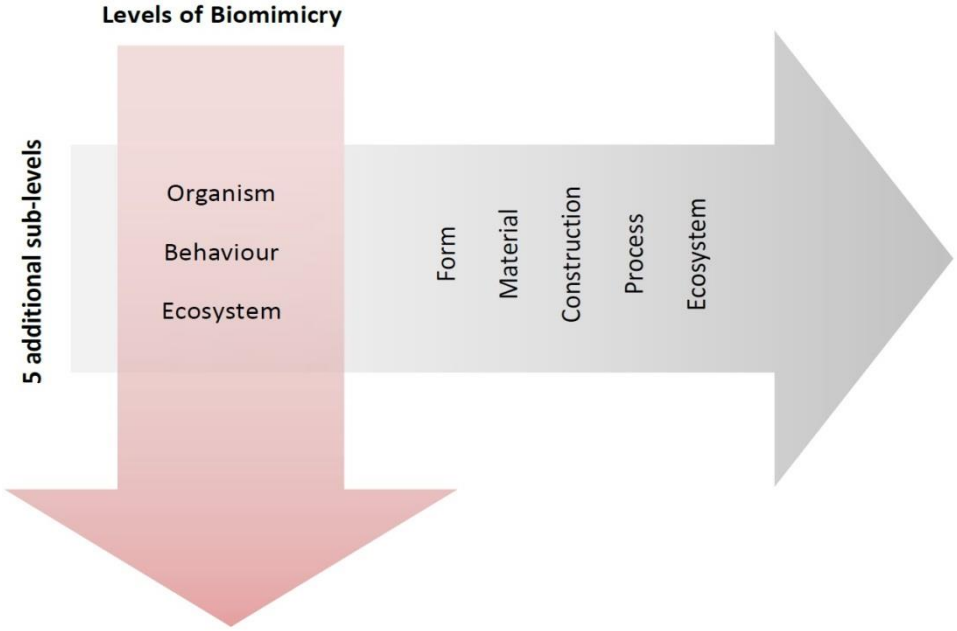

Figure 2.6: Three main levels of biomimetic design as explained by Zari (2007) which are the organism, behaviour, and ecosystem level. Additionally, each level could be applied in five different sub levels which are the form, material, construction, process, and function.

It is worth noting that these levels of biomimetic design could be seen from a different perspective that leads to a different classification. They could be perceived as ascending scales, starting from the cellular scale of living organisms; including material make-up and cellular growth laws for example. The second scale could include anatomical and structural aspects of the organism itself as a whole. The third scale includes the micro-environment such as the influence and interaction with other organisms and immediate surroundings. The fourth and final scale is the macro-environment including the context and ecosystem within which it survives and develops.

Any of these scales or levels could be beneficially applied in architecture, and not necessarily on the same corresponding scale. For example, studies on a cellular scale (their shape, packing, functions, interactions, etc.) could be useful for the development of nano-

[1] The Biomimicry Guild, is a for-profit consulting company founded by Janine Benyus. In 2010 they united with, Biomimicry 3.8, as a non-profit/for-profit hybrid organisation. In 2014, the two entities decided to revert to the original model of dual brands in order to more effectively achieve their missions. The for-profit consultancy is now Biomimicry 3.8, while the non-profit organisation is the Biomimicry Institute (The Biomimicry Institute, 2015).

materials, the development of building forms, and even for an urban-scale development (such as applications of cellular automata studies). In addition, studies on a macro-environmental scale and ecosystems (such as concepts of adaptation and evolution) could be applied on the scale of the design process of a building.

2.2.5 Similarities and differences between design in Nature and Architecture

Similarities and differences between nature and architecture are numerous and cover wide range of aspects; design concepts, morphology, material structures, behaviour, and so on. Regarding energy usage in particular (as this is the main focus of this research), the following quotation describes a general common base of design between nature and technology and hence architecture:

> *'Design in technology is based on the same laws of physics as animate nature, and that it is for this reason that similar problems, analogies, convergence and role models exist'* (Gruber, 2011 p.108).

Despite these similarities in design between nature and technology, and architecture in particular, differences also exist. Steven Vogel briefly made a comparison between built and grown structures in term of the most obvious differences between them, shown in Table 2.1.

Table 2.1: A brief comparison by Steven Vogel highlighting the main differences between man-made and natural constructions (Vogel cited in Gruber, 2011). Reproduced by the author.

Natural construction	Technical construction
Round form	Right angle
Few parts, varied properties	Many parts, homogeneous
Diffusion, surface tension, laminar flow	Gravity, thermal conductivity, turbulent flow
Strength	Stiffness
Toughness	Brittleness
Bending, twisting	Sliding
Flexible	Streamlined
Non-metallic	Metallic
Tension	Compression
-	Wheel, rolling
Submarines	Surface boats
Big 'product' compared to factory	Small products
Continuous rebuilding	Minimal maintenance
Wet	dry

2.2.6 Biomimicry Design Methods

There are two different approaches regarding biomimetic design; the problem-based approach and the solution-based approach. They are explained in the following paragraphs.

Problem-Based Approach 'Problem analogy'
Throughout the literature reviewed, this approach was found under different names, such as "Challenge to biology" (Biomimicry 3.8, 2013) "Design looking to biology" (Zari, 2007), "Top-down Approach" (Knippers, 2009) and "Problem-Driven Biologically Inspired Design" (Helms, et al., 2009) all referring to the same meaning. In this approach, designers explore nature for solutions and are required to identify problems in specific abstract terms. Then biologists need to match these problems to organisms that have solved similar issues. This approach is mainly initiated by designers identifying initial goals and parameters for the design.

The framework of problem-driven biologically inspired design follows a progression of steps which, in practice, is non-linear and dynamic in the sense that output from later stages usually influences preceding ones, providing iterative feedback and refinement loops (Helms, et al., 2009).

Solution-Based Approach 'Solution Analogy'
As stated in the previous approach, this approach was also found to have different naming such as and "Biology to Design" (Biomimicry 3.8, 2013) "Biology Influencing Design" (Zari, 2007), "Bottom-Up Approach" (Knippers, 2009) and "Solution-Driven Biologically Inspired Design" (Helms, et al., 2009). Here the process is primarily dependant on and initiated by people with biological knowledge and expertise rather than on a predefined design problem. A known example is the scientific analysis of the lotus flower which despite its presence in swampy waters, emerges clean. This led to many design innovations including Sto's *Lotusan* paint which enables buildings to be self-cleaning (StoCorp, 2015).

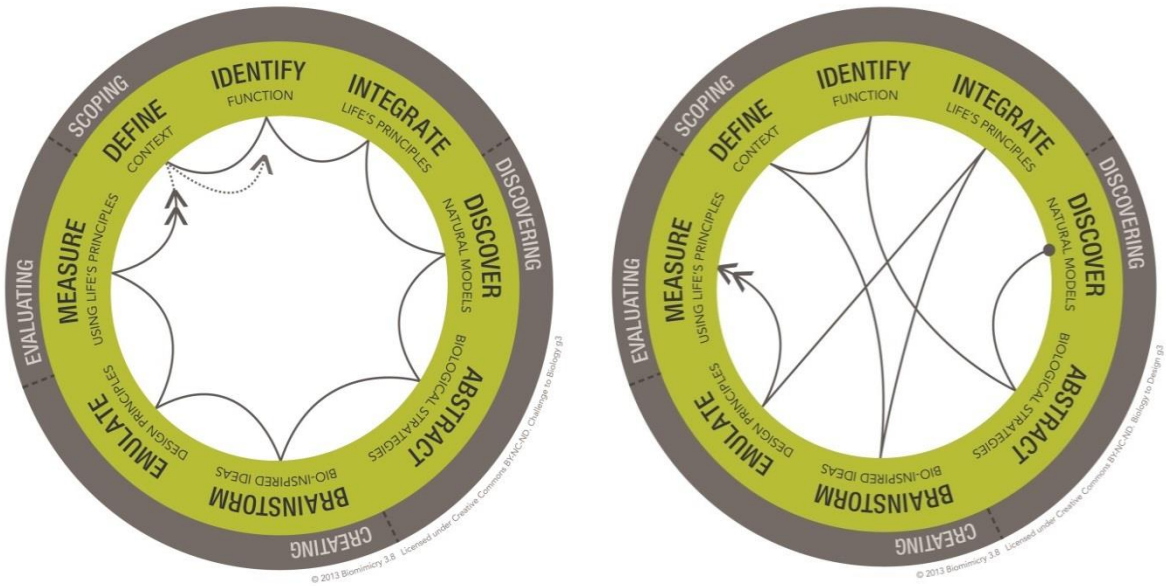

Figure 2.7: The two different biomimicry design methods illustrated by the Biomimicry Institute; Challenge to Biology (left), and Biology to Design (right) (Biomimicry 3.8, 2013).

2.3 General Biological Principles

Many references discuss general principles and concepts in biology as will be described in this section. They could be sometimes referred to as life's principles, criteria of life, or ecosystems principles. This section briefly highlights these principles in a number of references, stating in the end what is seen as common between them.

2.3.1 The Biomimicry Institute (2013b)

The *Biomimicry 3.8 Institute* defined a set of principles based on the recognition that life in general is interconnected and interdependent and is influenced by the same set of conditions. These principles represent repeated patterns found in most living species, with a common aim that they create conditions conductive to life as shown in Figure 2.8. These principles are:

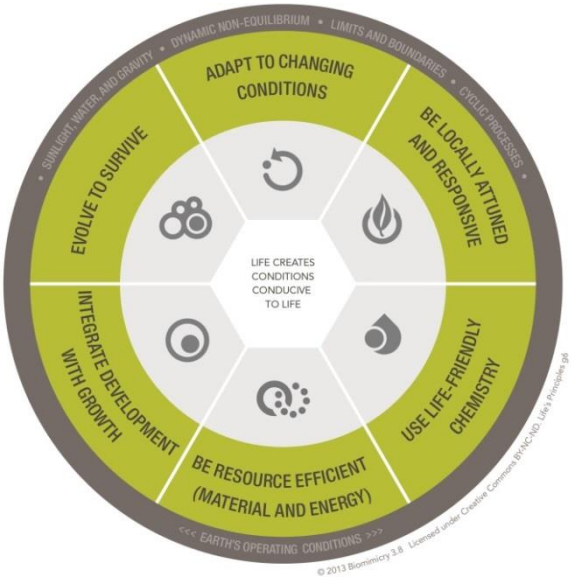

Figure 2.8: Life's Principles by the Biomimicry Institute (Biomimicry 3.8, 2013b).

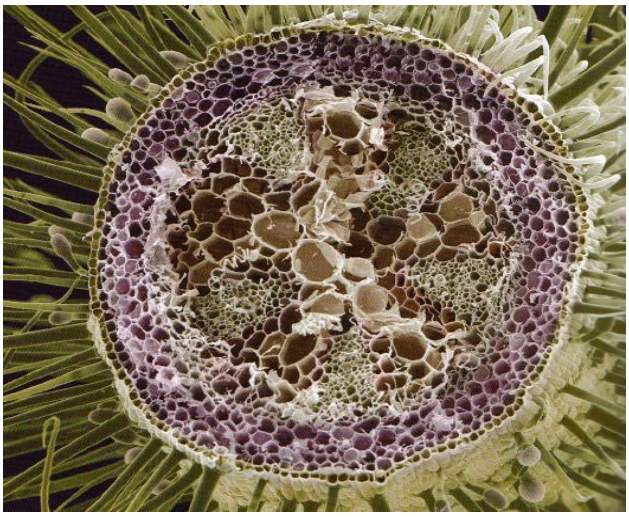

Figure 2.9: Cross section through the stem of a geraniim illustrating variation in their cross section and different organisations of cells in successive hierarchies. Cells have a structural role (such as supporting the plant itself and resisting wind loads on a macro scale) in addition to distributing carbohydrates, hormones and water in the same time (micro scale) (Castle, 2004).

a) Adapt to changing conditions

Nature adapts to changing contexts. It maintains its integrity by self-renewal, constantly adding material and energy for healing and system improvement. It maintains resilience and survival by diversity and variation. This way, systems survive and functions are met after the occurrence of disturbance or change in context, as the same function could be achieved by a variety of organisms or ways. For example, in the built environment a city has different modes of transport like, buses, subway, trams, cycling and walking lanes, if one of these modes encounters a problem, the main function (which is the transport of people) can be still achieved by an alternative mode.

b) Evolve to survive

Through the process of evolution, nature continually embodies information to ensure enduring performance. Through trial and error, successful survival strategies are preserved and repeated throughout generations. Information is also shuffled and exchanged to create new options. Unexpected results or mistakes are incorporated in ways that could lead to new forms or functions. Genetic mutations are the source of many new strategies or forms

for living organisms. These strategies that aid the organisms in survival are passed along in genetic material.

c) Resource efficient

Nature takes advantage of local resources such as energy and materials. Everything is recycled and contained within a closed loop of material flow from one form to another. Multi-functional design is favoured where more than one need could be met by the same element. For example the cells of plant stems have a structural role of supporting the plant, in addition to the transport and distribution of water and carbohydrates at the same time as shown in Figure 2.9. Nature uses low energy processes by reducing consumption as well as the required temperatures and pressures for reactions. Shells and bones are a good example of strong natural matrerials that are formed in regular temperatures and conditions. Finally, shapes, patterns and form are always based on need.

d) Locally attuned and responsive

Nature fits into the surrounding environment and integrates with it through win-win relationships. Abundant local materials and energy are used, and local phenomena that are repeated in the environment are made useful, so that needs are fulfilled with what is available. The changing seasons are an obvious example of cyclic processes on Earth, and natural organisms expect and take advantage of these repeating patterns to have a better chance of survival. Information flows to trigger reactions in response to changing circumstances.

e) Use life-friendly chemistry

Biochemistry in nature takes place by using small subsets of elements that are arranged in numerous elegant ways to fulfil certain functions, and decomposition does not result in harmful by-products. For example, venoms and poisons in nature are made of basic elements and proteins that are combined and assembled in different ways. Once a prey is infected by a venous predator such as snake, the toxin decomposes back to basic elements and no traces would be found of it in the faeces of the snake. This is in contrast to man-made toxins that are harmful to the environment and do not usually decompose back into natural elements.

f) Integrate development with growth

Nature invests in strategies that integrate both development and growth. What is meant by development in this sense is the investment in the infrastructure that enables growth to occur. An example is a city that experiences population growth. Without the necessary infrastructure, the increasing population would encounter many difficulties and lack of services necessary for living. Nature is self-organising, where systems do more than individual parts. A bottom-up process is nature's method of building, where organisms are built one cell at a time, progressing from simple to more complex forms.

2.3.2 Pera Gruber (2011)

Gruber (2011) in his book Biomimetics in Architecture also refers to the same topic with the name of *Classical Criteria of Life* that were defined by Neil Allison Campbell (2000). They are supposedly present in any living system according to the author. The concepts are more or

less similar to those stated by the Biomimicry Institute with some minor differences. The *Criteria of Life* were stated as follows:

a) Order

Living organisms exist in some sort of chemical order, in the sense of thermodynamic laws. Autotrophic[2] organisms use energy from the sun to form complex molecular material to store energy. Heterotrophic[3] organisms internalise food and hence highly ordered material. On a molecular level, this material is reduced to even lower levels to deliver energy required for survival.

b) Propagation

Organisms have the capability of reproduction and passing on genetic information. Unicellular organisms reproduce by cell division. Most plant and animals reproduce by combining a male cell and female cell containing a complete set of chromosomes. The strategy of reproduction promotes genetic recombination, which leads to diversity and variety in the genome (which is a set of all the inheritable traits of an organism) representing the basis of evolution.

c) Development and growth

DNA information controls the processes of growth and development which generate organisms and thus represent species. Development processes occur both throughout the life of the organism or throughout generations of the species. Growth depends on cell division, differentiation and assembly to form building material for the organism. Growth does not occur by a predefined plan specifying the position of elements in space, but rather by concept and rhythms regulated by chemical processes. These concepts vary in nature, such as addition, extrusion, growth on the edge, budding and so on.

d) Energy use

Living organisms absorb energy and convert it into nutrients required for activities and survival. In order to survive they have to use energy in the most efficient manner possible. Consequently, to achieve this specific goal we find that nature applies certain strategies such as optimising the whole instead of single elements, using integrated rather than additive construction, preferring multi-functionality over mono-functionality, using sunlight directly or indirectly, and complete recycling instead of accumulating waste. To solve a given problem nature uses the least possible energy. Gruber emphasises the physical law that energy is neither created nor destroyed, but could transform from one form to another.

e) Reactions to the environment

Sensing and reacting to the environment and surroundings are crucial for the adaptation of living organisms. They have to sense external stimuli, process them, and react accordingly to survive.

f) Homoeostasis, metabolism and autopoiesis

[2] Autotrophic: capable of self-nourishment by using inorganic material as a source of nutrients and using photosynthesis or chemosynthesis as a source of energy, as most plants and some bacteria (Dictionary.com, 2013).

[3] Heterotrophic: capable of utilizing only organic materials as a source of food. (Dictionary.com, 2013b).

The definitions of these terms according to the Oxford Dictionary are as follows: Homoeostasis is the tendency toward a relative stable equilibrium between interdependent elements, especially as maintained by physiological processes (Oxford Dictionaries, 2016). Metabolism is the chemical processes that occur within a living organism in order to maintain life (Oxford Dictionaries, 2016b). Two kinds of metabolism are often distinguished: constructive metabolism, the synthesis of proteins, fats and carbohydrates that form tissue and store energy, and destructive metabolism, the breakdown of complex substances and the consequent production of energy and waste matter.

Autopoiesis is the self-maintenance of an organised entity through its own internal processes; (in extended use) self-organisation, self-regulation (Oxford Dictionaries, 2016c). Despite changing environments, the internal conditions of organisms' bodies are kept constant within certain limits. Living systems *change to stay the same,* and that is the main concept of autopoiesis. This concept applies on a cellular level, all the way up to the level of biospheres. When applied on the scale of whole species, it leads to evolution.

g) Evolutionary adaptation

Evolution is defined as the process by which different kinds of living organisms are thought to have developed and diversified from earlier forms during the history of Earth (Oxford Dictionaries, 2016d). It is the gradual development of something, especially from a simple to a more complex form. Evolution and natural selection result in organisms that are more and more adapted to their environment. At the same time, these environments are being shaped by them as well. Gruber presented an architectural interpretation of these life criteria, addressing architecture as the whole built environment that includes urban design, building, processes and materials that are all influenced by living systems. Not all criteria of life have parallels in the field of architecture. He adds to the aforementioned criteria the following:

- Openness: nature involves open systems that exchange resources, energy and information. The opposing needs of openness and enclosure have to be met. This is true also in architecture.
- Self-organisation: the capability of a system of sustaining order without outside influence. The overall behaviour of the system is complex, but simple rules are followed in local interactions.
- Limitation: limited space and time define the existence of natural systems as well as built ones.
- Information processing: information is passed on in the form of matter during the replication of organisms.

According to Gruber, modern architecture witnesses a gradual increase in the presence of life criteria. However they do not appear in a particular order. Some of these criteria are already inherent characteristics in architecture such as openness and limitation for example while others are quite difficult to apply in reality such as self-replication and propagation. He presents an interesting illustration (Table 2.2) which gives a general overview of the applicability of each life criterion in architectural terms, along with a small example for each interpretation.

Table 2.2: A general overview of the applicability and interpretation of each life criterion in architecture. Light grey fields are important in current architecture discussion and experimental designs; dark grey fields are still unexplored and should be followed by a strategic search for new architectural vision (Gruber, 2011).

	Urban Design	Building	Process	Material and Structure
Openness	Yes	Yes	Yes/Not Applicable	Yes
	Cities as open systems	Buildings as open systems	Processes open to input and influences	Permeability
Self-organisation	Yes	Yes/No	Yes	Yes
	Cities as self-organised structures	"Self-building"	Planning and building processes	Material processing and structuring
Limitation	Yes	Yes	Yes/Not Applicable	Yes
	Limits are being exceeded	Limits are being exceeded		Limited in space and time
Information processing	Yes	Yes	Yes	Yes/No
			Processing is based on information	Not enough inherent information
Order	Yes	Yes	Yes	Yes
Propagation	No	Yes/No	Yes	No
	More growth than propagation	Propagation of typologies	Cyberspace	
Growth	Yes	Yes	Yes	Yes/No
	Urban growth	Extension and increase in size	Growth processes used for design	Sustainable materials, but no growth in applied state
Energy processing	Yes	Yes	Yes	Yes/No
				Production, but no harvesting
Reaction	Yes	Yes/No	Yes	Yes
		No intelligent reaction yet		Smart Materials
Homoeostasis and Metabolism	Yes	Yes	No	No
Evolution and Natural Selection	Yes	Yes/No	Yes	Yes
	Evolution as development	Yes on typological level		Evolution as development

2.3.3 Zari and Storey (2007)

A third reference (Zari & Storey, 2007) discussing the same topics under the name of 'Ecosystem Principles' is reviewed. By comparing multi-disciplinary understandings of how ecosystems operate, a set of ecosystem principles was developed by Zari and Storey (2007). By analytically comparing related knowledge of ecosystem principles in various disciplines, they developed a set aiming to capture cross disciplinary understandings of ecosystem functioning. These principles are stated as follows. Ecosystems:

a) Depend on contemporary sunlight.

Energy from the sun is the only input (apart from the moon's gravitational forces) into the Earth's closed loop ecosystems, serving as the only source of energy whether in a direct or indirect way. Most ecosystems depend on contemporary sunlight (which is recently received from the sun) that has been transformed into biomass by photosynthesis. This biomass forms the basis of the food chain.

b) Optimise the system rather than its components.

Ecosystems utilise materials and energy in a manner that optimises the system as a whole rather than its individual components. Matter is continuously recycled in a loop where waste of an organism is used by another. Energy is effectively used and materials tend to serve more than one function, as this means less energy expended. Allen (2002) in (Zari & Storey, 2007) discusses how biological systems degrade energy in a small number of large steps rather than in a small number of large steps. This leads to the flow of energy from an organism that has done work to be used by another, and therefore energy use is most efficient.

c) Are attuned to and dependent on local conditions and situations.

Species of a certain ecosystem tend to have multiple relationships with other species with which they share the environment. They use resources available in their immediate range of influence and are tailored and adapted to their specific microclimate.

d) Are diverse in components, relationships and information.

A diverse system is a strong one capable of withstanding obstacles and adapting to changing circumstances. The number and strength of relationships among organisms of an ecosystem is more important to its stability than the number of species itself. These relationships include both competition and cooperation. They include relationships among the organisms themselves, and between them and their environment. As an ecosystem becomes more diverse and complex, *emergence* tends to occur which is the phenomena of new unexpected organisation in complex systems.

e) Create conditions favourable to sustained life.

Organisms grow and perform the activities necessary for their survival in a manner that does not damage the ability of their ecosystem to survive. Organisms process and manufacture the required materials and chemicals for their existence using what is available in their local environment. Materials are formed in normal temperatures and water is usually the chemical medium. As organisms live and die, the environment is regenerated and strengthened.

f) Adapt and evolve at different levels and at different rates.

Adaptation and evolution are two interlinked processes that allow organisms and their ecosystems to survive in their constantly changing environment. Reap et.al. (2005) in (Zari & Storey, 2007) refers to adaptation as the means by which an organism adjusts to change throughout its life time, while evolution is the process by which slower genetic changes occur throughout successive generations of a species through the medium of the gene.

These general principles were intended to aid designers in evolving design methodologies and aim at the development of a more sustainable built environment. Although the comprehensive application and fulfilment of all ecosystem principles in one single project may be yet difficult to achieve, numerous examples that employ some of them do exist.

These three references reviewed share more or less the same principles despite some different naming. For example they all mentioned the concepts of evolution, adaptation, responsiveness and dependence on natural energy sources. This research focuses on the principle of adaptation; how it occurs in nature and what are its possible applications. The means by which natural organisms adapt to their surrounding environments is very inspiring and provide a very useful source of possible architectural solutions. Architects still need to improve adaptation properties of the built environment for better energy performance of buildings. The following section elaborates on the principle of adaptation in nature and then in architecture.

2.4 Adaptation in nature and building skins

2.4.1 How organisms adapt

Adaptation and Evolution

Life develops as organisms and their environment interact with each other. Resulting from evolution and natural selection, organisms become more and more adapted to their environment while shaping it at the same time. Evolution is one of the most important principles in nature. Based on Darwin's theory, it occurs by means of mutation, genetic recombination and natural selection.

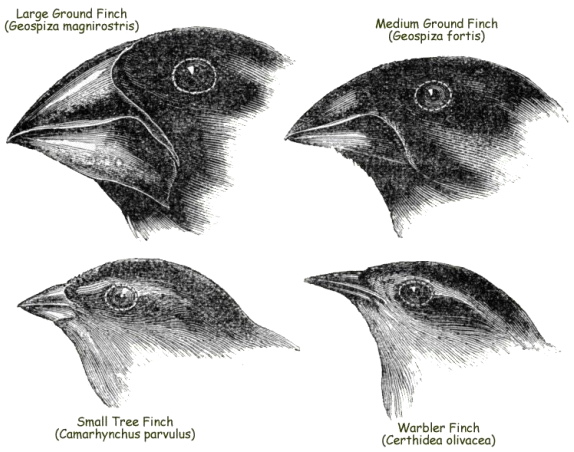

Figure 2.10: Over many years, the finches' beaks have evolved to suit their eating habits. For example, seed and fruit eaters have claw-like beaks to grind and crush their food, while grub eaters have longer, thinner beaks to poke into holes to attain their food.
Source:
http://www.animalcorner.co.uk/galapagos/finches.html.

Mutations are the small genetic changes that occur in the organism's DNA. Genetic recombination is used to describe the production of offspring, who combine genetic combinations of their parents. Mutations cause the required genetic variations, so that even in unexpected

environmental contexts certain organisms could cope better than others. Recombination ensures the passing-on of the genetic material. Finally, natural selection is the successful reproduction of natural organisms as a result of their interaction with the environment.

It is important to note that if an organism has a certain feature that is advantageous in a specific environment, then this organism has a higher *fitness* than others without it. This improves their reproductive success and therefore it is likely that this specific feature would be passed on to new generations. In this manner, the existence of the organism and the feature is continued. The consequence of this process could be seen in remarkable adaptations of organisms to their environments, especially remote ones as they help in developing unique flora and fauna particularly suited to them. Darwin illustrates for example how finches (which are a species of birds) in the Galapagos Islands, have adapted to their habitat and developed a variety of beaks according to their eating habits as seen in Figure 2.10 (Keynes, 2001).

Steadman (2008) elaborates on this subject, stating that the concept of *fitness* is not absolute; it is a relative quality depending on the particular environment in which the plant or animal lives. What could be regarded as fitness in one environment could be a disadvantage in another. For example, some moths have evolved to have the light colour of tree barks and therefore they are camouflaged against predatory birds. But if tree barks become darkened by industrial smoke, this characteristic makes it no longer fit to the new environment. It is then advantageous (more fit) for the moth to be black or dark in colour. The wide variety of natural forms may seem to the regular observer as unaccounted for. But the fact is that each detail in the forms of natural organisms has its functional purpose as mentioned by Horatio Greenough in his book: 'Form and Function: Remarks on Art, Design and Architecture' first published in 1947. He mentions that: 'If there be any principle of structure more plainly inculcated in the works of the Creator than all others, it is the principle of unflinching adaptation of forms to functions'. By studying adaptation means of living organisms, architects could derive beneficial solutions for buildings. This means that it is necessary to study the context as a whole in which the building is located including its climate, site, functions and needs of its users.

Morphological adaptations as well as behavioural ones, are aquired through evolution and are the product of trial and error. Certain forms of very basic learning processes in animals may be also be (in part at least) based on trial and error. Animals could repeatedly experiment with various modes of bevhaviour, available tools, or certain foods to eat and discover through failure and pain which of these were successful and which were not.

Skins in Nature

Plants and animals have a huge variety when it comes to skins and surface coverings. Animals offer a remarkable range of different types of fur, feathers, scales, hair, exoskeletons and shells, each have multiple roles and is specifically adapted to certain functions, environment and context. Skin in natural organisms has many functions, for example it aids in the thermoregulation of the body by the mediation of heat loss and gain. It regulates the balance of water in the body as well as allowing the diffusion of elements like oxygen and nitrogen into it. Nerve endings are present in the skin allowing sensation, and the colour and pattern of the skin have an important role in communication and camouflage (Mazzoleni & Price, 2013).

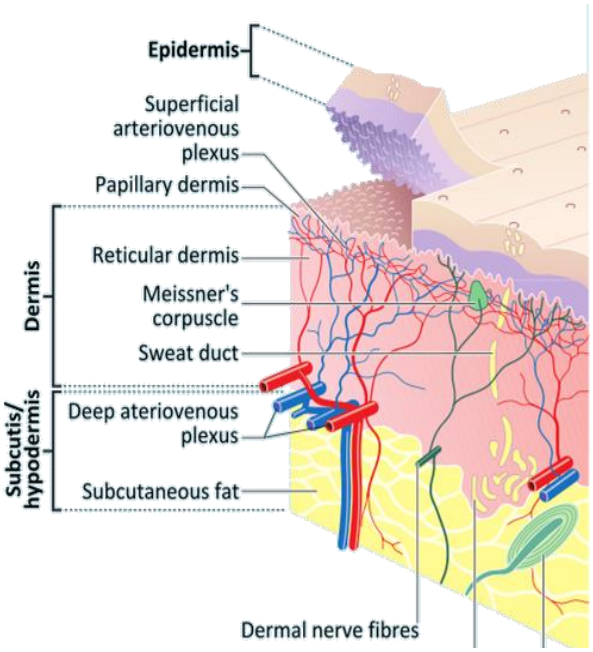

Figure 2.11: Diagram illustrating the layers of human skin.
Source: https://en.wikipedia.org/wiki/Human_skin.

Vertebrates have skins that are composed of multiple layers. The human skin, shown in Figure 2.11, has three main layers; the epidermis, the dermis and the hypodermis. The first one is a thin protective layer which keeps out water, harmful chemicals and protects against sun damage. The following layer is the dermis, allowing blood circulation to provide the epidermis with oxygen and nutrients. It is the initial source of input for the nervous system, sending signals to brain for sense such as heat, cold, touch, pressure, etc. Thermoregulation also occurs in this layer. If the body is hot, blood vessels conduct heat to the epidermis to allow surface cooling by radiation and sweat. If the body is cold, the vessels retain body heat. The final layer which is the hypodermis contains major blood vessels, fat, cells that store energy. It is an insulating layer as well as a shock absorber. Other vertebrates also have skin composed of multiple layers functioning in a similar manner to that of humans. But unlike humans who have small amount of hair on their skin, animals usually have a significant skin covering. Fur for example is composed of two layers; ground hairs at the bottom that are thick and provide insulation, and guard hairs which are longer and coarser. Guard hairs contain colour pigments, and protect against the elements especially rain as it contains water-repellent properties. Fur helps in thermoregulation of the body as it responds to heat and cold. Fur hairs could either be erect creating insulation air spaces in between, or flatten so that less hair is trapped and the animal could release heat (Mazzoleni & Price, 2013).

This is very similar to the role of building skins and therefore animal skins present an important source of possible ideas. Other ideas could also be inspired from the behaviour of animals in their environment in order to survive, in addition to plants and their adaptations to different climates.

2.4.2 How buildings adapt

As mentioned earlier, in the natural world form is always a reflection of its function which, in turn, is related to the environment. The degree of appropriateness of a form to its function and environment is referred to as adaptation or fitness as Darwin puts it.

Returning to the built environment and designed artefacts, maybe it is suitable to mention in this context Louis Sullivan's famous slogan: 'Form follows function' (Sullivan, 1896). It implies that built forms should be a result of their intended function, in other words, buildings should be a consequence of their functions and their 'fitness' could be measured as the degree of appropriateness to the context and reasons for which they were designed in the first place. The context could include aspects of the physical environment in which the building is placed, such as the site, micro and macro climate. It also includes non-physical aspects such as social, economic, cultural issues, available construction means, budget, in addition to required function itself and user preferences. However, the non-physical aspects (despite their importance) are not the focus of this research.

The importance of the environment in affecting the designed artefact was emphasised by researchers such as Herbert Simon in his book 'The Sciences of the Artificial' (Simon, 1996) where he refers to the environment as a *mould* to man-made objects. He stated that adapting to a goal involves a relation among three things: the purpose or goal, the character of the artefact, and the environment in which the artefact performs. He implies that the question of measuring fitness (which is the evaluation according to predefined goals) is related to the lowest levels of detail of the design problem.

Types of Adaptation

Adaptation in architecture has many forms but it could be mainly categorised into non-reactive and reactive adaptation as shown in Figure 2.12. *Non-reactive* adaptation is commonly observed in buildings aiming to achieve context-adaptation with basic passive design strategies. It is applied in a wide range of design decisions; basically any aspect of the context in which the building is designed. This type of adaptation includes for example the well-known environmental design theories which take into account the local environment and translate it into decisions such as the placement of the building in its site, minimum damage to existing ecology, building orientation, massing, zoning of floor plans, size and location of openings, use of static shading devices, façade morphology, selection of local appropriate materials and many other passive design techniques that aid in the adaptation of the building to its environment. In this type, no change of state or movement occurs in any of the building parts.

These decisions are very important, and they improve the adaptation as well as the environmental performance of the building. But the environment itself is never static, always changing whether throughout the timescale of the year, or even the day. This is why a *reactive* architecture has been developing for the last decades, one that is able to increase the performance of the building and apply adaptation at a higher level by sensing environmental stimuli and reacting to them. This *reactive* adaptation is usually concerned with the building skin. It is worth noting that the author thinks that there could be in the future a kind of *proactive* adaptation, one that is able to predict events that would occur in

the very near future and respond accordingly. For example, buildings could detect forthcoming weather conditions and therefore take necessary actions and adjustments.

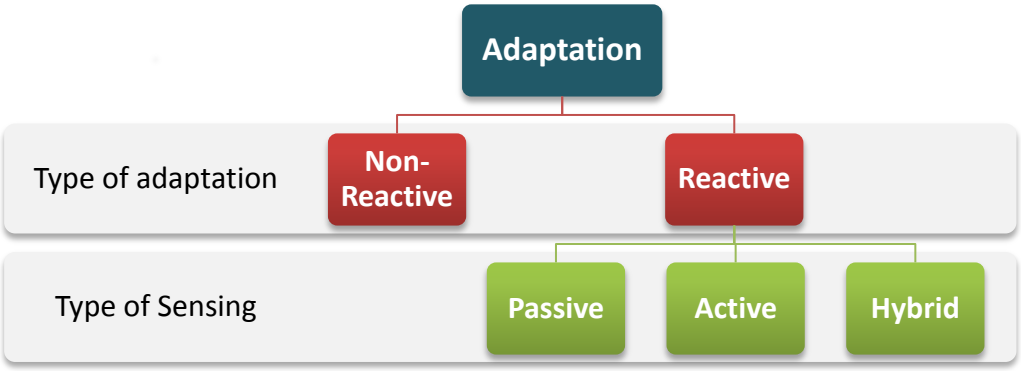

Figure 2.12: Types of adaptation and sensing. Source: the author, based on description from Gruber (2011).

Sensing Strategies

Reacting to the environment indicates that there is some kind of sensing, signalling, regulating and finally actuating. Petra Gruber in his book 'Biomimetics in Architecture' provides a thorough explanation on this topic. The action of sensing is a precondition to reacting, and it could be passive, active, or hybrid (Figure 2.12). *Passive* sensing indicates that there is some kind of material property change according to environmental stimuli, where the change of physical conditions directly initiates actuation. It is usually decentralised, energy efficient, and is embedded in architectural systems as integrated elements and not as add-ons. Its disadvantage is the invariability of reaction. An example of passive sensing is presented in section 2.6.1.

Active sensing strategies are much more common as they are installed in many technical building systems. They detect information regarding temperature, pressure, humidity, intensity of light, and wind speed for example. These sensors transform this information into an electric signal which then has to be interpreted to obtain meaning and transform it into an action. These actions are made either by human decision makers or decision-making technical devices and in both cases they rely on information to assist in taking these decisions. This enables designers to make buildings 'do' what they are planned for. Reactions of buildings could take place in the form of movement of certain building elements, opening, and closing, changing the properties of spaces or built elements.

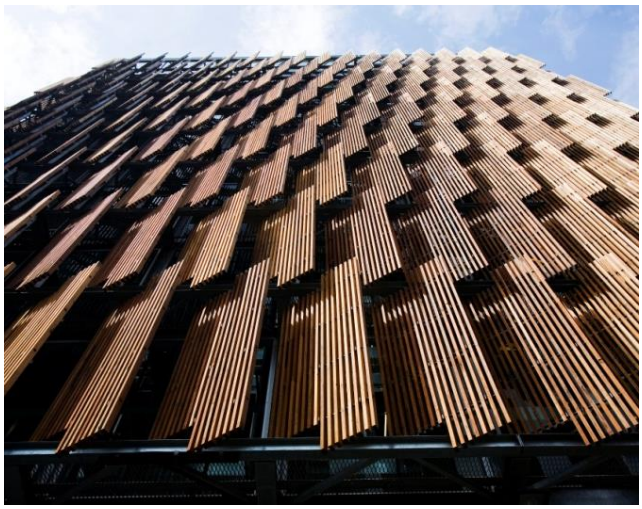

Figure 2.13: CH2 Melbourne City Council House. Image shows movable louvers on the western façade. Source: http://www.melbourne.vic.gov.au/AboutCouncil/MediaCentre/ImageGallery/Pages/CH2imagegallery.aspx

Hybrid systems have the advantages of passive strategies in combination with an active system that can be modified and adjusted in case the passive reaction is not enough.

Similar to nature, movement of building parts allows the adaptation to external climatic conditions. Movement could be triggered by the sun for example, as in the case of the CH2 building in Melbourne City (Council House 2), where louvers placed on the western façade move according to the sun's position to reflect as well as collect heat (active sensing) as seen in Figure 2.13. Opening and closing are the most common forms of movement in buildings. They permit/prevent visual and physical access, privacy, control of the amount of light, heat and wind entering the building. They could also be used to control resources such as water, gas, and waste in infrastructural systems.

Figure 2.14: Jean Marie Tjibaou Cultural Centre by Renzo Piano in New Caledonia. Source: http://www.fondazionerenzopiano.org/project/85/jean-marie-tjibaou-cultural-center/.

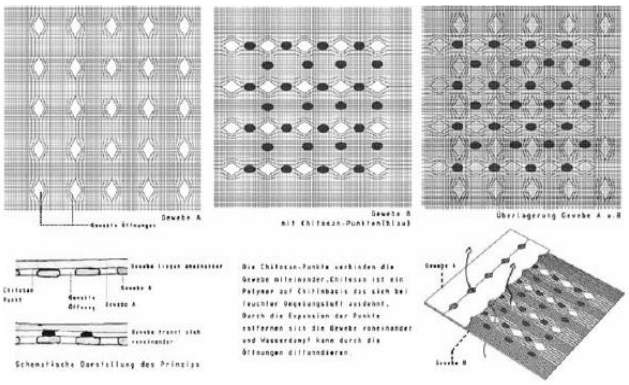

Figure 2.15: ***Michael Murauer, "smart fabric"*** **- inspired by stoma: ventilation according to humidity, in Gruber (2011).**

Renzo Piano's Jean Marie Tjibaou Cultural Centre, constructed in 1998 in Nouméa, New Caledonia is an example of a building adapting and reacting to wind conditions (active sensing) as shown in Figure 2.14. He aimed at passively ventilating interior spaces using wooden wind catchers, a double façade and movable shutters. Arup Engineering Company performed the required calculations for the wind concept, and glass shutters in the partitioning walls can adapt the building to different wind conditions. When there is a light breeze, the shutters open up to improve ventilation, and if wind speed increases they gradually close.

An example of sensing and reacting on a material scale (passive sensing) is a project[4] by Michael Murauer in a design program at the Vienna University of Technology (Figure 2.15). It was an experimental design project of a passive smart fabric inspired by stoma, which are openings in plant leaves for gas exchange and ventilation according to humidity. Two layers

[4] "Smart fabric inspired by stoma", project by Michael Murauer for the design program "Bionik - natürliche Konstruktionen" taught by Petra Gruber at the Vienna University of Technology in 2005.

of fabric are overlapped in a manner so that the pores would not lie on top of each other. Between these two layers a polymer is placed which changes its volume with changing humidity. When the volume of this polymer increases the distance between the two layers increases as well, allowing for better air flow and ventilation. Another example on the material scale is dimming glass panels that change their state from clear to cloudy at a threshold temperature.

Current technological advances produce the so called 'smart materials' that have responsive abilities and adaptive behaviour. They usually react due to changes in electric voltage. Some have different stimuli, for example shape-change materials whose shape deform with low temperatures and then transforms back to its original form at higher temperature. Piezoelectric materials have the ability to transform mechanical energy into electric energy. Currently these kinds of materials are not common in architecture but they are expected to be used more frequently in the future.

Challenges to reactive adaptation

Reactive adaptation faces a number of obstacles at different phases of a project; the design phase, maintenance phase, and post-occupancy phase. During the preliminary design phase, clients have difficulty accepting such reactive architecture that is usually associated with high risk taking. It is concerned with new technologies that have possible chances of long payback times due to higher investment, operation/failure costs. If architects expect clients to take such chances then they must be supported with well-informed design decisions. This increases the demand and need for tools that could accurately predict the performance of the building (Loonen, et al., 2013).

One of the main difficulties facing a reactive adaptation is maintenance and durability, especially with technologies that are dynamic. Dynamic solutions often come with mechanical and operational difficulties. A famous example is Jean Nouvel's Institute du Monde Arab in Paris, where the building's south façade mimics the behaviour of the eyes in response to light. The façade panels are programmed to open or close according to sunlight intensity, aiming to improve interior comfort and light conditions. Unfortunately these panels are currently not functioning due to mechanical and maintenance problems (Mazzoleni & Price, 2013).

End users also could present challenges since the inability to override system decisions is one of the most common complaints (Loonen, et al., 2013). There should be some degree of flexibility and freedom to allow for personal preferences.

2.4.3 The building skin

The building skin is considered one of the most important elements of the building. This is due to the fact that it is the interface between building occupants and the external environment. It visually connects them to the exterior and also protects from environmental elements such as wind, sun, rain, noise, etc. The building skin is also important as it is what we 'see' of the building from the outside, defining streets and urban context. It is one of the major factors affecting the amount of energy needed for cooling and ventilation, and that is why it was selected for this study. The roof and façade of a building are exposed to the same environmental conditions, and serve the same functions (although with different degrees of

intensity) and therefore the term 'skin' would be used in a global manner to include both façade and roof.

Adaptive skins- Terminology

The idea of building facades/skins responding to changing environments has taken various terms used by researchers and practitioners. These terms may include: kinetic, dynamic, active, interactive, smart, intelligent, and responsive. They all have similarities and variations, and are addressed (often separately) in much literature[5]. The following definition was found to be most explanatory:

> *'A climate adaptive building shell (CABS) has the ability to repeatedly and reversibly change some of its functions, features or behaviour over time in response to changing performance requirements and variable boundary conditions, and does this with the aim of improving overall building performance'* (Loonen, et al., 2013, p.485).

Loonen et al. (2013) interpret the building shell as all the built elements that separate the interior of a building from the exterior environment. This interpretation gives it much wider meaning than that of the building *façade*. However, the author would like to add the aforementioned passive strategies (section 2.3.2) to this definition as part of being adaptive. It is important to simultaneously consider -when possible- both passive and actives adaptation strategies to combine their benefits.

Functions of the building skin

Similar to skin in animals and clothing in human beings, the building skin serves numerous simultaneous functions achieved by appropriate design decisions and construction means. According to Lang (2001), an investigation into building skins must address the following issues that are critical to their design and performance:

- Function
- Construction
- Form
- Ecology

In terms of thermal comfort, 'function' obviously plays the most important role. However, these four issues are interdependent and affect each other, therefore it is important to consider all of them and give them equal weight during the design process. Construction issues include studies of materials used, façade components, how they are assembled and fabricated for example. Addressing the form of the façade regarding its morphology would inform the required constructions means to build it, in addition to the resulting ecological performance which addresses questions like: what is the energy consumption of the building skin? How does it reduce cooling/heating loads? (Lang, 2001).

As mentioned earlier, the building skin has many functions such as lighting, ventilation, protection from rain, sun, wind, glare, noise, excess humidity and fire. It is also important in insulating against heat/cold, in visual continuity, safety, and -if possible- in energy gain.

[5] Examples of such literature include books like *Intelligent Skins* by (Wigginton & Harris , 2002) and *Designing Kinetics for Architectural Facades* (Moloney, 2011) among many others.

Since the scope of this research is concerned specifically with thermoregulation characteristics of the building, only a number of these functions will be chosen for the evaluation of the proposed building skin. They are:

- Thermal performance
- Daylight performance

These factors together may be considered the most important ones that affect thermoregulation and consequently the required cooling loads and energy consumption of the building during its lifetime. These functions have conflicting design requirements, since less cooling loads means smaller openings which in turn means less daylighting. So the use of parametric design tools and evolutionary algorithms could prove useful in this challenge (by the use of fitness functions that help find best combined solution for all criteria).

2.5 Biomimicry and Computation

Within the last thirty years, new theories in architecture and design have developed that don't just try to understand and mimic natural forms, but aim at deeper understanding of biological processes from which designers could learn. One of the reasons encouraging this development is the escalating environmental crisis and the rise of sustainable design where new ideas and innovation are needed. It is thought that to design architecture in harmony with nature and its context, we need to take lessons from nature itself.

Another reason was the increasing availability of computers in the practice of designers and engineers. When computers have spread in the 1980s along with graphics and modelling software, this enabled designers to explore new possibilities of complex, fluid, curvilinear shapes. Simulation software for the behaviour of designed artefacts in terms of their structural and environmental behaviour for example, allowed designers to introduce new methods for optimising performance. Genetic and evolutionary algorithms were developed, whose mode of operation closely resembles natural evolution. Design researchers have been developing these algorithms since the 1990s, which could 'evolve' the design of buildings and other artefacts (Steadman, 2008).

'Computer Aided Design' vs. 'Computational Design'

Development in available software enabled the shift from *computer aided design* processes (CAD) to *computational* design processes. In CAD, forms are created by modelling geometric entities (such point, lines, solids, surfaces, etc.) which are defined only by their coordinates. In this case, the software is only a digital alternative to the previously used manual tools such as pencil and T-square, making it easier to edit, erase, copy, and so on. Even after the introduction of NURBS geometries which enabled the creation of more complex forms, these forms are still the result of a set of drawing commands where the computer plays a passive role. In computational design however, form is created by a set rules and relationships. Achim Menges defines computation as *'the processing of information and interactions between elements which constitute a specific environment; it provides a framework for negotiating and influencing the interrelation of datasets of information, with the capacity to generate complex order, form, and structure.'* (Menges & Ahlquist, cited in Peters, 2013, p.10). So in this case the role of the computer is extended to be a more active player in the design process.

Biologically-inspired computation

Since the emergence of computational theories and methods in the past decades, extracted principles from natural systems have been influential in the design and computation domain. These biologically inspired means have influenced architecture, by introducing computational form-generation techniques.

The main challenges to finding new solutions relate to the identification of suitable biological models and the extraction of the main principles from them. Hypothetically, this identification can be approached from two different standpoints: mimicking the characteristics of a specific natural phenomenon versus learning from general principles of natural organisms. The first method offers novel ideas for designers by revealing hidden aspects of physical, chemical and mechanical properties that are not common in our surroundings. In this approach the biological models are best investigated by biology experts. A close collaboration and mutual understanding among these biologists and designers is the essential key for the initiation and progress of any bio-inspired projects.

Conversely, the second approach (learning from general principles in natural organisms) proposes new solutions for the development of methods, processes and systems in engineering and computation. One of the best examples in this category is evolutionary computing and genetic algorithms initiated by John Holland in the 1970s, which was inspired by natural evolution (Steadman, 2008).

Nature's systems and organisms are a result of ever-continuing evolutionary processes. Architecture could be seen as a sort of artificial life and hence subject to the ideas of genetic coding, replication, survival of the fittest etc. (Frazer, 1995). Design could be described as a human activity where the evolutionary mechanisms of nature are able to aid in creating a diversity of new forms. These forms are able to survive the environment within which they are set, and then serve as a basis for further evolution and improved solutions. Through the use of genetic algorithms (GAs), this evolutionary design process aids in resolving multiple (and often conflicting) criteria by producing outputs that learn from experience of previous generations (Rosenman, 1996). This process usually aids in creativity and produces unexpected results.

An evolutionary algorithm (EA) is represented by rules for a computer program. These rules start with a certain *population* representing possible solutions to a problem. Members of the population are *parents* to a new generation of *offspring*. They pass on their *genes* with some random variations mimicking the concept of mutation in natural evolution. Some EAs allow children to inherit genetic material from their parents as in sexual reproduction. The children undergo an evaluation process to measure their fitness based on criteria that designers specify. Children that pass this evaluation process are considered to be fit and act as parents to a new generation. While other that do not meet the specified criteria simply die off. This process keeps repeating until the designer is satisfied with the produced results or until breeding produces very small improvements (Steadman, 2008).

Pioneers in this field include John Frazer who is considered one of the ground breakers of computation form generation as he proposed the idea of evolutionary architecture in 1969 in the Architectural Association in London and was further developed in the 1990s. Michael Rosenman and John Gero have worked on methods for evolutionary architecture in the 1990s at the University of Sydney. They specifically concentrated on generating complex genes for generating architectural floor plans. In 2001 computer scientists Martin Hemberg and Una-May O'Reilly in collaboration with designer Peter Testa at MIT have developed a computational design tool named GENR8 to apply evolutionary computing in the domain of architecture (Sherif, 2010).

Some researchers and designers are seeking some analogies of the design process with growth. Some experiments with computation include software that 'grow' designed artefacts, and then 'evolve' them. One of the techniques used in this field of study is the Lindenmayer Grammar. In the late 1960's, the biologist Aristid Lindenmayer proposed a string-rewriting algorithm which can model simplified plants and their growth processes. This theory is now known as L-Systems. The applications of this system is not restricted to growing plant-like forms, but could be also used within the field of architecture. Architects such as Dennis Dollens uses software based on these L-systems to design architectural elements with complex curved morphologies analogous to plants and animals (Dollens, 2009).

Computational theories could be inspired from other biological principles found in nature. These principles include fractals, cellular automata, swarm systems and artificial life. More information regarding algorithms inspired by nature is available in many references such as Steadman (2011) and Zang et al. (2010).

Programming Languages

As the use of computers spread among architectural practice, a growing exchange of knowledge among the disciplines of programming and architecture took place. Architects are becoming more interested in personalising available tools by re-writing their code to build more customised solutions for their design problems. A number of Text-Programming Languages (TPLs) such as RhinoScript and Processing and Visual Programming Languages (VPLs) such as Grasshopper are becoming increasingly used. Each of these two types has its advantages and drawbacks depending on the task at hand. For example, one of the most important differences between them is that TPLs are only one-dimensional while VPLs are two-dimensional or more, which makes their use much more intuitive and user-friendly and therefore it requires less background knowledge than TPLs. On the other hand, VPLs might be difficult to understand and keep track of a script if it becomes too big as they become quite 'messy' with lots of connecting wires between different components. Users must continuously organise their script to avoid losing track of it. Another drawback of VPLs is the absence of advanced abstraction means which forces users sometimes to rely a lot on copying and pasting leading to redundancy in their scripts (Leitão, et al., 2012).

The VPL Grasshopper for Rhino 3D modelling was chosen for this research due to a number of reasons. The highly interactive and visual interface is among the most important. The immediate visual feedback makes it easy to detect defects and adjust accordingly. Input parameters could be easily adjusted at any point, and the resulting form is immediately

altered. Another important reason is the wide variety of free plugins for Grasshopper, which are usually programmed by architects and tackle specific problems encountered in design practice. These plugins could work together and freely exchanging data with one another. This is due to the software's capabilities created by David Rutten, which formalise the exchange of data around simple collections of basic geometric primitives. This 'geometric content- based' data exchange is in contrast to BIM's 'assigned attribute-based' data structures, and is a simplification that enables plug-ins to easily work together (Davis & Peters, 2013).

Geco for example is a plug-in that explores the possibility of creating real-time links between Grasshopper and Autodesk's Ecotect analysis sustainable design software that evaluates environmental performance in early design stages. Ecotect in general requires designers to export or restructure 3d models to analyse them. Geco however allows the exportation of models to Ecotect and imports the simulation results back in Grasshopper immediately without the need of reworking the model over and over again. This live link improves workflow, maintains the original file format and provides much faster feedback.

Other examples include Galapagos and Octopus plug-ins that apply evolutionary algorithms in problem solving, Kangaroo is a Live Physics engine for interactive simulation, and Weaver Bird which performs surface subdivisions and tessellations. There are numerous other plug-ins available and are being shared on the internet, each tackles a design problem or presents new opportunities. This creates a new rapidly growing design environment based on sharing.

This research intends to apply biological inspiration by mimicking certain aspects of organisms that help them in thermoregulation. The solutions would then be modelled using parametric software as mentioned earlier. The research also intends to utilise evolutionary algorithms for their benefits in form generation and selection between numerous possible solutions.

2.6 Current Research and Examples

Examples of adaptive biomimetic buildings skins could be found in both academia and, less commonly, in professional practice. They originate in contexts where creativity and sustainability are prioritised, and costs are relaxed to some extent (Loonen, et al., 2013).

The study of Biomimetics has spread in universities all over the world. For example, the Institute of Computational Design (ICD) at Stuttgart University as well as the Emergent Technologies and Design (EmTech) studio at the AA in London have shown particular interest in biomimetic design within the last few years. Other examples include centres for Biomimetics in Reading University in the UK, which was set up by George Jeronomidis and Julian

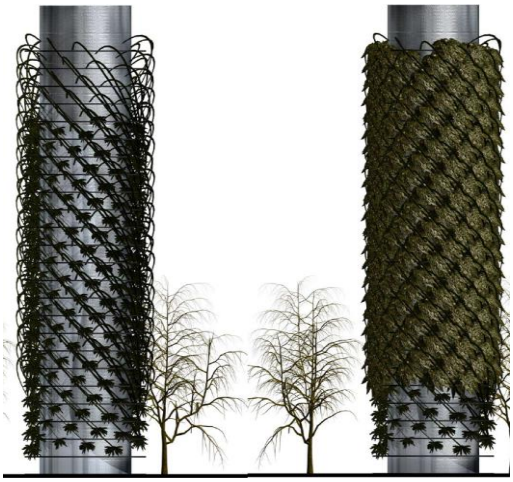

Figure 2.16: BioTower by Dennis Dollens. Digitally grown tree, branches, leaves, and flowers programmed as an experiment dealing with environmentally active functions in order to create biomechanical, living, architecture (Dollens, 2009).

Vincent. Research in this centre has concentrated on the properties of organic materials such as bone, collagen, chitin (from which the carapaces of insects are made), cellulose, and the silk of spiders' webs. Other examples are the Biologically Inspired Systems Lab in Sweden, the MIT Media Lab, the Austrian Institute of Technology, the Centre for Biologically Inspired Designs at Georgia Tech, Atlanta, and the Centre for Biologically Inspired Materials and Material Systems at Duke University, North Carolina. A new journal of *Bioinspiration and Biomimetics* has started publication in 2007, and conference on *Design and Nature* at the Wessex Institute of Technology also started in 2007.

Frei Otto is known for pioneering construction innovations in many materials and building forms, especially light-weight structures. One of his interests is the study of natural systems regarding their geometry, mathematics and structural behaviour. He believes fibres are the secret of understanding biological structures, emphasising on their remarkable resistance to tearing. They are composed of simple yet diverse geometric material whose study could be very useful for the design and construction of buildings. He states that architects should understand living nature, not just copy it (Hensel, et al., 2004). Another example is the Genr8 design tool developed by Una-May O'Reilly, Martin Hemberg and Achim Menges of the Emergent Design Group at MIT and the Emergent Design and Technologies Group at the Architectural Association in London. This tool is based on Evolutionary Computation and Artificial Life, and it uses an organic growth algorithm mimicking the growth of plants, and their reaction to environmental stimuli such as sunlight and gravity (Hemberg, et al., 2008).

Within the field of practice also exist some examples like the famous Beijing National Stadium (The Bird's Nest), The Beijing National Aquatics Centre (The Water Cube). Some leading architectural studios show interest in biomimicry such HOK Architects (who have been closely working with the Biomimicry Guild) and Grimshaw Architects who designed the Eden Project in the UK (Figure 2.17). Biomimetic design in practice could be also seen in some of the works of Michael Pawlyn and Atelier One, Soma-Architecture among others. The following section includes some detailed examples of biomimetic design both in academia and in practice.

Figure 2.17: Eden Project by Grimshaw Architects. Source: http://www.edenproject.com/.

2.6.1 Project HygroSkin: ArchiLab Exhibition, 2013

Research at the Institute of Computational Design[6] (ICD) at Stuttgart University has shown great interest in biomimetic design, and this pavilion is an example. The research was based on the study and exploration of a surface that could passively respond to humidity changes, based on inspiration from Conifer cones and is a result of over six years of design research experience in this particular topic (Menges & Reichert, 2012).

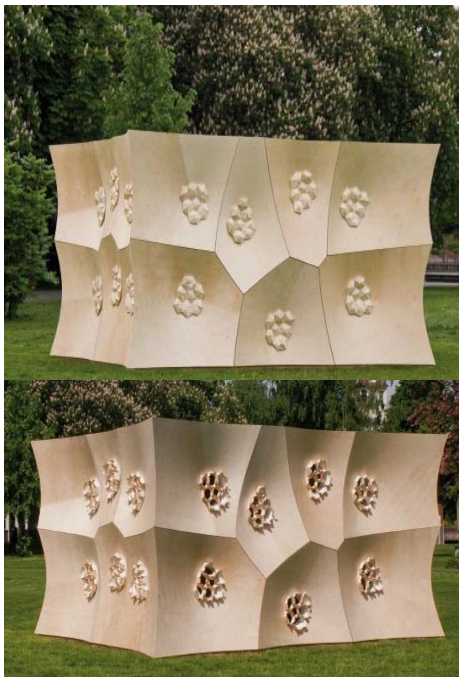

Figure 2.19: HygroSkin Pavilion in a closed state (top) and opened state (bottom) (Menges, et al., 2013).

Biological Inspiration

The initially moist Conifer cones contain seeds necessary for reproduction which are released when the cones are dry and therefore opened. What is really interesting is that even if the cones are not anymore attached to the tree, they continue to open and close as humidity levels change. This is due to the cone's material itself which is capable of interacting with the environment even if its tissues are no longer living.

The ability of the cones to continuously open and close (Figure 2.18) is due to the structure of the scales' material itself. The scales consist of two layers; an outer one made of parallel, long densely packed thick-walled cells that react to changing humidity by expanding or contracting, and an inner layer that almost doesn't change. Therefore the research focused on mimicking this material structure by developing bi-layered materials that could react in a similar way.

Figure 2.18: : Project by Iva Kremsa, Kenzo Nakakoji and Etien Santiago, Performative Wood Studio (Achim Menges), Harvard University Graduate School of Design (GSD), Cambridge, Massachusetts, 2009. Left: Conifer cones in open and closed states. Right: a responsive system component was developed that can adapt its shape by being based on a four-, five-, six- or seven-sided polygon (Menges & Reichert, 2012).

Application

The envelope of the HygroSkin Pavilion adapts and responds to changing weathers. When the humidity is relatively low on sunny days, the envelope is fully opened, and when it rains for example or the humidity increases, a response is triggered and the skin is closed automatically as seen in Figure 2.19. The anisotropy[7] and hygroscopicity[8] of wood is similar to that of cones and therefore synthetic wood composites were studied and developed. The dimensional change of wood is directly proportional to changes in moisture content. Given a specific piece of wood, a certain increase or decrease in moisture content will always cause

[6] For more information: http://icd.uni-stuttgart.de/?p=9869

[7] Anisotropy denotes the directional dependence of a material's characteristics (Menges & Reichert, 2012).

[8] Hygroscopicity refers to a substance's ability to take in moisture from the atmosphere when dry and yield moisture to the atmosphere when wet (Menges & Reichert, 2012).

the same swelling or shrinking. When different synthetic veneer composites are combined, they could be physically programmed to differently respond to humidity changes.

The skin of the pavilion (which simultaneasly acts as a load-bearing structure and a weather-sensitive skin) was computationally designed and derived from the elastic behaviour of thin sheets of plywood. It is composed of 28 geometrically different panels, with 1100 humidity responsive openings which respond to relative humidity changes ranging from 30% to 90%. These openings could transform from an opened to a closed state within a few minutes given a rapid change in humidity (Menges, et al., 2013).

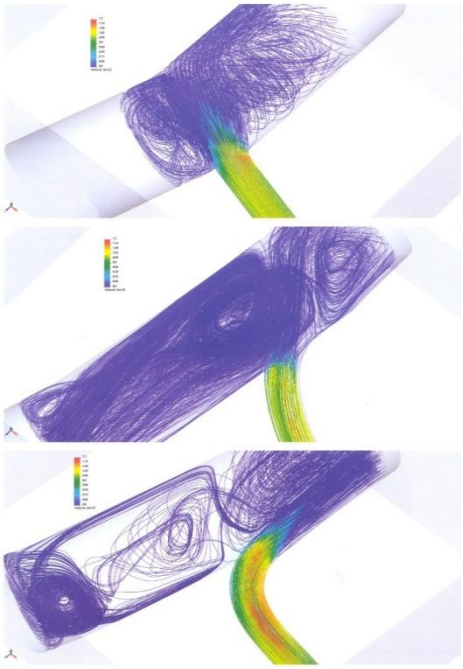

Figure 2.20: Computational Fluid Dynamics tests of different branching connections. Masters Dissertation of Yukio Minobe, 2008 (Hensel, et al., 2010).

2.6.2 Branching Systems for Ventilation

The Emergent Technologies and Design Programme[9] (EmTech) at the Architectural Association School of Architecture (AA) hosts many research projects and theses related to biomimetic design. An investigation on the design of branching systems for ventilation needs was done in the Masters dissertation of Yukio Minobe in 2009 illustrated in the opposite figures (Figure 2.20Figure 2.21Figure 2.22). The aim of this research was to computationally develop a branching ventilation system for a domed-shape envelope (Hensel, et al., 2010).

Figure 2.21: Computational Fluid Dynamics of airflow in branching ventilation system. Masters Dissertation of Yukio Minobe, 2008 (Hensel, et al., 2010).

Biological Inspiration

The research was based on a detailed analysis of termite mounds, especially their behaviour in reducing thermal impact by ventilation. This involved studying:

- Upward airflows from the nest through the buoyancy effect.
- The lateral air distribution from the mound chimney via lateral connections towards surface conduits.
- Airflow towards the negative pressure zone of the mound due to pressure differentials.
- Suction from the negative pressure side of the mound.

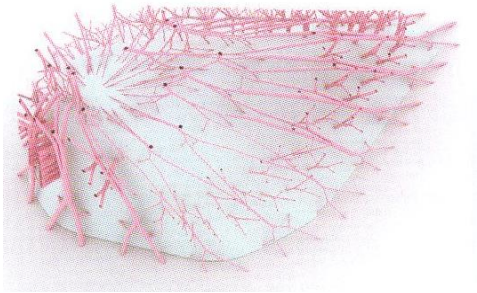

Figure 2.22: 3D model of branching morphology. Masters Dissertation of Yukio Minobe, 2008. (Hensel, et al., 2010)

[9] For more information: http://emtech.aaschool.ac.uk/category/biomimetics/

Application

The research first examined three different types of branching connections (Figure 2.20). They were analysed in terms of their airflow patterns using computer fluid dynamics to determine which had the least turbulent flow.

This was followed by the development of two algorithms that could form branching ventilation networks; a centroid branching algorithm, and a sphere-packing algorithm. They apply different logic in the branching patterns they generate, and were therefore analysed with respect of their branching network, angles between branches and the resultant airflow pattern of each.

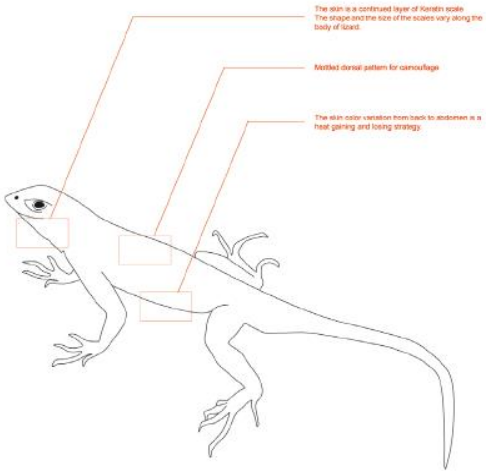

Figure 2.23: Side-blotched Lizard (Uta stansburiana) (Mazzoleni & Price, 2013)

2.6.3 Lizard-inspired skin for hot climates

Ilaria Mazzoleni in her book "Architecture Follows Nature" presents the investigation of her on-going research and the academic collaboration with her students in the Southern California Institute of Architecture during the spring of 2010. They worked with biologists and focused on animal skins as inspiration sources for building envelopes (Mazzoleni & Price, 2013).

Figure 2.24: Rendered model of proposed residence inspired by the Side-blotched Lizard (Mazzoleni & Price, 2013)

Biological Inspiration

One of the projects was inspired by the skin of the Side-blotched Lizard (Uta stansburiana) shown in Figure 2.23, by students Yuan Yuan & Juan San Pedro. The lizard's skin is composed of scales forming a continuous epidermal sheet. The scales overlap and are connected by hinges of thinner keratin material. They vary in both size and colour, where they are relatively small in body parts that experience more movement and flexibility, compared to other larger sizes in ares that experience little movement. Colour patterns are dark on its back, to maximise heat absorbtion from the sun, and are of lighter colours on its abdomen facing the ground. The behaivour of the lizard also contributes to its thermoregulation, as it adjusts its body perpendicular to the sun's rays during the day, and curls up during the night.

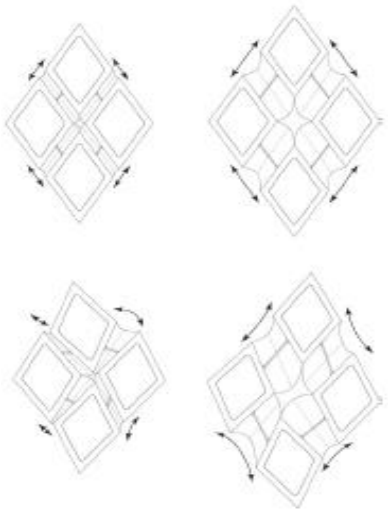

Figure 2.25: Skin panels movement diagram (Mazzoleni & Price, 2013).

Application

The students propose a design for a residence in California, shown in Figure 2.24, which attempted to achieve thermal comfort for its residents. The walls of the building were composed of photovoltaic panels with hydraulic pistons and flexible membranes between the panels. These membranes enabled the expansion and rotation of the panels, increasing the surface area of the whole building and adjusting angles with respect to the sun. The panels contained two layers of phase change material (PCM) and a flexible air passage sandwiched between them. This permitted the flow of air within the thermal mass, to absorb heat or to cool down depending on the time of day. The panels vary in size, as smaller ones were used for areas that move.

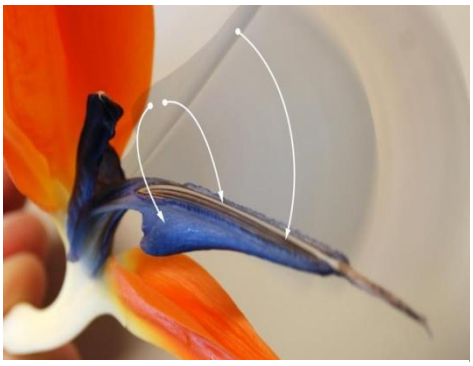

Figure 2.26: Elastic deformation of the kinetic system in the *Strelitzia reginae* flower. When mechanical force is applied (as indicated by the arrows), the sheath-like perch opens (Knippers & Speck, 2012).

Figure 2.27: Full scale prototype of the Flectofin shading system. (Knippers, et al., 2012).

2.6.4 Flectofin Project

Flectofin is a research project at the ITKE (Institute of Building Structures and Structural Design) at Stuttgart University. It is a hinge-less louver system that could move its fin by 90 degrees by inducing bending stresses or temperature change to it. The research is based on the investigation of elastic plant movement and folding mechanisms as an inspiration for kinetic architecture as seen in Figure 2.26 (Knippers & Speck, 2012).

Biological Inspiration

In nature, plants have evolved a variety of moving mechanisms that are based on elasticity without the presence of hinges as seen in the open/closing of many types of plant leaves and flowers. This is in contrast to current building practice which heavily depends on a combination of multiple elements using hinges and rolls, which increases its need of continuous maintenance and risk of failure by time. This project was inspired by the pollination mechanism in the Strelitzia reginae flower (commonly known as the Bird-of-Paradise). The weight of pollinating birds that land on the flower's petals causes temporary deformation and the plant's pollen is released. When the bird is no longer present the petals move back to their original position closing the pollen sack.

Application

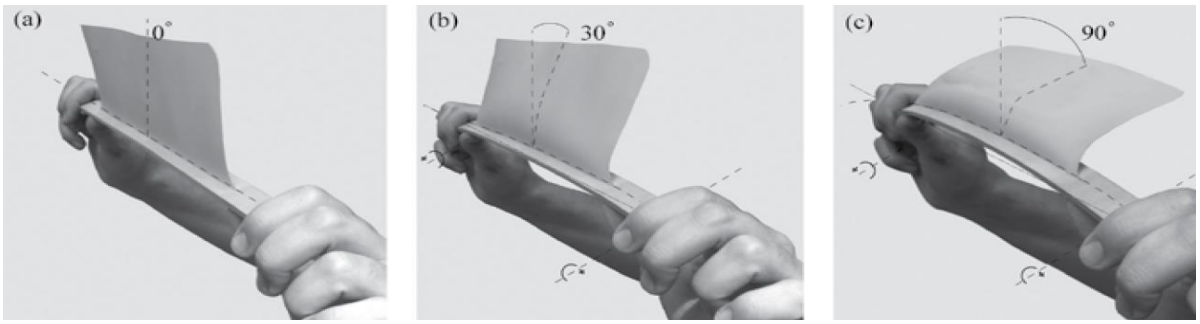

Figure 2.28: Physical model of the Strelitzia reginae flower principle of deformation. Bending the backbone causes the attached lamina to deflect 90 degrees sideways (Knippers, et al., 2012).

The team worked on an abstraction of the flower's elastic motion into a simple mechanism which consisted of a shell element with relatively thin thickness attached to a beam (Figure 2.28). This shell element has an equilibrium path that is non-symmetrical and is triggered by torsional buckling induced by uniaxial bending of the beam to which it is attached. This phenomenon of torsional buckling is known to engineers as is usually regarded as a failure. However, this same concept is effectively used by nature to achieve required movements. In Figure 2.28 a prototype of a façade shading system was built of fiberglass-reinforced plastics. The material offers high elastic deformations due to its tensile strength and low bending stiffness. The fins allow for opening angles that range from -90° to +90° offering views as well as complete closing of the façade whenever desired.

This prototype has been applied to the façade design of an actual building (Figure 2.29) which is the perminant pavilion for the 2012 Expo in South Korea by Soma-Architecture. The façade is composed of kinetic lamellas that control the light conditions during the day, and then after sunset LEDs are used to intesify the visual effect of their movements. This kinetic media façade represents a rare example of biomimetic design on a constructed building scale in which form, material, movement and light are seamlessly interrelated (Soma, 2012).

Figure 2.29: Theme Pavilion in South Korea by Soma-Architecture. Left: the main entrance façade to which the biomimetic inspiration was applied in the form of kinetic lamellas that control daylight. Right: close-up of the lamellas in their open position (Soma, 2012).

2.7 Research Approach and Focus

Biomimicry in architecture throughout history has been mainly applied to building form. This research aims at applying biomimicry at a higher level, one that considers not only the form but also the behaviour and functions of natural organisms and their relationships with surrounding context. The biological principle of adaptation is at the centre of this study where adaptation means of living organisms will be the main field of investigation. All kinds of biological adaptation are open to investigation, whether they are morphological or behavioural. Additonally, the principle of evolution would play an important role in the development of the design proposal, since evolutionary algorithms will be part of the computational apporach used as will be discussed later in the thesis.

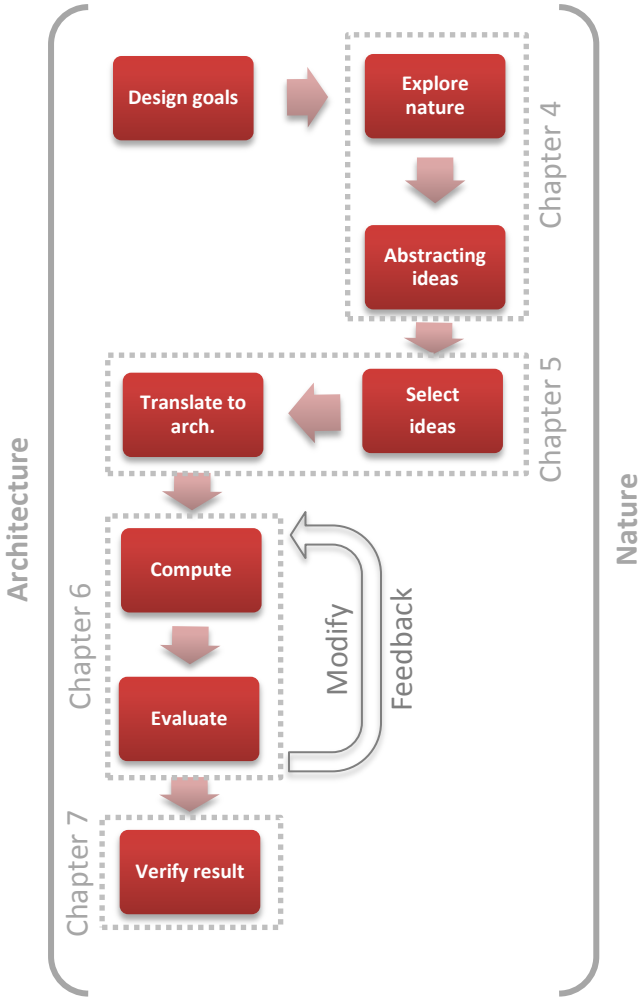

Figure 2.30: General stages of the biomimetic-computational design approach and the corresponding chapters in which they are addressed. Source: author.

Also the research is not restricted to a certain scale, whether it is a cellular scale or an ecosystem scale, they all present possible ideas that could be applied in building skins as explained in section 2.2.4. In terms of adaptation in architecture, both passive and reactive techniques could be considered. However this research focuses mainly on passive strategies to avoid problems related cost and maintenance often associated with dynamic facades.

The biomimetic design approach followed here is a problem-based approach. Figure 2.30 demonstrates this design approach and the chapters corresponding to the application of each phase. It is based on the problem-based approach described in section 2.2.6 but adjusted by the author to be more suitable for an architectural context, and applied with computational tools. This methodology is expected to be better understood and refined along the way during its actual application on a real design challenge.

The specific design challenge or goal is defined which is the requirement of decreasing cooling loads. It is then abstracted as much as possible to facilitate the search for parallels in nature. A list of possible inspirations will be set for this design challenge, followed by a brainstorming phase, where each inspiration would be abstracted, analysed and its main concept determined to serve as an architectural solution. One or more ideas would be

chosen as solutions for the addressed design challenge. The choice will be based mainly on two things; the possibility of being parametrically modelled, and its suitability to be combined with solutions of other challenges.

Thermoregulation characteristics of the building skin is the specific focus of this research, with an aim to propose solutions that would decrease cooling loads in hot climates and increase the efficiency of buildings. So the research sets out by asking questions like: how does nature insulate in hot climates? Why do desert plants look like this? How do animals regulate their body heat? How do skins of animals function? How does air exchange/movement occur?

Proposed solutions will be parametrically designed using Grasshopper for Rhino 3D modelling software. The choice of this visual programming language was due to a number of reasons. The interactive environment and immediate visual feedback are among the most important. Another reason is the availability of a wide range of plugins that easily work together and are capable of performing various environmental simulations. This is particularly important as it will be useful in the testing and evaluation phase of the research, since it provides real-time environmental simulations facilitating immediate feedback. Choosing parametric software in general would facilitate managing different and often conflicting design requirements.

This design method is intended for the preliminary conceptual phase of design in general. The early stage is usually the most important where critical decisions are taken that affect the overall performance of the building in the end, and it is usually the most creative as well.

2.8 Summary

Nature provides us with role models that can be pursued currently and in the future. It is still difficult to see buildings with evident qualities of living organisms. Reasons include technical problems, and the issue of having power and control over the building. Applying 'life's principles' in temporary small-scale structures is easier and more commonly found such as in examples shown in section 2.6. Such examples gradually encourage and push ahead the building industry. One must note that superimposing biological principles onto architecture is not the same as claiming that architecture is alive.

The discussion of the main biological principles in section 2.3 improves the understanding of the connection between the two fields of architecture and biology. Taking this into consideration, inevitably innovative architectural practice will move towards more sustainability and ecological compatibility. New findings and discoveries in life sciences research should be more easily accessed especially to non-biologists to support the spread of information across many disciplines. Architects working alongside biologists, material scientists, etc. is very important for the transfer of knowledge and exchange of information between different fields of expertise. A focus has been made on the principle of adaptation in both nature and architecture. It has been decided in this research to seek passive strategies for adaptation.

This chapter represents a background on which the rest of this thesis is based. Biomimicry was explained in terms of its origins, methods, levels, relationship with architecture and current examples. It ended with the design methodology that will be applied in Part 2 and Part 3 of this thesis. The main aim of the forthcoming chapters is applying and evaluating this methodology in the end to see if it helps us as architects in finding innovative solutions for our design problems. Using this methodology, a new building skin will be proposed for an existing building with the main objective of reducing its energy consumption for cooling. Parametric design software will be used as tools during the application of this methodology. The research also intends to utilise evolutionary algorithms for their benefits in form generation and selection between numerous possible solutions.

By the end of the thesis, the proposed methodology will be presented once more in its final refined form after learning from its actual application. It will also be criticised based on the following criteria:

- The degree of success of the output of this methodology (which is the design proposal itself; to what extent did it achieve the required objectives)
- The capabilities and limitations of the software tools currently available
- Challenges addressed during the application of this methodology

Before the application of this methodology begins, the following chapter demonstrates the basics of Double-Skin Façade (DSF) design and simulation.

Chapter 3

Design and simulation of Double Skin Facades (DSF) in hot climates

3.1 Introduction

The decision of considering Double Skin Facades (DSFs) as the building element to which biomimetic inspirations would be applied came at a later stage in the development of this thesis. It was not until the biomimetic design process had already been applied (specifically in Chapter Five) that it was decided that DSFs are a potential application due to many advantages as will be discussed. Hence, a basic understanding of them was required in order to proceed with the design process based on informed design considerations from available literature. However, it was decided to place this current chapter within the contents of Part One of this thesis for the sake of not interrupting the explanation of the design proposal in Part Two, and also because it more appropriately aligns with the nature of Part One as a literature reviewing section.

This chapter demonstrates a *general* overview of Double Skin Facades (DSFs) with particular interest in their application in hot climatic areas in addition to the simulation methods commonly used for predicting their daylight, thermal and airflow performances. Although literature concerning DSFs focuses on their application in relatively cold climates, this is not the scope of this thesis. To appropriately outline the most important guidelines needed to be taken into consideration during the design process, a number of case studies of DSFs in hot climates are demonstrated.

It is not an objective of this chapter to make an extensive review of DSFs, but rather to get a basic understanding of the important design considerations and simulation techniques used to evaluate their performance. This will help in the development of the Biomimetic design proposal intended in the chapters to follow.

3.2 Overview of DSFs

3.2.1 Definition

Poizaris (2006) provided an extensive review of DSFs and presented many definitions by different authors such as The Source book of the Belgian Building Research Institute (BBRI), (2002), Harrison and Boake, (2003), Arons, (2001) and Saelens, (2002). What most of these definitions have in common can be explained as follows:

A double skin façade is a system comprised of two façade layers; an external one which is usually fully glazed, and an internal one which can be partially or fully glazed. The resulting space between them is usually called the ‘cavity’ and could range from 20 cm to a few meters in depth. The cavity acts as a buffering zone between the building and the exterior weather and site conditions, and could be naturally ventilated, mechanically ventilated or not ventilated at all. The DSF can cover a part or the whole of a building.

It is an architectural trend that was developed mainly in Europe driven by aesthetic desires, better acoustics, better indoor environments and reduction in energy use during the operation of the building. These motivations caused DSFs to be quite popular despite being more expensive (in both construction and maintenance costs) than conventional single facades.

3.2.2 Categorisation

DSFs can be categorised based on ventilation type, manner of operation, and most commonly based on their structure as seen in Figure 3.1, or geometrical configuration as follows (Oesterle et al., cited in Poizaris, 2006 and in Barbosa and Ip, (2014).

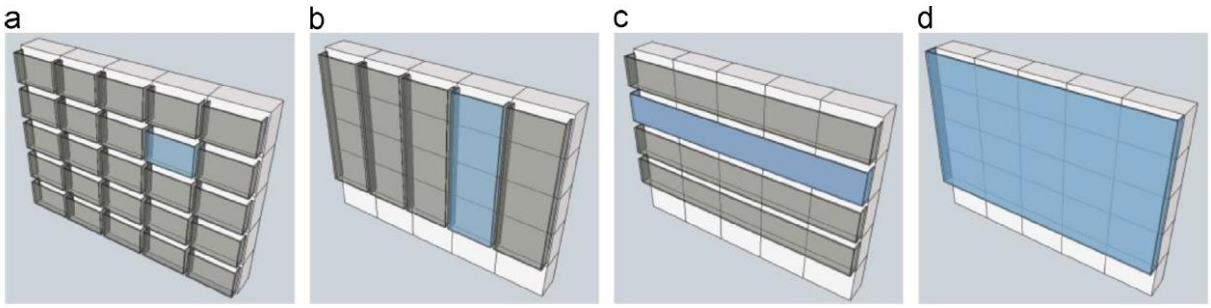

Figure 3.1: DSF categorisation based on its structure: (a) Box Window,(b) Shaft-Box, (c) Corridor and (d) Multi-Storey double skin façade (Barbosa & Ip, 2014).

- Box window type: The façade is divided vertically and horizontally by partitions, creating small independent boxes.
- Shaft box type: It is a special case of the Box window type, in which columns of boxes are vertically connected together without horizontal separations to create vertical continuous shafts supporting the stack effect. Fewer openings are needed in this type with respect to the previous one.
- Corridor façade: Another special case of the Box window type in which rows of boxes are connected horizontally without vertical separations. Openings in the external façade layer are usually located at each floor and ceiling level.
- Multi storey Double Skin Façade: In this case, the space between the internal and external façade layers is continuous without any vertical or horizontal partitioning. The cavity is usually ventilated by openings located at the bottom and the top of the building height. The multi storey type has the greatest temperature gradient and hence the strongest stack effect which means more captured warm air is being released from the cavity top and thus the ventilation rate of the cavity increases.

3.2.3 Design considerations regarding heat transfer and airflow

As mentioned earlier, DSFs were developed mainly in Europe and therefore most design guidelines were based on studies done in relatively cold climates. While the design and construction of DSFs is already quite abundant in literature, the context of hot climates is not often considered in which they would behave in a different manner. Therefore the application of DSFs in hot climates is still under investigation (Poizaris, 2006; Barbosa and Ip, 2014; Shameri et al., 2011). It is somewhat a controversial issue since some claim that DSFs may cause an increase in cooling loads in the summer if not well designed (Papadaki, et al., 2014; Poirazis, 2006; Gratia & De Herde, 2007).

Stec and van Paassen's study in 2003 (cited in Poizaris, 2006) point out the main design parameters that affect the temperature and airflow inside the cavity:

- Size of upper and lower air openings

- Depth of the cavity
- Position of the shading device in the cavity and its material (especially the absorption coefficient)
- Solar transmission, U-value and absorption coefficient of inner and outer glazing.

In addition, a paper by Barbosa and Ip (2014) identified the main parameters influencing the thermal and energy performance of such facades and both summarised and categorised them to outer façade, inner façade and site parameters. For each parameter they specified guidelines for its potential application in the design double facades even for warmer climatic areas. Since most of the papers reviewed (but not all) were addressing DSFs in cold climates, *therefore these guidelines are to be considered with caution, mainly with the aim of understanding how double facades work.*

Table 3.1 includes some of the design considerations reviewed in Barbosa and Ip (2014) that are seen most relevant to the application of DSFs in hot climates. They concluded that double facades do have great potential in providing thermal comfort even in hotter climates. However, it is unlikely that natural ventilation can be provided all year round, and therefore a mixed-mode system alternating between natural and mechanical ventilation is the probable scenario.

Table 3.1: Summary of most relevant guidelines reviewed in Barbosa and Ip (2014).

Building component	Parameters	Guidelines
Outer façade	Cavity depth	▪ Heat transfer rates decrease with cavity depth due to high ventilation rates. A cavity size between 0.7m and 1.2m can balance between solar gain and heat transmission (Radhi et al., 2013).
	Shading device	▪ Preferably placed in the middle of the cavity to be protected from weather. However in warmer climates they can be a heat absorber in summer, so it is best to put them outside (Gracia and De Herde, 2007). ▪ Vertical shading elements have a lower heat transfer coefficient than horizontal ones (Jiru et al. 2011).
	Outer skin glazing properties	▪ Double glazing is preferred in warmer climates as it reduces heat transfer across the façade (Mingotti et al., 2013).
	Structure	▪ The multi-storey and shaft type structures have a stronger stack effect increasing ventilation rates (Torres et al., 2007).
	Cavity openings	▪ Bigger openings aid in extracting warm air out of the cavity (Torres et al., 2007). ▪ Cavity temperature decrease does not vary in a linear way with opening sizes (Gracia and De Herde, 2007).
Inner facade	Inner skin materials	▪ Using a shading device with a high thermal mass reduces thermal gain (Fallahi et al., 2012).
	Window to wall ratio and openings	▪ Higher WWR improves airflow inside rooms, but they also increase heat gain. A 50% to 70% Window to Wall Ratio (WWR) range is recommended (Chou et al., 2009).
	Cavity height	▪ A solar chimney above the cavity is recommended to be at least two floors high to improve ventilation rates in the upper floors (Ding et al., 2005).
Site	Solar irradiance and orientation	▪ Cavity temperature in a south-facing façade may be up to 20°C higher than ambient temperature on sunny days (in a temperate climate) if no shading device is used (Gracia and De Herde, 2007). ▪ Façade orientation has a major influence on cooling loads, and the south facing DSFs (with 45° variations) are the most efficient ones (Haase et al., 2009). ▪ East and west orientations might increase cooling loads (Gracia and De Herde, 2007; Hamza, 2008).
	Wind	▪ A 10°C difference can be observed between null wind speed and 4 m/s in a clear summer day (Gracia and De Herde, 2007). ▪ Double façade is preferably placed in the leeward side of the building where the highest pressure coefficients take place. Airflow in the cavity is lowest when the wind is parallel to the facade (Lou et al., 2012). ▪ Cavity air velocity is directly proportional to wind speed and is around four times lower. (Stec and Paassen, 2005).

Most design considerations regarding naturally ventilated DSFs mainly aim for the enhancement of buoyancy-driven not wind-driven natural ventilation. Since most of the reviewed studies were in temperate climates, having a 20°C difference between cavity and external temperature would not be a major problem. In fact, the bigger the temperature differences the better the buoyancy effect and natural ventilation. However in hot climates where ambient temperatures are relatively higher, it would therefore not be favourable to have such a great increase in cavity temperature.

Therefore the main concern of DSFs in hot climates is the avoidance of over-heating of the cavity space as much as possible.

The main differences between DSFs in cold and hot climates according to the researcher can be summarised in the following table.

Table 3.2: Some aspects of DSFs in cold climates as reviewed in Barbosa and Ip (2014) and Poizaris (2006). Due to the nature of hot climates having higher ambient temperatures and solar exposure, therefore they have clear differences between DSFs in colder climates.

Cold climates	Hot climates
Focus on the improvement of buoyancy-driven natural ventilation	Focus on the improvement of wind-driven natural ventilation
A higher temperature gradient in the cavity is encouraged as it means a better stack effect	A higher temperature gradient in the cavity is avoided since external temperature is already relatively high
Heating is needed in winter	No heating is often required in winter
Glare problems could exist	Serious glare problems could occur due to higher solar exposure than cold climates

In case of naturally-ventilated DSFs, airflow in the cavity is affected by free convection which is the buoyancy or stack effect occurring due to warm air rising. It is also affected by surrounding winds which could either strengthen or weaken the stack effect. Air temperature and airflow interact and affect each other and influence the final performance of the DSF. Hence understanding the physics going on is not a trivial task, and the use of simulation tools to help designers predict the resulting performance of the choices they make is becoming more and more important. The following section demonstrates the main modelling approaches used in the simulation of heat transfer and airflow in DSFs as well as their daylight performances.

3.3 Daylight simulation methods and software used

There are a number of daylight simulation algorithms available and used by popular simulation programs. To model the Daylight phenomena in buildings, these algorithms depend on one of three commonly used methods; BRE split flux, radiosity and raytracing (Reinhart, 2011). The BRE split flux method, or otherwise called protractor method, was developed at the British Building Research Establishment (BRE) and only models diffuse sky conditions. This method could be used when the simulated scene is exposed to a lot of direct and not reflected light. But if the scene is far from the facade opening or heavily obstructed, this method is quite unreliable. The other two remaining methods are capable of modelling different sky conditions and spaces with or without obstructions from the entering light.

Radiosity was initially developed to solve problems related to heat transfer between surfaces, and since the 1980s it has been applied in the calculation of illuminance levels for electric light or daylight. Here, each surface is treated as a perfectly diffuse reflector with a constant luminance so that radiation exchanged between two surfaces can be described as a single number depending on their reflective properties and on the overall geometry of the scene.

In Raytracing, light rays in a scene are simulated to represent the overall luminous distribution from the available light sources. This method can support complex optical surface properties. This method has two types; either forward or backward Raytracing. In the former, rays travel from a light source to scene objects, and in the latter, rays are emitted from a point of interest (view point or a virtual sensor) and traced backwards until they hit a light source or an object. If the rays hit an object, the luminance of that object must be calculated by secondary rays. A ray path is aborted when a certain number of reflective bounces has been reached (specified by the user) or when the relative weight of a ray decreases below a given threshold. Backward raytracing is typically used in relatively complex scenes. It is considered more efficient since most of rays that are emitted by the light source(s) never reach the specific viewpoint or sensor in which the user is interested, so by specifying beforehand the viewpoint of interest the simulation naturally concentrates on those objects, thus saving computation time.

Radiosity requires less calculation time for straight forward geometries which do not contain too many surface elements. But this advantage no longer applies when the model complexity increases as the calculation time in radiosity increases with the square of the number of considered scene elements. While in raytracing this relationship is linear. These approaches are applied in numerous simulation software that provide a user interface to these algorithms. Radiance is powerful simulation software that uses backwards raytracing. A survey by Reinhart and Fitz (2006) (cited in Reinhart, 2011) showed that 50% of the programs used by the participants used Radiance which has been validated by comparison of its results with real measurements. Hence, in this research Radiance will be used for daylight analyses, due to its advantages over the other methods such as: simulating complex geometries, supporting complex optical material properties and different sky conditions.

3.4 Thermal & Airflow simulation methods and software used

The cavity could be either mechanically or naturally ventilated (due to wind and/or buoyancy). In the first case the amount of airflow in the cavity is known, however in the second it is not and must be calculated (Li, cited in Poizaris, 2006). To study the performance of double facades, researchers and designers use computational tools, some of which are gaining increasing credibility which encourages their use especially in the early design phase as they are faster and less expensive than constructing physical models which might hinder the quick flow of design in its initial stages. Challenges of numerical modelling of natural ventilation in general often include unpredictable variables such as the wind and user behaviour and complex physics as the airflow rate affects the temperature, which in turn affects the airflow rate itself (Chen, 2009).

Based on the level of resolution of building simulations, they can be categorised into either macroscopic or microscopic (Hensen, 2002). The macroscopic level deals with whole building systems, interior and exterior conditions over periods of time. The microscopic level focuses on smaller spatial and time scales. Accordingly, airflow modelling in buildings also is divided generally to two main approaches; Airflow Network (AFN) models for the macroscopic level and CFD models for the microscopic level (Djunaedy et al., cited in Poizaris, 2006). The following sections describe in more detail the AFN and CFD modelling approaches.

3.4.1 Airflow Network Model (AFN)

AFN models treat every building component and relevant HVAC fluid flow systems as a network of nodes that represents rooms and parts of rooms. It also includes inter-nodal connections that represent flow paths of doors, pipes, ducts, fans, etc. The concept of mass conservation for inlet and outlet flows leads to non-linear equations which are integrated over time to characterise the flows. It calculates airflow and contaminant transport between building zone and between the building and external air based on pressure differences. Because of its abilities it can be used with thermal models, in such cases it is integrated with a thermal network which solves the heat balance at each node. Each thermal zone has just one node at its centroid and is assumed to be ‘well-stirred’. A thermal model of the building as well as the double façade must be included. The buoyancy effect created by the thermal gradient along the cavity, together with the wind effect is taken into account. It provides useful information about bulk air flows quickly without the need of high computational resources making it suitable especially if annual calculations are needed (De Gracia, et al. 2013; Poirazis, 2006).

A main advantage is that, compared to other airflow models, it is the main method used to predict the overall ventilation performance of a building (Chen, 2009). However, it neglects momentum effects and assumes uniform air temperature in a zone. Also it does not provide detailed information about air velocities inside zones which is important for evaluating thermal comfort. A way of overcoming this and increasing the accuracy of network models is by representing the DSF zone by several nodes instead of just one.

Known software examples include COMIS, which is coupled with TRNSYS for the thermal modelling, and CONTAM which is coupled with TAS. The energy modelling software ESP-r and EnergyPlus have AFN models included in them making them very useful tools. The AFN

is considered the main tool for the prediction of ventilation performance in an entire building (Chen, 2009). The validation of airflow network modelling has been conducted using experiments which show that current airflow tools (COMIS, COMTAM, ESP-r and EnergyPlus) can be used keeping in mind that the simulation accuracy is dependent on the adjustment of some ambiguous coefficients (You, et al., 2013).

The main limitations of the AFN include:

- Not appropriate in cases when the temperature distribution in a zone is significant.
- Only provides information about bulk flows of air (Hensen, 2002).
- The default wind pressure coefficient values are based on ASHRAE (American Society of Heating, Refrigerating and Air conditioning Engineers) database which are limiting in the evaluation of changes in building form and detailed façade designs (You, et al., 2013).

3.4.2 Computational Fluid Dynamics (CFD)

CFD is the science of predicting fluid flow, heat transfer and mass transfer by solving the differential equations that govern these physical phenomena using numerical methods. These numerical methods replace the differential equations with a system of algebraic equations that are much easier to solve using computers. The purpose of a CFD simulation is to calculate the desired flow quantities (such as velocity, temperature, etc.) at a large number of points connected together and distributed throughout the physical domain at hand, forming what is called a *mesh* or a *grid*. In CFD models the geometry under investigation is surrounded by a two or three-dimensional grid of nodes and for each node the conservation equation for mass, momentum and thermal energy is solved. They are capable of performing many tasks that the network model cannot achieve (Poirazis, 2006).

They are the most popular and are based on replacing partial differential equations by algebraic equations either by the finite element method (FEM) or finite volume method (FVM) and most commonly the finite difference method (FDM) (Chen, 2009). CFD is used to determine the convective heat transfer coefficient, detailed information about the nature of the flow field, flow around venetian blinds, openings, and different shading devices. CFD is considered the only way to simulate detailed airflow values of a DSF (De Gracia, et al., 2013). Examples include OpenFOAM, Fluent, Flovent and Phoenix.

Limitations of CFD in practice as mentioned by numerous authors such as De Gracia, et al., (2013), Hensen, et al., van Dijk and Oversloot, Ding, et al., Jaroš, et al. and Chen (all cited in Poizaris, 2006) include:

- Too detailed and sophisticated for the design stage.
- Need high computer power and time.
- Uneven boundary conditions.
- Not user friendly as they require advanced knowledge to be used.

3.4.3 Coupling of CFD and AFN

According to Poizaris (2006), digitally modelling a double façade cavity is a complicated task as there are three main elements that interact with each other and affect the resulting behaviour. These elements are airflow, air temperature (thermal performance), and daylight. Specifically, neither airflow nor temperature can be accurately estimated alone without the other as they are highly interrelated.

Manz and Frank (cited in Poizaris, 2006 p.60), point out that:

> *"The thermal design of buildings with the DSF type of envelope remains a challenging task. As, yet, no single software tool can accommodate all of the following three modelling levels: optics of layer sequence, thermodynamics and fluid dynamics of DSF and building energy system."*

Since modelling of DSF is too complex for the AFN alone, many researchers suggest combining them with CFD models to compensate each other's limitations (Djunaedy, et al., 2002; Beausoleil-Morrison, 2001; Manz and Frank, 2005 in Poizaris, 2006). This is seen as a way of overcoming the lack of accuracy of the network models and 'over accuracy' of CFD models.

Integrating building energy simulation (which typically uses the AFN) software such as EnergyPlus with airflow modelling in CFD can offer accurate predictions of the thermal performance of a DSF or a whole building. EnergyPlus can provide information regarding certain boundary conditions to be fed to the CFD software which in turn would calculate important values such as the convective heat transfer coefficient, or the wind pressure coefficient that cannot be calculated by the AFN (De Gracia, et al., 2013). Examples illustrating such coupling techniques are presented in the following section.

The complete thermal and airflow description of double façade systems requires a coupled model of optics, thermodynamics and fluid dynamics of the air cavity and the room space, in addition to a building energy simulation tool. Challenges facing such coupled models include discontinuity in time-scale, modelling, and speed (Chen, 2009).

3.4.4 Examples of DSF simulations using the Airflow Network model and CFD

This section illustrates some examples of simulated DSFs with particular focus on the AFN used in EnergyPlus, as it is more commonly used in early design phases, and also because of the controversy regarding its accuracy in predicting the performance of DSFs.

Experimental validation of the Airflow Network Model

Kim and Park (2011) question if whole building simulation tools (such as TRNSYS, ESP-r, TAS, EnergyPlus, etc.) are appropriate for simulating the complex heat and mass transfer phenomena that take place in DSFs. They conducted a series of empirical experiments to validate the use of EnergyPlus (v.6.0) simulations for DSFs.

They constructed an experimental test facility representing a low-rise naturally ventilated DSF with venetian blinds for a single window as shown in Figure 3.2. They measured internal and external surface temperatures of each façade layer, as well as cavity temperature and airflow. Then these values were compared with simulated results. Significant errors were observed as simulated temperatures were generally overestimated. Simulated cavity airflow velocity was similar to measurements only when certain ventilation modes were set (Figure 3.3).

They aimed at studying the reasons behind the discrepancies found between actual measurements and simulated results, resulting in a set of considerations to take into account while using EnergyPlus for modelling DSFs. They found that main errors are caused by:

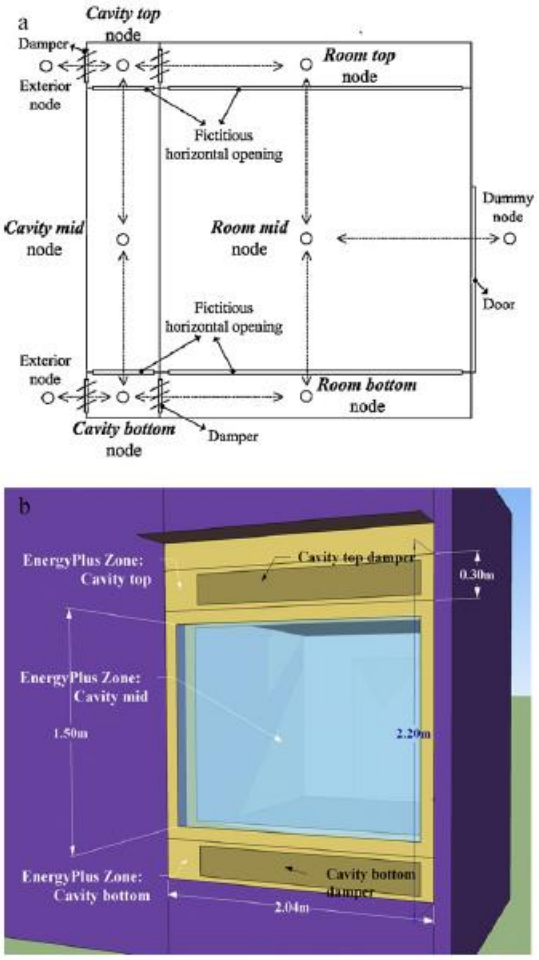

Figure 3.2: (Top) Section view of the modelled cavity and room divided into three stacked zones (showing the connection of the airflow network nodes, blind slats not drawn for clarity), and (bottom) perspective view to the south front (Kim & Park, 2011).

a) Uncertainty of measurement and simulation input parameters:
   - Effective leakage areas for the window, door, floor ceiling and walls were taken from ASHRAE.
   - Discharge coefficient of ventilation dampers.
   - Wind pressure coefficient.
   - Properties of installed glazing obtained from manufacturers were not complete. Reflectance and emissivity of the blind slats were assumed.

b) Assumptions and simplifications of the reality during the modelling process:
   - The cavity was modelled as three vertically stacked zones with fictitious horizontal openings in between. They used the Airflow Network model to simulate airflow driven by wind pressure and buoyancy.
   - None of the algorithms in EnergyPlus that calculate the exterior convective heat transfer coefficient is specifically known for its use in DSFs. Users must choose among them based on judgement and engineering intuition.
   - Curvature of blinds, and their support strings, tapes and rods are ignored.

c) Limitation of the tool:
   - In EnergyPlus v.06 blinds could not be assumed to cover a part of the window as it is in the real model.
   - None of the algorithms in EnergyPlus that calculate the interior convective heat transfer coefficients take into account the cavity airflow pattern.

They tried to improve simulation results by calibrating the model. They measured actual leakage areas and fed them back as new simulation input parameters and repeated the tests. New results show some improvement in the surface temperatures of the outer glazing layer and cavity temperature.

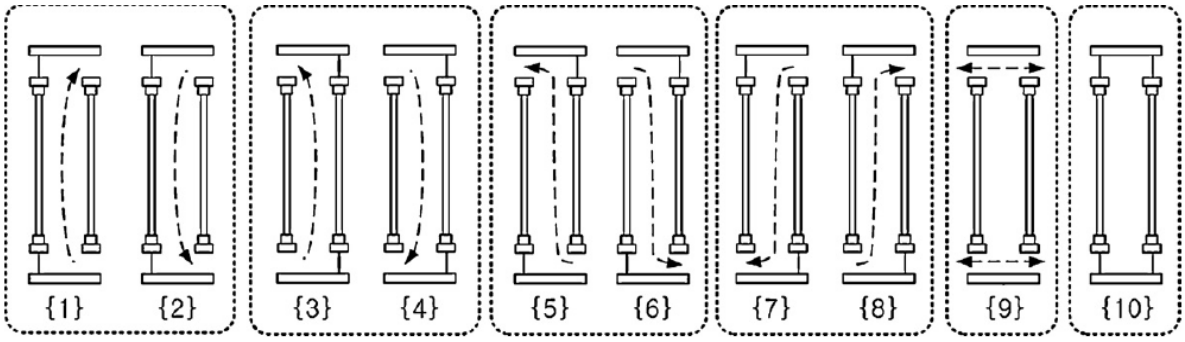

Figure 3.3: Six ventilation mode settings (and ten possible flow patterns) of the DSF. Simulated cavity air velocity profile was similar to actual measurements in the first and second setting (Kim & Park, 2011).

They concluded with the recommendation of integrating CFD with EnergyPlus (or similar tool) specifically for calculating the convective heat transfer coefficients.

Experimental validation of the Airflow Network Model by the International Energy Agency

A report done by the International Energy Agency by Kalyanova, et al. (2009) aimed at performing empirical validation assessed the suitability of current building energy simulation tools (ESP-r, IDA ICE 3.0, VA114, TRNSYS-TUD and BSim) for modelling DSFs. Even if Energyplus was not one of the tools compared, it uses the Airflow Network model which is similar to that used in some of them.

Figure 3.4: The *Cube* at Aalborg University with a South-facing double façade (Kalyanova, et al., 2009).

The researchers constructed a *Cube* at Aalborg University, Denmark, with the following dimensions: 3.5 m width, 0.58 m depth and 5.45 m height and a South facing façade as seen in Figure 3.4.

When all air openings of the double façade were closed, some models had simulated results that were consistent with measurements except during peak solar loads. However when they are opened, most models underestimated cooling loads. They noted that occasionally models had good agreement with measurements, but this agreement was not consistent.

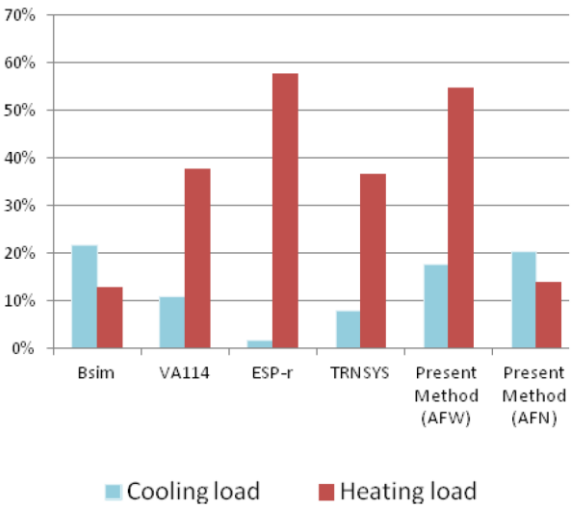

Figure 3.5: The percentage of the error that each program produced in estimation of the heating and cooling loads of the Cube in comparison with the experimental data (Sabooni, et al., 2012).

Reasons for the underestimation of cooling loads include:

- Underestimation of DSF cavity air temperature
- Errors in prediction of cavity mass flow rate
- Underestimation of solar gains to DSF and/or experiment room
- Limitations of the experimental set-up

They concluded that further research is needed to derive solid conclusions on the capabilities of these models in simulating DSFs.

This Cube was investigated again later by other researchers (Sabooni, et al., 2012) by comparing the empirical results obtained in 2009 with their own simulations using EnergyPlus. They tried two simulation methods; the Air Flow Window method (AFW) coupled with CFD, and the Air Flow Network (AFN) method. They concluded that the AFN method provided more accurate results regarding the heating and cooling loads of the Cube, and that the AFN method even had less percentage of errors (Figure 3.5) when compared to other software used by Kalyanova, et al. in 2009.

Validation of EnergyPlus thermal simulation of a double skin naturally and mechanically ventilated test cell

Another more recent example by Mateus, et al. (2014) validated the results obtained by EnergyPlus v.7.1 by comparing them with measurements from a test cell of a DSF in Portugal. The test cell was built in the Portuguese National Civil Engineering Lab in Lisbon. It represents a single room with a South-East facing DSF. The cavity has 45º fixed shading slats and it is split into two adjacent volumes; one is naturally ventilated and the other is mechanically ventilated (Figure 3.6). The external glazing of the DSF is single while the internal is double. In the case of the naturally ventilated DSF model in EnergyPlus, the authors considered only buoyancy driven natural ventilation and neglected the effects of wind.

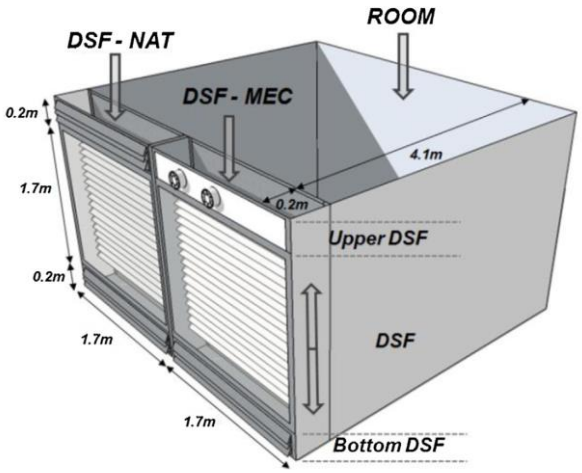

Figure 3.6: Zones of the digital model of the test cell. The DSF cavity is divided into two halves; one is naturally ventilated (left) and the other is mechanically ventilated (right). Furthermore, the cavity in both halves is divided vertically into 3 thermal zones; upper DSF, DSF, and bottom DSF (Mateus, et al., 2014).

They also compared two digital models of the DSF to test the effect of approximating vertical stratification in the cavity. One model had a cavity represented in a single thermal zone while the other had a cavity represented in three thermal zones that are vertically connected by internal openings spanning the entire cross-section area of the DSF. The values compared in all cases were the air temperature and the radiant temperature.

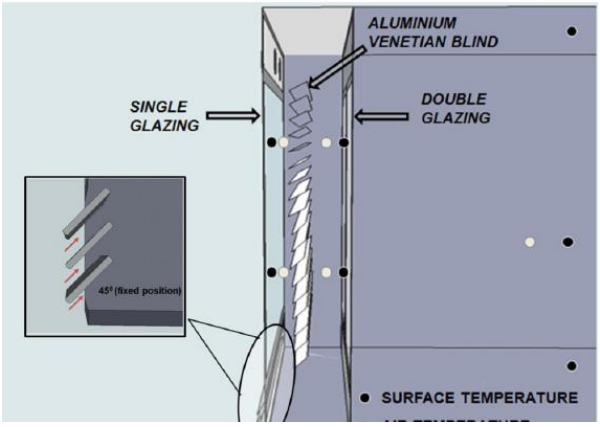

Figure 3.7: Locations of the thermocouple sensors used in the ventilated facade and room measurements (Mateus, et al., 2014).

Their results can be summarised as follows:

- Simulated and measured values showed good agreement with an average simulation error in air and radiant temperatures of 1.4˚C and an average daily maximum error of 2.5˚C.
- The air temperature was lower in the mechanically ventilated DSF. Additionally, it had a higher average difference between air and radiant temperatures than the naturally ventilated one. The simulations were not capable of predicting this behaviour.
- During the day, radiant temperature tends to be over predicted while air temperature is under predicted.
- The use of a single vertical thermal zone for the DSF (as opposed to three vertical zones) resulted in a significant increase in error in radiant temperatures.
- The impact of solar radiation measurement accuracy on the simulations was assessed using two sensor technologies. The standard single horizontal global radiation sensor technique proved inadequate, leading to an increase in of 15% in the daily maximum error indicator.

An attempt to couple EnergyPlus and CFD FLUENT

Zhan et al. (2013) attempted to couple EnergyPlus with CFD tool FLUENT in simulating the airflow rates of a retrofit building in Philadelphia. Although no double skin facades were addressed in this study, it represents a good example of coupling both software tools together. The authors attempted to couple both CFD and nodal models to complement each other's limitations. The nodal model provided the following values to be set as boundary conditions in the CFD model:

- Interior and exterior surface temperatures of the building envelope.
- Outdoor weather conditions such as ambient temperature, wind speed and direction to determine the boundary type of the surfaces representing the simulation domain.

Then the CFD tool performs a steady state natural ventilation simulation to calculate the temperature profile and velocity fields. A post processing program takes these values to calculate the following:

- Airflow rates through all the openings.
- Average air temperatures through the openings.
- Surface heat transfer coefficients for all of the envelope surfaces.

Limitations of nodal model such as the Airflow Network model used in EnergyPlus include:

- Users must input in the simulation parameters various coefficients such as wind pressure coefficient, heat transfer coefficient, loss factor and friction factor. These values are difficult to define.
- Thermal and airflow patterns cannot be represented by the model. The lack of knowledge of the airflow patterns leads to errors in the prediction of heat transfer in the cavity which is complex by nature.

Limitations of CFD models:

- They need much more computation power than nodal models.
- Difficulty of modelling the thermal storage capacity of building components.

The coupling platform was based on Building Controls Virtual Test Bed which allows users to couple different simulation programs for co-simulation, and to couple simulation programs with actual hardware (Nouidui, 2016). The authors designed a new Object in EnergyPlus called ExternalInterface:Airflow which sets the airflow rate for each piece of the openings in the building. They used FlowPlus program for executing CFD simulation and extracting coupling variables.

They compared the simulated airflow rates (of all windows and doors) from the AFN alone and from the coupled AFN and CFD models in a time frame of 8 days in July. No real measurements were taken to verify simulations results. They observed that the AFN generally predicts smaller airflow rates for the openings with a difference ranging from 100% to 200% from results of the coupled model. AFN results were extremely different in particular cases. They were highly underestimated when there was an obstacle in front of the façade that causes complicated airflow patterns. They were also highly overestimated in clearstory openings with a difference up to 600% from the coupled model results.

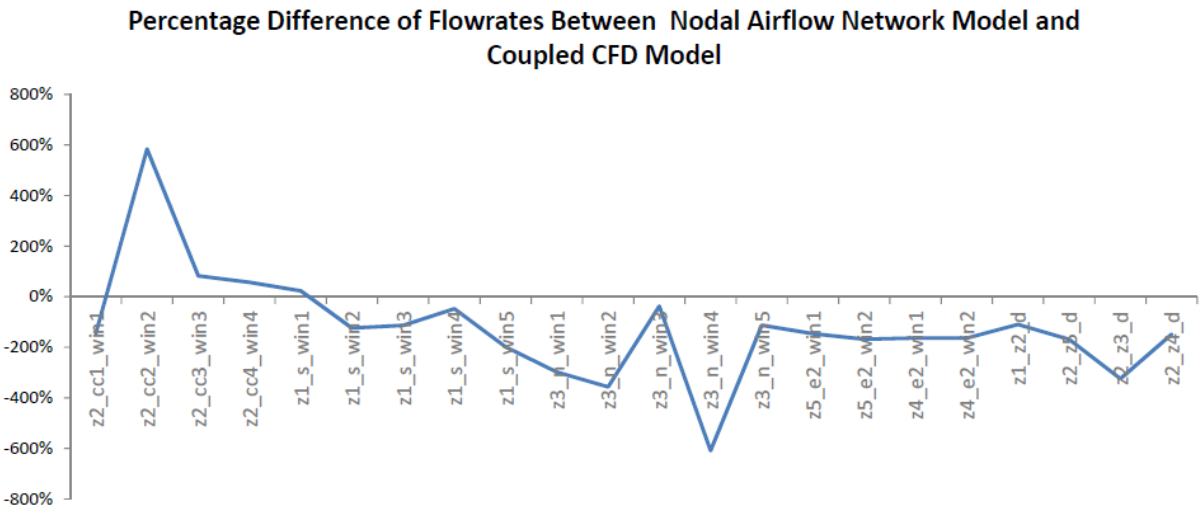

Figure 3.8: The averaged percentage difference of airflow rate values during run period of June 1st to June 8th between values generated with nodal airflow network and coupled simulations (Zhang, et al., 2013).

3.4.5 Selected simulation software for this research

After reviewing the main airflow modelling techniques, their capabilities and limitations, it has been decided for this research to choose a tool based on the Airflow Network model which is EnergyPlus for the following reasons:

- Its capability of analysing airflow in buildings without the high computational power and time required by CFD models
- Its capability of being integrated in building energy models, most importantly EnergyPlus which is the running engine for many Grasshopper energy simulation plugins.
- Suitable for early design stages when the overall building performance (ventilation, thermal, and daylight) are very important in taking informed decisions

CFD models would be used in a later stage after the main geometrical and structural configurations of the proposed building skin have passed the conceptual phase.

3.5 Case studies in hot climates

This section presents a number of studies of DSFs in warm, hot and extreme hot climatic areas. The objective is to learn from previous research and identify the main design aspects they followed and the tools they used in thermal/airflow simulations.

3.5.1 Warm climates

An interesting study done in central Italy by Baldinelli (2009) explored the use of a double façade in a relatively warm climate that needs summer cooling as well as winter heating. It was assumed to be a façade for a square office room 10 m wide and 3.2 m high. He proposed an external layer made of L-shaped movable glass and aluminium shading panels that could rotate using hydraulic jacks to take one of two positions (Figure 3.9):

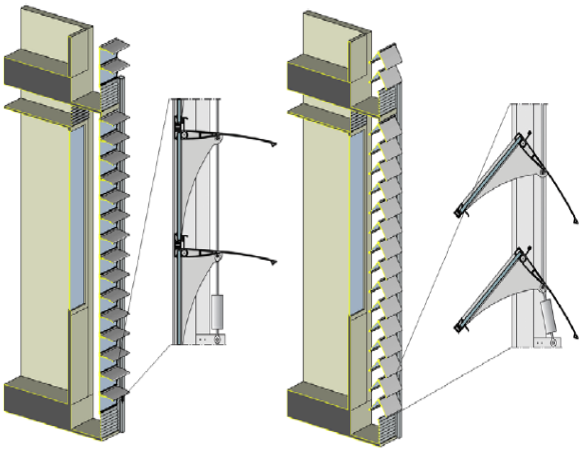

Figure 3.9: double façade proposed by Baldinelli (2009) with movable glass and shading device in closed state (left) for winter and open state for summer (right).

Open state: This was the summer position that allows air to enter/exit the cavity through distributed openings along the façade height. It reduced the greenhouse effect which is usually the main concern in the application of double facades in hot climates. The aluminium shading panels were tilted in this position to decrease solar radiation entering the cavity. In fact, it was found that the temperature of the air flowing near the inner façade layer was close to ambient air temperature (33.8°C) on a typical summer day in central Italy.

Closed state: this was the winter position where the shading devices were in a horizontal position thus allowing a large amount of solar radiation to enter the cavity as the sun is low in winter. Also reflection from the aluminium shading devices added to the solar gain.

The proposal was applied to a south orientation and calm surrounding winds were assumed. Since wind pressure is variable and unpredictable, calm outdoor conditions were assumed throughout the whole study. Defining just a single value for wind pressure would make results too dependent on that particular case study. Simulations of air flow

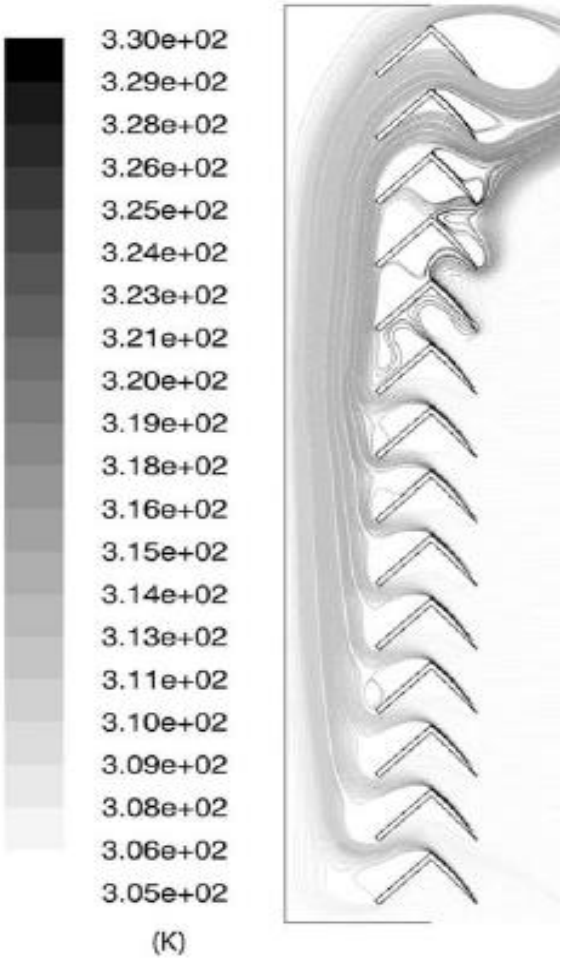

Figure 3.10: Temperature air streamlines (K) in summer configuration (July 15th, 12:00, central Italy) (Baldinelli, 2009).

rates using FLUENT CFD were confirmed by physical experiments which showed that errors never exceeded 6% of the real measure values.

The cooling season was assumed from June till September, and the cooling loads of this proposal were compared with three façade types; single fully glazed, 50% glazed and opaque facades. Simulations showed good summer behaviour of the proposal due to the high shading level and multiple openings.

Results:

Cooling loads were 10.3 KWh/m^2 for the proposed design, 151 KWh/m^2 for a fully glazed single façade and 77 KWh/m^2 for 50% glazed single façade, which showed that double facades could be used in warm climates if certain design aspects were taken into consideration.

Observations:

- Wind effects were not studied.
- Different orientations were not addressed.
- Effect of shading on daylighting was not addressed.
- Strong emphasis on external shading and multiple openings: air temperature in the cavity was close to ambient temperature.
- Natural ventilation of the rooms in summer was not considered.

The external skin was composed of two layers of 5mm float glass with a 0.37 mm film of polyvinyl butyral in between, and the shading device was made of anodized aluminium which is an alloy that combines good mechanical resistance properties with a relatively low density and good performance against weather conditions. The inner skin was transparent, made of double glazing composed of a layer of glass as that of the external skin, and an inner 4 mm float glass layer with a 10 mm air gap.

Another study in a relatively warm climate was conducted by Papadaki et al., (2014) in which they modelled an existing single-façade building in Crete then introduced different DSF configurations (as seen in Figure 3.11) to the digital model to evaluate their performance. The existing building had double glazing with a 12 cm air gap and had an annual cooling energy consumption of 54 KWh/m^2 which the authors considered high and needed reduction. They introduced a corridor-type DSF made of double glazing as well. They compared the performance of the DSF with and without natural ventilation, and with different positions of shading devices. Their results showed that both the ventilation of the DSF cavity and the use of shading devices (which preferably are placed externally) could produce up to 24% in annual energy savings.

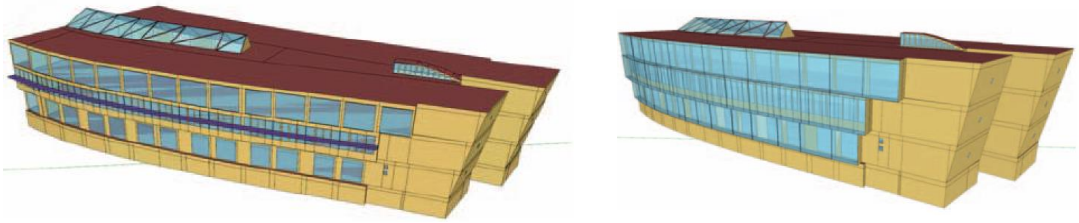

Figure 3.11: A digital model of the existing building studied in Crete by Papadaki et al. (2014) with (right) and without (left) their proposed double façade.

3.5.2 Hot climates

There are very limited investigations of double façade behaviour in hot climates. A study by Hamza (2008) represents one of the few available in literature to this date, where a comparison was carried out between single façade and a double façade with three possible glazing options; transparent, tinted and reflective.

In Hamza's study, the single façade acted as a benchmark base case representing a typical office building in Cairo. Data was collected from 33 existing office buildings to determine the construction methods, materials, and occupancy profiles to model the benchmark case. Data regarding monthly energy consumption was also collected from 10 of the 33 buildings for validation and calibration of the model. However, only one of them provided accurate sub-metered data which was the World Trade Centre. It was a major energy consumer as it used around 5,000,000 KWh/year.

Figure 3.12: Cairo World Trade Centre. The first tower on the right was the one used in the study of Hamza (2008).

The simulation tools used were the dynamic thermal modelling software IESVE (Version 5.1) ApacheSim is at the core of the IES suite of thermal analysis products, each of which simulates an aspect of thermal performance. The simulation results indicated a pattern which matched the real consumption values, with an error between 2 and 8%.

Characteristics of the modelled benchmark case:
Square floor plan, 6 storeys high, WWR= 40%, glazing= 6 mm clear reflective panels, walls= single brick leaf, uninsulated wall infill between the concrete columns, plaster rendering from both sides, overall U value of walls= 1.4W/m^2K.

Characteristics of the double façade:
It was placed on all four orientations, started at the first floor, 1 m wide cavity, top and bottom of cavity are 100% open, no shading devices were placed in the cavity due to high levels of pollutants and dust particles which reduce air quality and increase maintenance cost. Three different types of external glazing were compared; clear, tinted and reflective.

Table 3.3: Glazing properties for each type of double façade. The internal glazing is common for all of them (Hamza, 2008).

External glazing type	U-value (W/m^2K)	Solar coefficient	g-Value	Thickness (mm)	Transmittance (%)	Reflection (%)	Absorption (%)
Clear glazing	5.6	0.85	0.87	10	73	7	20
Body tinted green	5.6	0.59	0.51	10	35	5	60
Reflective glazing active blue	5.6	0.27	0.42	10	21	12	67
Internal glazing type: clear	5.6	0.95	0.82	6	79	7	14

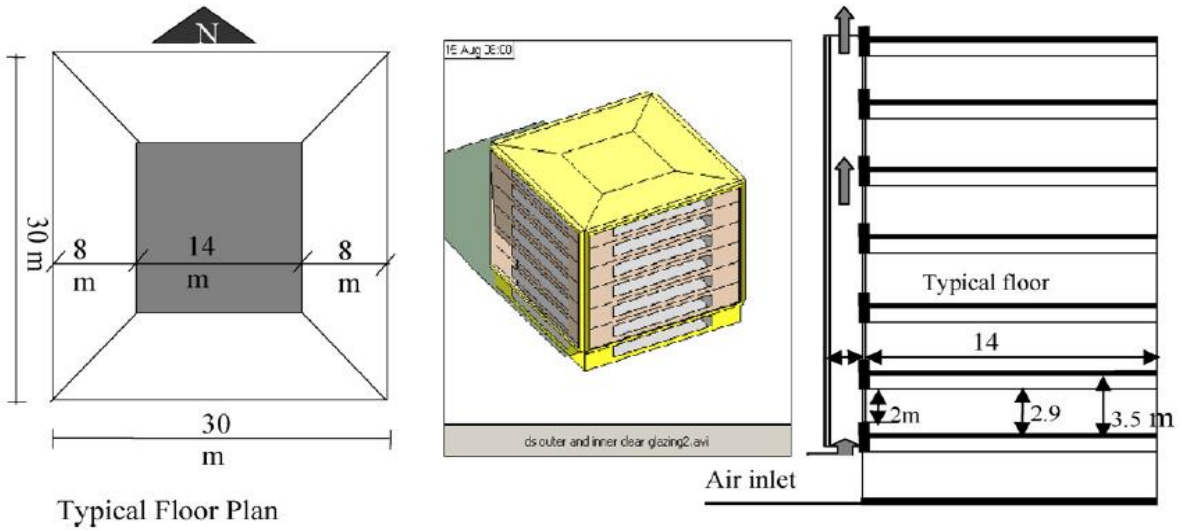

Figure 3.13: Single skin plan (left), double skin isometric (middle) and cross-section configuration (right) (Hamza, 2008).

Results:

Table 3.4: Comparison of the annual cooling loads of the benchmark case with three different glazing types of double facades (Hamza, 2008).

	Annual cooling loads of Benchmark single skin (KWh/m^2)	Double façade: clear	Double façade: tinted	Double façade: reflective
East	1299	7% increase	11% decrease	32% decrease
West	1311	7% increase	11% decrease	32% decrease
South	1311	7% increase	11% decrease	32% decrease
North	1121	2% increase	18% decrease	32% decrease

Results of this study indicate that careful material choice is critical to the thermal performance of the double façade, as reflective glazing provides the most reduction in cooling loads. It also dismisses hypotheses that claim that double facades do not provide considerable energy saving especially in hot climates.

Observations:

- Effect of wind was not addressed.
- Use of shading devices was not addressed.
- No openings other than the top and bottom ones were used.
- Results were *not* in accordance with Radhi et al. (2013) who mentioned that the double façade in the north orientation had the least reduction of all. Radhi et al. also mentioned that performance in the south was less than the east and west, which was not evident here.
- The study emphasised the importance of glazing properties.
- Natural ventilation was not possible from March to November due to high ambient temperatures in Cairo in these months (average high temperatures range between 24°C and 36°C.
- It was somewhat strange that east, west and south orientations always had exactly the same percentage of increase of decrease in cooling loads. Differences were expected to occur even if they are small.
- No physical measurements were taken from the existing building.

Hamza along with others (Hamza, et al., 2007) has previously done another investigation about double facades in Cairo. They compared a 6-floor high typical double façade in which the cavity was continuous with openings only at the top and bottom, with another 'corridor' type double façade in which the cavity was divided vertically every two floors by a perforated walkway (50% solid) and had openings at each floor level (Figure 3.14). The DSF in both cases was 30 m long and 21.1 m high. Both outer and inner glazing was single. They respectively had the following properties: thickness of 10 mm and 6 mm, transmissivity of 0.45 and 0.78, absorptivity of 0.49 and 0.15.

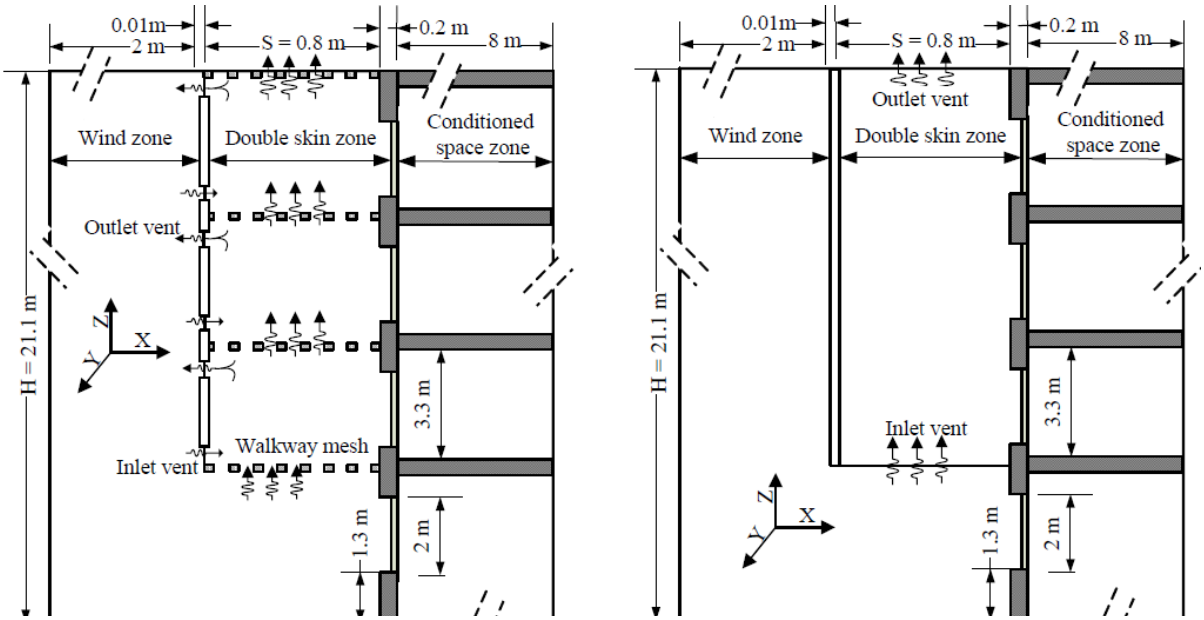

Figure 3.14: The corridor (left) and continuous (right) double facades compared (Hamza, et al., 2007).

Using Fluent v.6.2.16 CFD simulations, they compared different heat gain sources (direct solar radiation, surface radiation, and convective heat gain), cavity temperatures, and

airflow in both cavities, in addition to luminance levels using Radiance. This was done for East and West facades.

Results:

The results showed that direct solar radiation was the main heat gain source compared to surface radiation and convection heat fluxes in both orientations (Figure 3.15). The corridor type cavity temperature was 1.5°C lower than the continuous one, as it experienced turbulent flow at inlet and outlet openings that caused a cooling effect. Air velocity was lightly slowed down due to the presence of the walkways. The wind had more influence on airflow in the corridor type, while buoyancy had more effect in the continuous type.

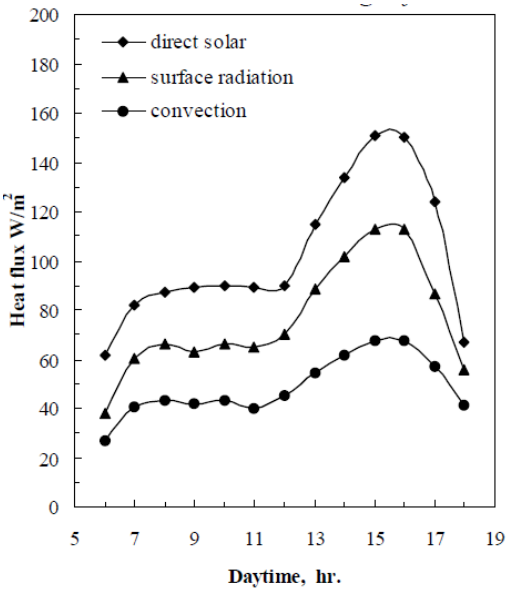

Figure 3.15: A comparison between radiation, convection and direct solar heat fluxes passing through the inner building skin in the West orientation (Hamza, et al., 2007)

The main factor affecting the airflow in the cavity in the case of the obstructed corridor type DSF was the wind due to the presence of multiple openings, aided by the buoyancy effect. However in the continuous DSF, the airflow was mainly affected by buoyancy due to the lack of openings along the height of the cavity which trapped heat inside. This caused it to have a higher temperature difference between the inside and ambient external temperature.

There were minor differences in the daylight performance between East and West orientations. Both double façade configurations resulted in glare problems near the windows which would require the use of blinds. The corridor type façade had a darker indoor environment and reflections from the walkways produced sharp contrasts. It was concluded from this paper that natural ventilation that was seen in the corridor cavity type was important to decrease its temperature. However this type has caused a decreased daylight performance leading to the need of more artificial light. They recommended further research to be conducted to improve daylighting the corridor type double façade.

Observations:

- The presence of openings along the height of the DSF was very important to reduce cavity temperature.
- Improved thermal performance in the corridor type DSF was associated with decreased daylight performance inside the rooms.
- The use of shading devices was not studied.

Another study of DSFs in hot arid climates was done by Hashemi et al. (2010). They studied an existing DSF of the Supreme Court building in Tehran, by measuring the cavity temperatures and the exterior surface temperatures of the inner wall. This was performed for all four orientations of the building from the period of 6th to 21st of July, and from the 5th to 13th of January.

The building is 11 floors high. The DSF starts at the second floor; it is a corridor type DSF separated horizontally every two floors. The cavity width is 0.7 m. They used single glazing in the inner and outer façade layers. Aluminium vents are 1.5 m high distributed throughout the façades as shown in Figure 3.16 . No shading devices were used.

Figure 3.16: The Supreme Audit Court in Tehran. Source: http://pubs.sciepub.com/ajcea/1/6/3/

They made a digital model of the building and simulated its thermal performance using EnergyPlus v.2.1. Some of their important results are summarised in the following paragraphs.

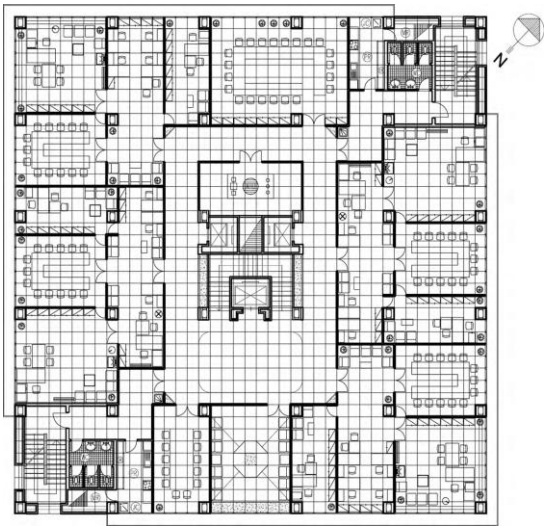

Figure 3.17: Typical floor plan showing that the DSF is connected in the NE and SE and also in the NW and SW (Hashemi, et al., 2010) .

Results

- Cavity temperatures in 7th and 11th floors:

They measured the cavity temperature at the 7th and 11th floors. During daytime hours in summer, the temperatures at the 11th floor were always lower (with a difference up to 8°C), and were sometimes even below outside temperature. This was mainly due to the poor ventilation on the 7th floor as they had less surface area of vents.

- Simulated vs measured cavity temperatures on a typical summer day and winter day:

Thermal simulations overestimated cavity temperatures on a summer day (18th of July). This over estimation increases during the daytime with a maximum difference of 4.5°C between measured and simulated values. On a winter day (6th of January) the simulations were more accurate, but it sometimes underestimated the cavity temperatures during the daytime with a maximum difference of -2.5°C.

Both simulated and measured results indicate that the North West DSF is the warmest in the summer, and the SE is the warmest in the winter.

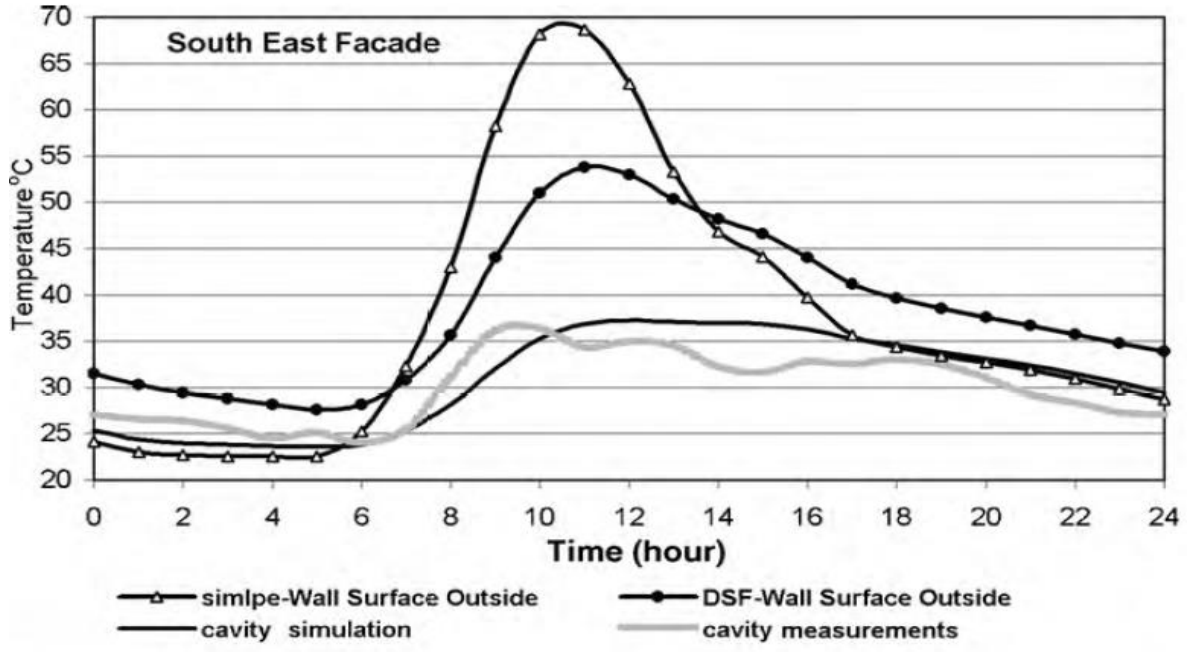

Figure 3.18: Surface temperatures of the external building with and without the DSF. Simulated and measured cavity temperatures are also illustrated (Hashemi, et al., 2010).

- Annual cooling loads with and without the DSF:

Cooling loads in daytime were reduced, however during the night they increased due to the lack of night ventilation in the office rooms, causing accumulated heat to be trapped. On an annual scale, cooling loads were generally reduced even if the building didn't have night ventilation.

Observations

- It was expected to have a difference between measured and simulated cavity temperatures due to many reasons such as software limitations, and also due to possibility of measured weather data not corresponding 100% to those in the used weather files in EnergyPlus on that specific simulated day.
- It was not possible to have an idea of the effect of wind on the measured results, since the wind direction was not mentioned and no airflow measurements were taken in the cavity.
- Despite the lack of shading devices, and the use of single glazing in both the outer and inner facades layers, natural ventilation alone was able to improve the overall performance. This was clearly seen when the 7^{th} and 11^{th} floor temperatures were compared, showing the big influence of ventilation on cavity temperature.
- If appropriate shading was studied the DSF thermal performance would have improved.

Other examples of DSFs with measurements from reality were always just one-storey high. This example was particularly interesting as it demonstrated real measurements of a relatively high DSF in a hot climate.

3.5.3 Extreme hot climates

Another study addressing the performance of double facades was conducted by Radhi et al. (2013) but in the hotter climate of the United Arab Emirates. Although their work was cited in the review paper of Barbosa and Ip (2014) there was not much focus on the fact that the double skin studied was in an extremely hot climate, and unlike almost all other double facades, this one has openings in the outer layer at each floor level. This made this example particularly interesting for the scope of this thesis and therefore it will be reviewed in the following pages.

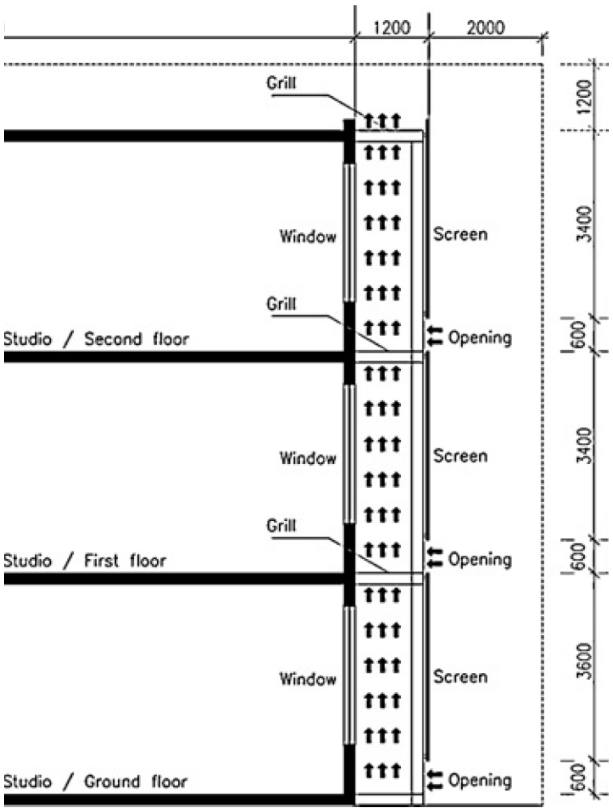

Figure 3.19: The double façade studied by Radhi et al. (2013). The outer layer is a single 10 mm glazing screen with openings at each floor as well as at the top. It is 12 m high and 65 m long with a 1.2 m wide cavity and grills at each floor slab level. The inner walls are of masonry and windows are double glazed, 2.9 m high and 12 m wide as they are openings for 13x13m design studios (which are air conditioned).

In their paper, Radhi et al. (2013) modelled an existing building with a double facade which was the Architectural and Engineering Department in Al Ain city, and studied its performance in a typical summer day with a monthly average maximum temperature of 47°C and North-West prevailing winds with an average speed of 4 m/s.

They compared an East-facing double façade system that has a configuration as shown in Figure 3.19 with a classic single façade system. They measured airflow, temperature and cooling loads in both cases. Both systems were then studied in the four different orientations. They used Design Builder software that runs on EnergyPlus for the construction of 3D geometrical models, establishment of boundary conditions and calculation of overall thermal performance in terms of heat gain and cooling loads. Then PHEONIX CFD software was used to study the airflow and temperature distribution.

Figure 3.20: Architectural and Engineering Department in Al Ain city in the UAE (Radhi, et al., 2013).

Then they compared 5 different cavity depths (from 0.5 to 1.5 m) and 4 different glazing properties (U-value, heat gain coefficient and emissivity shown in Table 3.5) to the reference DSF to see the impact of these variables on thermal gain and cooling loads. The most important results of their investigation are summarised in the following paragraphs.

Table 3.5: Different properties of the external glazing of 5 different Double Facades. The single glazing is the existing reference case (Radhi, et al., 2013).

External Glazing	Single	Double 1	Triple	Double 2	Double 3
U-Value (W/m^2 K)	5.7	2.79	2.32	3.1	3.25
Solar transmission (ST)	0.78	0.6	0.59	0.64	0.64
Light transmission (LT)	0.88	0.78	0.74	0.31	0.32
Solar heat gain coefficient (SHGC)	0.82	0.7	0.65	0.4	0.40
Emissivity	0.96	0.92	0.9	0.92	0.92

Results

- Airflow:

Two forces affected air movement; which were mainly the stack effect and wind forces. Air entered from the openings and moved mainly upwards, while a small percentage of it moved downwards through the aluminium grills. The rising heated air in the cavity created a high pressure at the bottom and at each opening thus inducing air to enter.

- Air and surface temperatures:

In the double façade, temperature at the bottom and at the openings of the cavity was lower than that at the top opening. Heat was transferred to the top by the rising warmed air. What is very important to note is that the air temperature inside the cavity was not much different than the air temperature outside due to the presence of openings along the cavity height. However the radiation temperature was high when compared to the single façade which reflects the greenhouse effect. The upper cavity openings induce the stack effect causing upper floor to experience more heat gain, but at the same time it was responsible for removing the heat out of the cavity. The single façade and the outer layer of the double façade were hotter than the inner layer as it received less direct solar radiation.

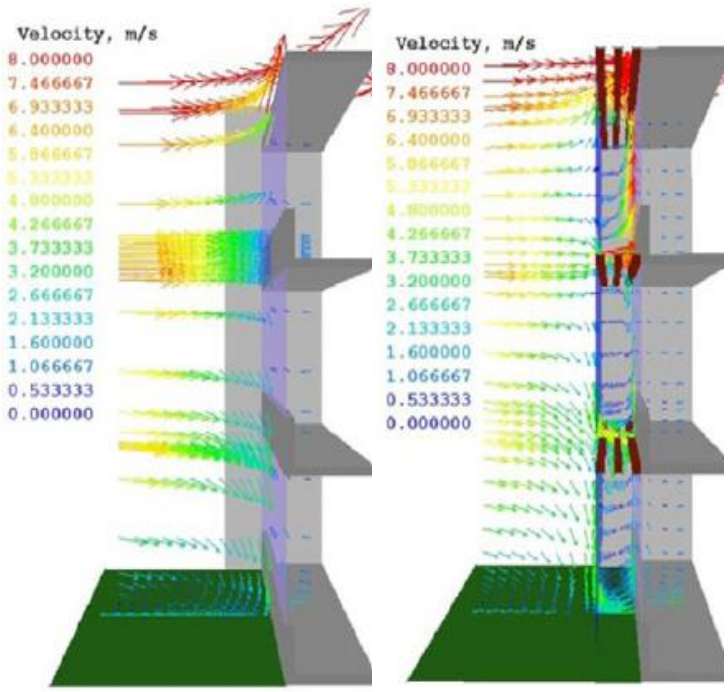

Figure 3.21: Comparison between airflow pattern and velocity between a single façade (left) and a double façade (right) (Radhi, et al., 2013).

- Cooling loads:

Two main factors affected cooling loads which were the solar gain and the heat transmission of the façade. Their study showed that these factors were reduced in the double façade thus reducing cooling loads. They estimated a 17% reduction in cooling energy on a typical summer day due to the performance of the double façade.

- Effect of orientation:

The double façade had lower heat transfer rates than the single façade in all orientations, but these rates were different from one orientation to the other depending on the level of irradiance and the angle of incidence of the sun.

For example, it was noticed that despite the south orientation receiving the highest amount of irradiation, the difference in heat transfer between the single and double façade was minor. This was because when the sun is in the south, it had the highest position and hence the reflection by the vertical glazing is high in both façade types. The double façade caused a greenhouse effect which was particularly strong in the south orientation. This caused just a 5% decrease in cooling loads, with respect to 15% in the east and west orientations. In in north orientation, simulations showed a 3% increase in cooling loads. This was attributed to

the low level of irradiance and relatively large amount of heat and solar trapped within the cavity, which increased the transmission of heat into the space.

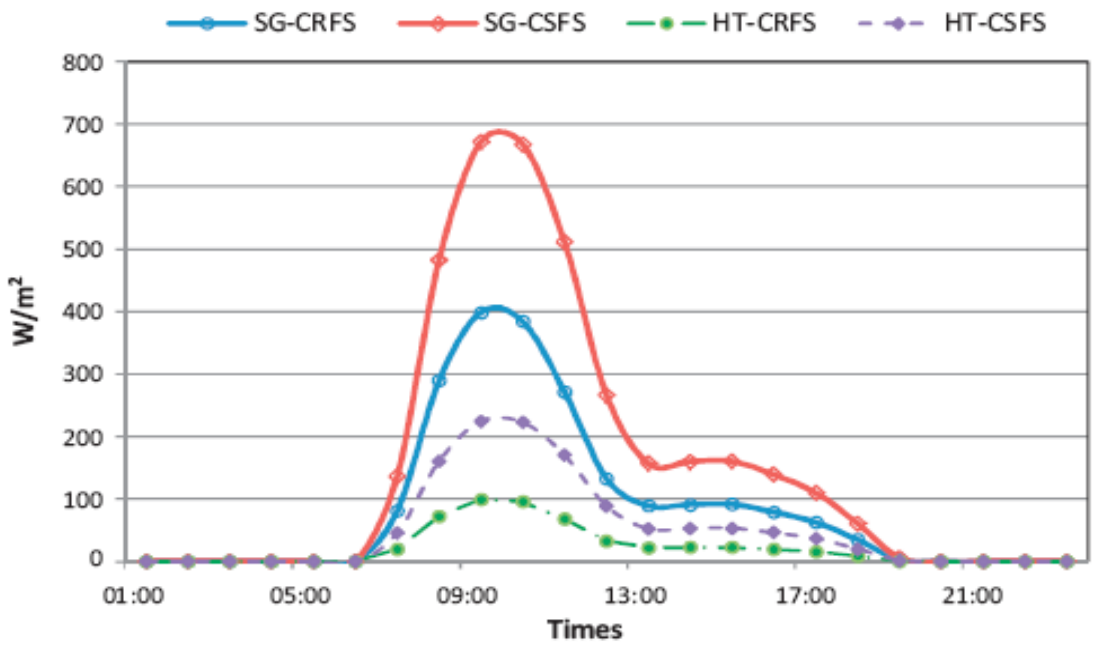

Figure 3.22: Heat transmission (HT) and solar gain (SG) through inner layer (windows). The Figure shows a comparison between the performance of the double facade, and a classic single façade system (Radhi, et al., 2013).

- Cavity depth and openings:

Decreasing the cavity depth had two different effects; it reduced the mass flow rate of circulating air hence reducing cavity temperature, while increasing the direct solar radiation that reached the inner layer. A balance was found between the depths of 0.7 m and 1.2 m.

The presence of the cavity openings had a critical role in airflow and in avoiding the greenhouse effect. The glazing properties (especially the solar heat gain coefficient) also had a major role in the efficiency of the double façade and the greenhouse effect. CFD simulations showed that using single glazing in the outer layer of the DSF decreased its efficiency by 26%.

- Glazing properties:

The optical and glazing properties influence the solar gain as well as the amount of daylight that entered which both had a large impact on cooling loads. Logically there was linear relationship between the U-Value of glazing and heat gain. However in their results, a smaller U-Value did not *always* mean a smaller convective heat transfer coefficient. On the other hand the decrease in SHGC always showed a decrease in the heat transfer coefficient. Therefore the SHGC was seen to be the most effective glazing property that reduced cooling loads.

Observations:

- Use of shading devices was not addressed.
- Multiple openings used are very important for cavity ventilation.
- Importance of glazing properties and cavity depth on the thermal performance of the DSF.
- The effect of low thermal and optical properties of glazing on the amount of daylight entering the rooms was not investigated.
- Natural ventilation of indoor spaces was very difficult due to extreme hot climate of the UAE (annual average high temperatures range from 24°C to 45°C).
- DSFs could cause an increase in cooling loads in the north orientation.
- No physical measurements were taken from the existing building.

3.5.4 Non-uniform DSFs

Most studies regarding double facades usually considered the outer façade layer a as a flat vertical surface with not much geometrical complexity. This study by Hamza et al. (2011) was particularly interesting (despite being applied in a temperate climate) as they considered three different configurations for the outer façade layer as shown in Figure 3.23.

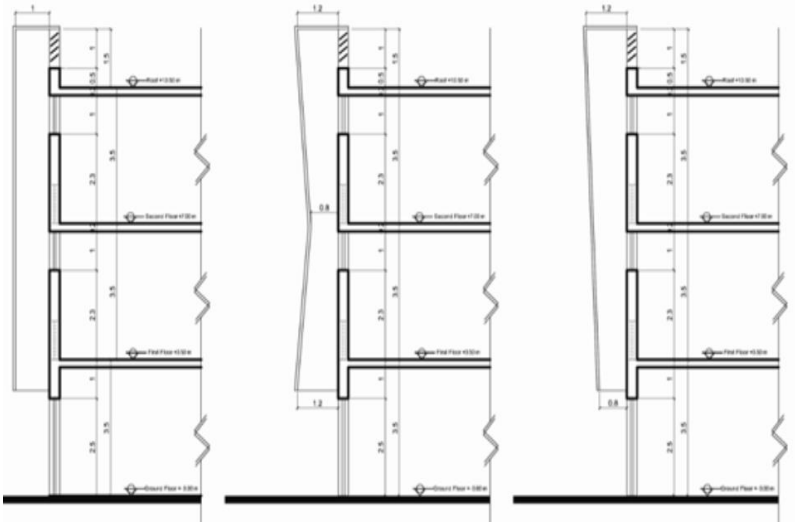

Figure 3.23: Three façade configurations studied by Hamza et al (2011).

They compared the cavity air temperature and velocity, room temperatures and fresh air supply rate in these three cases for an average summer day in a temperate climate (ambient temperature assumed 21°C). They used IESVE v.6 for coupled with CFD simulations using ANSYS CFX[10] code. Interesting design considerations for the double façade included:

- It started 2 m above the ground level to minimise thermal exchanges with the ground and also for better quality of air entering the cavity.

[10] ANSYS CFX is a high-performance computational fluid dynamics (CFD) software tool that delivers reliable and accurate solutions quickly and robustly across a wide range of CFD and multi-physics applications. For more information visit: http://www.ansys.com/Products/Fluids/ANSYS-CFX.

- The outer layer extended about 1 m higher than the building roof which was recommended to improve ventilation rates in the upper floors as they usually experience less air pressure due to weaker buoyancy effects at the top.
- The surface area of the cavity outlets were just 25% of inlet areas for a more effective airflow.
- Single sided ventilation in the rooms was assumed, and inlet/outlet openings were placed in opposite corners in a staggered way to prevent the exhaust of a room from entering the inlet of the room above it.

The results of this comparison showed that all three configurations have very similar heat stratification in the cavity with a 2-3°C difference between inlet and outlet temperatures. Air velocities were highest when they are adjacent to the outer cavity surface which was warmer and most of the air coming from room outlets joined this high velocity stream.

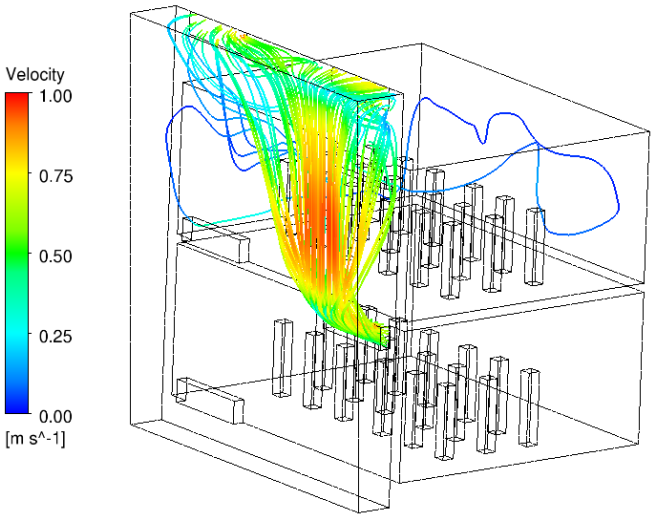

Figure 3.24: Study of air movement and velocity in the DSF cavity by Hamza et al. (2011).

Fresh air supply rate was 28 l/s (11.8 m^3/hr) per person in the first for and 22 l/s (79.2 m^3/hr) in the second floor, and both are above the recommended value of 8 l/s (28.8 m^3/hr) per person. The mean air temperature in the rooms was around 25°C which was above comfort levels and suggested the need of mechanical ventilation (Hamza, et al., 2011).

Observations

- Effect of wind was not addressed.
- No shading devices were used.
- No openings other than top and bottom ones were used.

Hamza & Abohela (2013) also carried out a similar investigation of other non-uniform double façade configurations (Figure 3.25) in Newcastle Upon Tyne, UK. This time they focused on studying both the thermal and daylight performance of the building in each case. They used IESVE v.6.4.0.12 and Radiance for their simulations.

Results showed that all three configurations had very similar thermal performance. The average cavity temperature was about 3°C higher than ambient temperatures in winter and 7-8°C higher in summer. Temperatures of the cavity at the second floor levels were generally 2°C higher than the first floor. The staggered configuration provided self-shading to the building and cavity temperature followed the ambient temperature profiles more closely than other configurations thus having a lower thermal stratification profile. This showed the influence of direct solar radiation and shading techniques on the building performance.

Regarding the daylight performance, the straight and inclined facades had similar performances, having the possibility of glare near the windows. The staggered configuration had the darkest indoor environment even on a clear summer day indicating that more artificial light was needed. This indicated the importance of studying the thermal and daylight performance that result from shading since energy savings in cooling loads might be associated with more energy consumption for lighting (Hamza & Abohela, 2013).

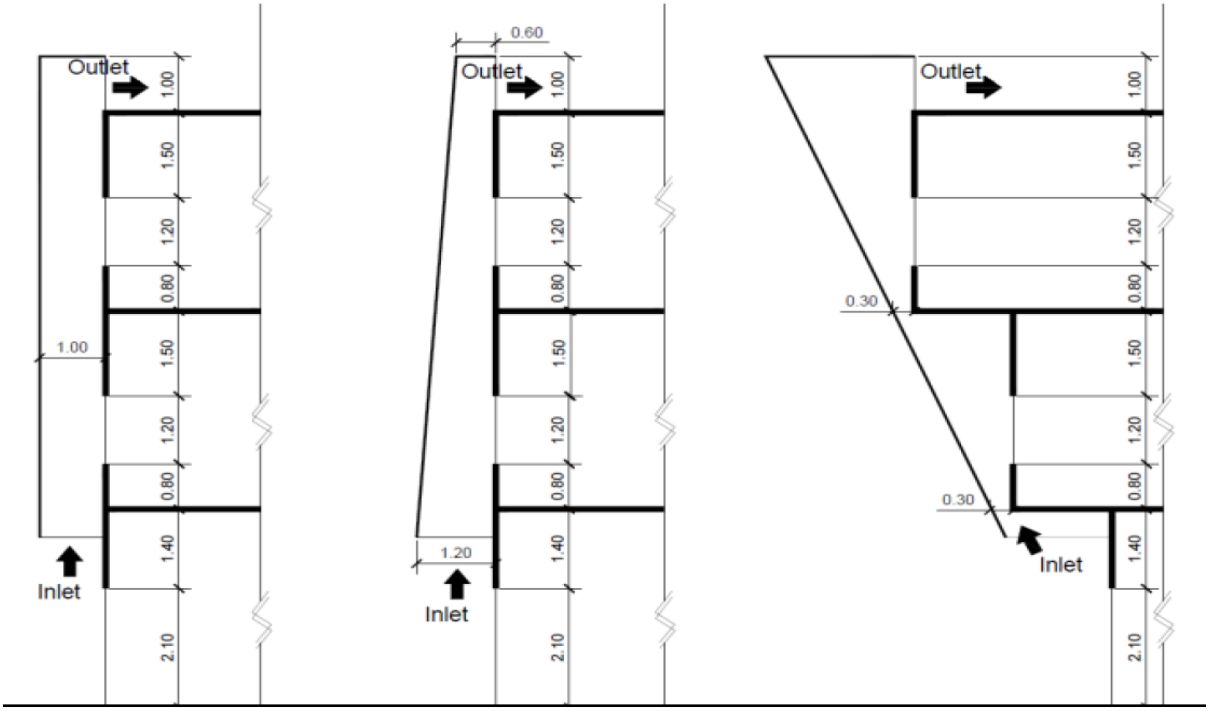

Figure 3.25: Three façade configurations studied by Hamza & Abohela (2013) in Newcastle Upon Tyne, UK. From left to right: straight, inclined and staggered configurations.

3.5.5 Summary of case studies

Table 3.6: Summary of the case studies reviewed in this chapter. Source: author.

Author	Location	Software used	Actual measurements	Shading used	Daylighting studied	Façade variables compared	Performance criteria	Important results and observations
(Baldinelli, 2009)	Central Italy	Fluent CFD v.6.2	Yes	Yes	No	▪ Single (glazed/opaque) vs. double façade	▪ Cooling loads	▪ Minor differences between simulated and measured values (didn't exceed 6%). ▪ Cooling loads are much less when DSF is used. ▪ Strong emphasis on external shading and multiple openings: air temperature in the cavity was close to ambient temperature.
(Hamza, et al., 2007)	Cairo, Egypt	Radiance & Fluent CFD v.6.2.16	No	No	Yes	▪ Continuous vs corridor DSF ▪ East & West orientations	▪ Cavity temperature and airflow ▪ Difference sources of heat gain ▪ Daylighting	▪ Direct solar radiation is the main heat gain source compared to surface radiation and convection heat fluxes. ▪ The corridor type cavity temperature was 1.5°C lower than the continuous one, with a slightly lower air velocity. ▪ Minor differences in the daylight and thermal performance between East and West orientations. ▪ The corridor type façade had a darker indoor environment.
(Hamza, 2008)	Cairo, Egypt	IESVE, v. 5.1	No	No	No	▪ Single vs. double façade ▪ 4 orientations ▪ 3 glazing properties for outer layer	▪ Cooling loads	▪ Minor differences between simulated and measured values (between 2 and 8%). ▪ Reflective glazing provides the most reduction in cooling loads (32% in all orientations) compared to double clear and double tinted glazing. ▪ Clear double glazing caused a 7% increase in cooling loads in S, E, & W orientations, 2% increase in N. ▪ S, E, and W orientations always had same reduction/increase in cooling loads.
(Hashemi, et al., 2010)	Tehran, Iran	EnergyPlus v.2.1	Yes	No	No	▪ Single vs. double façade ▪ 4 orientations	▪ Cavity temperature ▪ Cooling loads	▪ Simulations overestimated cavity temperatures in summer, & sometimes underestimated the cavity temperatures during the daytime in winter. ▪ Both simulated and measured results indicate that the NW DSF is the warmest in the summer, and the SE is the warmest in the winter. ▪ Cooling loads in daytime were reduced, however during the night they increased due to the lack of night ventilation in the office rooms. ▪ Despite the lack of shading devices, and the use of single glazing in both the outer and inner facades layers, natural ventilation alone was able to improve the overall performance.
(Radhi, et al., 2013)	Al Ain, UAE	Design-Builder 2.1 & Pheonix CFD	No	No	No	▪ Single vs. double façade ▪ 4 orientations ▪ 3 glazing properties for outer layer ▪ 5 cavity depths	▪ Cavity temperature and airflow ▪ Cooling loads	▪ Cavity temperature is not much different than the air temperature outside due to the presence of openings along the cavity height. ▪ The DSF has lower heat transfer rates than the single façade in all orientations except the North, but with varying degrees. 17% to 18% estimated reduction in cooling loads. ▪ The North can lead to a 3% increase in cooling load. ▪ Recommended cavity depths: 0.7 m and 1.2 m. ▪ Optical properties of the screen, particularly SHGC & U-value, are the most effective way to reduce cooling loads.

3.6 Observations

3.6.1 Design guidelines for hot climates based on reviewed literature

For the context of hot climates, it is concluded that double facades could be used and the following design aspects were observed to be the most important for the successful use of double facades:

- Multiple openings in the outer layer to ensure sufficient ventilation of the cavity.
- Shading elements placed externally and not in the cavity.
- Use of shading devices with a high thermal mass.
- Recommended cavity depth range: 0.7 m to 1.2 m.
- Cavity should be higher than ground level and higher than roof level.
- Low Solar Heat Gain Coefficient of the outer glazing is very important.
- Double façade is preferably placed in the leeward side of the building where the highest pressure coefficients take place. Airflow in the cavity is lowest when the wind is parallel to the façade.

Shading devices

Generally if a shading device is used in a DSF it is usually placed inside the cavity as it would be protected from external weather conditions and easily maintained. However it affects airflow depending on its geometrical configuration and position within the cavity and it also absorbs heat which increases cavity temperature. Since most research and applications regarding double facades are in temperate climates, this was not a major issue. When considering hot climates, it is important to decrease heat gain as much as possible inside the cavity, therefore shading devices might be placed outside despite being exposed to the weather. Preferably it should have a high thermal mass.

It was surprising that among the presented examples, shading devices were only used in the study of Baldinelli (2009) despite being all in hot climates thus requiring shading elements. When shading devices were not used, then strong attention was given to the glazing properties of the external façade layer. It was also surprising that single glazing is used in the outer façade layer of existing DSFs in Hashemi, et al. (2010) and Radhi, et al. (2013).

Cavity depth

It is important to note that the effect of cavity depth in particular on the façade's performance is somewhat tricky. Stec and Paasen (2003) in Poizaris (2006) point out that in general, as the cavity gets thinner, the flow resistance increases and the convective heat transfer increases causing increased air temperature in the cavity and an improvement in the stack effect. They estimate that the flow resistance can be negligible if the cavity depth is equal to or greater than 40 cm. In hot climates, it is difficult to say for certain whether thin or deep depths are better because in one case the cavity temperature is higher and in another case the temperature of the shading device (if it is placed in the cavity) is higher.

The decision regarding the cavity depth is influenced by many other factors such as aesthetics, presence/type of shading device, need of maintenance space and the ventilation strategy selected for the cavity, whether is natural, mechanical or mixed.

To the author's knowledge, up to the date of writing this thesis the following aspects were not yet investigated in the context of hot climates:

- Different wind directions: which was more studied in temperate climates and it was found that double facades are more effective in the leeward side of the building.
- Different geometrical configurations for the outer layer and shading elements other than the classic flat fully glazed façade.
- The effect of low Solar Heat Gain Coefficient which greatly reduces heat gain on the resulting amount of daylight entering the occupied spaces.
- The climate in Cairo is not as extreme as that in the UAE and other gulf countries, which opens up the possibility of natural ventilation for at least in some part of the year.
- Cooling the air in the cavity to be used for natural ventilation in the occupied spaces.

3.6.2 Importance of simultaneous study of daylight and thermal performances

As seen from literature review, the daylight performance has been rarely addressed alongside its thermal performance. This is particularly important in hot climatic areas where shading devices, small window sizes or highly reflective glazing (which clearly affect daylight performance) are needed in order to reduce heat gain in the cavity. It is important to note that studying the daylight performance along with different façade configurations was only addressed by Hamza et al. (2007). It was the only example found (to the author's knowledge) that studied both daylighting and thermal performances of double facades in a hot climatic area.

3.6.3 Accuracy of the AFN

The advantages and limitations of the AFN have been mentioned in section 3.4.1. Examples have been presented of studies that applied the AFN in simulating the performance of DSFs and compared these results to actual measurements. It has been observed that there are different opinions regarding the accuracy of the AFN.

Mateus et al. (2014) showed that there was good agreement between measured and simulated air and radiant temperatures, given that the DSF digital model was divided vertically into three thermal zones. Hashemi et al. (2010) saw that the cavity temperatures were overestimated in summer and underestimated in winter, however both simulated and measured values indicated that the NW orientation is the warmest in the summer, and the SE is the warmest in the winter. This study is the only one found to compare measurements from an existing office building at different heights and not a typical single-storey test cell. Kalyanova, et al., (2009) occasionally observed good accordance with simulated and measure data, but it was not consistent. Kim & Park, (2011) observed significant errors in cavity temperature, and some errors in airflow values depending on the configuration of openings.

It can be observed from these studies that the AFN can sometimes produce reliable results but definitely not always. At least we can say that it can somewhat *point us* to the right direction as in the case of Hashemi et al. despite the numerical errors.

It is also important to emphasise that almost all the reviewed examples were of flat DSFs with fully glazed outer skins. No complex geometrical configurations were studied, either in cold or hot climatic areas. So it is expected that the errors of the AFN would be even more if the geometry of the DSF was more complicated. Nevertheless, the AFN remains almost the only feasible way for designers to have a basic understanding of their DSF proposals at least in early conceptual phases.

3.7 Summary

This chapter presented a brief overview of DSFs focusing on their application in hot climatic areas and the simulation methods often used to predict their daylight, airflow and thermal performances. These three elements interact and affect each other and the final performance of the building skin, hence simulating their behaviour all together is a complicated task.

DSFs in hot climates are somewhat controversial as they may lead to increased energy consumption. After outlining design guidelines available in existing literature, case studies of DSFs specifically in warm/hot climates were presented since most other researches focused on cold climatic areas. Hence a number of design guidelines and considerations were observed to be the most important for the successful application of DSFs in *hot* climatic areas as discussed in sections 3.6.1 and 3.6.2.

The most common simulation methods used are backward Raytracing for daylighting, and the Airflow Network model for general thermal and airflow simulations and for annual building energy simulations as well, and finally Computational Fluid Dynamics for very detailed simulations of a part of a building in very brief moments in time. These methods will be applied in this thesis in forthcoming chapters, and the software chosen are Radiance for daylighting, EnergyPlus for the early design phase and OpenFoam for the verification of the results of EnergyPlus. The benefits and limitations of these methods have been outlined, indicating that there are attempts to couple the AFN and CFD together in order to compensate for each other's' limitations.

The brief review presented in this chapter serves as a background for the design development of the biomimetic skin that will be proposed in chapter five. Part Two of this thesis begins in the following chapter. It represents the empirical phase of this research in which the application of the biomimetic-computational design method begins.

Chapter 4:
Biomimetic Inspirations & Analyses

4.1 Introduction

After reviewing biomimetic-computational design and Double-Skin Facades in Part One of this thesis, in this chapter the biomimetic design process commences as a means of exploration for innovative ideas for thermoregulation problems in building skins.

The applied biomimetic design methodology is a problem-based approach, which means it starts by defining specific design problems and then search for parallels in nature. More specifically, this chapter will focus on the *searching* phase in an attempt to prepare a list of possible solutions that either reduce heat gain or increase heat loss to adapt to hot climatic conditions.

The process of searching and exploring nature could be done by multiple ways. One way is to start looking in same habitat of the design problem at hand, as organisms in the same habitat would be the most adapted to this specific environment. However, solutions to the same problem could also be seen by organisms belonging to different habitats as well such as the behaviour of burrowing and seeking shelter underground which is seen in both extreme hot and cold environments (as shown in Figures 4.1 and 4.2). Therefore exploring native organisms is preferred but will not be a limit to this search.

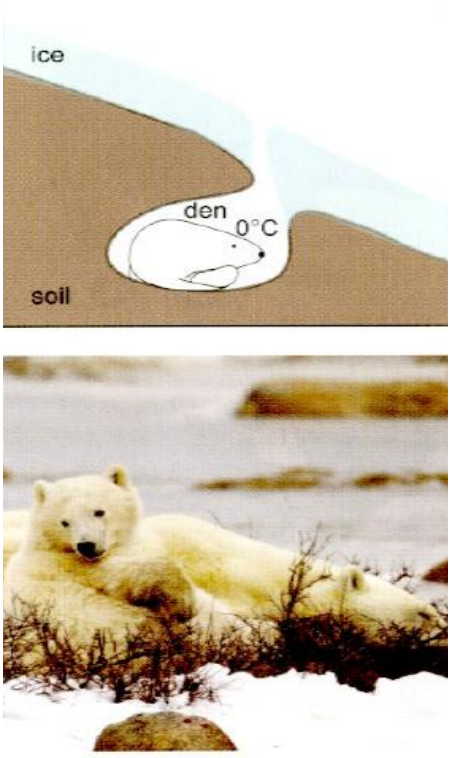

Figure 4.1: Polar bear seeking shelter underground from extreme cold (Mazzoleni & Price, 2013)

Figure 4.2: Sidewinder snakes use abandoned rodent burrows. The snakes use them for protection from predators as well as the hot and cool extremes of desert climate.
Source: http://education.nationalgeographic.com/education/encyclopedia/burrow/?ar_a=1.

Another way is to investigate the online database; asknature.org which works on categorising biological literature based on function to facilitate the search and retrieval of the solutions to each function. Another benefit is to link designers with the biologists (and other researchers) who have presented their work on the database. In parallel, it is useful to explore work done in similar research to benefit from and build upon work already achieved and to avoid duplication. Finally, going directly to biologists is another important way, whether to seek detailed explanation of a certain organism or to have some suggestions of organisms to look up.

Since the main concern of this research is thermoregulation in hot climates then the design goal is the minimisation of heat gain and maximisation of heat loss through the building skin. Heat is transferred by one of four processes:

- Radiation
- Conduction
- Convection
- Evaporation

Therefore the output of the searching phase of living organisms will be categorised depending on the means by which they regulate heat, which is one of these four processes. Then each organism will be analysed in order to understand exactly how did it regulate heat, then its strategy would be simplified and abstracted to facilitate the identification of the potential corresponding architectural feature(s).

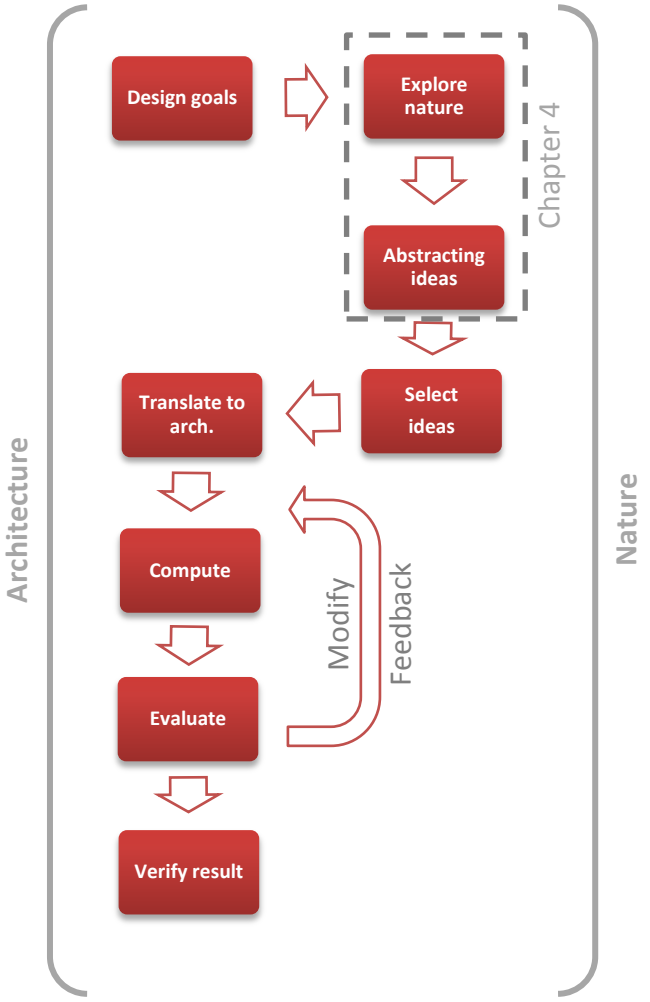

Figure 4.3: Scope of this chapter within the biomimetic design process. Source: author.

By the end of this chapter there would be numerous organisms and possible ideas. It is therefore necessary to undergo a selection process based on:

- The coherency of the chosen ideas together in one design solution (minimum conflicting ideas)
- Whether or not the idea is multi-functional (such as serving structural and environmental purposes simultaneously as in nature)
- The applicability of the chosen idea using parametric design means (which means the possibility of *quantifying* and translating the design idea into geometrical and mathematical relationships)

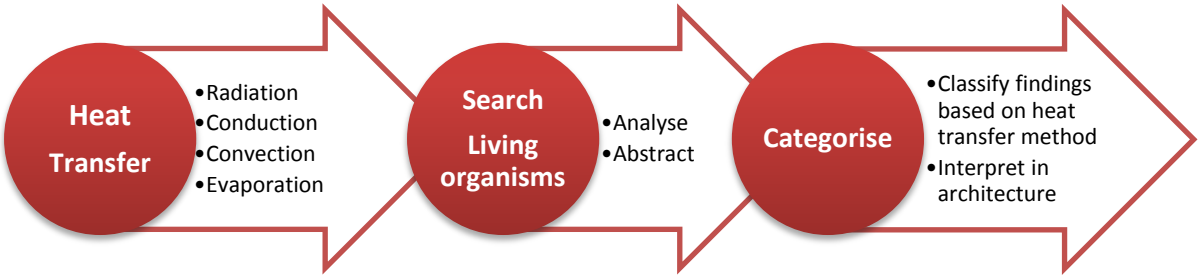

Figure 4.4: Methodology followed in this chapter. Source: author.

Thermoregulation in nature

Mazzoleni and Price (2013) provide an overview regarding thermoregulation in nature as follows. Living organisms fall into two main categories in terms of their metabolism. Ectotherms, including invertebrates, reptiles and fish, obtain most of their required heat from their environment. Endotherms, which include mammals and birds, produce their own energy by metabolic processes enabling them to maintain a rather constant body temperature (thermal homeostasis).

Many strategies were evolved by animals living in extreme hot arid climates to prevent overheating. These strategies are both physical as well as behavioural. Examples include being light in colour to reflect heat, having long limbs to be farther from the ground, having more blood vessels near the surface of the skin in order to increase heat loss, staying active only at night and dawn, taking refuge underground, in pools of water if available, and even going into a type of dormancy called estivation within the hottest months of the year.

The issue of an animal's ratio of surface area to its volume is very important when the idea of heat gain and loss is considered. When a shape gets bigger in size, its surface area with respect to its volume decreases. This means that larger animals are better in maintaining their body heat when compared to smaller ones, because the surface is where the heat is gained and lost to the environment. This explains why big animals tend to exist in cold climates, where smaller animals tend to exist in hot ones. In cases of relatively big animals existing in hot climates, they tend to have less fur, and longer, bigger extremities (such as big ears and long limbs) to facilitate heat loss.

Contrasting to hot climates, other animals have adapted to living in extreme cold environments. Adaptations include having some sort of thick insulation taking the form of fur, feather, or fat. Fur and feather have the ability to trap warm air pockets, and release them when required. Some animals could curl up while sleeping to decrease heat loss, others evolved a counter-current heat exchange system that enables them to warm up cold blood coming from limbs using warm blood pumped by the heart. Some types of fish and insects have evolved a kind of protein that prevents ice from forming in their bodies. Other behavioural strategies include gathering up in groups, hibernating, digging up dens and burrows.

There are four main mechanisms through which heat is gained and lost (Lienhard IV & Lienhard V, 2016). These mechanisms are explained in the following section, highlighting the specific building skin features that are most relevant in each mechanism.

4.2 Heat Transfer

4.2.1 Radiation

Radiation is the process of heat transfer by electromagnetic waves through space or air from a warm object to a cooler one. All objects (whether living or not) release and receive heat from the surrounding objects. The sun is the best example in this case, emitting heat mostly in the form of visible light. Other objects on the earth mainly radiate heat in the infrared range but behave exactly the same. This means that if two objects can '*see*' each other, they will exchange heat. If a barrier comes between them, then this direct exchange is blocked. This is what happens when we are in the shade of a tree, which is a barrier between us and the sun (Lienhard IV & Lienhard V, 2016).

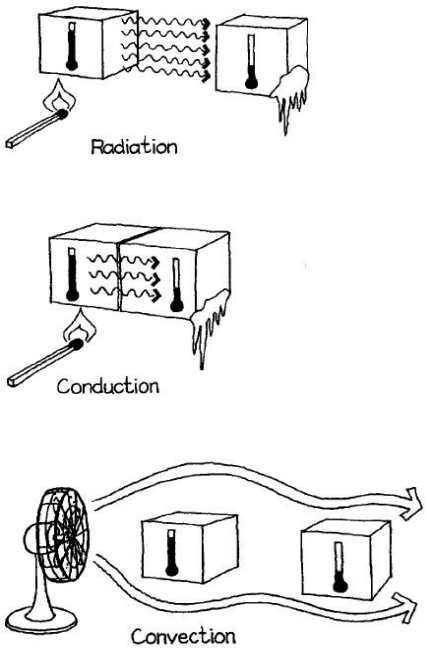

Figure 4.5: Heat transfer processes in buildings (Allen, 2005).

Buildings are exposed to two kinds of thermal radiation; solar radiation coming from the sun which has an extremely high temperature and therefore heat is emitted in short wavelengths, and thermal radiation emitted from surroundings (such as surrounding buildings, ground, people and vehicles) which have relatively low temperatures and therefore emit heat in long wavelengths. It is important to note that buildings react quite differently to these two kinds of wavelengths. For example, white paint is an excellent reflector of solar radiation, but in contrast it only reflects about 10% of heat emitted from its surroundings. This is useful to be put in consideration when choosing building materials, depending on its context (Allen, 2005).

Natural daylight is very important both for the reduction of artificial lighting and for the wellbeing of building occupants. However, the study of natural lighting should be carefully studied along with sun-protection systems to achieve a critical balance between optimum daylight and prevention of unwanted short-wave and long-wave spectrum of solar radiation.

The location of sun protection system in a building has a direct impact on its energy consumption and comfort levels. Studies have shown that cooling loads could be halved when external blinds are used on conventional east and west facades if compared to a glass façade without sun screening. In the case of external screening elements (especially movable ones) it is important to consider the local climate condition, especially wind resistance as strong winds could lead to maintenance problems. However, the use of internal blinds could only decrease energy consumption by 20% as they have the disadvantage of absorbing and transmitting solar radiation into interior spaces (Schittich, 2001).

Specific building skin features according to the researcher which affect the transfer of heat by radiation include:

- Size and shape of openings for day lighting.
- Shading elements.
- Morphological features such as the colour and texture (self-shading) of the skin.
- Reflectance and emittance of the external surface of the skin.

4.2.2 Conduction

Conduction is the transfer of heat through a solid medium which occurs when two objects come into contact and heat is transferred from the warmer to the cooler one. A material's ability of resisting this flow of heat (insulation) is measured by its thermal resistance which is one of the important factors affecting the rate at which the building gains or loses heat. Usually designers tend to choose materials with maximum possible thermal resistance for thermal comfort as well as energy saving. The effectiveness of an insulating material depends on the position in which it is placed in the building skin with regards to the direction of heat flow, as it is usually placed close to the point of heat flow entry.

It is worth noting that every surface has a thin surface film of still air caused by friction between this surface and the surrounding air. This thin film becomes thicker as the roughness of the surface increases. This is why fur for example has great insulating properties as its roughness traps more air than other flat surfaces. Thermal capacity is another material property that affects conduction. It is the ability of a material to store heat, and is usually proportional to the mass of the material. Designers often combine materials with high resistance with others of high thermal capacity to achieve desired thermal performances (Allen, 2005).

Specific building skin features according to the researcher which affect the transfer of heat by conduction include:

- Thermal resistance (insulation) and thermal capacity of the building materials
- Arrangement of materials
- Thickness of materials
- Texture of skin

4.2.3 Convection

In convection, heat is carried away by a stream of moving fluid, be it gas or liquid, which is heated by a warmer object then release this heat to a cooler one. The fluid that is directly adjacent to the body forms a very thin region called the Boundary Layer in which its velocity is very low. Heat is first conducted to this layer then it is swept away by convection (Lienhard IV & Lienhard V, 2016).

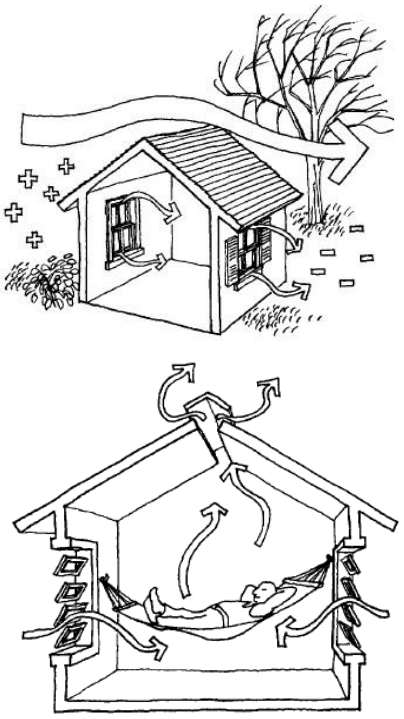

Figure 4.6: Types of air flow in buildings; either wind-driven (above) or thermally-driven (below) (Allen, 2005).

Thermal comfort requires the continuous movement and circulation of air, to remove excess body heat and evaporate perspiration. Any ventilation system in a

building has four main components: a source of air (of adequate temperature, moisture content and cleanliness), a moving force, a controlling mechanism, and a recycling mechanism for old air. The most basic ventilation system is a natural one. Outdoor air is its source, and the moving force could be either the wind (forced convection), or buoyancy (free convection). Air circulates within a building because of its tendency to move from areas of high pressure to areas of lower pressure.

In the case of buoyancy, the difference in pressure is formed by different densities of warm and cool air, which causes warm air to rise up. The rate of ventilation in this case depends on the distance between the openings and on the difference in temperature between the warm and cool air. In the case of wind, air flows from one side of the building with high pressure to a lower-pressure area on another side. The use of either or both of these two cases is determined by the designer and depends on the climatic conditions (Allen, 2005).

Specific building skin features according to the researcher which affect the transfer of heat by convection include:

- Ventilation system
- Size of openings
- Location of openings
- Humidification/dehumidification elements

4.2.4 Phase-change

Heat could also be gained or lost when a given substance changes its physical state from one to another (as from gas to liquid, liquid to solid, etc.). Latent heat is the amount of energy absorbed or released by a substance during a change in its physical state that occurs without changing its temperature (Encyclopædia Britannica, 2013). Lienhard IV and Lienhard V (2016) refer to heat transfer in this method in particular as mass transfer. For example when water is exposed to dry air, its vapour pressure can produce a relatively high concentration of water vapour in the air that is closest to the water surface. The difference in concentration of water vapour in the air and that in the water surface drives the diffusion of vapour into the air stream. The process of evaporation is the most known and experienced by humans and therefore is explained in more detail.

The human body performs a number of processes in order to maintain its temperature within tolerance. It could be cooled by warming respired air, by diffusing small quantities of water vapour through the skin, by convection, and by radiation. When the body needs to be cooled furthermore, we sweat. The skin produces water which evaporates into the air, and the latent heat of vaporisation required for this evaporation is lost by the body and therefore it is cooled. The effectiveness of this process depends on the existing moisture content of the air. If the air is dry then perspiration evaporates rapidly and the body is cooled even if the air temperature is higher than the body. However, if the humidity of the surrounding air is high, then evaporation is slow and perspiration accumulates on the body causing an uncomfortable feeling. It is therefore important to consider the humidification (in case if extreme dryness) or dehumidification of the air to enhance thermal comfort (Allen, 2005).

However, since we are currently dealing also with buildings (not just living beings) and their constituent materials, therefore according to the researcher it was better to generalise this type of heat transfer so that it would include the heat lost or gained from the change of a material from *any* physical state to another not just from liquid to gas an in the case of vaporisation. Other cases include condensation and freezing. Phase-change materials that have a large value for latent heat are being continuously studied for thermal energy storage. Within the last forty years numerous types of materials have been studied, and among the most common are paraffin waxes and hydrated salts (Farid, et al., 2004).

Specific building skin features according to the researcher which affect the transfer of heat by phase-change include:

- Humidification/dehumidification elements
- Ventilation system
- Use of phase-change materials

With the aim of reducing heat gain and consequently improving thermal comfort and reducing cooling loads, the physical processes of heat transfer were selected for further study to address this aim. There are numerous building features that affect heat gain and loss, this research will focus only on features related to the building skin. Figure 4.7 summarises the features of the building skin that are affected by each method of heat transfer.

In the following sections a number of inspirations from nature are investigated. They will be analysed and each inspiration will be categorised based on the main method of heat transfer. This facilitates linking it with the potential building skin feature to which it can be applied.

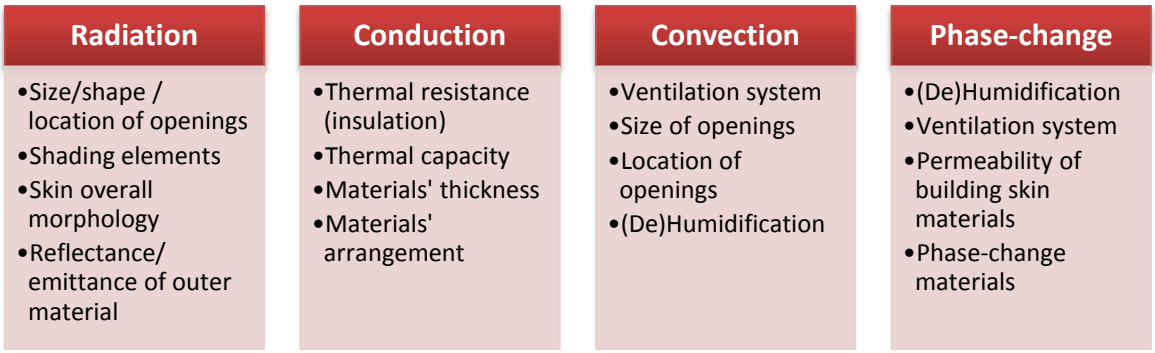

Figure 4.7: Heat transfer processes and the related building skin features. Source: author.

4.3 Trees and plants

Introduction

Climatic conditions have an important influence on the forms and functions of living organisms that were evolved as means of survival. Trees and plants are flexible structures that are sensitive to climatic conditions and as a response, they have evolved a number of techniques and features that aid in overcoming such situations. These features aid in thermal regulation either by minimising heat gain, or maximising heat loss. In the following section, leaves, tree barks and succulents will be addressed and analysed to explore *some* of the strategies which they have in general to aid in thermoregulation. Strategies that depend on bio-chemical processes are not presented here.

4.3.1 Leaves

Leaves are physical and biological entities that are extremely differentiated, either on the level of different species, or even within the same one. The huge variation of shapes and sizes of leaves have long been a topic of research, indicating that it is a part of an adaptive response to different climates, and different microclimates within the same tree or plant (Schuepp, 1993).

They only absorb the energy required for photosynthesis (which is a sensitive process and occurs within a temperature range between 30 and 40 degrees Celsius) and the energy required for the tensile water transport upwards along tree barks (Henrion & Tributsch 2009; Zähr, et al. 2010).

It is worth noting that leaves depend on two types of convective heat loss; thermally-driven (free) convection in the form of upward flows, and wind-driven (forced) convection represented in lateral air movement, which is the most effective. An individual leaf will experience the free convection of neighbouring leaves as forced convection on itself. In the case of lack or insufficient air movement for forced convection, some leaves experience temperatures up to 20°C above ambient air temperature creating a challenge for leaves in warm and windless spaces (Vogel, 2009).

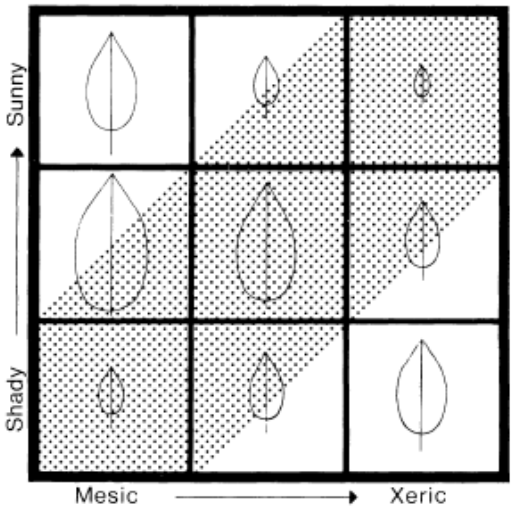

Figure 4.8: Optimal leaf size in different situations ranging from mesic (moisture-abundant) to xeric (dry) environment, and from sunny to shady situations. The stippled area indicates the range of habitats likely to be encountered in nature (Givnish & Vermeij, 1976).

Five strategies are discussed here that are likely to decrease the effect of very low air movement and full sunlight in warm climates. Comparisons have been made between sun leaves and shade trees of species mainly in North America, and have found that sun leaves have features that resemble those of leaves located in hot habitats, and therefore will be presented (Schuepp, 1993, Vogel, 2009, Givnish, 1988 and Ehleringer, et al., 1976):

- Size

Smaller and narrower leaves have evolved as they have thinner boundary layers[11] (BL) and therefore less resistance and more heat loss by convective dissipation as seen in Figure 4.9. For example, it has been found that warm environments and seemingly still air, broad leaves could reach 20°C above ambient temperature while relatively smaller conifer leaves (such as pine, spruce and fir) reached only 10°C (Vogel, 2009).

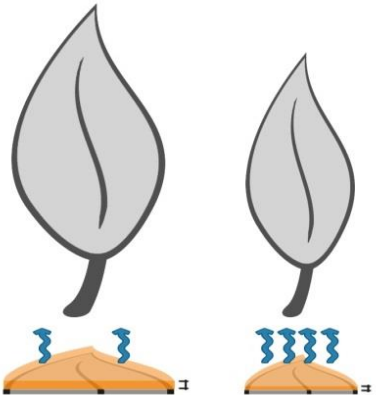

Figure 4.9: Smaller leaf size decreases the boundary layer resistance hence improving free convection. Source: author.

- Shape

The shape of the leaf also has a role, as temperature on a given point on a leaf increases approximately with the square root of the distance from an edge (Vogel, 2009). So this distance decreases if a leaf is lobed, dissected or pinnate and narrow in addition to being smaller in size. Lobes and serration in leaves decrease the boundary layer resistance and improve free convection (Schuepp, 1993). Winn (cited in Vogel, 2009) made some field experiments comparing dissected and cordate leaves of *Viola septemloba*, and found that the dissected leaves were substantially cooler. He also found that around 73% of leaves took the lobed form in winter, while in summer they were only 12%.

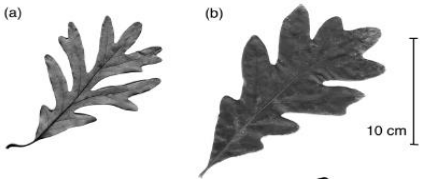

Figure 4.11: difference between a sun leaf (left) and a shade leaf (right) of white oak (*Quercus alba*). Sun leaf is smaller and more lobed (Vogel, 2009).

Figure 4.10: difference between a cordate leaf (left) and a lobed leaf (right). Lobes improve free convection (Wikipedia, 2016).

A trick that un-dissected or un-lobed leaves have evolved by time to overcome excessive heat gains in the summer is producing phytochemicals which lures certain types of insects to produce non-lethal holes in its blade. These holes permit buoyancy-driven convective airflow through the leaf rather than around it. Leaf tearing has also been observed in large leaves such in the banana (*Musaceae*) in hot environments as a similar protective mechanism (Schuepp, 1993).

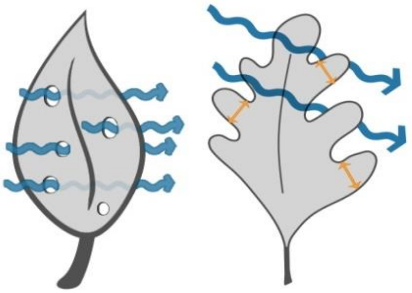

Figure 4.12: Holes (left) and lobes (right) in leaves decrease the distance to the closest edge and decrease the boundary layer resistance and improve free convection. Source: author.

Another observation regarding the form of leaves is that some have evolved a folded form that enables young leaves to fit inside small buds. This form allows self-shading and hence reduces heat gain. There are numerous folding patterns in plants (Patil & Vaijapurkar, 2007); among the well-known is common beech (Fagus

[11] Boundary layer (BL): a thin zone on the surface of a leaf where air does not move due to surface friction. For transpiration to take place, water vapour must pass this layer to reach the atmosphere. The bigger and wider the leaf, the thicker the boundary layer becomes and therefore resistance to transpiration increases (Schuepp, 1993).

sylvaticus) as seen in Figure 4.13, and hornbeam (Carpinus betulus) leaves. The leaves have a central primary vein and secondary parallel veins arranged symmetrically about the main one (Kobayashi, et al., 1998). This folding pattern is the inspirational source of a two-dimensional expandable array proposed by Miura (1980) for the design of a solar pattern, and is still inspiring researchers today.

Figure 4.13: Leaf of common beech tree (Fagus sylvaticus) in folded and unfolded states (Kobayashi, et al., 1998). Schematic cross-section (right) though a folded leaf, indicating that the folds shade parts of the leaf from incident sunlight. Source: author.

The concept of leaf folding exists also in a more dramatic fashion, where leaves could dynamically fold at night, or in response to certain stimuli such as touch (either responding environmental stimuli like rain, or for trapping insects) and excessive heat. An example is the leaf folding shrub (Mimosa pudica), commonly called as "Sensitive Plant" as it quickly folds and droops downward when touched (Patil & Vaijapurkar, 2007). The study of geometry and folding patterns of such leaves might be particularly useful in the design of an adaptive responsive building skin.

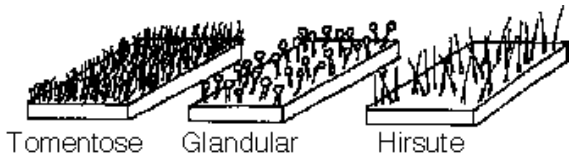

Figure 4.14: Three examples of numerous possibilities of leaf pubescence (Wilson, 2016).

- Orientation

The effects of changing orientation are usually seen in un-lobed leaves. They tend to avoid near-horizontal positions reduces incident radiation in addition to improving convection between the leaf blade and surrounding air. Mangrove leaves are a good example where sun leaves are almost vertical while shade leaves are almost horizontal. Some leaves are capable of rotating throughout the day to adjust their position and reduce heat gain such as the *Alibizzia* (julibrissin) leaves (Vogel, 2009).

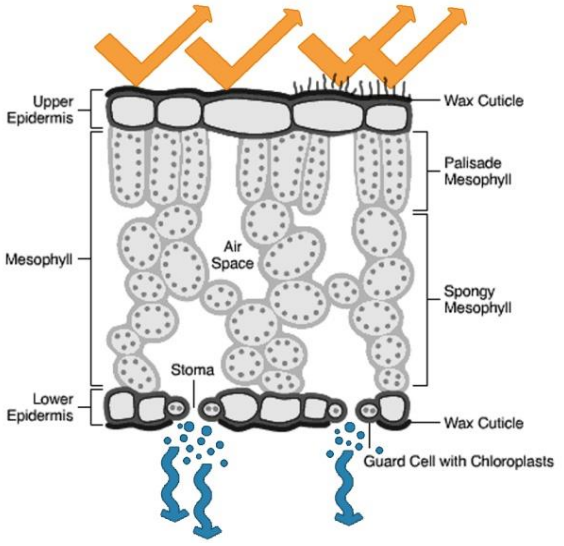

Figure 4.15: Schematic cross-section through leaf indicating a reflective upper surface either by was or pubescence to minimise incident radiation. Stomata openings in the lower side are responsible for evaporative cooling.

- Leaf surface

Another way of reducing incident radiation is by decreasing absorptivity. Silvery and shiny leaves have around 20% less absorbance than others (Nobel, 2005 in Vogel, 2009). Thus the presence of a waxy coating for reflection proves useful. Pubescence (leaf hair) as shown in Figure 4.14, has been observed as a feature of plants in arid climates, because they reduce the heat load of leaves by increasing

the reflectance from the leaf surface which reduces amount of radiation absorbed (Ehleringer, et al., 1976). Pubescence also affects the leaf boundary layer in different ways. Widely distributed hair decreases the effect of this layer's resistance, while dense hair traps the air and therefore the boundary layer thickens (Schuepp, 1993).

Stomata distribution is another very important aspect that leaves have evolved, since sun leaves general have more stomata per unit area than shade leaves (Vogel, 2009). Increased stomata mean better heat loss through transpiration; it has been observed that sun leaves could transpire up to 12 times faster than shade leaves. This feature is particularly important in the case of very low speed of air movement where free convection becomes dominant (Schuepp, 1993). However, it is only beneficial in water/moisture abundant environments where plants can afford to lose water to cool through transpiration.

- Venation system

Venation systems have two main functions which are transporting substances from one point to another with the least investment in energy and mass and sustaining the mechanical behaviour and structural support of leaves (Kull & Herbig, 1994; Nebelsick, et al., 2001). However, this research is interested in the contribution of venation systems to the thermoregulation of leaves, as they transport water which is vital for cooling by transpiration.

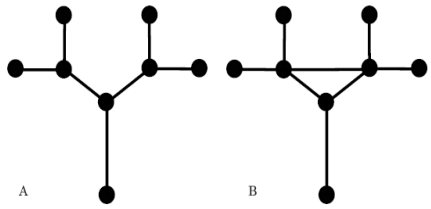

Figure 4.16: Types of venation systems; open (left) & closed (right) (Nebelsick, et al., 2001)

The wide variety of venation patterns imply a strong evolutionary selective process, however the functional background of this variety is still not well understood (Nebelsick, et al., 2001; Sack, et al., 2012). Nevertheless, studies addressing this issue show general differences between sun leaves vs. shade leaves within same species, and between leaves in hot climates versus temperate ones. These observations are summarised as follows:

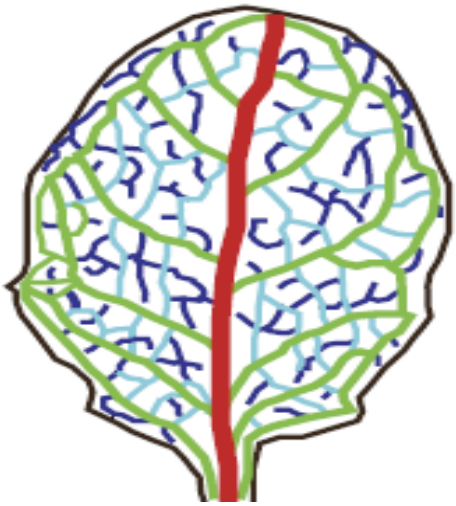

Figure 4.17: Diagram illustrating orders of veins. Red: 1º, Green: 2º, Cyan: 3º, Blue: 4º. Leaves could have orders up to the 7th degree. The first 3 degrees are the ones considered major veins (Sack, et al., 2012).

Regarding the venation type; closed venation systems (Figure 4.16) occur more frequently than opened ones in areas with less water availability than others. This could be due to the fact that in closed systems there are multiple paths available to reach a certain point so the water could take the shortest possible one. Another reason is the increased safety when compared to open systems, if one path is damaged due to injury then water and other substances could still reach areas beyond the damaged route due to the existence of other alternative bypasses. A third reason is the capability of providing homogeneous pressure difference across a leaf in the case of varying stomatal opening degrees and varying transpiration rates (Nebelsick, et al., 2001).

Regarding venation density and radii; studies have shown that with decreasing leaf surface area (as seen in sun leaves and in hot climates) the diameters of only the *major* veins (Vein hierarchy shown in Figure 4.17) decreases, but their density increases (density= vein length per unit area), minor veins however are independent of leaf size. Smaller diameters come with less vascular costs to construct them, and higher densities provide a redundant 'super highway' system for water transport which contributes to drought tolerance by easily routing water around blockages caused by drought and protecting the overall hydraulic system from vein damage (Sack, et al., 2012; Kull and Herbig, 1994).

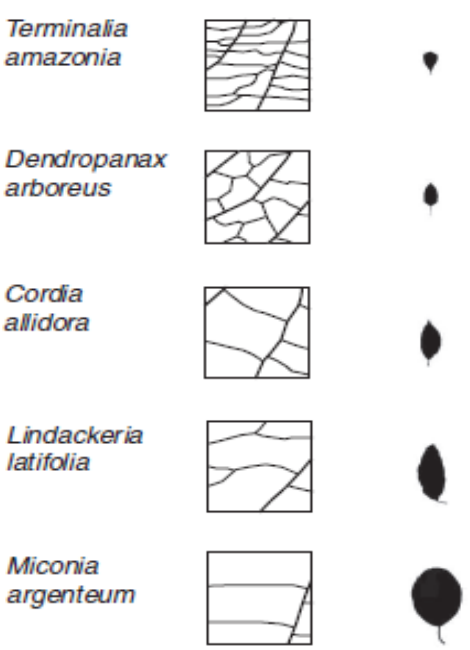

Figure 4.18: General decrease of major vein density with the increase of leaf size (Sack, et al., 2012).

Summary of leaf strategies

Table 4.1: Summary of leaf strategies for thermal regulation. Source: author.

Strategy	Description	Feature	Main principle
Small, narrow size	It decreases Boundary Layer resistance enhancing heat dissipation by convection	Size	Increase loss by free convection
Lobes and dissections	This decreases the distance from any point on the leaf to the closest edge thus decreasing its temperature, & decreases the Boundary Layer resistance	Shape	Increase loss by free convection
Holes	Holes permit air to pass through the leaf & decreases the Boundary Layer resistance	Shape	Increase loss by free convection
Tears	Tearing permits air to pass through the leaf and decreases the Boundary Layer resistance	Shape	Increase loss by free convection
Folds	Folds result in parts of the leaf to be constantly in the shade	Shape	Decrease incident radiation
Avoid horizontal position	Decreasing the angle of incident light reduces heat gain	Orientation	Decrease incident radiation
Shiny surface	Increasing the reflected portion of solar gain decreases the absorbed portion	Surface Texture	Decrease incident radiation
Pubescence	Hairs increase reflection and in some cases decrease the Boundary Layer resistance	Surface Texture	Decrease incident radiation and Increase loss by free convection
More or bigger stomata	Increase the leaves' ability to lose heat through transpiration	Molecular surface properties	Increase loss by evaporation
Venation system	Efficient transportation of fluids throughout the leaf	Internal structure	Increase loss by evaporation (indirectly)

4.3.2 Tree Stems

a) Bark

Leaves are not the only tree elements that contribute to cooling and thermal regulation, but also tree barks have an important role.

Tree barks have always attracted people's attention due to their appearance. Despite their diversity that makes it seem difficult to find common thermoregulation strategies, they all serve the function of efficiently delivering water to leaves. And since leaves (usually) could sustain temperatures no more than 40 to 50 degrees Celsius, the water that reaches them must therefore be cool even in hot environments. Excessive heating could also affect the tensile water flow in the Xylem[12] tissue below the bark (Henrion & Tributsch, 2009).

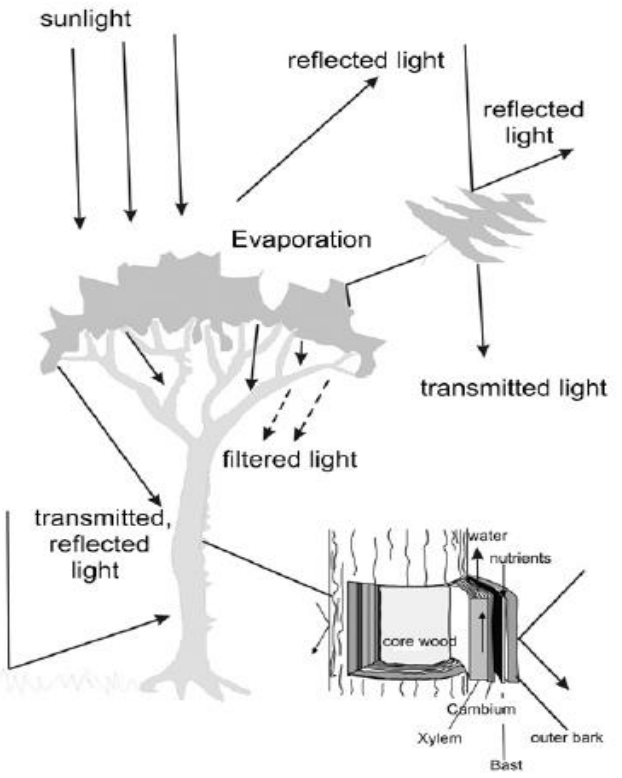

Figure 4.19: Drawing of crown, leaves, and bark of a tree visualizing their involvement in optical atmospheric processes (Henrion & Tributsch, 2009).

Unlike leaves, barks are not capable of cooling by evaporation. Therefore they have evolved other strategies to remain cool. These include morphological ones such as:

Figure 4.20: Different bark morphologies. Barks of Araucaria (Auracariaauracana; left), Canary Island pine (Pinus canariensis; center), and Cuivertree (Aloe dichotoma; right) (Henrion & Tributsch, 2009).

- Barks are usually round, which means they have the minimum exposed surface area to incident solar gain and surrounding temperature thus preserving its own internal temperature as much as possible.
- Barks have a very thick insulating outer layer, which in some cases can reach 50 cm in thickness (as in sequoia barks).
- Some trees have developed rough bark textures that provide shaded areas thus decreasing the heating effect of incident light.
- Other barks that are not very thick, have evolved an outer layer that peels off like paper, creating air gaps that improve insulation and reduce heat gain by conduction.

In addition to these morphological features, Henrion and Tributsch (2009) noticed that there are features regarding the reflectivity and emissivity of tree barks. Light is usually filtered first by leaves in the tree canopy, this means that in most cases the light that

[12] A type of vascular tissue in terrestrial plants, and is primarily involved in transporting water and nutrient (from the roots to the shoot and leaves) and providing structural support (Biology Online, 2009).

reaches tree barks is either solar light reflected from surrounding vegetation or light that has been transmitted through thin leaves of the same tree, and this kind of reflected and transmitted light has wavelengths that are different from that of direct incident light.

Henrion and Tributsch (2009) made an experiment where they collected eleven different samples of tree barks from different environments to measure their optical reflection and emission properties (see Figure 4.21). They found that tree barks were optimised not for reflecting the visible spectrum of solar light (of wavelengths between 380 and 750 nm), but rather for the filtered (transmitted) and reflected light from surroundings (which is a part of infrared light of wavelengths of 700 to 2000 nm). This was particularly important since infrared light in general comprises about 53 % of incident solar light at ground level, while visible light is 44% and ultra violet is 3% (Nobel, 1991). This gave the importance for refletive properties of skin properties to be considered.

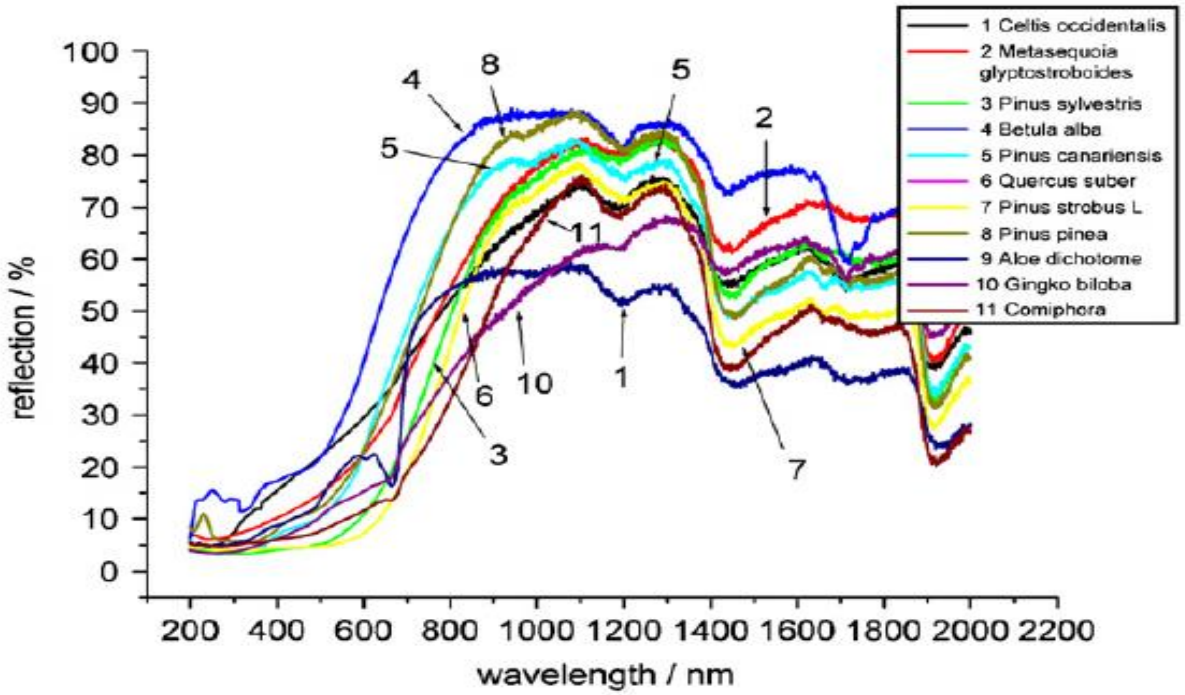

Figure 4.21: Reflection spectra of 11 tree barks from different parts of the world. Reflection is optimised in wavelengths between 700 and 2000 nm rather than within the visible light spectrum (Henrion & Tributsch, 2009).

b) Tree stem vascular system

Investigating into the internal structure of tree stems also may provide interesting ideas. Raven et al. (cited in Yowell, 2011) explained the internal transport system in a tree which generally consisted of two types of conducting tissues; the xylem and phloem, serving two different purposes.

The Xylem is the main water-conducting tissue, transporting water (as well as minerals) in a one-way movement from the roots upwards to different parts of the tree. The upward pull of water is caused by tension and hydrostatic pressure due to water evaporation through transpiration in the leaves. Water lost in leaves creates a negative pressure causing suction of water from the soil (Figure 4.22).

The Phloem hosts a two-way movement of food substances. After photosynthesis takes place in a certain leaf, sucrose is formed and loaded to the phloem tissue creates an increase in sucrose concentration in that particular spot. Sucrose then moves *down* the concentration gradient causing it to move from its source to a sink (where it is needed and used) which could be either up or down the tree (Figure 4.23).

As repeatedly seen in nature, these vascular tissues are multifunctional. Not only serving as the main transport system but also the main structural elements supporting the tree itself.

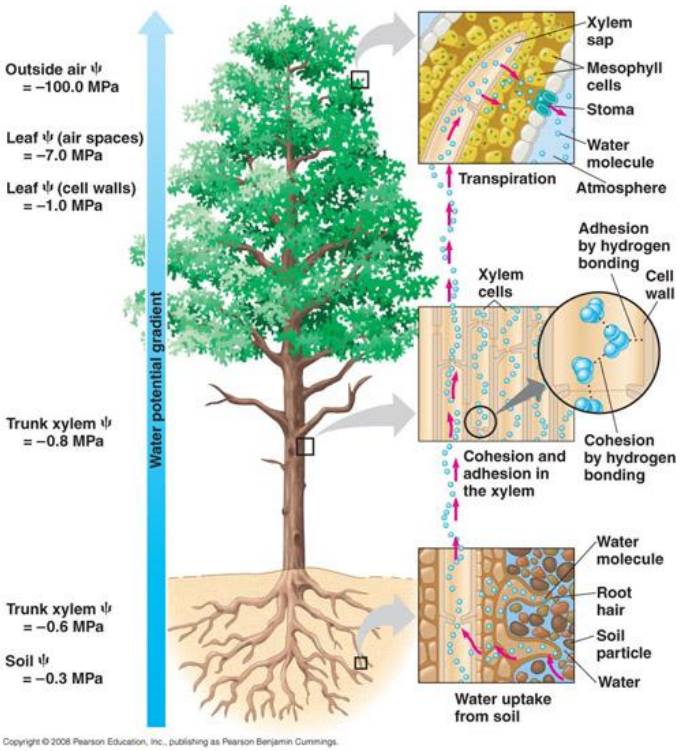

Figure 4.22: Diagram illustrating water following the potential gradient from soil to atmosphere, and is pulled together by the cohesiveness and adhesiveness of the molecules themselves. The negative pressure in the xylem tubes generated this way is known as shoot tension.

Source: http://www.bio.miami.edu/dana/226/226F09_10.html

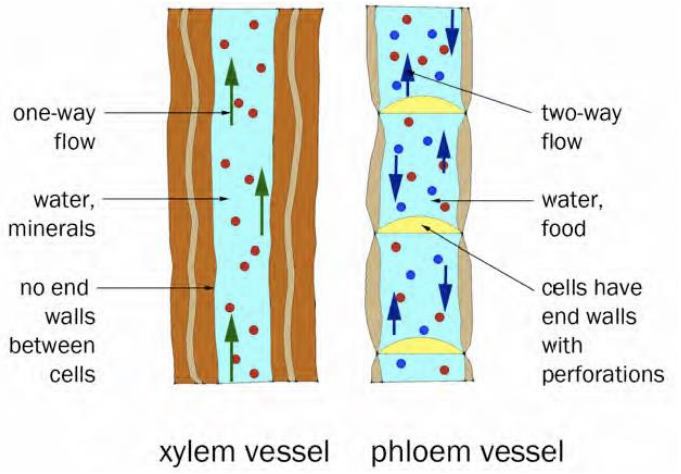

Figure 4.23: Diagram illustrating the main differences between Xylem and Phloem vessels in plant vascular systems (Yowell, 2011).

Summary of tree stem strategies

Table 4.2: Summary of tree bark strategies for thermal regulation. Source: author.

Strategy	Description	Feature	Main principle
Round cross-section	Decreases exposed surface area	Shape	Decrease incident radiation
Thick outer layer	Provides an efficient insulating layer	Shape	Decrease gain by conduction
Rough surface	Increases the area of shaded bark surface	Surface texture	Decrease incident radiation
Peeling surface	Peels create air gaps in between serving as additional insulation	Surface texture	Decrease gain by conduction
Reflection of non-visible light spectrum	Barks are optimised to the reflection of infrared light rather than visible light.	Molecular surface properties	Decrease incident radiation
Water transport through xylem	Water pulled upwards from roots due to evapo-transpiration occurring in leaves	Internal structure	Increase loss by evaporation

4.3.3 Succulents

Succulents are plants that have thick fleshy tissue that has adapted to the storage of water. Some of them such as cacti have no leaves (or very small leaves) and store water only in the stem, while others (e.g. agaves) store water in their leaves. They are native to environments with arid to semi-arid climates and have therefore evolved a number of features that help them survive the hot climate (Encyclopaedia Britannica, 2014).

Figure 4.24: Golden Barrel cactus (left) that has a relatively small surface area to volume ratio, spines, and V-shaped grooves among other strategies that aid in thermal regulation. Cereus schottii (right) has smooth alternate concave and convex surfaces for self-shading and light reflection.
Source (left): https://en.wikipedia.org/wiki/Echinocactus_grusonii
Source (right): http://plantlust.com/plants/lophocereus-schottii-monstrose/).

A number of strategies that desert succulents use for thermal regulation are mentioned as follows (Hadley, 1972; Jones & Rotenberg, 2011):

- The relationship between surface area and mass is one of the important factors that determine the rate of heat transfer between the organism and its environment. Heat transfer through radiation, convection and evaporation is proportional to the surface area of a plant or animal. Since small organisms have relatively big surface area to mass ratio, their temperature increase and decrease more rapidly and are easily influenced by surrounding temperature.

Some large succulents use this concept to their advantage and have a small area to volume ratio such as prickly pear (Opuntia littoralis) and barrel cacti (Figure 4.24, left), so they heat up more slowly.

- Many succulents close stomata during the day and open them at night when the temperature has decreased and relative humidity has increased to decrease water loss by transpiration. In this case the process of photosynthesis occurs at night as carbon dioxide is absorbed and combined with an acid in a process called Crassulacean Acid Metabolism (CAM). During the day this acid is decomposed and the carbon dioxide is released internally so that photosynthesis would be associated with minimum water loss.

- The concept of self shading is widely used among succulents. Varying from spines and protrusions, ribbed surfaces, grooves, or smooth alternating concave and convex surfaces such as in Senita (Cereus schottii) as shown in Figure 4.24 (right). These seeming irregularities decrease the incident angle of solar radiation as well as reflect and scatter part of it.

- Those which have hairy spines help also collect dew droplets by condensation and funnel them down the grooves to combine with other droplets forming bigger ones and decreasing their chances of being lost by evaporation as seen in Figure 4.25 and Figure 4.26.

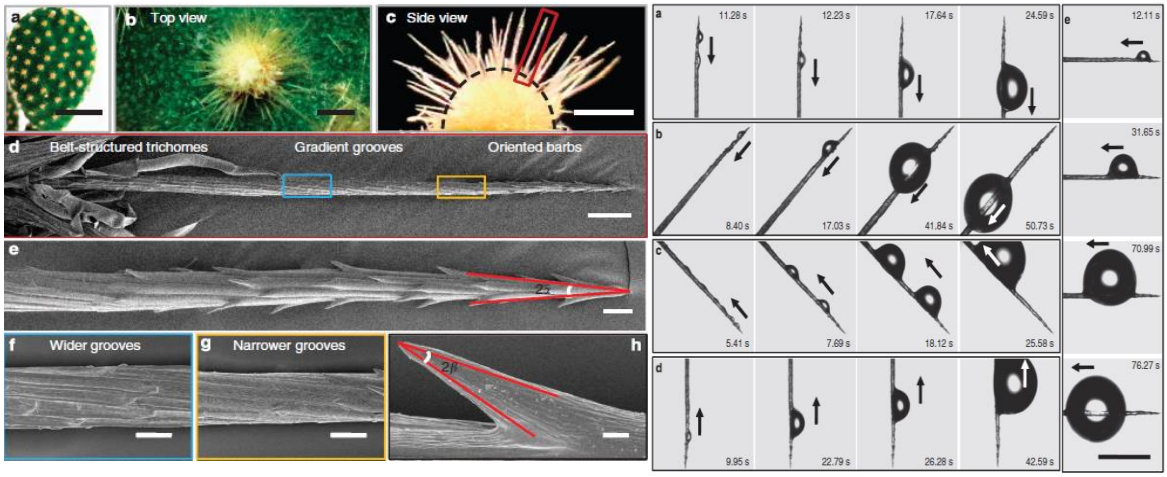

Figure 4.25: Appearance and surface structures of the cactus (Left). Microscopic observation of the directional water collection on the cactus spine placed at various angles (Right) (Ju, et al., 2012).

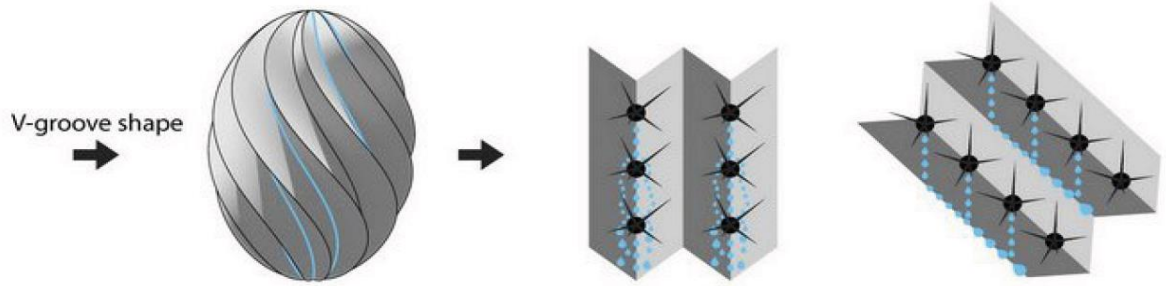

Figure 4.26: Diagram illustrating dew collected by spines of a cactus then funnelled down grooves (Erioli, 2010).

Summary of succulent strategies

Table 4.3: Summary of strategies used by succulents for thermal regulation. Source: author.

Strategy	Description	Feature	Main principle
CAM	Photosynthesis occurs at night so stomata are closed in daytime and preserve water lost in evaporation	Metabolism	Decrease water loss by evaporation
Surface area to mass ratio	Smaller surface area to volume ratio minimises exposed surface area in relative to its volume to decrease the rate of heat gained by conduction from the environment as well as the incident solar radiation	Shape	Decrease gain by conduction and incident radiation
Ribs and grooves	Increases the area of shaded surfaces	Shape	Decrease incident radiation
Spines and hairs	Hairs increase reflection and in some cases decrease the Boundary Layer resistance. Additionally they may help collect dew water.	Texture	Decrease incident radiation and increase water supply by condensation
Alternate curves	Increases the area of shaded surfaces	Shape	Decrease incident radiation

4.3.4 Architectural examples

Al Bahr Towers, Abu Dhabi

Aedas Architects won an international competition for the design of Abu Dhabi Investment Council Headquarters in 2007. The project includes two iconic 25-storey towers, each accommodating around 1000 employees.

Figure 4.27: overall view of Al Bahr Towers in Abu Dhabi. Image source: http://www.arup.com/Projects/Abu_Dhabi_Investment_Council_Headquarters.aspx

The façade design includes an adaptive kinetic shading system based on the general concepts of *Mashrabeya* design which is a traditional Arabic wooden lattice screen, typical of the Middle Eastern architecture. The folding tensile fabric façade will unfold when exposed to excess sunlight thus reducing glare, solar gain and cooling loads. Computational design tools helped in developing the parametric geometrical configuration and its responsive properties. This design concept is predicted to decrease 20% of the solar energy entering the building and contributes in meeting the US Green Building Council LEED Silver rating (Derix, et al., 2011).

Figure 4.28: Close-up of dynamic façade in folded and unfolded states. Image source: http://www.archiscene.net/firms/aedas/al-bahar-towers/

Although the design concept was not biomimetic intentionally, it greatly resembles folding techniques seen in leaves, and self-shading in general that was seen in numerous cacti which reduces heat gain by radiation. It represents an interesting example as it is one of the biggest constructed adaptive dynamic façades, and the building typology and site climate are similar to the proposed building design in this research.

Conceptual office building ventilation system

A research group at the Imperial College of Science in London (Yiatros, et al., 2007) investigated tree stems as a model for naturally ventilating an office building. They saw a direct analogy between water transport throughout a tree and ventilation systems.

Their idea was to circulate air under the natural forces of buoyancy due to temperature differences and well as wind. Buoyancy would be due to a temperature difference cause by solar gain and human activity. They designed a cylindrical office building with a central shaft and external atria around the circumference of the building. Air in these atria is heated and rises upwards due to buoyancy. This causes air to be pulled from the central shaft to replace it. Fresh air could be also drawn from the outside by opening windows. The hot air rising leaves the building from the top, assisted by prevailing winds.

Although this proposal was inspired from the vascular system of tree stems, it can also be related to the ventilation systems of *Macrotermes bellicosus* termite mounds as will be explained in section 4.4.7.

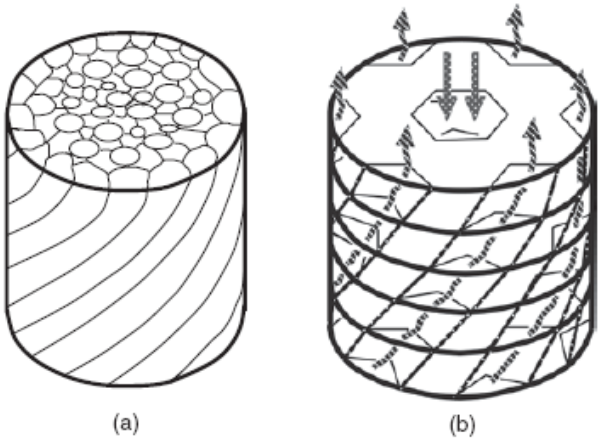

Figure 4.29: (a): schematic cross section through a tree stem. (b): conceptual diagram for the ventilation system of an office building inspired by the vascular system of trees (Yiatros, et al., 2007).

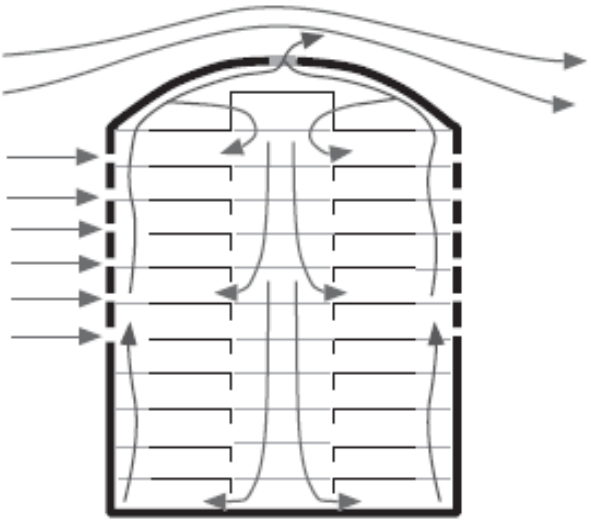

Figure 4.30: Section through the designed building, indicating desired airflow directions by natural ventilation. Hot air rises to the top where it is either cooled by evaporation and filtered by green plants, or escapes from the top. Cooled air is driven downwards through the central shaft, covered by a small pond/fountain. External air also enters from the sides where green plants are positioned close to windows such that they act as filters and wind buffers (Yiatros, et al., 2007).

4.4 Animals

4.4.1 Introduction

Animals inhabiting hot arid climatic regions face two major problems, which are excessive heat and dehydration. This is due to the conditions that they continuously face such as strong solar radiation, low relative humidity, dry winds and scarce rain. These animals have evolved thermoregulatory adaptations that help maintain their internal temperatures below lethal limits, and keep water loss as minimum as possible (Hadley, 1972). Thermoregulation in animals can be categorised into morphological, physiological and social (or behavioural) adaptation (Abere & Oguzor, 2011).

Examples of behavioural thermoregulation include for example changing location to seek shade, nocturnal activity and burrowing. Since rock and sand have low specific heat, at night they quickly cool off, and this encourages animals to be active during the night. Also rock and sand are poor conductors of heat, so even if their temperatures at the surface is much hotter than air, there could be around a 15-degree drop in temperature just 5 centimetres below, which encourages burrowing (Cole, 1943).

Despite the importance of behavioural strategies in animal thermoregulation, in the following sections a focus will be made on morphological and physiological adaptations. They were observed among animals that live mainly in hot arid regions in addition to relatively temperate ones in which animals are subjected to long period of sun exposure. Some of the adaptive strategies were observed to be common among several species (with some differences) while others were unique to specific ones.

4.4.2 Respiratory evaporative cooling

Respiratory cooling occurs when water in the upper airways and buccal cavity evaporates during breathing. In various animals -and specially in reptiles- the effects of this kind of cooling are of much use as they produce temperatures often 5°C lower than body or brain temperature (Tattersall & Cadena, 2010; Tattersall, et al., 2006). It results from one of the following breathing patterns:

- Normal breathing pattern
- Panting; a shallow rapid pattern which induced more extensive cooling of the nasal passages
- Open mouth gaping and protruding tongue which increases the exposed surface area for evaporation and is supposed to cool the entire upper airways. This is seen in many birds, mammals and especially reptiles as it allows them to bask in the sun while keeping the head from overheating.

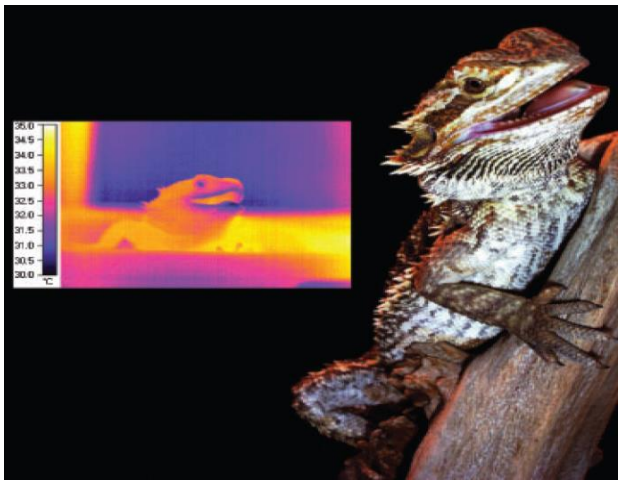

Figure 4.31: Bearded dragon lizards (Pogona vitticeps) increasingly exhibit open-mouth gaping as they experience body temperatures higher than their normal, preferred temperatures. This open-mouth breathing promotes evaporation from the moist inner lining of the mouth, manifesting as the cooler temperatures observed along the margin of the mouth (inset thermal image). This evaporation is thought to prevent overheating of the head and brain at elevated air temperatures (Tattersall & Cadena, 2010).

- Gular pumping; high amplitude movements in the throat (often seen in some frogs), and gular fluttering; high frequency movements (often seen in some birds).

The more the deviation from the preferred temperature of the animal, the more evident these respiratory responses are. Therefore they are evident in many lizards that inhabit extreme hot habitats. It is important to note that such cooling mechanisms that depend on evaporation of water are carefully used for short periods when the animal's body reaches an upper limit of toleration, due to the scarcity of water in some regions.

Figure 4.32: Common nighthawk (above). Birds of this order are most common in warm climates, and frogmouths, potoos, and nightjars all roost and nest in the open where they can be subjected to long periods of direct sun exposure. The gular sac is rapidly expanded (below) to increase the speed of air moving through the sac and buccal cavity. As the fast air passes, heat is lost from the blood vessels close to the surface (convective heat loss) and also through the moist membranes (Harrington, 2012).

4.4.3 Counter current systems

Vascular system

Reptiles have a unique heat exchange system in their heads that helps in maintaining a non-lethal temperature range in the head. This is particularly important for reptiles as they are ectotherms and need to spend a lot of time basking in the sun.

The heat exchange occurs between the internal carotid arteries (that supply the head with oxygenated blood) and the internal jugular veins (that bring deoxygenated blood from the head back to the heart) and this exchange is controlled by a constrictor muscle (Figure 4.33). While in the sun, warm blood is carried away from the head by the internal jugular vein. Since the cooler internal carotid artery is very close to this vein, heat is transferred from this vein to the artery thus keeping the head warm.

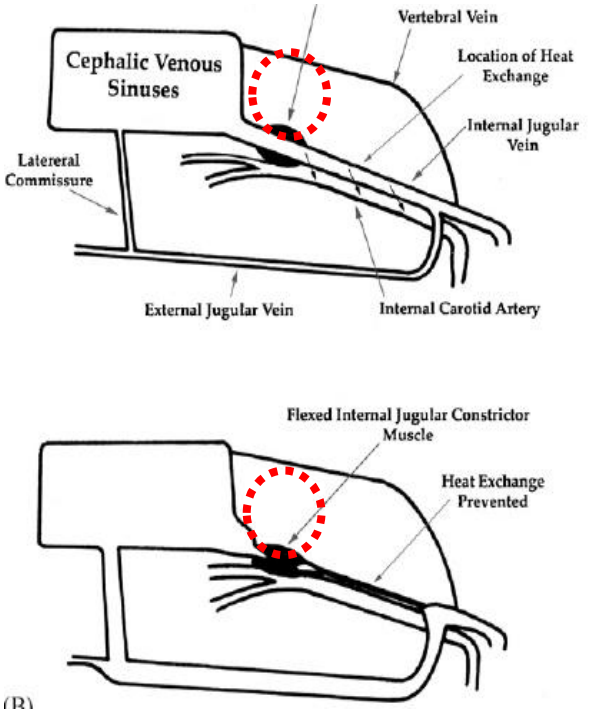

Figure 4.33: Counter-current heat exchange system in the head of reptiles. A muscle controls blood flow to allow/prevent heat exchange between the veins and arteries (Tattersall, et al., 2006).

When body temperature increases (in the lizard *P. coronalum*) up to 30°C, the muscle contracts and acts like a valve preventing the flow of blood through the internal jugular vein. The blood then accumulates in the venous sinuses (appearing to us externally as eye-bulging) and the increased pressure opens certain shunts through which the blood eventually flows out back to the heart and by-

passing its normal route. Thus no heat exchange occurs and blood in the carotid artery remains cool and no heat is transferred to it (Tattersall, et al., 2006).

Respiratory system

Another form of counter-current heat exchange takes place in the nasal passages of mammals, birds and reptiles. It is very similar to the function but not to the flow of vascular heat exchange where blood flows in two opposite directions and heat is transferred between parallel arteries and veins. There is a spatial separation between both passageways and heat transfers between them due to their proximity. Here there is only temporal separation, as air flows in and out within the same passageway.

When these animals exhibit high body temperatures, their respiratory patterns change and strategies like panting, gaping and fluttering occur (by evaporative cooling as described in the previous section). When this happens, the carotid artery is cooled and therefore the blood inside it heading for the brain is cooled (Tattersall, et al., 2006).

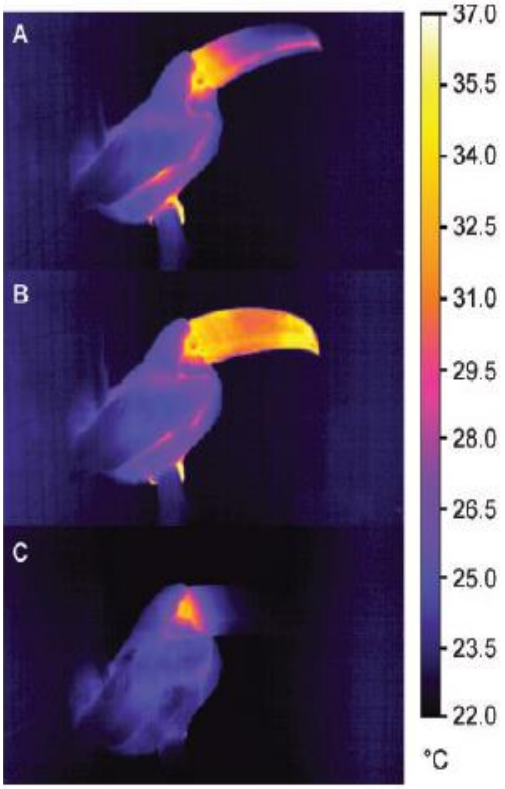

Figure 4.34: The bill of the Toco toucan (Ramphastos toco) acts as a thermal radiator. In the above infrared thermal images, relative to the awake state (A), entry into sleep (B) is associated with a transient increase in heat loss from the bill as superficial blood vessels receive increased blood flow. Once sleep occurs, the bill cools down towards air temperature (C), being virtually indistinguishable from the background temperature. Toucans are capable of modulating blood flow to the bill surface to conserve or release heat as necessary (Tattersall & Cadena, 2010).

4.4.4 Peripheral blood flow: Vasodilation

The surface temperature of animals is determined by many factors such as ambient temperature, metabolic heat production, insulation and blood flow. Here a focus is made on the ability of changing blood flow through the vessels just beneath the skin as an important instrument in regulating body temperature and heat loss.

Such blood flow changes often occur under surface areas of the animal's skin that have relatively less fur (or feathers) and almost no insulation. These surface areas are usually highly vascularised and could be called *thermal windows or thermal radiators* and include ears, feet, and the nose of mammals, and bills, feet and facial skin of birds.

A known example is the enormous bill of the Toucan bird which can dissipate up to 60% of excess body heat. The bill has all the features of a thermal window as it is not insulated, it is enlarged and well vascularised. As the body temperature increases, blood flow in the bill increases thus enabling more heat loss through radiation as well as convection (Tattersall & Cadena, 2010; Tattersall, et al., 2009).

Greenberg et al. (2011) provide similar examples of salt marsh sparrows also using their bills as radiators and observed that sparrows had larger bills in areas with higher summer temperatures. The same concept of heat loss could be seen in flippers of seals and sea lions, ears of hares, foxes and elephants, head wattles of chicken and turkey (Greenberg, et al., 2011) and lizard appendages (Dzialowski & O'Connor, 1999). This concept of radiative heat loss through appendages is of particular importance for animals living in poorly buffered areas with minimum water sources. It serves as a valuable alternative method of heat loss to the costly evaporative cooling in which valuable water is lost.

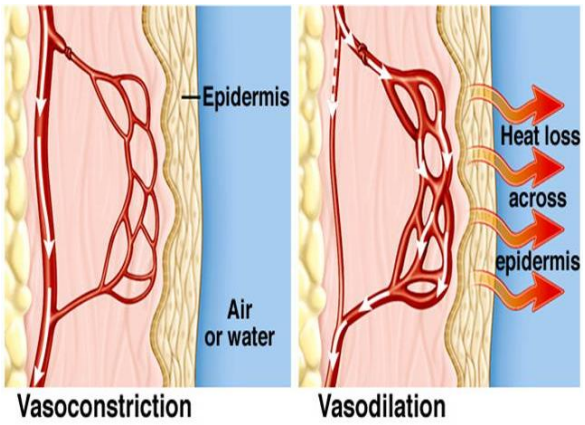

Figure 4.35: Generally, endotherms and ectotherms can alter blood flood at skin surface for thermoregulation. In hot weather, vasodilation occurs in which blood flow increases at skin surfaces (especially in appendages) to allow more heat to be dissipated. Image source: (Gillam, 2014)

Another good example of thermoregulation by changing peripheral blood flow is elephant ears. Due to their large size, elephants have a small surface area to volume ratio making it relatively difficult to dissipate excess heat. They also neither pant nor have sweat glands, which limits the effect of evaporative cooling. However, their large ears that could reach 183 cm in length (in the case of African Elephants) represent a fifth of the animal's surface area, and they have an extensive vascular network which makes them ideal *thermal windows.* When ambient temperature rises above 15°C dilation of the blood vessels occurs to increase blood flow and radiate excess heat (Figure 4.36). These thermal windows appear in thermal imaging as sharply contrasting spots with skin temperature difference up to 14°C higher than surrounding skin (Weissenböck, 2010).

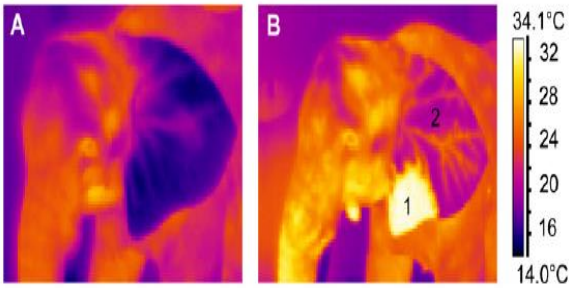

Figure 4.36: Two successive thermograms of an African Elephant. A: 17 minutes after entering an indoor space whose temperature is 19.5°C. B: 68 minutes after entering the space, a thermal window could be clearly seen. Skin temperature at location 1=33.0°C and at 2=22.2°C (Weissenböck, 2010).

4.4.5 Rain & moisture harvesting

a) Lizards

Some lizards have developed unique abilities to harvest rain and moisture which are most invaluable for survival. There are three known lizards from three different continents (*Phrynosoma cornutum*, *Moloch horridus* and *Phrynocephalus arabicus*) that have skin properties that enable them to capture rain and moisture on their bodies and deliver them to their mouths for drinking. This is quite useful in cases of light rain that would otherwise be absorbed by the usually dry and porous soil.

These three lizards have a broad body and a network of channels between their scales that carry water through capillary action in a radiating way from the channels to the lizards' jaws.

An important property they all have (regardless of the species or shape of scales) is the wettability of their skin. When a water droplet is applied to their skin it incredibly gets absorbed (Figure 4.37) very fast as the outer face of the scales have a 10 degree contact angle with water, which makes them super hydrophilic[13] (Comanns, et al., 2011).

This water absorption is very effective that *M. horridus* lizards are actually capable of drinking water from damp soil just by rubbing their ventral (lower body) scales on the ground after it rains.

This water-acquisition system has three main features (Sherbrooke, et al., 2007):

1) Narrow, deep spaces between the scales (called scale hinges) that partially close off a semi-tubular network (called hinge joints) where the water is accumulated and transported.
2) Convolutions in the hinge joints that increase their cross-sectional surface area which increases the possible amount of water to carry.
3) Different scale morphology at the rear end of the jaws to facilitate the ingestion of water coming from this network.

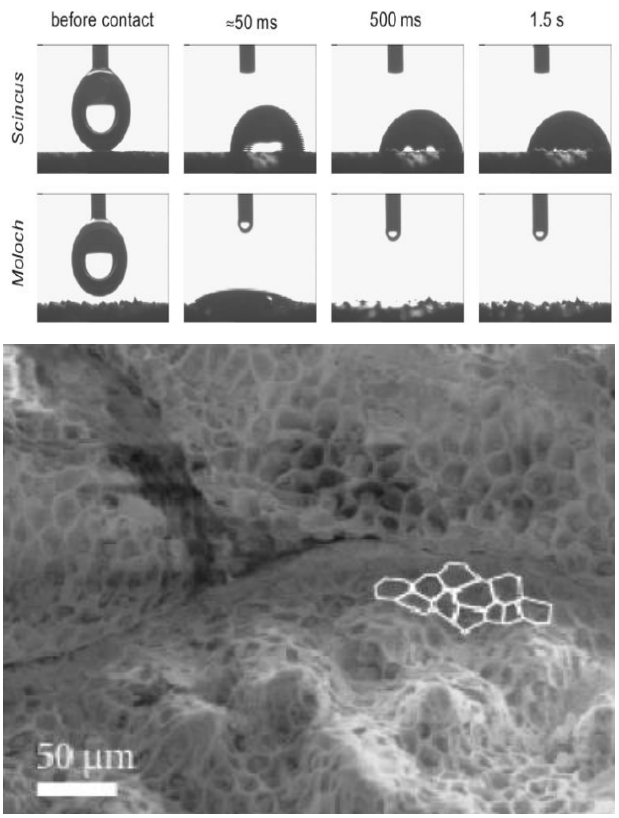

Figure 4.37: Water spreading on the surfaces of scales of 2 lizards. A droplet of 5 µl was applied through a syringe and brought into contact with the surface by the use of a micro manipulator. While on the non-moisture harvesting lizard *Scincus scincus* the droplet hardly changes over time, an almost immediate spreading of the droplet on the moisture harvesting lizard. Micro ornamentation of *Moloch horridus which* shows the honeycomb like micro ornamentation virtually all over all scales (Comanns, et al., 2011).

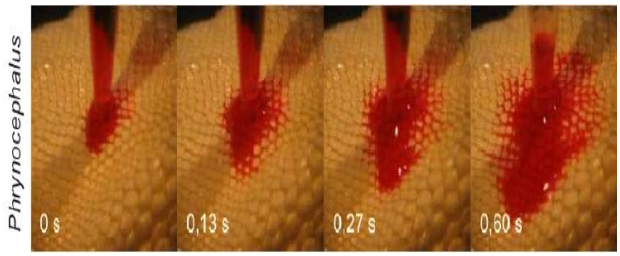

Figure 4.38: Immediate water transport in inter-scalar capillaries (Comanns, et al., 2011).

It is important to note that the size and number of a reptile's scales have an important thermoregulatory role by affecting its water balance. This is because the size and number of scales affect the amount of skin surface area that is exposed to the atmosphere. Reptiles living in arid places often (but not always) have large scales that overlap which decreases the rate of dehydration. While others living in more humid places tend to have smaller scales (Calsbeek, et al., 2006).

[13] Having a tendency to mix with, dissolve in, or be wetted by water (Oxford Dictionaries, 2016e).

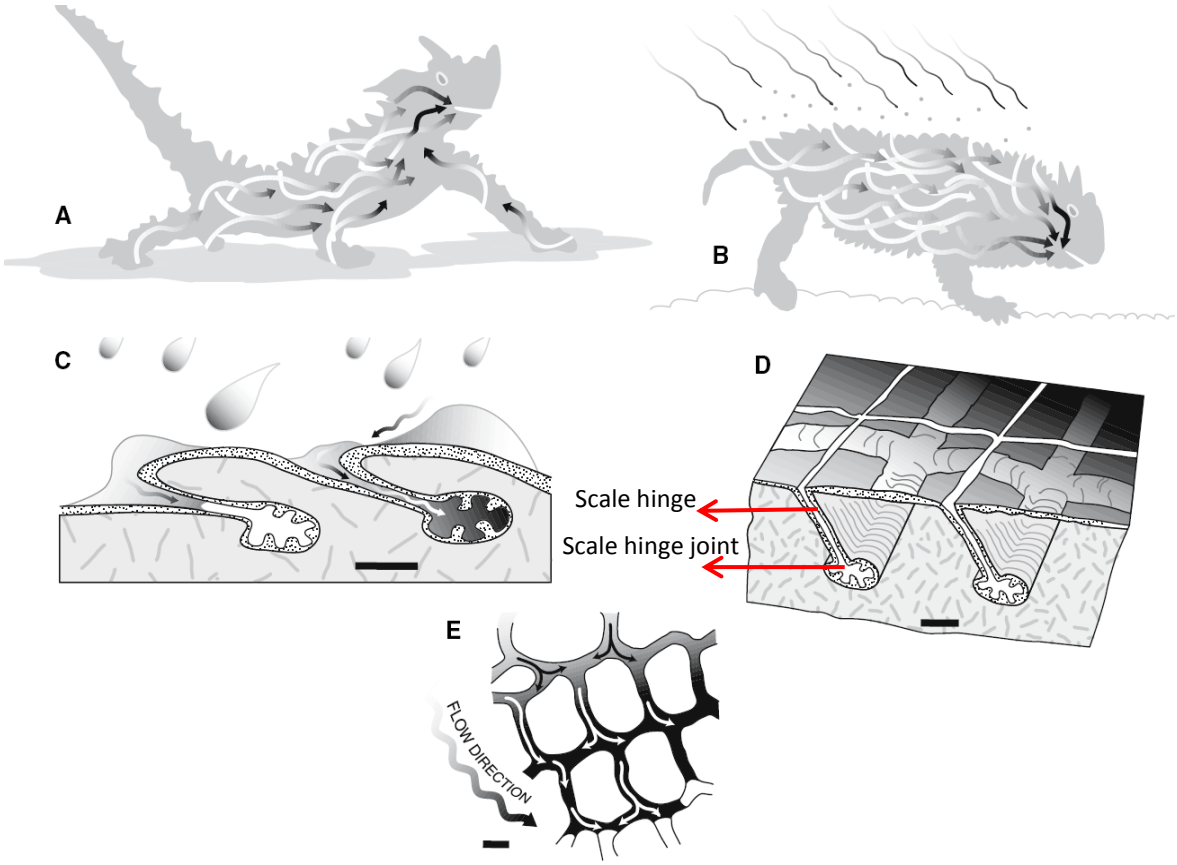

Figure 4.39: A) *M. horridus* illustrates uptake of water from a water puddle by capillary forces generated in limb scale channels and its transport throughout its body surfaces leading to the rear angle of the jaws for drinking. B) *P. cornutum* similarly, illustrates the capture of raindrops. C) Cross-sections through two scales (outer surface, stippled keratin, above, and dermis/muscle tissue, shaded/lined, below). Scale hinges have narrow elongated entry from scale surfaces to expanded scalehinge joints below. The scale hinge fills as raindrops falling on the surface of the skin are pulled, by adhesive forces, into the scale hinge and down to the scale hinge-joint channel. D) illustrates channel connections below scale surfaces to a continuous semi-tubular network. E) Schematic horizontal section of skin below scales (above outlined white spaces), illustrating continuous semi-tubular, scale-hinge-joint channel system (Sherbrooke, et al., 2007).

b) Insects

The moisture harvesting capability is not only seen in lizards but in some insects as well. Norgaard and Dacke (2010) have made an interesting comparison between 4 fog harvesting beetles in the Namib Desert which are famous examples of collecting moisture from fog events that occur in the desert. These events could reach 100 km inland and occur around 30 times per year, bringing water represented in minute droplets that can add up to a litre of water per square meter on a mesh of artificial fog screen during a day. They represent a predictable and therefore reliable water source for desert life. The main principle of heat transfer for thermoregulation in this case is the *condensation* of water vapour in the air to form water droplets.

Some beetles harvest the fog by digging trenches or ridges in the sand, while others use their own body as fog collectors which are affected by two factors (Norgaard & Dacke, 2010):

- The surface properties of the beetles' dorsal surface (Elytra). Experiments show that elytra surfaces of these beetles is hydrophobic (water repelling) and not hydrophilic

(water loving) as previously thought. Morphological features may vary. For example *Onymacris unguicularis* has a smooth surface with 0.5 mm wide grooves divided by narrow ridges in the posterior half. This is in contrast with *Stenocara gracilipes* for example which has jagged bumps forming irregular lines. However both of them are equally efficient in fog collecting. Studies show that fog collecting beetles survive in large numbers during the times of low rainfall, in opposite to other beetles that lack this adaptation as they decline to less than 1% of their mean abundance.

Figure 4.40: The Namib Desert beetle (genus Stenocara) collecting fog. Image source: http://www.corbisimages.com/stock-photo/rights-managed/42-28710929/the-namib-desert-beetle-genus-stenocara-fog?popup=1.

- Fog basking: This is a behaviour that includes facing the wind and adopting a head standing position. *O. unguicularis* holds its ventral side at an angle of 23 degrees to the horizontal. This helps the water droplets to roll down and form larger ones by the time it reaches the head so it could drink. This behaviour has so far been seen only in 2 out of 200 species living in the Namib Desert.

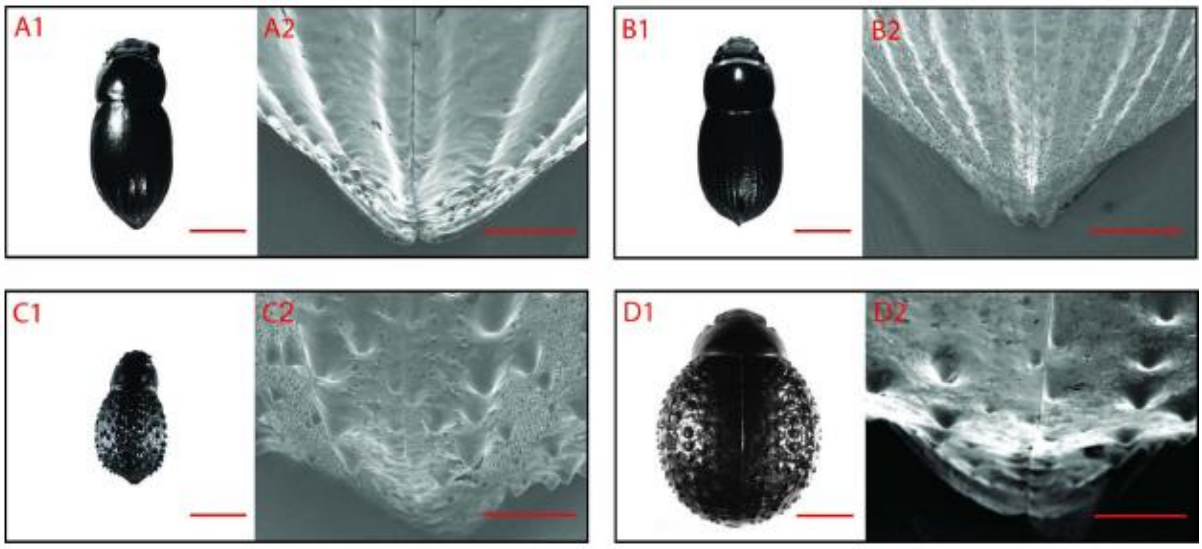

Figure 4.41: Four fog harvesting beetles in the Namib Desert and a close up of the Elytra of each one. A) Onymacris unguicularis, B) Onymacris laeviceps, C) Stenocara gracilipes, and D) Physasterna cribripes (Norgaard & Dacke, 2010).

4.4.6 Coloration

Skin colour is another feature that helps animals to adapt to their environment. It serves many functions such as concealment (camouflage), signalling, and also for thermoregulation. In general, darker colours increase heat absorption and help in rapid heating, while lighter colours reduce heat absorption which is important to reduce overheating for example in reptiles (Langklide & Boronow, 2012). The same concept could be seen in some mammals as well, for example a Zebra seen in an infrared image clearly show its black stripes to be around 10°C warmer than the white strips (Mccafferty, 2007). This causes air movement and a cooling effect by convection.

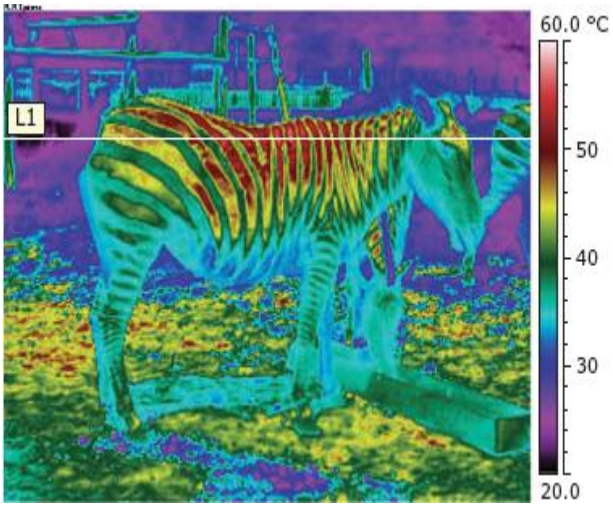

Figure 4.42: The zebra *Equus burchelli boehmi* in an infrared image showing black stripes 10 degrees warmer than the white ones (Mccafferty, 2007).

4.4.7 Termite Mounds

Nature is filled with of structures built by animals that aid in thermoregulation and natural ventilation of its occupants, and examples of those include prairie dog burrows, wasp hives, and bee hives. Termite mounds in particular have received great interest by both biologists and designers for their remarkable structures that comprise complex ventilation systems.

Macrotermes is a species of termites that cultivate fungus and build mounds up to 8 meters high housing millions of insects. They exist in tropical and sub-tropical regions of Australia, South East Asia and Africa (Korb, 2003). There are mainly 2 types of mounds (Figure 4.43); open ones with a chimney (exposed to higher wind velocity due to height) and side holes closer to the ground so a 'stack effect' occurs drawing fresh air from the ground openings up through the chimney. Secondly, there are also closed ones with no openings where ventilation was thought to occur mainly through a 'thermosiphon' mechanism driven by metabolism-induced buoyancy of nest air. Turner and Soar (2008) highlight some misconceptions often associated with these ventilation mechanisms and offer a more accurate explanation of how the ventilation system really works, especially regarding closed mounds. Two species will be demonstrated; *Macrotermes michaelseni* and *Macrotermes bellicosus* which both build closed mounds.

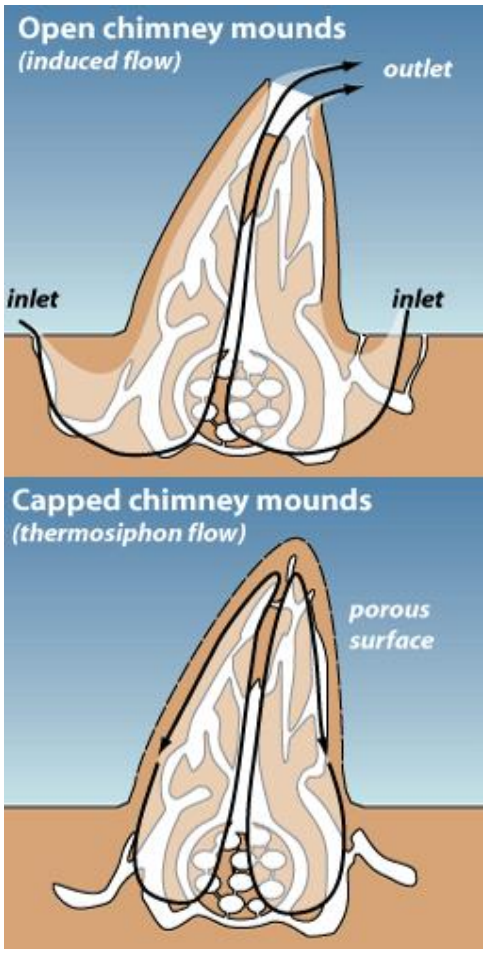

Figure 4.43: Two main types of ventilation systems previously thought in open (top) and closed (bottom) termite mounds (Turner & Soar, 2008).

a) Macrotermes michaelseni

Macrotermes michaelseni termite mounds for example are distributed in sub-Saharan Africa and are explained here in more detail. They are closed cone-shaped mounds that could extend several meters in height, with a porous skin and an underground nest with a diameter of 1.5 to 2 meters (Turner, 2001).

Ventilation system

The mound comprises a central chimney that starts right above the underground nest all the way up reaching about 2 thirds of the mound height. A series of smaller vertical shafts called surface conduits are distributed around the chimney but close to the mound surface, separated from external air just by a 1 to 3 centimetres thick porous layer. The surface conduits extend throughout the entire mound height and are also connected to peripheral underground conduits that surround the nest. Between the chimney and surface conduits exists a reticulum of tunnels that connect surface conduits with each other and with the central chimney.

Air flowing in the surface conduits is vigorously-mixed and highly affected by wind speed and direction due to the porosity of the mound surface. The high connectivity among them allows air to flow from one side of the mound to another (depending on the pressure gradients caused by the wind on the mound's conical form) sometimes without even passing through the chimney. The porous surface and lateral connectives act as a damping network and reduce the speed of the air as it reaches the chimney.

In the nest and the subterranean network however, air movement seems to be dominated by buoyancy-driven natural convection produced by the metabolism of the termites and their cultivated fungus causing the air to move upwards.

What is particularly interesting is the airflow in the chimney itself. It is influenced by a balance of two main forces (Figure 4.44); the natural convection pushing upwards from the nest, and the forced convection taking affect in the upper parts of the chimney (which could be directed up or down depending on wind direction, but usually a suction effect occurs pulling air up). The flow in the chimney will depend on the resultant of these two forces. Turner (2001) found that air in the middle of the chimney oscillates in rough synchrony with the ambient winds. He concluded that a '*Tidal'* ventilation system is a more accurate description to airflow in these termite mounds resembling it to tidal airflow in mammalian lungs (Turner & Soar, 2008).

It is worth noting that nest temperature is not regulated to constant value, this could be explained by the use of deep soil as a thermal sink and closly following its temperature variations (Turner & Soar, 2008). The ventilation network as a whole is illustrated in Figure 4.46.

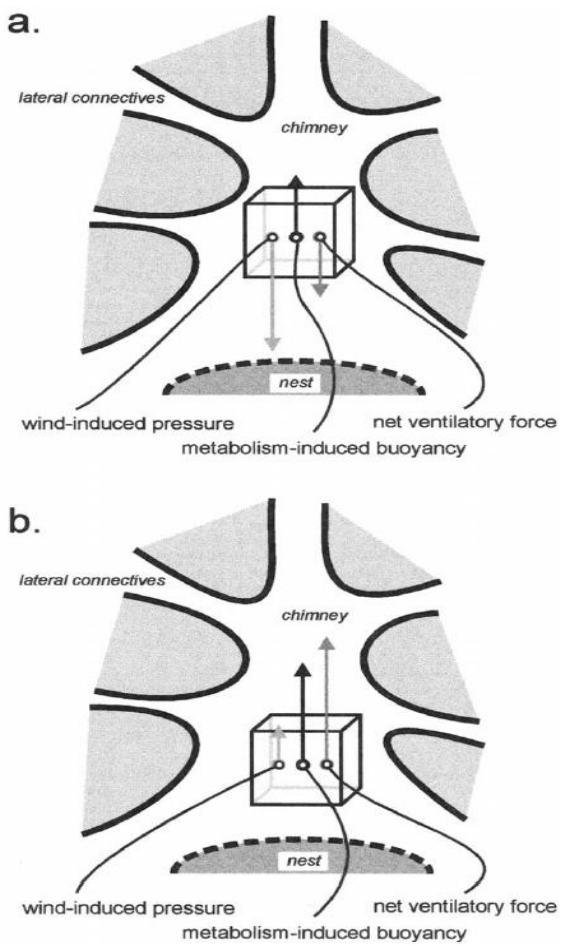

Figure 4.44: Diagram representing balance of forces on a parcel of air, represented by the cube. As the magnitude and direction of the wind-induced pressure vector fluctuates, air in the middle chimney moves up or down in a tidal pattern (Turner, 2001).

Figure 4.45: Plaster cast of *macrotermes michaelseni (Left)* and a detail showing the surface conduits and small egress channels close to the surface (Abou-Houly, 2010).

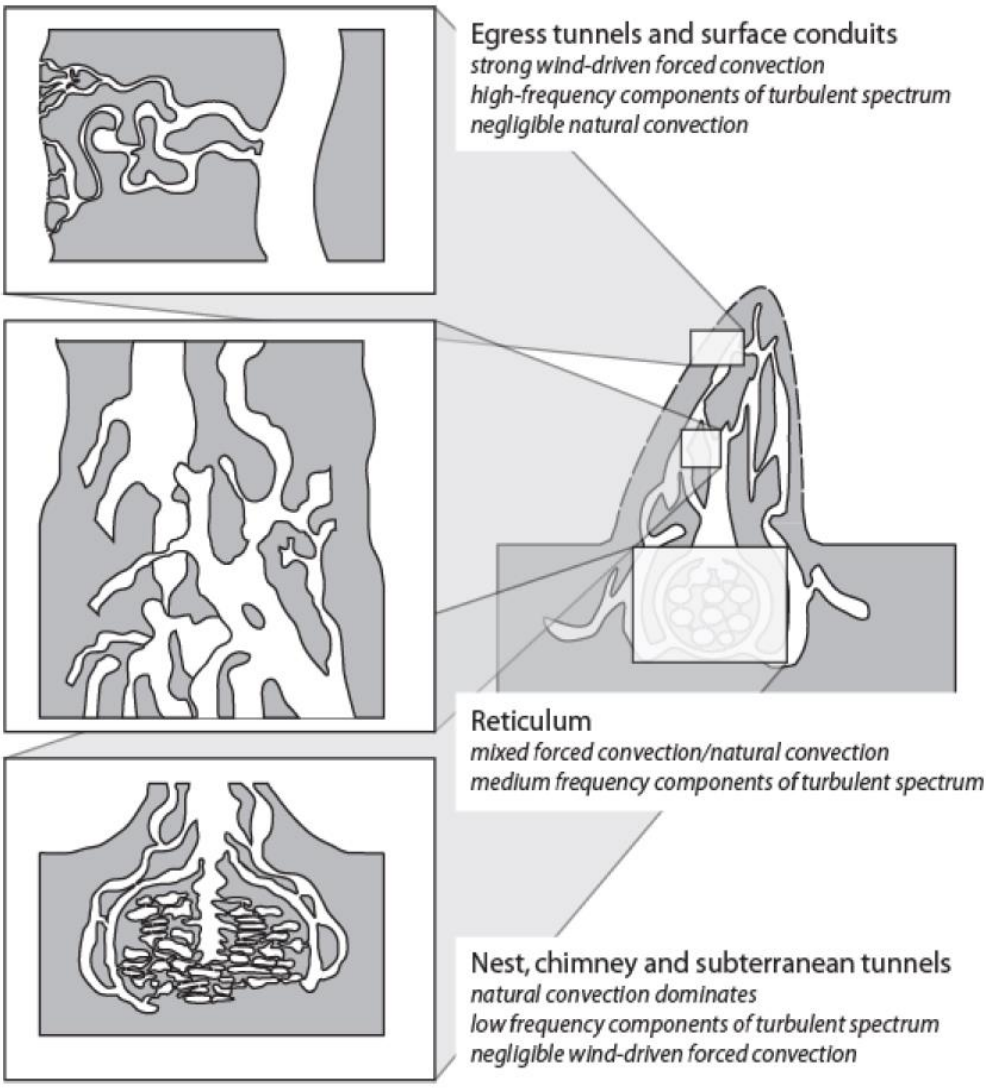

Figure 4.46: schematic diagram illustrating the ventilation system in the closed mound of *macrotermes michaelseni* (Turner & Soar, 2008).

Mound surface

The surface conduits mentioned earlier extend towards the outer surface by branching up, till they reach the surface itself through egress channels. These channels are distributed throughout the mound and are usually closed from the mound external surface unless conditions cause more permeability to be needed for increased ventilation so termites adapt by opening and closing them as required (Turner & Soar, 2008).

The existence of these channels play a critical role in the porosity and overall ventilation system, as airflow through the skin doubles with the presence of closed channels and increases 6 times with the presence of open ones. Airflow also depends on the depth of the channel from the skin surface. Egress channels are closest to the surface in the upper third of the mound height which is exposed to more wind velocities and greater pressure gradients with comparison to the rest of the mound (Abou-Houly, 2010).

Another advantage of the porosity and egress channels is that they enable the termites to benefit from the current winds regardless of their direction. Winds by nature are turbulent and not entirely predictable, which makes any system trying to catch wind coming from just a specific direction not efficient.

Mound Morphology

The mound's conical form also affects the flow of air within it. Wind causes positive pressure on the mound at the upwind side, and its value increases with increasing height. And negative pressures occur at the lateral and downwind sides, also increasing with height. This means that the maximum pressure difference occurs at the top third of the mound's height which causes a great suction effect of the airflow inside. This also means that the surface area through which air enters the mound is much smaller than the surface area through which it leaves, hence the air velocity decreased as it exits (Turner, 2001).

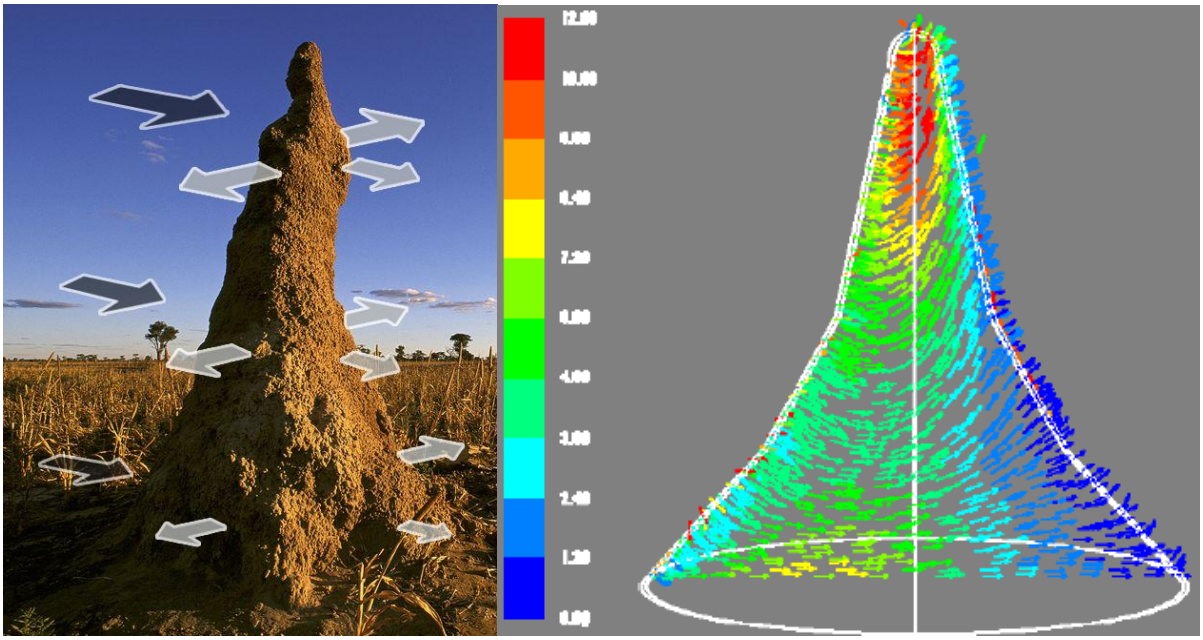

Figure 4.47: Left: Diagram illustrating the varying wind pressure on the mound; dark arrows represent positive pressure and light arrows represent negative pressure. The arrow size roughly indicates the strength of the pressure. The greatest pressure difference occurs at the top of the mound which causes a suction effect of the air flowing inside dragging it upwards as seen in the CFD simulation for internal airflow velocity on the right. The digital model of the mound is simplified; no internal tunnel network is modelled (Abou-Houly, 2010).

Source of image on the left: http://news.nationalgeographic.com/news/2014/07/140731-termites-mounds-insects-entomology-science/.

b) Macrotermes bellicosus

Macrotermes bellicosus termites also build closed mounds seen in the savannah of Cote D'Ivoire in Western Africa. Unlike the cone-shaped mounds explained in the previous section, these termites build cathedral-shaped mounds with many ridges and increased surface complexity. This increases the exposed surface area of the mound allowing more airflow inside (Korb, 2003).

Figure 4.48: Macrotermes bellicosus mounds in the Como National Park in Cote d'Ivoire (Korb, 2003).

They have their nests underground as *Macrotermes michealseni*, opening up to a central chimney that reaches the top. Peripheral air channels (corresponding to the surface conduits described by Turner for *Macrotermes michaelseni*) start at the bottom of the nest and run vertically just beneath the surface in ridges. A significant difference is that while winds seemed to be the main influence affecting ventilation in *Macrotermes michaelseni* mounds, here solar radiation plays a critical role. This leads to a variation in mound ventilation between day and night as follows:

During daytime, solar radiation heats up the peripheral air in the ridges above nest air temperature causing a temperature gradient in the air. This causes the warm air to rise up, pulling cooler air from the nest and causing buoyancy-driven natural convection. Air circulates through the mound and returns back to the nest through the central chimney.

The ventilation system changes through the night where nest air temperature is higher than ambient and mound temperature so it rises in the central chimney from the nest to the top like a thermosiphon effect. Warm air might also rise through the ridges so a circulatory motion of air back to the nest is not likely to occur.

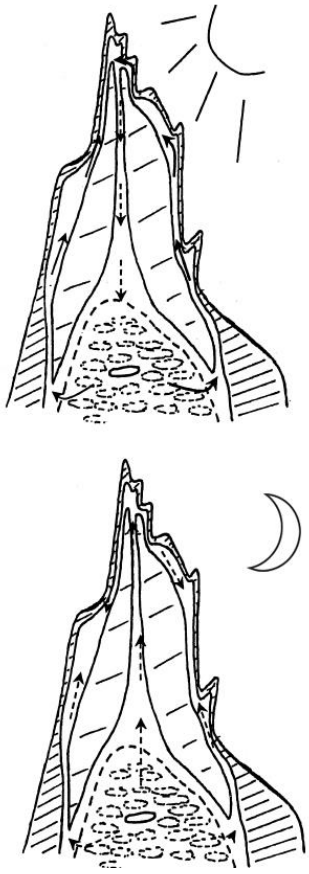

Figure 4.49: Suggested ventilation system in cathedral-shaped *Macrotermes michaelseni* mounds during day and night (Korb & Linsenmairl, 2000).

Summary of animal strategies

Table 4.4: Summary of animal strategies used for thermoregulation. Source: author.

Strategy	Description	Feature	Main principle
Respiratory evaporative cooling	Breathing patterns in many endo/ectotherms increase heat loss by evaporation	Respiratory system	Increase loss by evaporation
Vascular counter current heat exchange	Contracting muscles control blood flow to allow/prevent heat exchange between veins and arteries in the head of lizards	Blood flow	Decrease gain by conduction
Respiratory counter current heat exchange	Respiration cools blood in arteries preventing overheating in the brain	Respiratory system	Increase loss by evaporation and convection
Vasodilation	Endo/ectotherms increase blood flow in appendages to expel extra heat	Blood flow	Increase loss by radiation
Moisture harvesting (a)	Inter-scalar capillary system in some lizards capture moisture	Morphology	Increase water supply then cooling by convection from water to their bodies
Moisture harvesting (b)	Hydrophobic surface properties of Namib beetles enable them to collect fog	Morphology	Increase condensation then cooling by convection from water to their bodies
Colouration	Light colours in general decrease absorbed heat. Alternating dark and light colours in Zebras create areas with different temperatures inducing air flow	Morphology	Decrease gain by conduction and increase loss by convection
Tidal airflow	Air oscillates in central chimney under a balance of forces (wind vs buoyant air from warm nest) in rough synchrony with winds	Mound ventilation system	Increase forced and natural convection (induced by metabolism)
Porous termite mound surface	Porous surface enables the use of winds regardless of their direction	Mound surface properties	Increase loss by forced convection

Egress channels in termite mounds	Egress channels increase surface porosity and allow air to infiltrate the mound while damping it. Porosity is controlled through opening and closing egress channels as needed	Mound surface properties	Increase loss by forced convection
Mound Ridges in termite mounds	Mound surface area is increased through ridges in which sun heats up air causing it to flow upwards through these vertical tunnels pulling along air from nest	Mound ventilation system	Increase loss by natural convection (induced by solar heat gain)
Soil as thermal sink	Nest energy balance is strongly driven by soil's large thermal capacity	Underground nest	Increase loss by conduction
Air suction at termite mound top	Pressure difference due to mound morphology and height causes a string suction effect on internal airflow	Mound form	Increase loss by forced convection
Vascular counter current heat exchange	Contracting muscles control blood flow to allow/prevent heat exchange between veins and arteries in the head of lizards	Blood flow	Decrease gain by conduction
Respiratory counter current heat exchange	Respiration cools blood in arteries preventing overheating in the brain	Respiratory system	Increase loss by evaporation and convection
Vasodilation	Endo/ectotherms increase blood flow in appendages to expel extra heat	Blood flow	Increase loss by radiation

4.4.8 Architectural Example

Davis Alpine House, Kew Gardens, London

An interesting example of a biomimetic ventilation system is the Davis Alpine House at Kew Gardens, by Wilkinson Eyre Architects with environmental engineering and expert in termites Patrick Bellew of Atelier Ten. The building is an energy efficient greenhouse providing the cool climatic conditions required for a collection of Alpine plants.

Taking inspiration from termite mounds, designers created an underground chamber within a concrete double slab. Through its thermal mass and large surface area, it acts as a heat sink for the following day. Air during the day is cooled in this underground chamber then circulated at plant level. Then a stack effect is created due to the considerable height of the two back to back arches that form the main structure of the building. Openings exist around the bottom perimeter of the overhanging cladding as well as at the very top to allow passive ventilation (WilkinsonEyre, 2014).

Figure 4.50: Exterior view of the Davis Alpine House at Kew Gardens (WilkinsonEyre, 2014).

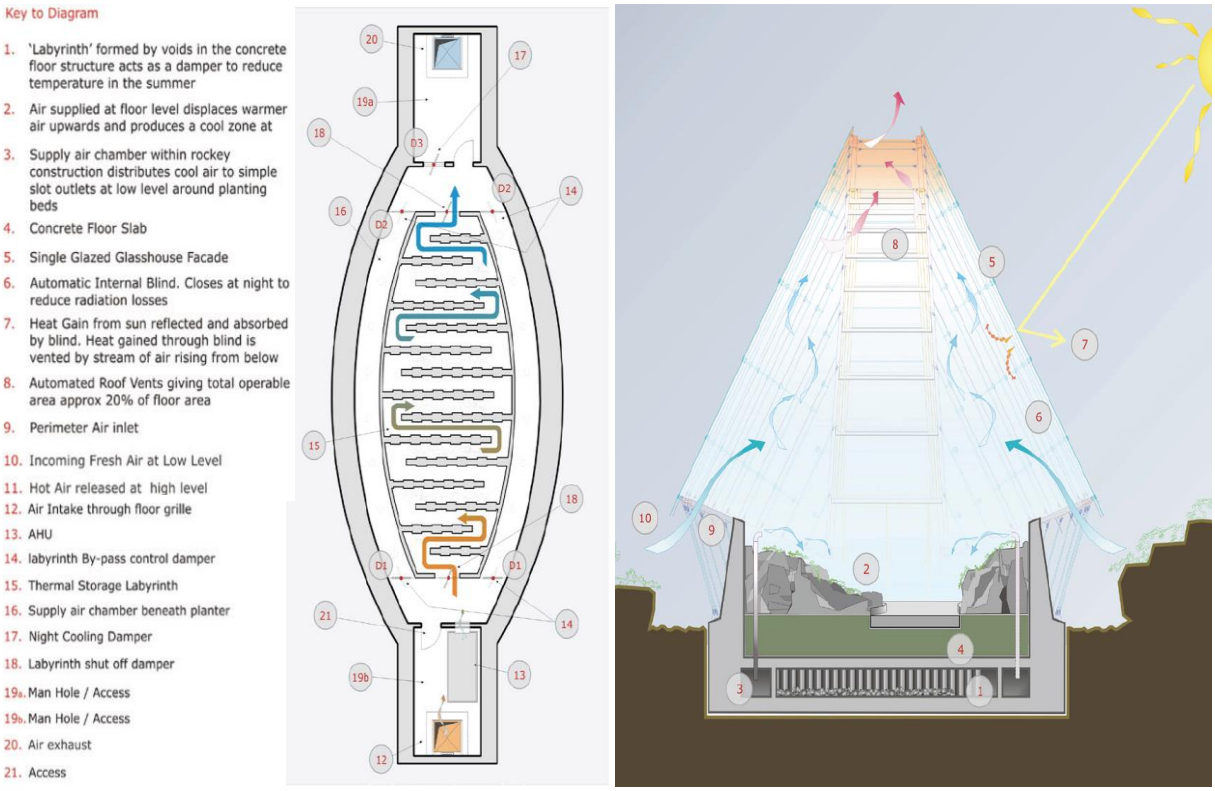

Figure 4.51: Diagrams illustrating cooling mechanisms. Right: cross section showing the side and top openings causing the stack effect. Left: plan of underground chamber acting as a thermal sink for air cooling (WilkinsonEyre, 2014).

4.5 Humans

Humans possess complex thermoregulatory mechanisms (many of them exist in other animals) that are able to lose excess heat by cutaneous (skin) vasodilation and sweating, retain heat by vasoconstriction, and generate heat by shivering. Internal (core) body temperature is the main trigger of these mechanisms, in addition to a secondary trigger which is skin temperature (Charkoudian, 2003). Blood flow close to the skin plays a critical role in human thermoregulation, while normally receiving 5% of cardiac input in thermo-neutral conditions, it could receive as much as 60% during extreme heat and as low as 0% in cases of extreme cold (Kellogg Jr., 2006). The role of skin in thermoregulation is stronger and more evident in appendages such as hands and feet which act as insulators, radiators and evaporators for the human body (Taylor, et al., 2014). Factors affecting the thermal exchange between the body and environment include:

- Exposed surface area to mass ratio
- Network of blood vessels that deliver heat to the skin by convection and conduction
- Temperature and water vapour gradients

Some of these factors are highlighted here as follows:

4.5.1 Surface area to mass ratio

The morphological features of hands and feet enable them to have relatively high surface area to mass ratio (S/M) if compared to that of the whole body. An average man has a S/M of 0.024 m^2/kg, while that of hands and feet are 3 and 4 times greater respectively. This facilitates the radiation of excess heat, which is also enhanced given that hand muscles are poorly insulated, and feet are in constant contact with large heat sinks (Taylor, et al., 2014).

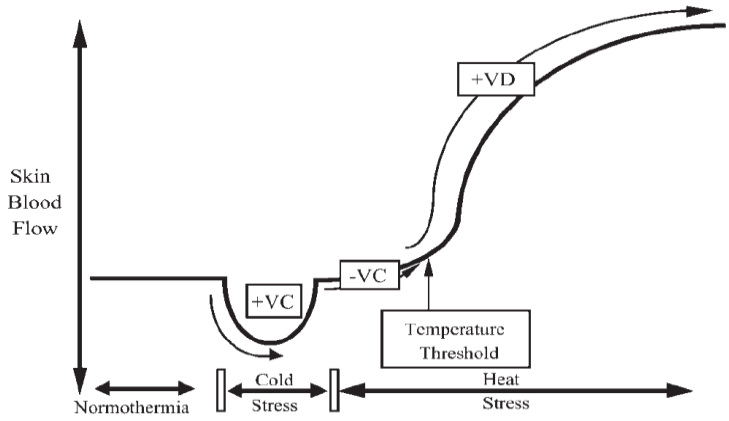

Figure 4.52: High skin blood flow acts in conjunction with evaporation of sweat to reduce body heat. +VC, increased active vasoconstrictor nerve activity; -VC, decreased active vasoconstrictor nerve activity; -VD, increased active vasodilator activity; Threshold, coincident core temperature at which cutaneous active vasodilation and sweating begin under resting conditions (Kellogg Jr., 2006).

4.5.2 Vascular network

As seen in other mammals, humans also utilise vasoconstriction and vasodilation to regulate heat. During cold, thermo-neutral or exercising states, vasoconstriction occurs in hands and feet as well as in nose, ears and lips. The strong constriction of the capillary veins near the skin surface directs blood flow to deeper vessels which are better insulated. Blood flow in extremities may fall below metabolic requirement in extreme cold. This causes appendages to behave as a protective barrier where a physiological amputation of them conserves deep body heat.

However when the body is heated, vasodilation occurs and blood flow increases to maximise heat dissipation. Heat is transferred from the core to the surfaces by convection

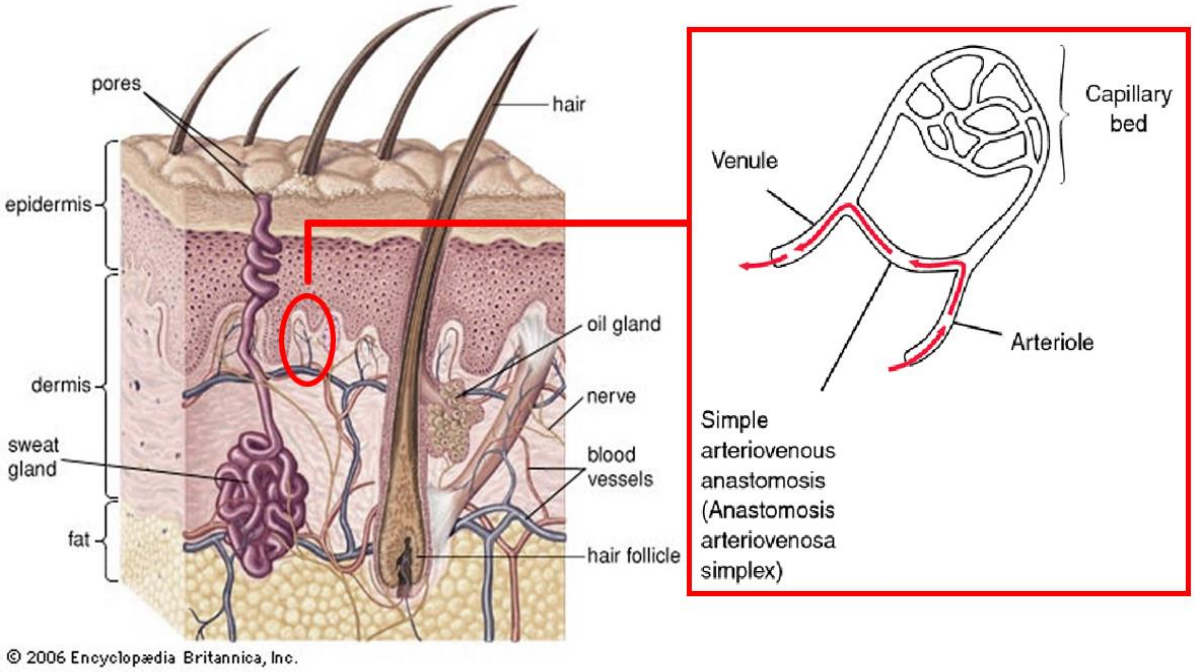

Figure 4.53: basic layers of human skin, zooming in on papillary capillaries near the surface and the arteriovenous anastomoses that act as shunt by-passing the smaller capillaries in cases of vasodilation to maximise the possible amount of blood flow and enhance heat dissipation.

Image sources:
Right: http://medical-dictionary.thefreedictionary.com/anastomosis
Left: http://www.britannica.com/EBchecked/topic/547591/human-skin

through the veins, and then is dissipated at the surface by radiation. This is enhanced by arteriovenous *anastomoses* (which are links between an arteriole and a venule). These vessels are deeper than the superficial capillaries and have much wider radii. They act as capillary by-passes, and although this may seem rather odd as the blood is directed slightly away from the surface, it enables much more blood to flow due to larger radii (up to ten times bigger than capillaries) and therefore more heat can be dissipated. In fact, extreme vasodilation enables 75 and 90 times more blood flow than extreme vasoconstriction in hands and feet respectively. Blood flow in hands and feet is rarely stable; in fact even in thermo-neutral states it is continuously changing to modify the convective delivery of heat to the skin (Taylor, et al., 2014).

4.5.3 Perspiration

In parallel to cutaneous vasodilation, sweat also occurs to decrease skin temperature by evaporative cooling and therefore cooling the blood flowing in the skin before it returns back to deeper blood vessels (Charkoudian, 2003). Sweat is secreted from eccine glands that are distributed all over the body with varying densities. Sweating increases through two ways; first increasing the number of activated sweat glands then increasing the amount secreted per gland (Shibasaki, et al., 2006). It is essential to the thermoregulatory process in heated states as heat lost for example from hands due to evaporative cooling reaches 336 W/m^2 from each hand (at 22 mL/hr assuming complete evaporation). Total whole body water loss may amount to 16 litres per day in extreme heat and exercising (Taylor, et al., 2014).

4.5.4 Architectural Example

Homeostatic Façade system

Decker Yeadon is an architectural material technology firm that designed a prototype of a double-skin façade system that is capable of autonomously opening and closing in reaction to indoor temperature. The system is inspired by concept of homeostasis found in endotherms, and also by the concept of expansion and contraction of muscles. Homeostasis in organisms allows them to regulate their internal conditions such as temperature (Minner, 2011).

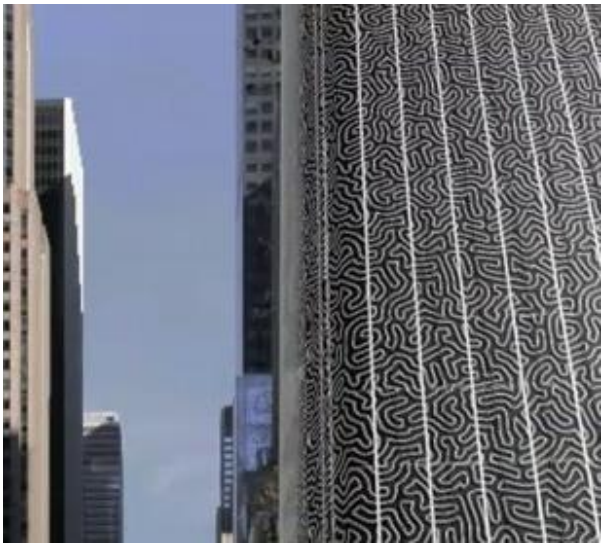

Figure 4.54: Rendering of the Homeostatic Facade System by Decker Yeadon (Minner, 2011).

The swirling lines on the façade are actually ribbons of an elastomer[14] wrapped over a flexible polymer core. This elastomer has a coating that distributes an electric charge causing it to deform. The charge is triggered by sunlight as the temperature increases during hot days, so the system expands and reduces the amount of sunlight entering. When it cools the system contracts and more light is allowed to enter. Its main advantage over other façade systems is its low power consumption since the material itself is the also the motor. It represents an example of localised control at any point on the façade. No computers or humans are needed to activate it as it is the sensor and activator in the same time.

However, one might automatically think of an expected situation where occupants would want or need to open or close the system for reasons other than thermoregulation. They do not have any control and therefore the practicality of the concept is debatable despite its advantages.

Figure 4.55: The façade prototype (right) and detail (left) in their expanded open state and contracted closed state (Minner, 2011).

[14] An Elastomer is a natural or synthetic polymer having elastic properties, e.g. rubber (Oxford Dictionaries, 2016f).

4.6 Summary of All Strategies

Table 4.5: Summary of strategies used by animals for thermal regulation. Source: author.

Strategy	Description	Feature	Main principle
	LEAVES		
Small, narrow size	It decreases Boundary Layer resistance enhancing heat dissipation by convection	Size	Increase loss by free convection
Lobes and dissections	This decreases the distance from any point on the leaf to the closest edge thus decreasing its temperature, & decreases the Boundary Layer resistance	Shape	Increase loss by free convection
Holes	Holes permit air to pass through the leaf & decreases the Boundary Layer resistance	Shape	Increase loss by free convection
Tears	Tearing permits air to pass through the leaf and decreases the Boundary Layer resistance	Shape	Increase loss by free convection
Folds	Folds result in parts of the leaf to be constantly in the shade	Shape	Decrease incident radiation
Avoid horizontal position	Decreasing the angle of incident light reduces heat gain	Orientation	Decrease incident radiation
Shiny surface	Increasing the reflected portion of solar gain decreases the absorbed portion	Surface Texture	Decrease incident radiation
Pubescence	Hairs increase reflection and in some cases decrease the Boundary Layer resistance	Surface Texture	Decrease incident radiation and Increase loss by free convection
More or bigger stomata	Increase the leaves' ability to lose heat through transpiration	Molecular surface properties	Increase loss by evaporation
Venation system	Efficient transportation of fluids throughout the leaf	Internal structure	Increase loss by evaporation (indirectly)
	TREE STEMS		
Round cross-section	Decreases exposed surface area	Shape	Decrease incident radiation
Thick outer layer	Provides an efficient insulating layer	Shape	Decrease gain by conduction
Rough surface	Increases the area of shaded bark surface	Surface texture	Decrease incident radiation
Peeling surface	Peels create air gaps in between serving as additional insulation	Surface texture	Decrease gain by conduction

Reflection of non-visible light spectrum	Barks are optimised to the reflection of infrared light rather than visible light.	Molecular surface properties	Decrease incident radiation
Water transport through xylem	Water pulled upwards from roots due to evapo-transpiration occurring in leaves	Internal structure	Increase loss by evaporation
SUCCULENTS			
CAM	Photosynthesis occurs at night so stomata are closed in daytime and preserve water lost in evaporation	Metabolism	Decrease water loss by evaporation
Surface area to mass ratio	Smaller surface area to volume ratio minimises exposed surface area in relative to its volume to decrease the rate of heat gained by conduction from the environment as well as the incident solar radiation	Shape	Decrease gain by conduction and incident radiation
Ribs and grooves	Increases the area of shaded surfaces	Shape	Decrease incident radiation
Spines and hairs	Hairs increase reflection and in some cases decrease the Boundary Layer resistance. Additionally they may help collect dew water.	Texture	Decrease incident radiation and increase water supply by condensation
Alternate curves	Increases the area of shaded surfaces	Shape	Decrease incident radiation
ANIMALS			
Respiratory evaporative cooling	Breathing patterns in many endo/ectotherms increase heat loss by evaporation	Respiratory system	Increase loss by evaporation
Vascular counter current heat exchange	Contracting muscles control blood flow to allow/prevent heat exchange between veins and arteries in the head of lizards	Blood flow	Decrease gain by conduction
Respiratory counter current heat exchange	Respiration cools blood in arteries preventing overheating in the brain	Respiratory system	Increase loss by evaporation and convection
Vasodilation	Endo/ectotherms increase blood flow in appendages to expel extra heat	Blood flow	Increase loss by radiation
Moisture harvesting (a)	Inter-scalar capillary system in some lizards capture moisture	Morphology	Increase water supply then cooling by convection from water to their bodies
Moisture harvesting (b)	Hydrophobic surface properties of Namib beetles enable them to	Morphology	Increase condensation

	collect fog		then cooling by convection from water to their bodies
Colouration	Light colours in general decrease absorbed heat. Alternating dark and light colours in Zebras create areas with different temperatures inducing air flow	Morphology	Decrease gain by conduction and increase loss by convection
Tidal airflow	Air oscillates in central chimney under a balance of forces (wind vs buoyant air from warm nest) in rough synchrony with winds	Mound ventilation system	Increase forced and natural convection (induced by metabolism)
Porous termite mound surface	Porous surface enables the use of winds regardless of their direction	Mound surface properties	Increase loss by forced convection
Egress channels in termite mounds	Egress channels increase surface porosity and allow air to infiltrate the mound while damping it. Porosity is controlled through opening and closing egress channels as needed	Mound surface properties	Increase loss by forced convection
Mound Ridges in termite mounds	Mound surface area is increased through ridges in which sun heats up air causing it to flow upwards through these vertical tunnels pulling along air from nest	Mound ventilation system	Increase loss by natural convection (induced by solar heat gain)
Soil as thermal sink	Nest energy balance is strongly driven by soil's large thermal capacity	Underground nest	Increase loss by conduction
Air suction at termite mound top	Pressure difference due to mound morphology and height causes a string suction effect on internal airflow	Mound form	Increase loss by forced convection
HUMAN SKIN AND APPENDAGES			
Vasodilation and Anastomoses	Cutaneous blood vessels act as by-passes to conduct more blood flow in cases of vasodilation to dissipate more heat	Blood flow	Decrease loss by convection and Radiation
Evaporative cooling by perspiration	Sweat secretions in humans account for up to 16 lt/day of water loss dramatically increasing heat loss	Human skin	Increase loss by evaporation
Surface area to mass ratio	Higher ratio means increased exposed surface area hence more heat could be dissipated by radiation	Hands and feet	Increase loss by radiation

4.7 Summary

This chapter addressed the concept of thermoregulation in nature, as well as highlighting the four possible methods through which heat is transferred. These four methods were important in analysing the biological inspirations that followed as they acted as the link between the biological strategy and the corresponding architectural feature to which it could be applied in the building skin design. The biomimetic design process began in this chapter by trying to find solutions and adaptation strategies for thermoregulation problems in hot climates. These strategies aim at minimising heat gain or maximising heat loss through any of the four heat transfer methods. The researcher started looking for answers in biological literature, online databases and previous research done in similar topics.

After applying the biomimetic design strategy in this chapter a better understanding of the process itself was achieved. Hence, the diagram presented in the introduction of this chapter can be expressed in more detail as seen in Figure 4.56. A number of challenges were faced in this phase, starting with choosing the correct terminology to use while searching in biological literature. Terms like 'adaptation to heat' and 'thermoregulation' for example resulted in general search outputs. While they were useful in understanding general thermoregulatory concepts in nature, they usually did not provide in depth knowledge about a specific organism or strategy. Therefore, came the necessity to know exactly what to look for; either a specific organism or specific strategies like: vasodilation, counter-current heat exchange, turbinate functions in birds, etc.

After finding a number of relevant strategies, another obstacle emerged which was to eventually understand the strategy at hand due to terminology that seem unfamiliar to non-biologists. This came in parallel with the necessity of having at least a rough idea of a possible architectural application to this strategy in order to decide if it is worth further investigation or not. After investigating a number of organisms and the various means by which they achieve thermoregulation, the architectural equivalent (building skin feature) corresponding to each strategy is specified as shown in Table 4.6. The ideas in the presented table are by no means all of those available in the plant and animal kingdoms. They only represent what the researcher has investigated up to this date.

It is important to note that some strategies found along the way were not included in this thesis because they dealt with nano-scale morphological skin features of organisms, which makes potential solutions fall within the scope of work of a material scientist in order to be applied. Behavioural adaptation strategies of animals -which are very important- were also not included here as they often included moving and relocating for example, making it quite difficult to imagine a possible architectural application based on them.

It is observed that numerous strategies focus on thermoregulation specifically by minimising the heat gained due to incident solar radiation. This indicates the important role of morphological aspects and surface properties of the organism in its adaptation to hot environments. Some architectural features (such as morphology, shading elements and cladding materials) could have more than one possible biomimetic strategy. It is therefore necessary to undergo a selection process and choose exactly the ideas that would be further explored. The criteria on which we could base the selection include:

- Available technology and materials.
- Construction and maintenance costs.
- Designer and client preferences.
- Coherency/contradiction of the selected idea with others.
- Multi-functionality of the idea; whether it has simultaneous benefits such as structural, environmental, or aesthetic advantages.

The selection of ideas however will not indicate any importance over others. The following chapter discusses the application phase of this research, where a number of ideas are selected and translated into mathematical and geometrical terms so that they can be digitally modelled.

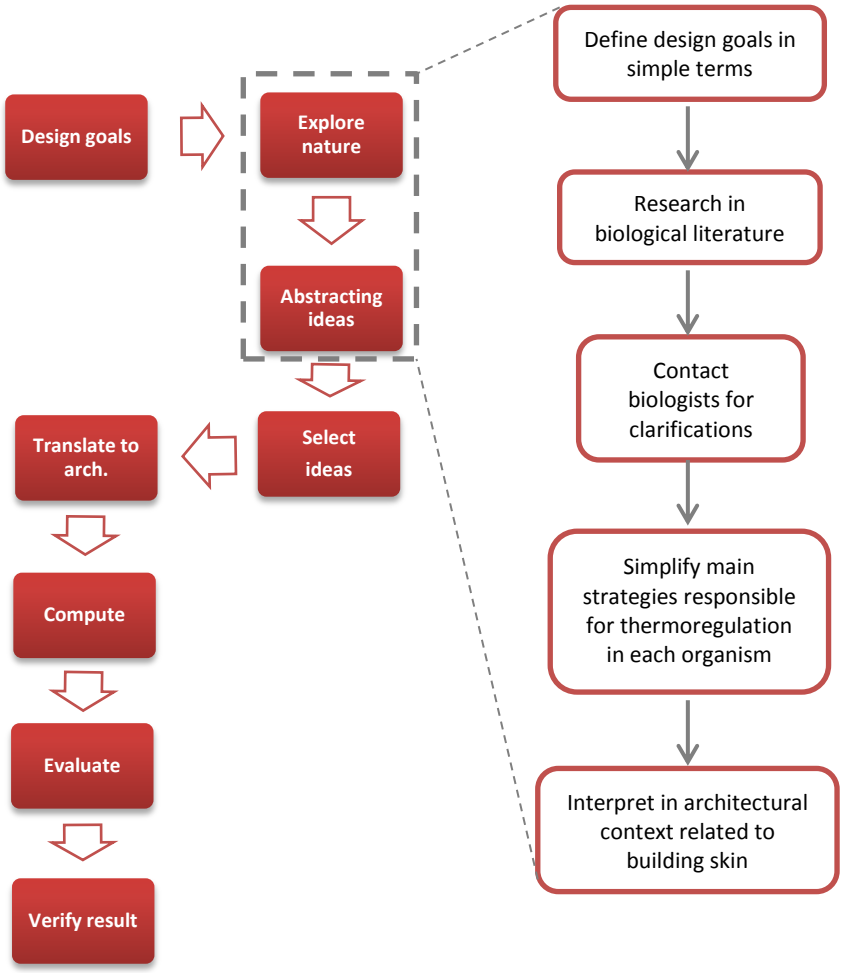

Figure 4.56: Detailed diagram of the design methodology that represented the scope of this chapter. Source: author

Table 4.6: Summary of all investigated strategies and the corresponding building skin features to study, categorised according to the four main heat transfer methods.

RADIATION			CONVECTION		
Organism	**Strategy**	**Arch. feature**	**Organism**	**Strategy**	**Arch. feature**
Leaves	Folds	Overall Morphology Shading elements	**Leaves**	Small narrow sizes	Shading elements
	Avoid horizontal position	Overall Morphology Shading elements		Lobes and dissections	Perforations
	Shiny surface	Cladding material		Holes and tears	Perforations
	Pubescence	Cladding material		Pubescence	Cladding material
Tree Barks	Round cross-section	Overall Morphology	**Tree Barks**	X	X
	Rough surface	Cladding material	**Succulents**	X	X
	Reflection of non-visible light spectrum	Cladding material	**Animals**	Respiratory counter current heat exchange	Ventilation system
Succulents	Ribs and grooves	Overall Morphology Shading elements		Tidal airflow	Ventilation system
	Spines and hairs	Cladding material		Porous termite mound surface	Ventilation system Cladding material
	Alternate curves	Overall Morphology Shading elements		Egress channels in termite mounds	Ventilation system Perforations
Animals	Vasodilation[15]	Ventilation system		Mound Ridges in termite mounds	Ventilation system Overall Morphology
Humans	Vasodilation	Ventilation system		Air suction at termite mound top	Ventilation system Overall Morphology
	Surface area to mass ratio	Overall Morphology		Colouration	Cladding material
			Humans	Anastomoses	Ventilation system
CONDUCTION			**EVAPORATION/CONDENSATION**		
Organism	**Strategy**	**Arch. feature**	**Organism**	**Strategy**	**Arch. feature**
Leaves	X	X	**Leaves**	More/bigger stomata	Ventilation system
Tree Barks	Thick outer layer	Insulation Cladding material		Closed, dense venation system	Ventilation system
	Peeling surface	Overall Morphology Cladding material	**Tree Barks**	Water transport through xylem	Ventilation system
Succulents	Surface area to mass ratio	Overall building design	**Succulents**	CAM	Ventilation system
				Spines and hairs	Cladding material
Animals	Vascular counter current heat exchange	Ventilation system	**Animals**	Respiratory evaporative cooling	Ventilation system
	Soil as thermal sink	Ventilation system		Respiratory counter current heat exchange	Ventilation system
	Colouration	Cladding material		Moisture harvesting	Ventilation system
Humans	X	X	**Humans**	Evaporative cooling by perspiration	Ventilation system

[15] All the strategies listed under the radiation section of the table aim at minimizing the heat gain caused by radiation. Vasodilation is the only strategy observed that aim at maximizing heat loss by radiation.

Chapter 5

Biomimetic design & computation

5.1 Introduction

After exploring nature and defining a set of biomimetic inspirations (Section 4.6 of the previous chapter), in this chapter the biomimetic design approach continues focusing on the selection and translation of the inspirations into an architectural context as seen in Figure 5.1. Two of the inspirations are selected to be digitally modelled in an architectural context. The chosen ideas were strategies related to heat transfer by radiation and convection. Those related to conduction and phase-change mainly dealt with applications regarding material science or the building ventilation system, which are out of the scope of this thesis and represent a different field of study on their own.

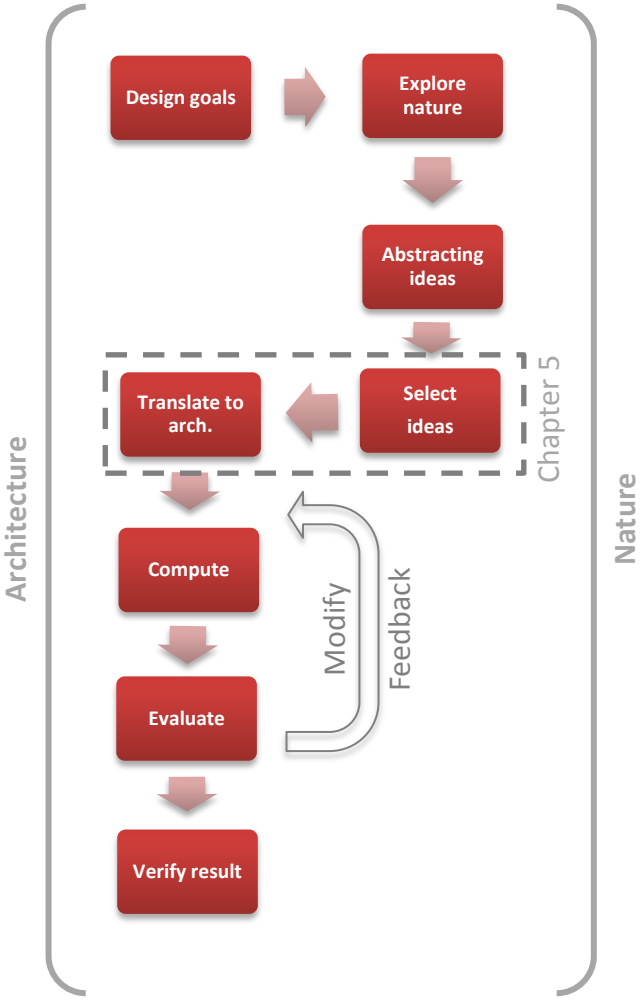

Figure 5.1: Scope of this chapter within the biomimetic design process. Source: author.

The possibility of digitally modelling the biomimetic strategy and combining it with other strategies were the main factors that affected their choice over others.

In this Chapter, the analogy of the selected ideas in an architectural context is explained, and then one of them is first applied in designing a shading screen for a typical office room in Cairo. It represents an initial design proposal and is evaluated by comparing the thermal and daylighting performances of this room before and after the placement of this screen. After seeing positive results, the proposal is further developed by increasing its complexity and integrating the second biomimetic inspiration to it. The final design proposal represents a Double-Skin Façade (DSF) instead of a shading screen. As discussed in Chapter 3, DSFs have many benefits over shading screens such as providing a better indoor environment, reduction in energy consumption and better acoustics.

It is important to note that although studying daylight was not among the main objectives of this research, it is inevitable to take it into consideration as it is directly linked to the building skin design and it is a major human need. In addition, the improvement of daylighting consequently means less dependence on artificial lighting and eventually less energy used, and better psychological wellbeing of the building occupants.

5.2 Selected biomimetic idea(s)

The first selected biomimetic idea is folding strategies inspired from leaves and cactus that provide self-shading, hence reducing heat gain by radiation. The concept of folding is inseparable from Origami explorations and is not new to architecture. Another selected idea is related to termite mounds. Many strategies are applied in termite mounds as discussed in the previous chapter, such as the mound morphology and its internal structure and ventilation network. However the chosen strategy here is the porosity of termite mound surface, which provides increased airflow inside the mound while buffering the exterior wind in the same time.

Figure 5.2: The two selected ideas; top: folding strategies of leaves (Kobayashi, et al., 1998), bottom: porosity of termite mounds (Abou-Houly, 2010).

Only these two biomimetic ideas are chosen and studied in this thesis. Ideas related to conduction and phase change were often associated with research related to material studies and/or the building ventilation system. A true investigation into such ideas and inspirations would need collaboration with material scientists and/or mechanical engineers. Most importantly, they would also require testing with physical experiments not just simulation software. This is currently beyond the capabilities of the researcher and therefore this thesis would mainly deal with morphological explorations of the building skin that can be tested through computer simulations.

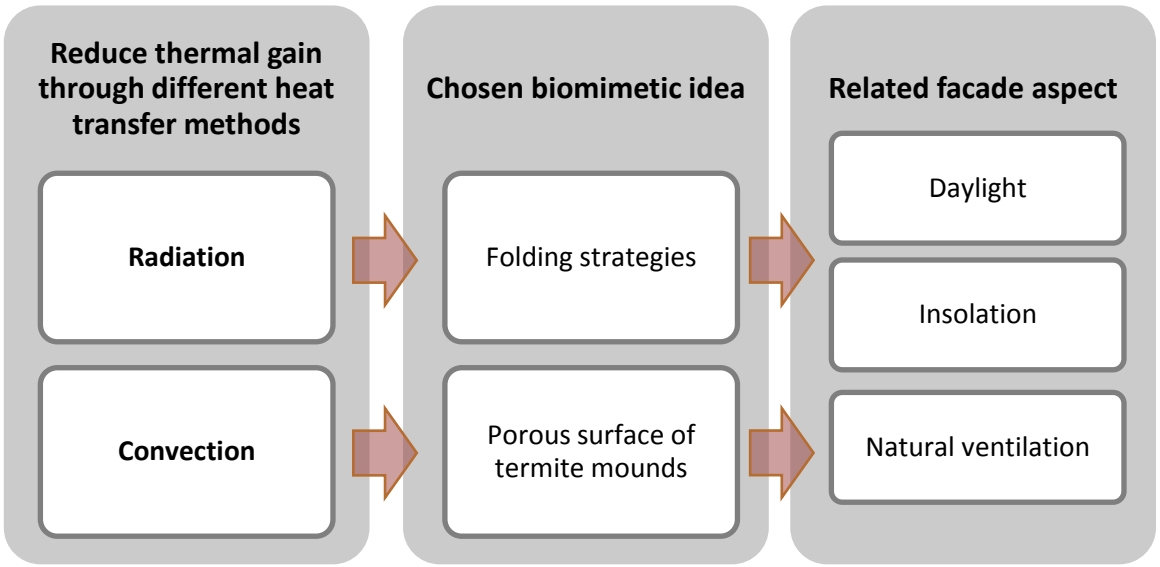

Figure 5.3: The addressed heat transfer methods and their corresponding biomimetic ideas and related façade features. Source: author.

5.3 Architectural analogies

Folding strategies and morphologies are relatively easy to imagine in an architectural context. They have been previously explored in architectural applications because of their potential as a creative form finding method, and also due to the resulting strength of the corrugated structures. The investigation here however is interested in the energy-saving benefits such forms can present. There are numerous possible folding patterns than can be applied to the skin of a building.

Regarding termite mounds, there are many similarities between a mound and a building, like being constructed above ground, being several meters high, having internal metabolism that affects airflow, aiming at protecting the interior from external turbulent conditions, aiming at improving interior ventilation of the structure, and being highly affected by wind.

However one must also acknowledge the obvious differences. Starting with scale, a man-made building is much bigger, increasing the influence of wind as it gets higher. Its inhabitants live in it and not underground, usually close to its surface, and they need light.

In an ideal case, one should think of 'whole-building' design and not just the façade design, especially when trying to optimise heat gain, airflow and daylight all together. But in this research the scope is limited to only façade design for an existing building and therefore the biomimetic inspiration is applied only to the façade to see its contribution alone in decreasing cooling loads.

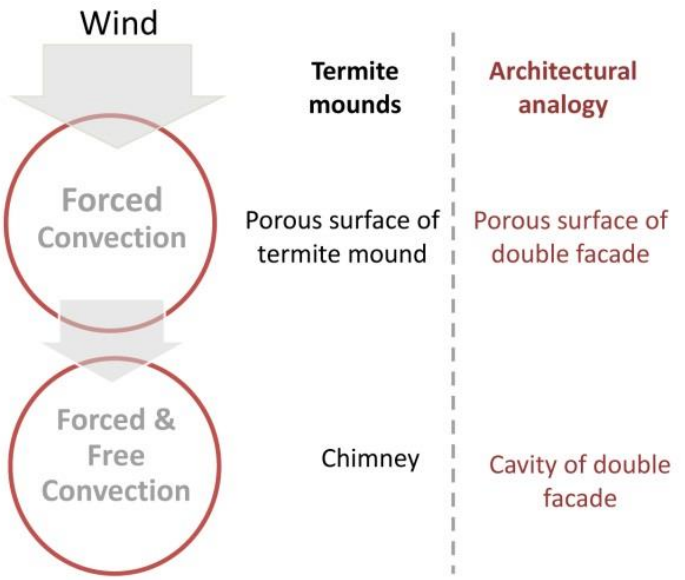

Figure 5.4: Inspiration of the porosity of termite mound surfaces and its analogy in designing a double façade. Source: author.

As mentioned earlier, ventilation in termite mounds is a complex process. Therefore just a couple of important features serve as the main inspiration here. One feature is the porosity of the mound surface that allows the air to enter end get distributed throughout the mound. Another is the concept of air flowing inside the chimney as a result of both free and forced convection, with forced convection being the dominant force. The concept is simplified and abstracted to be able to apply it in an architectural context. Figure 5.4 explains the addressed feature of the mound ventilation system and the corresponding architectural analogy.

Design objectives

- To design a double façade with a folded surface that minimises incident solar radiation.

- The folded surface is also porous and mimics an aspect of the ventilation behaviour in termite mounds in which exterior air passes through a porous wind-driven intermediate zone before entering the façade cavity.
- Air flow in the cavity would be in constant movement and is a result of both wind and buoyancy forces (forced and free convection) either reinforcing or opposing each other, thus attempting to increase convective heat loss of the building.
- Decrease cavity temperature as much as possible by increasing airflow rate and having folded surface that reduces heat gained by solar radiation due to self-shading.
- Provide natural ventilation in office rooms when exterior temperature is suitable.
- Even when natural ventilation is not provided in the office rooms, the cooling loads would decrease due to the presence of this double façade that shaded the internal building and in itself did not over heat.
- Maintain daylight in the office space at least as it was before the folded façade, if not improved.
- Opening size would be a factor of insolation falling on its surface, the bigger the insolation the smaller the opening to help in avoiding over-heating of the cavity.

Regarding the desired folding effect, many folding patterns can achieve the required result which is self-shading. Since we are dealing with the façade, the aesthetic aspect is also important when deciding which pattern to choose, as well as financial and structural aspects.

Difference between similar architectural analogies

Other buildings inspired by termite mound ventilation such as the Eastgate building in Harare, Zimbabwe shown in Figure 5.5, and the Davies Alpine House at Kew Gardens, London, usually apply the analogy on a whole building scale, by designing a central atrium within the building along with other features (Pawlyn, 2011). Their inspirations were based on other strategies related to the internal ventilation system or the overall mound morphology.

Figure 5.5: Eastgate building in Zimbabwe, inspired by termite mounds.
Image source: http://www.makingitmagazine.net/?attachment_id=104.

However, in this research the scope is focused only on façade design for an existing building, taking inspiration mainly from the concept of porosity of the mounds' surface. Therefore, the biomimetic inspiration is applied only to the façade to see its contribution alone in decreasing cooling loads.

Turner and Soar (2008) highlight some misconceptions often associated with the ventilation mechanisms in termite mounds and offer a more accurate explanation of how the ventilation system actually works. They explained that airflow is more complex than the two previously assumed airflow models; the thermosiphon model in closed mounds and the

induced flow model in open mounds. The famous Eastgate building although successful, is based upon these models that were found not to be entirely accurate. Rather, the system is closer to a 'tidal' ventilation model in which air flow depends on temporal variations of the wind as explained in the previous chapter in section4.4.7.

5.4 Software used for computational design and simulations

There are numerous software available that perform environmental simulations and energy analyses. The software vary among their capabilities and limitations, and they range between highly user-friendly such as Autodesk Ecotect but low in accuracy, to less user-friendly but more accurate such as Design Builder. Some are restricting in terms of input geometry and modelling capabilities, while others are more flexible. Table 5.1 illustrates a brief comparison between the most-suitable software for this study. The information was obtained from each software's official website, in addition to several studies that have been made to compare different environmental simulation software (Attia, et al., 2012; Panitz & Garcia-Hansen, 2013; Vangimalla, et al., 2011).

Grasshopper visual programming language has been chosen along with DIVA plug-in for Rhino (Lagios, 2016) since it provides a balance between accuracy, modelling flexibility and interoperability. A main advantage of this choice is the possibility of using an evolutionary solver (Galapagos in Grasshopper) to optimise between conflicting needs which are the decrease of incident radiation and cooling loads while improving daylighting. It is important to point out a limitation of DIVA thermal simulations, that it only performs it on single zones.

Galapagos[16] is an evolutionary solver integrated in Grasshopper where a number of desired variables (called *genes*) and a single numerical value representing the fitness function are inserted. The values can be minimised, maximised, or set a target value. The Galapagos fitness function optimises just one numerical value. If more than one value is needed it can be optimised then put in an equation where the result will act as the fitness. This equation is created manually. The solver starts with a first generation of random combinations of all the possible values of the variables (the range of each variable is set beforehand by the designer). It then calculates the fitness of each combination and sees whether or not it is close to what was intended. It selects the best-performing combinations or solutions to *breed* them and create the second generation of combinations.

The aforementioned biomimetic inspirations along with the chosen software are used to design a shading screen for a typical office room in Cairo as will be seen in the following section.

[16] For more information see the developer's explanation about Galapagos: http://ieatbugsforbreakfast.wordpress.com/2011/03/04/epatps01/

Table 5.1: Comparison between possible environmental simulation software. This data was collected in 2014 and might change in forthcoming versions of each software. Source: author.

Software	Capabilities	Limitations	Accuracy	Engine
Autodesk Ecotect[17]	▪ Whole building energy analysis ▪ Thermal performance ▪ Solar radiation ▪ Daylighting ▪ Shadows and reflections ▪ High interoperability ▪ User friendly	▪ No airflow simulations ▪ Limited modelling capabilities	▪ Validated only if DAYSIM/Radiance engine is used for daylight simulation. ▪ Solar radiation analysis is reliable	▪ CIBSE calculations
Autodesk Vasari[18]	▪ Daylight analysis ▪ Solar analysis ▪ Calculate and analyse energy models ▪ Air flow analysis around buildings (not inside) ▪ High interoperability	▪ Limited modelling capabilities	▪ Validated	▪ DOE2 ▪ Finite Volume Method approach. Turbulence is solved for using a Smagorinsky Large Eddy Simulation (LES) mode
DIVA[19] **for Rhino/ Grasshpper**	▪ Daylight analysis ▪ Thermal analysis ▪ Solar analysis ▪ Glare ▪ LEED daylight compliance ▪ High interoperability ▪ Strong modelling capabilities	▪ No airflow simulations ▪ Thermal simulations are limited to a single zone	▪ Validated	▪ Radiance/Daysim ▪ EnergyPlus
ArchSim[20] **for Grasshopper**	▪ Thermal analysis (multiple thermal zones allowed) ▪ Basic airflow calculations ▪ Basic daylight simulations ▪ User friendly	▪ Limited capability in daylight simulations	▪ Validated	▪ Radiance/Daysim ▪ EnergyPlus
Design Builder[21]	▪ Calculates heating and cooling loads ▪ Energy consumption broken down by fuel and end use ▪ Calculates internal air, mean radiant temperatures and humidity ▪ Heat transmission through building ▪ Shading and daylighting ▪ CFD analysis	▪ Limited modelling capabilities ▪ Low interoperability ▪ Imports only 3D geometry through gbXML, or 2D DXF formats. ▪ Not so user friendly	▪ Validated ▪ Tested against Pheonics for CFD results	▪ EnergyPlus

[17] (Autodesk Ecotect Analysis, 2010)
[18] (Autodesk Vasari, 2014)
[19] (Lagios, 2016)
[20] (Dogan, 2015)
[21] (DesignBuilder, 2014)

5.5 Typical office room

A digital model of a typical office room in Cairo is set up, with dimensions of 4x6 meters and 3 meters high. Only one room (one thermal zone) is studied as this is a limitation of DIVA simulation plugin. The façade of the room faces south and is made of clear low-E (low thermal emissivity) double-glazing. This glazing is the typical choice for a well-designed office building in Cairo where the room accomodates four employees (Figure 5.6).

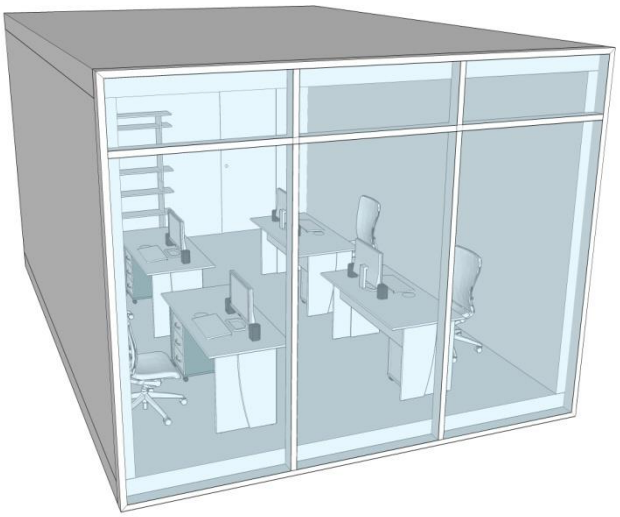

Figure 5.6: Typical furnished office room with double-glazed insulated curtain wall facing south. With dimensions of 4x6 meters and 3 meters high. Source: author.

The room ceiling, floor and walls are all considered adiabatic[22] surfaces in the digital model except its façade. This was important in order to undertand the contribution of the façade design alone on the thermal and daylight performances.

The shading screen will be placed in front of the façade of this room, then the thermal and daylight performances of the room will be compared before and after its placement.

5.6 Initial design proposal

5.6.1 Digital model

The modelling started with choosing a certain folding pattern. The pattern that is explored in the initial design proposal is that of the Hornbeam and Beach leaves. This pattern is also the basis of the famous Miura Ori pattern which is seen in Figure 5.7. However many folding patterns could achieve the same objective which is mainly self-shading.

The first step was to define a surface that would represent the screen placed in front of a building facade. This surface was divided in both the horizontal and vertical directions creating a grid of points. The even horizontal rows of this grid were selected and moved in the horizontal direction to create the fold displacement. Then the even vertical columns of points were selected and moved in a direction perpendicular to that of the façade surface to create the fold depth. A surface is created from the new set of points, forming the folded façade.

5.6.2 Design variables

The design variables that were used are demonstrated in Figure 5.7 and include:

- Number of folds in the X-axis

[22] Adiabatic means Relating to or denoting a process or condition in which heat does not enter or leave the system concerned (Oxford Dictionaries, 2016g).

- Number of fold in the Y axis
- Fold displacement
- Fold depth

There a lot of possible combinations between the variables stated above (Figure 5.8). Instead of manually trying every possible combination, these parameters were set as Genomes in Galapagos, and the fitness function was set to minimise the average value of insolation on all faces. The search range (minimum and maximum possible value of each parameter) was set at the beginning. After observing the results of the evolutionary solver the search range of each variable was adjusted accordingly. It was limited to the ranges that produced the best-performing results, to avoid wasting time in solutions that resulted in high insolation values anyway. The evolutionary optimisation was repeated, and one of the best performing results was selected.

So far we still do not have any openings yet. To determine their size, it was decided to calculate the annual insolation on each face, and then the opening size would be a function of that value. The bigger the numerical value of the insolation, the smaller the opening.

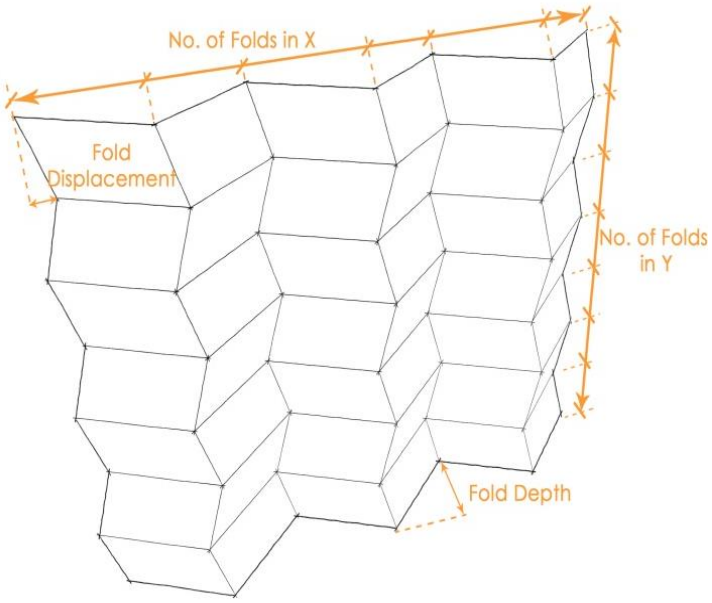

Figure 5.7: Conceptual sketch of the Miura Ori pattern, illustrating design parameters. Source: author.

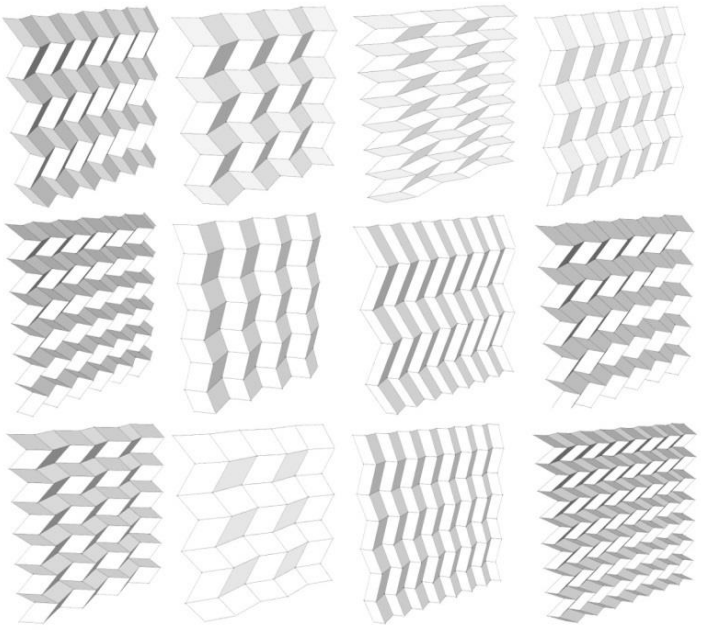

Figure 5.8: Examples of the numerous possible combinations among design variables. Source: author.

After adjusting the search range, daylighting simulations were performed. This time new design variables were added which are:

- Thickness of the skin
- Distance from the inner façade
- Smallest and biggest opening values

These variables had no influence on the amount of insolation on the faces and hence were not optimised in the previous stage. Rather, they have a direct effect of the amount of daylighting and heat gain in the room.

5.6.3 Performance criteria

The performance criteria of the design proposal are the cooling loads and the daylight inside the typical office room. The Galapagos evolutionary solver is used again for these new design variables, with the fitness function (Figure 5.9) set to minimise cooling loads while keeping a minimum illuminance value of 300 lux at four key nodes. The position of these nodes is the centre of four desktops placed the office room (Figure 5.12) with a height of 76 cm from the floor. So the solver first runs a daylight simulation, and if this minimum values is achieved it proceeds to run the thermal simulation and minimises the cooling load. If not, then the solution is ignored and another possible solution is tested.

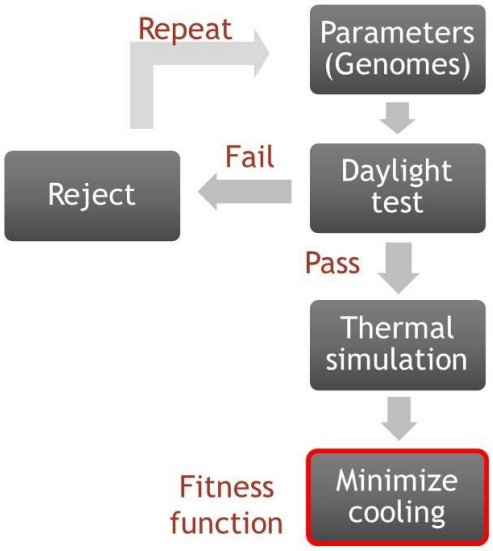

Figure 5.9: Diagram illustrating the workflow of the fitness function set up in Galapagos evolutionary solver. Source: author.

The spatial Daylight Autonomy (sDA) is a metric used to evaluate daylight performance instead of the more commonly used Daylight Factor. It is the first of a string of annual daylight metrics, now commonly referred to as 'dynamic daylight metrics'. It is represented as a percentage of annual daytime hours that a given point in a space is above a specified illumination level. It was originally proposed by the Association Suisse des Electriciens in 1989 and was improved by Christoph Reinhart between 2001 and 2004. It is a major innovation since it considers geographic location specific weather information on an annual basis. It also has the power to relate to electric lighting energy savings if the user defined threshold is set based upon electric lighting criteria (Reinhart, 2011).

Initially sDA simulations were intended to be used, however they take a lot of time, especially when used with Galapagos as it could keep on running for days using the available computers (Processor: Intel core i7, 3.5 GHz, RAM: 32 GB). Illuminance values were used instead just to give an initial indication of the best possible combinations of the new parameters.

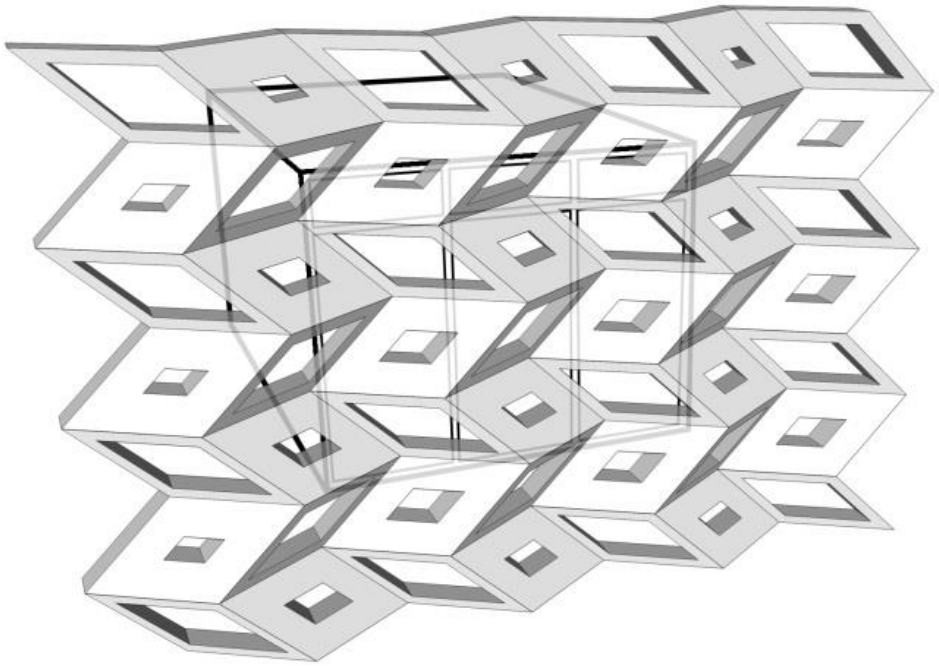

Figure 5.10: Final selected instance of the folded screen after optimisation: 7 folds in X & Y axes, displacement= 0.87 m, depth= 0.7 m, screen thickness= 0.34 m, panel sizes= 1.3*1.2 m. Source: author.

5.6.4 Comparison of performances before and after the screen

In the end, one of the results (Figure 5.10) achieving the least cooling loads was chosen to run a single accurate sDA simulation (Figure 5.12) on a grid of nodes with 60 cm spacing in the whole room to be sure that at least 55% of the analysis nodes receive 300 lux or more during half of the occupied hours. However, the sDA alone would not tell us if parts of the space are over-lit, which is particularly important to know in cities that have relatively low cloud coverage and almost continuous sunshine throughout the year as in Cairo. So a check was performed when certain points receive an illumination value above 3000 lux for more than 5% of the year. This check is important as glare and overheating could occur. Annual insolation on a vertical grid of points located just behind the glazing was also measured before and after the presence of the screen for comparisons.

The following values were calculated before and after the presence of the folded screen for comparison:

- Annual insolation on a vertical grid of points on the office windows
- Spatial Daylight Autonomy inside the room
- Over-lit areas
- Annual cooling loads

The same settings were always used such as materials, occupancy schedules, weather file, accuracy level, etc. Reduction in the cooling loads in the studied room due to the presence of the shading screen reached 25%. The results demonstrated in Figure 5.11 and Figure 5.12 show that traditional curtain-wall systems typically used in Cairo provide high sDA, however this is accompanied by high insolation and over-lit nodes. Here 60% of the space is over lit, usually causing occupants to use blinds and therefore decreasing the daylight entering the space and eventually using electric lighting most of the day. After the folded screen is

placed, a significant decrease in insolation and cooling loads is observed. The minimum daylight needs were achieved with a much less over-lit area (just 14% of the space).

This indicates a better distribution of light throughout the room. The decreased over-lit area not only means less heat gained by radiation, but also an increased real estate value and efficiency of the office space since a bigger area could be comfortably used.

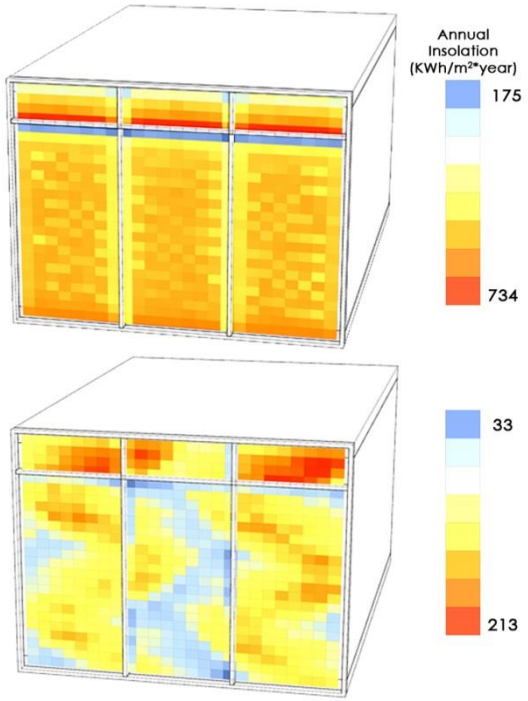

Figure 5.11: DIVA simulations of Solar Insolation analysis before (top) and after the screen (bottom). Source: author.

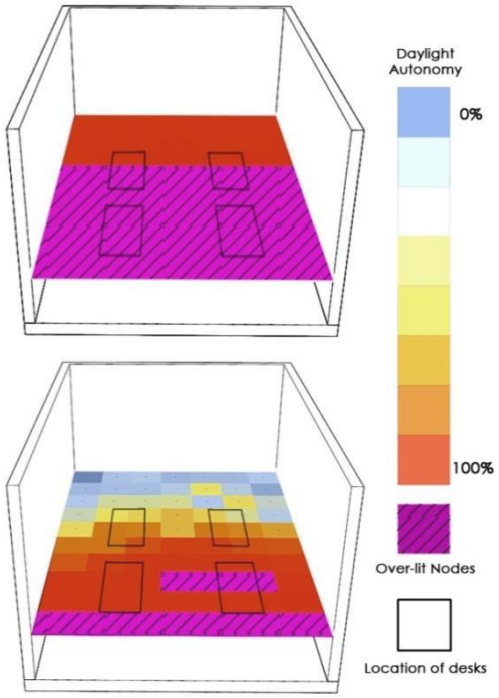

Figure 5.12: DIVA simulations of Daylight Autonomy and over-lit nodes before (top) and after (bottom) the folded screen. Positions of desks are outlined in black. Source: author.

Table 5.2: Comparison between simulation results of a typical office facade and the proposed folded skin, for a 24 m^2 office room in Cairo.

Value Measured	Traditional Skin	Folded Skin	Reduction
Annual insolation (average of all calculated points)	508.4 KWh/m^2	115.5 KWh/m^2	77%
Spatial Daylight Autonomy (300lux, for 50% of occupied time)	100% of space	62.9% of space	37%
Over-lit points (nodes above 3000lux)	60% of space	14% of space	76%
Annual cooling loads	3970.2 KWh	2964.5 KWh	25%

5.7 Final design proposal

After experimenting with folding patterns and having encouraging results, the design is developed to include the second selected biomimetic idea which was the porosity of termite mound surfaces. A different folding pattern is investigated here namely the triangular pinwheel pattern as will be explained in the following sections. It is seen as aesthetically pleasing and also all folded surfaces would be triangular and therefore flat, making it relatively easy to construct as opposed to double-curved surfaces.

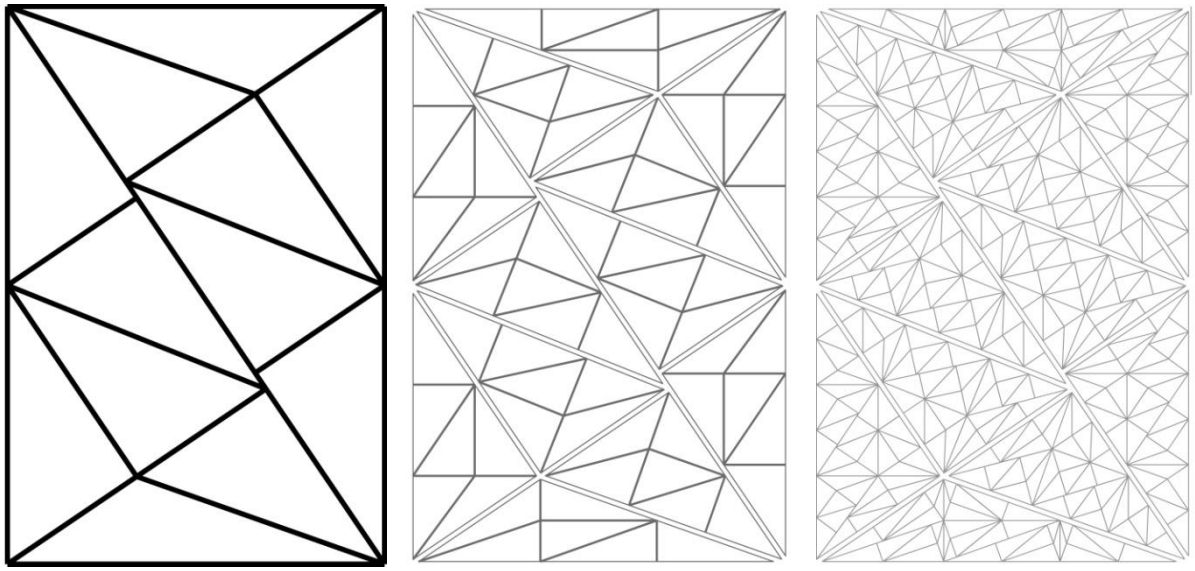

Figure 5.13: Since many patterns can achieve the desired behaviour of self-shading, another pattern is chosen to create the folded surface which is the triangular pinwheel pattern. It is an iterative fractal pattern that was found to be aesthetically more appealing. The first, second and third iterations of this pattern are represented in the figures on the left, middle and right respectively. Source: author.

In this proposal the model developed from being just a shading screen placed in front of the façade, to an actual Double-Skin Façade (DSF). This increases the complexity of the model, and opens up the possibility of benefitting from the advantages of DSFs in general that include better acoustics, better indoor environments and reduction in energy use during the operation of the building. DSFs were discussed in more detail earlier in Chapter 3.

5.7.1 Digital model

The triangular pinwheel is an iterative pattern that takes an input triangle and divides it in a certain way, then applies the same division logic again to the resulting triangles and so on. To have a folded surface made from this pattern, a certain point in input triangle is moved perpendicularly to its surface. The moved distance of this point controls the *fold depth* of each iteration. When applied to the double façade, three iterations were performed as seen in Figure 5.13, and the first iteration was selected to act as the main structural elements that would bear the load of the façade. They also serve another function as they contain a network of small 4x4 cm perforations. This network extends throughout the façade to create the intended *porous* effect.

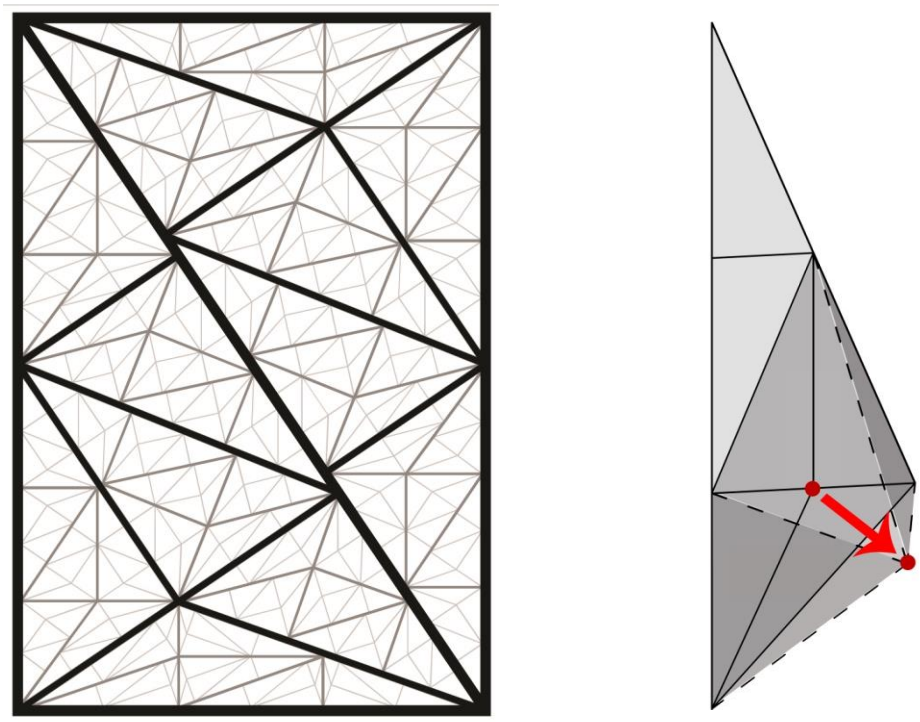

Figure 5.14: Left: hierarchy of 3 iterations of the triangular pattern in black, grey and light grey respectively. Right: adding a third dimension to the pattern to create a folding effect. Each iteration could have a different fold depth that could be positive (outwards) or negative (inwards). Source: author.

The main input in the Grasshopper script is a vertical rectangular surface placed in front of the office room to be studied, exceeding the width of the room from both sides by 2 m to ensure adequate shading.

To run energy simulations in EnergyPlus a thermal zone representing the double façade is created from an outer layer (folded surface), inner layer (the building façade), sides, and top and bottom. Each triangular face of the last iteration has a glazed opening that is not openable, and its size depends on the insolation value of its face (size decreases with increasing insolation). Even with this dependence on insolation, the maximum size of the glazed openings is controlled with a scale factor. A value of 1 means the surface area is completely glazed, and 0 means completely opaque.

The first iteration contains perforations and represents a ventilation network spreading across the façade area as explained earlier. These perforations mimic the porous surface of the termite mounds, while the façade cavity mimics the chimney as air inside it would move due to both free and forced convection forces (buoyancy and wind).

It was intended to model the ventilation network as an independent thermal zone in the digital model. But this turned out to be extremely difficult and beyond the capabilities of EnergyPlus. Even if it were possible, it would result in inaccurate results due to the complexity of its geometry.

5.7.2 Performance criteria

According to the required design goals, a number of performance criteria were chosen to represent the behaviour of the proposed idea. They include the cavity operative temperature, cavity air flow measured in air changes per hour (ach), and Daylight Factor (DF) in the office space. They represent the 'fitness' in the evolutionary algorithmic solver which would attempt to optimise the design variables to reach the solution that achieves the best balance or trade-off between these criteria.

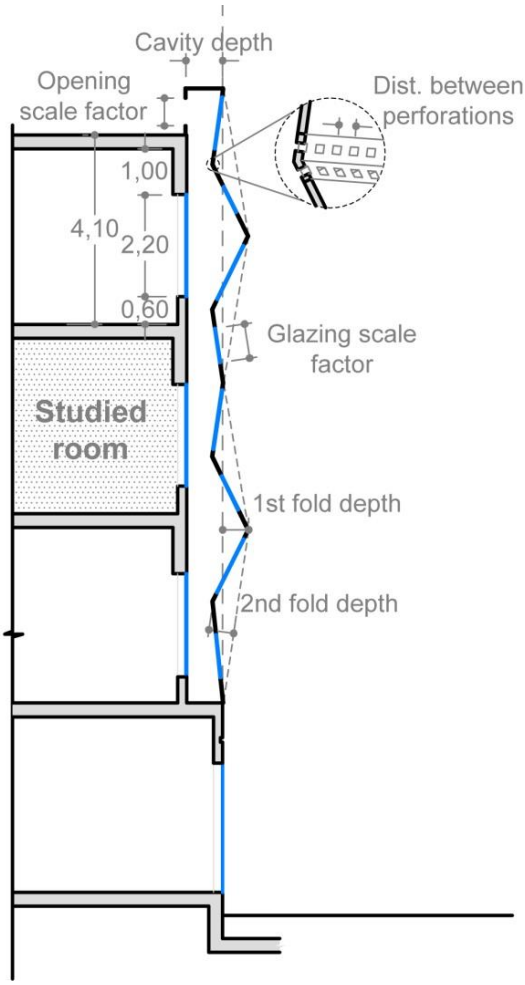

Figure 5.15: Schematic cross-section of the folded double façade illustrating its design variables to be optimised using evolutionary algorithms. Source: author.

Regarding daylight simulations, the Daylight Factor metric is selected for now instead of spatial Daylight Autonomy as a rough representation of the daylight performance. Again, as performed in the preliminary design proposal in section 5.6, when the optimisation process is finished and a solution is selected the daylight autonomy simulations will be performed.

The Daylight Factor is calculated on a 60x60 cm grid of points, 70 cm above floor level. The numeric value of this criterion will represent the number of nodes have a Daylight Factor value of 2 or more.

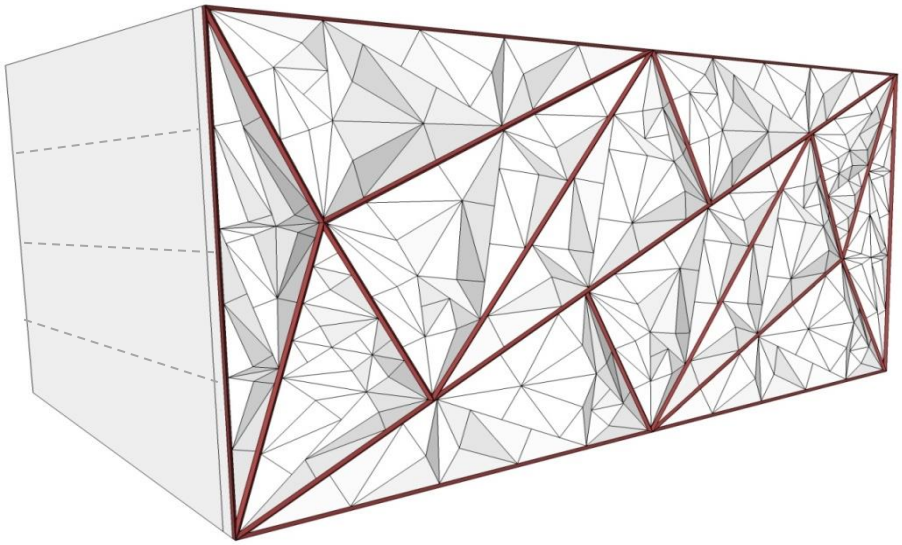

Figure 5.16: Diagrammatic perspective illustrating initial application of the folded pinwheel pattern on a hypothetical façade. Source: author.

5.7.3 Design variables

A number of design variables control the double façade morphology and openings, and therefore its behaviour. Table 5.3 demonstrates each variable and the criteria that it influences. Most variables affect all criteria simultaneously and in different ways. This makes the study and evaluation of the performance of this DSF challenging yet interesting in the same time as will be seen in detail in the next chapter.

Table 5.3: Design variables, their description and affected performance criteria. The search range of each variable is set after preliminary testing of a wider range for each variable alone to understand its influence. Source: author.

	Affected performance criteria			Variable description
	Cavity temp.	Cavity airflow	DF	
1st iteration fold depth	X	X	X	Distance measured from the cavity depth value (either added or subtracted). Zero means no folding is done.
2nd iteration fold depth	X	X	X	Distance measured perpendicularly from each new folded face of the first iteration. Zero means no folding is done.
3rd iteration fold depth	X	X	X	Distance measured perpendicularly from each new folded face of the second iteration. Zero means no folding is done.
Cavity Depth	X	X	X	Distance between the inner surface and outer base surface of the double facade.
Glazing scale factor	X	X	X	A scale factor of each folded triangular face to create glazed openings. The size of opening is inversely proportional to the amount of insolation falling on its face. This scale factor controls the maximum possible opening size. The minimum opening size is controlled by a fixed scale factor.
Distance between perforations	X	X	-	Area of openings is fixed 2x2=16 cm^2. Spacing controls their density. Zero means no openings are present.
Cavity top opening scale factor	X	X	-	A scale factor of rectangular openings at the top of the cavity. Zero means no openings are present.

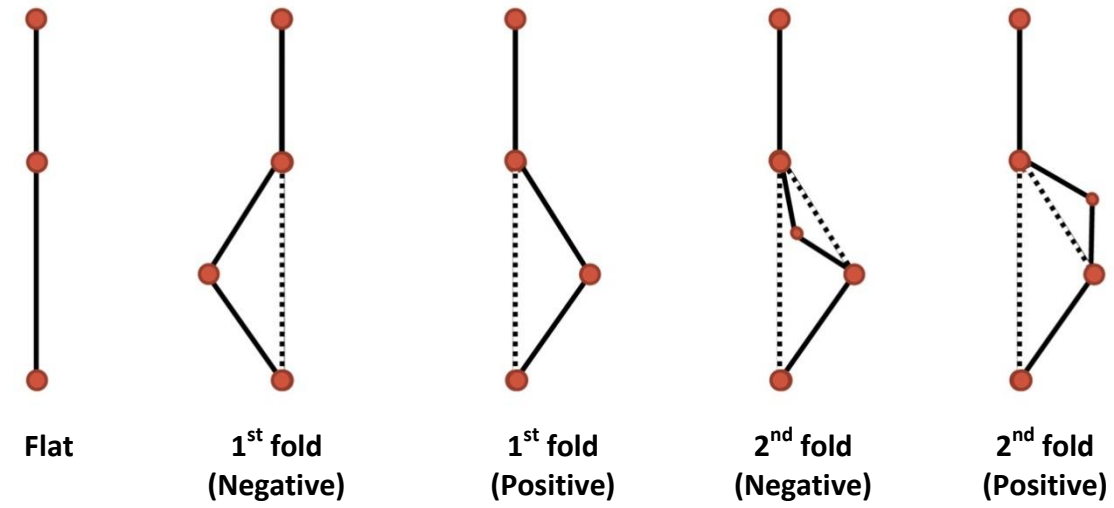

Figure 5.17: Diagram illustrating the fold depths of the first and second iterations, and that they can be either positive (folded outwards) or negative (folded inwards). The same applies for the third iteration as well but was not inserted in the diagram for simplification. Source: author.

5.8 Summary

This chapter represented a preliminary exploration of the application of selected biomimetic inspirations in an architectural context. After actually applying it, the design approach that was mentioned at the beginning of the chapter (Figure 5.1) can be now defined in more detail as seen in Figure 5.18. The selected ideas had to be abstracted into the simplest terms in order to be able to define the main parameters that describe them. Then these parameters were described in a mathematical/geometrical manner so that they would be applicable in an architectural context.

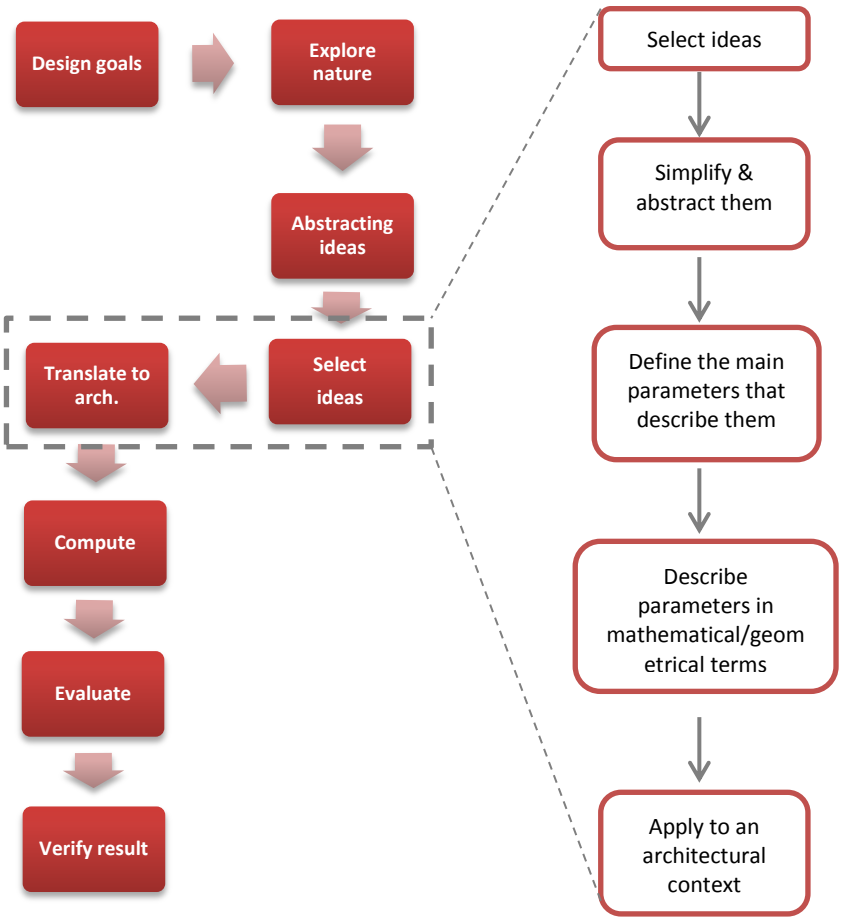

Figure 5.18: Detailed diagram of the design methodology that represented the scope of this chapter. Source: author.

Challenges faced include:

- Translating the biomimetic strategy into mathematical terms in order to be digitally modelled
- Integrating more than one strategy together into a single architectural solution
- Limitations in the simulation software (specifically the thermal simulations that run on EnergyPlus) caused certain simplifications to made in the digital model

A shading screen was proposed and is based on the first selected biomimetic inspiration which is folding, attempting to reduce heat gained by incident solar radiation. Preliminary comparisons of thermal and daylight simulations of a typical office room before and after the placement of the screen showed positive results and a reduction in cooling loads by

around 25%. This was associated with an improvement in daylight performance as well, since the over-lit area was reduced by 76% while maintaining the minimum spatial Daylight Autonomy requirements.

Since the main design objectives were met, this encouraged further development of the proposal to include the second biomimetic inspiration which is the porosity of termite mound surfaces. This is in the aim of increasing heat loss by convection. The shading screen developed into a Double-Skin Façade (DSF) as it has the potential of providing numerous benefits, most importantly improved indoor environment and reduction in energy consumption. A different folding pattern was explored and a more detailed proposal was developed, and represented the DSF. The following chapter includes the development and evaluation of the proposed DSF as it will be optimised and applied on an existing building in Cairo rather than on a hypothetical one as was done in this chapter.

It is important to note that the specific shape or pattern was not of great importance but rather the fact that it was folded and was able to reduce insolation on itself hence decreasing heat gain. The ideas presented in this chapter represent possible examples just for the sake of applying the selected biomimetic ideas and testing them, in order to proceed with the design methodology as a whole. Other patterns might achieve the same design objectives, if properly designed and optimised as well, to be adapted to the context to which they are applied. This gives more freedom to the architect to choose among various shapes and patterns, taking into consideration aesthetic needs as well.

Chapter 6

Application & evaluation of proposed DSF

6.1 Introduction

This chapter represents a detailed study of the final biomimetic design proposal illustrated in the end of the previous chapter. Here the research attempts to evaluate the proposal's thermal and daylight performances in more detail through the following means:

- Applying it to an existing building rather than a hypothetical one to act as a reference and compare its performance before and after its placement.
- Testing its performances in two orientations, South East (SE) and North West (NW). These are the two main orientations of the existing building.
- Comparing it to a typical flat Double Skin Façade (DSF).
- Studying the thermal performance throughout the three hottest summer months instead of July only to have more indicative results.

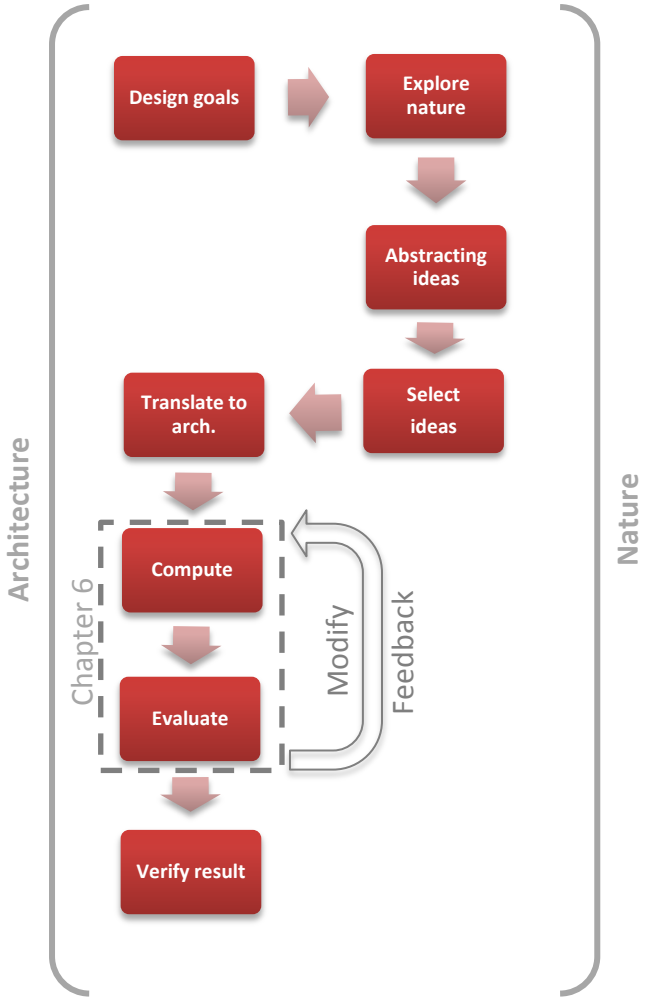

Figure 6.1: Scope of this chapter within the biomimetic-computational design process. Source: author.

The choice of an existing building is important in order to validate its digital model by comparing real and simulated cooling loads. This ensures that the reference case, to which the proposed façade is added, resembles reality as much as possible. In addition, it demonstrates the accuracy of the software used for these simulations which is EnergyPlus.

Many design variables control the morphology of the proposal and hence its performance, each variable is first tested individually to have a general idea of its effect. But since most of them affect both performance criteria (daylight and thermal gain) in different ways, and since there are numerous possible combinations among these variables, an evolutionary optimisation process is performed in order to search for the best possible combinations among them and to have a better understanding of their combined effects. And then one of the best-performing solutions (in each orientation) is selected and evaluated.

An important question followed: does this proposal perform better than a typical flat DSF? So a flat DSF was modelled based on recommendations from the literature reviewed in Chapter Three. The chapter ends with the comparison of the three cases; existing building acting as the reference case, typical flat DSF and proposed DSF. The effect of each

biomimetic inspiration (folds and perforations), and the effect of different orientations on the performance of the proposed DSF is discussed.

The software used in this chapter is Grasshopper visual programming language for Rhino 3D modeller as used in the previous chapter, together with the following plug-ins:

- Octopus (Vierling, 2014) plugin for evolutionary solving instead of Galapagos which was used in the previous chapter. The reason is that Octopus performs multi-objective optimisation of design requirements as opposed to single-objective optimisation in Galapagos.
- ArchSim (Dogan, 2015) Plugin which performs thermal simulations in EnergyPlus v.8.2. It was chosen instead of DIVA for the thermal simulations as it can accept multiple thermal zones and also because it can simulate airflow among them.
- DIVA for Rhino (Lagios, 2016) for daylight simulations that run using Radiance light simulation tool (Fuller & Mcneil, 2016).

6.2 Reference case: An office building in Cairo with a single facade

6.2.1 Context and building description

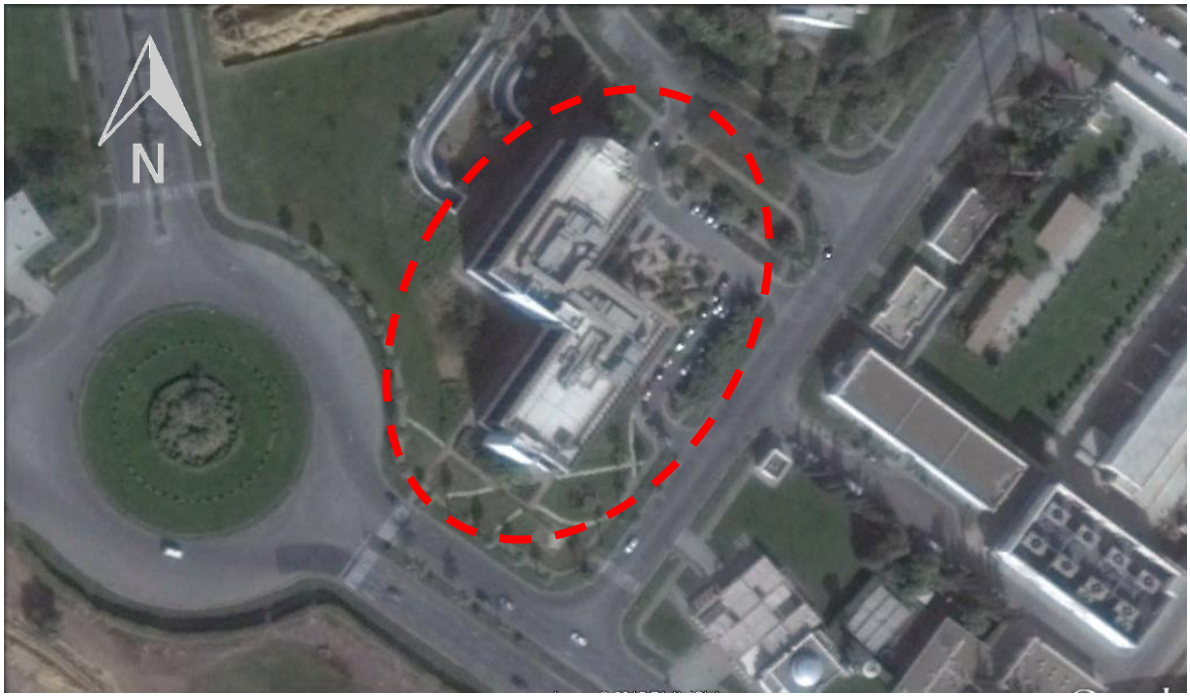

Figure 6.2: Site plan of the reference case B-19 office building in the Smart Village, Cairo, Egypt. Source: Google Earth.

The Smart Village in Cairo is a contemporary business district that represents the state of the art in office building design in Egypt. This business district is located around 28 Km West of Cairo, on the Cairo-Alexandria desert road, and it is considered a sub-urban area with low density mid-rise buildings.

One of these buildings was chosen for this application, which is the B-19 building (Figure 6.3). It currently includes three tenants; Nokia Company, the Egyptian Competition Authority and the Smart Village Company Headquarters. It is composed of two basement floors for parking, electrical services and storage areas, a ground floor and three upper

floors all dedicated to office use following an open-plan concept and some spaces are divided by glass partitions to form small office rooms. Working hours are from 8 am till 5 pm, and Fridays and Saturdays are off. This was particularly important in order to set the correct occupancy schedule in the digital model.

General information about the building includes:

- Location: 28 km, Cairo-Alex desert road.
- Consultant: ECG (Engineering Consultants Group).
- Main Contractor: Shuttering Construction Co.
- Year of completion: 2009.
- Project budget: 70,000,000 EGP.
- Building footprint: 2230 m^2.
- Total built up area: 13,380 m^2.

Figure 6.3: North West and South West views of the B-19 building in West of Cairo.
Source: http://alnoranarchitecture.com/projects/smart-village-b19-building.

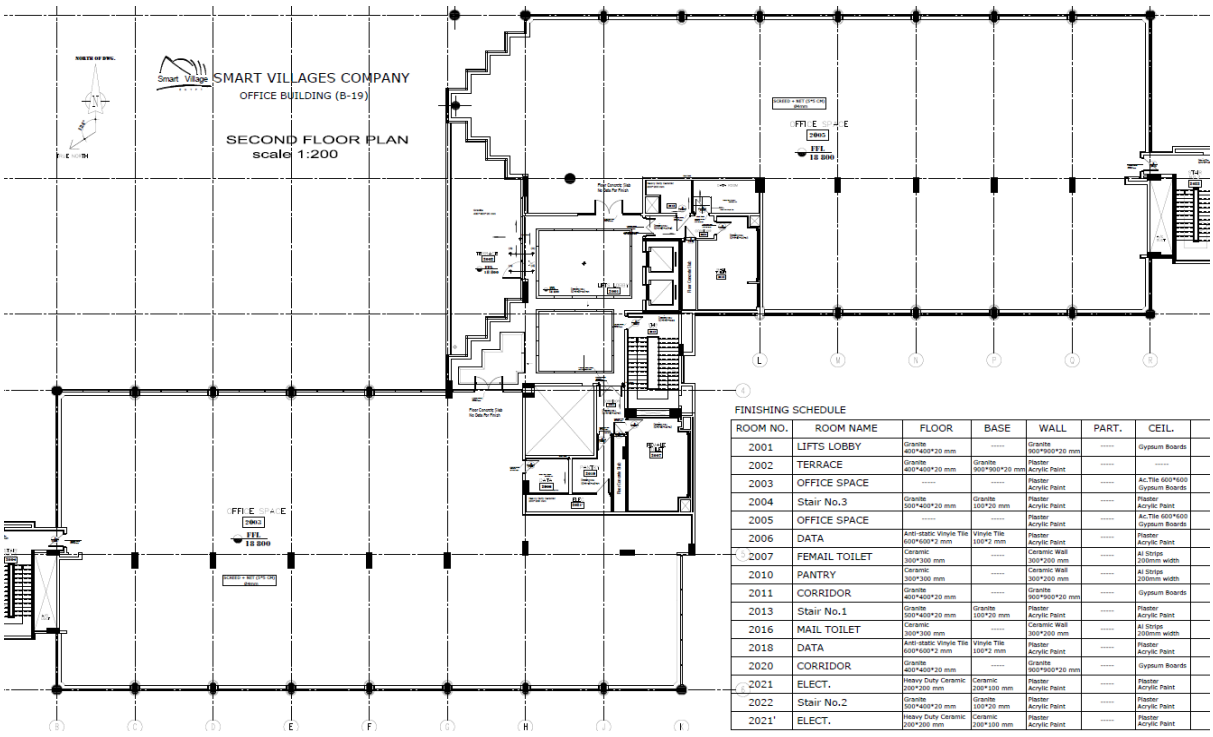

ROOM NO.	ROOM NAME	FLOOR	BASE	WALL	PART.	CEIL.
2001	LIFTS LOBBY	Granite 400*400*20 mm	-----	Granite 900*900*20 mm	-----	Gypsum Boards
2002	TERRACE	Granite 400*400*20 mm	Granite 900*900*20 mm	Plaster Acrylic Paint	-----	-----
2003	OFFICE SPACE	-----	-----	Plaster Acrylic Paint	-----	Ac.Tile 600*600 Gypsum Boards
2004	Stair No.3	Granite 500*400*20 mm	Granite 100*20 mm	Plaster Acrylic Paint	-----	Plaster Acrylic Paint
2005	OFFICE SPACE	-----	-----	Plaster Acrylic Paint	-----	Ac.Tile 600*600 Gypsum Boards
2006	DATA	Anti-static Vinyle Tile 600*600*2 mm	Vinyle Tile 100*2 mm	Plaster Acrylic Paint	-----	Plaster Acrylic Paint
2007	FEMAIL TOILET	Ceramic 300*300 mm	-----	Ceramic Wall 300*200 mm	-----	Al Strips 200mm width
2010	PANTRY	Ceramic 300*300 mm	-----	Ceramic Wall 300*200 mm	-----	Al Strips 200mm width
2011	CORRIDOR	Granite 400*400*20 mm	-----	Granite 900*900*20 mm	-----	Gypsum Boards
2013	Stair No.1	Granite 500*400*20 mm	Granite 100*20 mm	Plaster Acrylic Paint	-----	Plaster Acrylic Paint
2016	MAIL TOILET	Ceramic 300*300 mm	-----	Ceramic Wall 300*200 mm	-----	Al Strips 200mm width
2018	DATA	Anti-static Vinyle Tile 600*600*2 mm	Vinyle Tile 100*2 mm	Plaster Acrylic Paint	-----	Plaster Acrylic Paint
2020	CORRIDOR	Granite 400*400*20 mm	-----	Granite 900*900*20 mm	-----	Gypsum Boards
2021	ELECT.	Heavy Duty Ceramic 200*200 mm	Ceramic 100*100 mm	Plaster Acrylic Paint	-----	Plaster Acrylic Paint
2022	Stair No.2	Granite 500*400*20 mm	Granite 100*20 mm	Plaster Acrylic Paint	-----	Plaster Acrylic Paint
2021'	ELECT.	Heavy Duty Ceramic 200*200 mm	Ceramic 200*100 mm	Plaster Acrylic Paint	-----	Plaster Acrylic Paint

Figure 6.4: A typical floor plan of the B-19 office building. It demonstrates an open-floor layout, each floor can be partially or fully partitioned by its tenant according to their needs. Source: drawings provided by building owner.

6.2.2 Climate and weather data

Cairo has a typical hot desert climate that is usually dry from May till September, receiving an average annual rainfall of 26 mm. It has mainly two seasons; around eight months of summer and four months of winter, with the hottest months being June, July, and August. The average daily maximum and minimum temperatures in summer are 35°C and 21°C respectively. Summer temperatures can reach as high as 47°C in the peak of heat waves. Prevailing winds throughout the year range from North East to North West. Each year in the period between March and May, hot dry dusty winds blow from the South or South West. When these winds arrive they cause temporary increase in temperature and decrease in humidity (National Oceanic and Atmospheric Administration, 1990).

Figure 6.5 presents a visualisation of annual dry bulb temperature and relative humidity in which we can notice occasional heat waves represented in vertical strips in relatively darker colour. Figure 6.6 illustrates the Cairo wind rose.

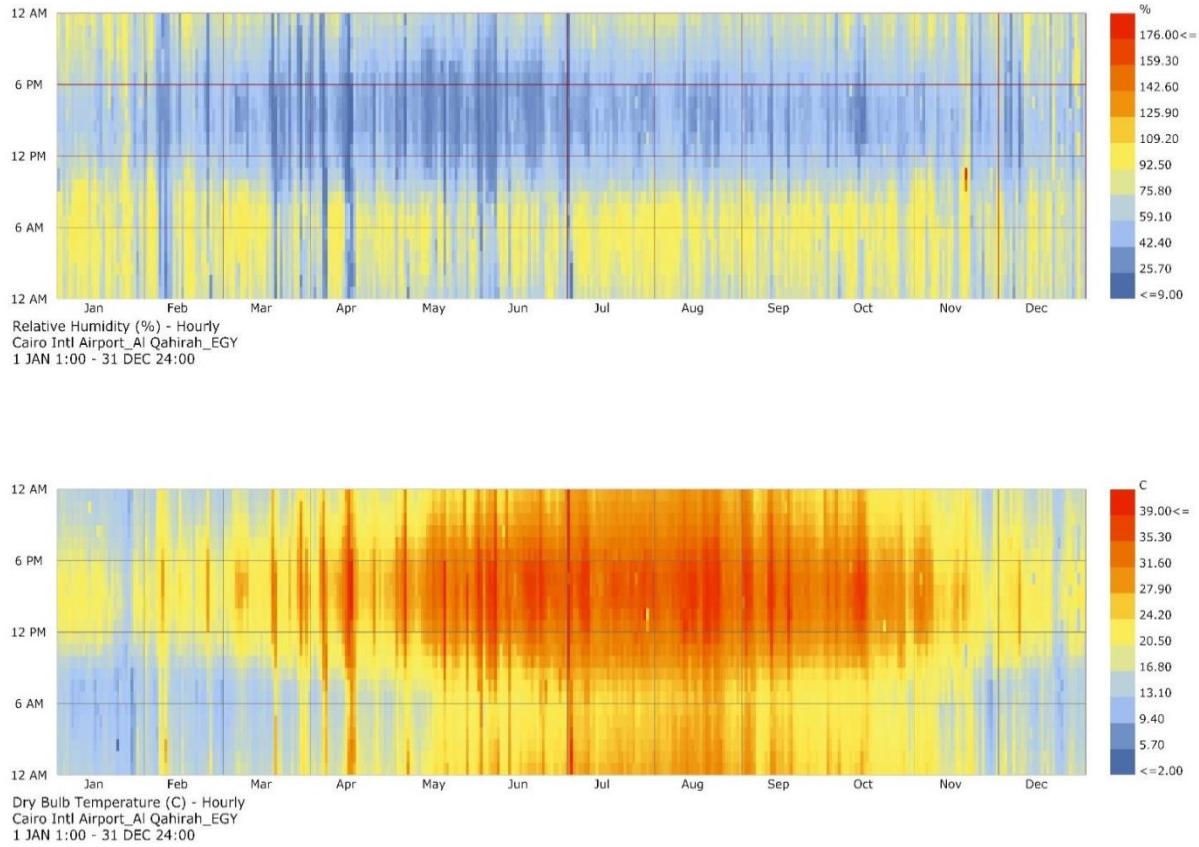

Figure 6.5: Visualised daily relative humidity (top) and dry bulb temperature (bottom) throughout a typical year in Cairo using Ladybug Plug-in for Grasshopper. The visualisation facilitates noticing the occasional heat waves that hit Cairo represented in vertical red strips. Source: author.

Weather files for a typical Egyptian meteorological year were obtained from the EnergyPlus website (EnergyPlus, 2014b). They represent data provided by the National Climatic Data Centre recorded from 12 to 21 years ending in 2003. This data is measured at the Cairo International Airport which has a sub-urban setting that is very similar to that of the reference case. This fact minimises the errors that could have been caused by the urban heat island effect for example, if the building were located within the city. This is often a problem that affects the accuracy of environmental simulations of buildings specifically if they are within a dense urban context.

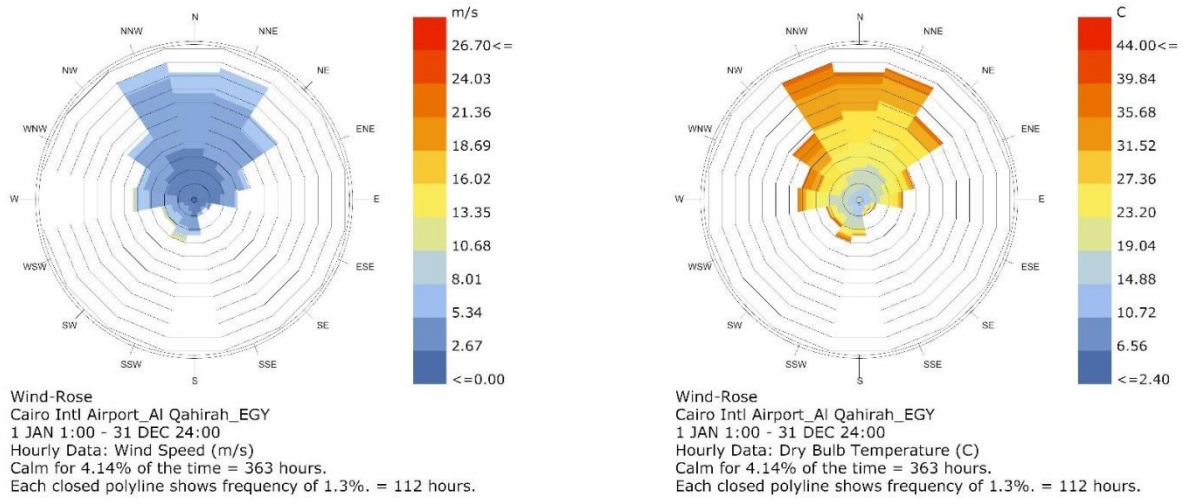

Figure 6.6: Cairo wind rose visualised using Ladybug Plug-in for Grasshopper. Colours represent the wind velocity (left) and the average dry bulb temperature (right). Source: author.

6.2.3 Studied room and façade type

Only one office room from the reference case is assessed throughout this chapter, representing a typical mid-floor space in the South Eastern (SE) façade with the surface area of 40 m^2 and dimensions of 5 m in width, 8 m deep, and 4.1 m high. Additionally, a similar room in the North Western (NW) façade is studied. These orientations represent the two main orientations on which most of the office spaces are located dues to the geometry of the building as seen in Figure 6.4.

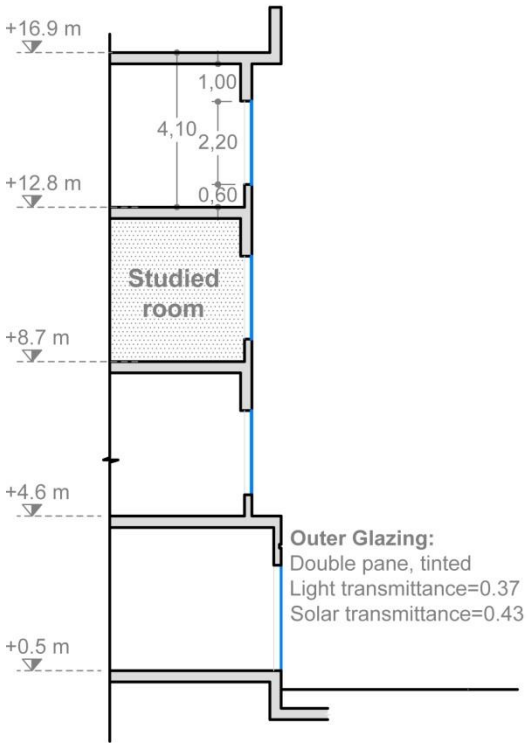

Figure 6.7: Schematic wall cross-section of the B-19 building. The studied room is on the second floor representing a typical mid-floor space. Source: author.

A digital model of the room and its surrounding spaces (not the entire building) was created, and the construction materials assigned were the same as those in the existing building; most importantly the façade had non-operable double-glazed tinted curtain wall panels and aluminium cladding as follows:

- Double glazing:
  - 6 mm blue tinted outer pane, 12 mm air gap, 6 mm clear float glass pane.
  - Shading Coefficient[23]= 0.43 maximum.
  - U-Value[24]= 2.8 W/m^2K, maximum.
  - Light transmittance[25]= 37% minimum.
- Exterior walls: 20 cm red brick and 30 cm reinforced concrete beams. No insulation.
- Aluminium cladding: used on exterior structural columns, standard RAL COLOR 9006 either Polyester Powder coated or PVDF Coat.
- Window to wall ratio (WWR): approximately 0.28.

The technical specifications of these materials were requested and obtained by interviews and email correspondence with the building owner.

[23] The Shading Coefficient is the ratio of the solar heat gain through a given glazing as compared to that of clear, 1/8 inch single pane glass. It is referred to also as Solar Transmittance or Solar Heat Gain Coefficient (Ander, 2014).

[24] The U-Value is the rate of heat flow due to conduction, convection, and radiation through a window as a result of a temperature difference between the inside and outside (Ander, 2014).

[25] The light transmittance is the percentage of the visible portion of the solar spectrum that is transmitted through a given glass product (Ander, 2014).

6.2.4 Actual cooling loads

The ventilation in the building is 100% mechanical; no openings are present in the curtain wall for natural ventilation. It has a central air conditioning (A/C) system which receives ready chilled water from a main chiller located elsewhere in the Smart Village. Occupants are able to switch the A/C on or off and control its temperature. Generally in winter months the A/C system starts 2 hours later and stops an hour earlier than the normal working hours.

Total annual cooling loads are equal to 234,143 ton refrigeration which is equivilant to 823,446 KWh. The spaces that need cooling in the building have a total area of 7,280 m^2 which means that the annual cooling consupmtion per area is 113 KWh/m^2.

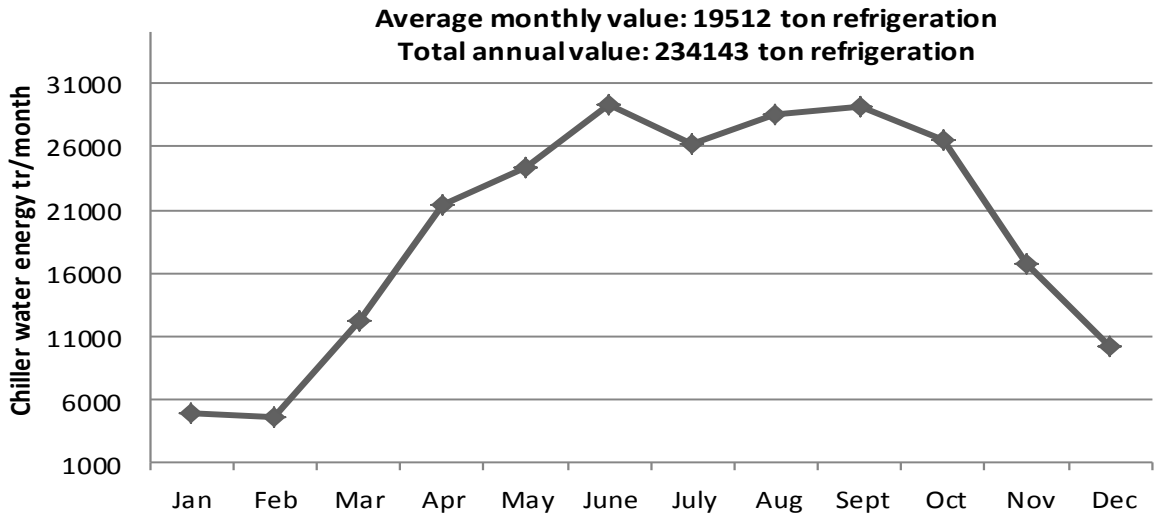

Figure 6.8: Actual monthly chilled water energy for the entire B-19 building in 2014. Source: author, based on data provided by the B-19 building owner.

Figure 6.8 demonstrates the monthly energy consumption needed for cooling in the year of 2014. Cooling loads closely follow the annual increase in temperature as expected. A sudden slight drop was noticed in the month of July, probably because this month corresponded with the holy month of Ramadan in which working hours are reduced and consequently the cooling system operates for a reduced number of hours during this month.

6.2.5 Thermal simulations (in SE/NW)

The digital thermal model was set up to be as closely-related to the real room as possible. Building drawings, material specifications, occupancy schedules, cooling set-points etc. were obtained from the building owners and incorporated into the model. Complete settings of the thermal model are placed in Appendix A. Simulations were performed once when the room faced SE and another time in the NW orientation as these are the two main orientations of the existing building.

The thermal model illustrated in Figure 6.9 consists of four zones:

- Zone 1: the office room itself located in the second floor.
- Zone 2: a block representing part of the third floor.
- Zone 3: a block representing the rest of the second floor spaces surrounding the room.
- Zone 4: a block representing part of the first floor.

It was not useful to model the entire building as this research is only interested in one room and its surrounding spaces that are in direct contact with it from all directions and therefore affect its heat gain and loss. All office spaces are constantly air-conditioned and kept at a temperature of 25˚C. Windows were placed only above and below the studied room because the flat and proposed DSFs will be added only to a portion of the façade and not to its entire length as will be discussed in sections 6.3 and 6.4.

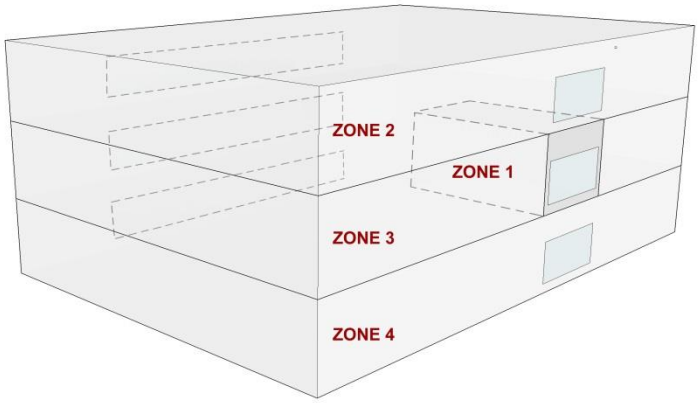

Figure 6.9: Diagram illustrating the zones of the thermal model of the reference case to be simulated using EnergyPlus. Source: author.

Cooling loads for June, July and August which are the hottest months of the year were simulated as they will serve as reference values to be compared with the proposed and flat DSFs later in this chapter. In the SE orientation the cooling loads for these three months were 2253.4 KWh for the 40 m^2 room, and are slightly higher in the NW orientation and are equal to 2284 KWh (Figure 6.10). However, when simulations are made for an entire year, the SE consumed more cooling loads as will be seen in the following section.

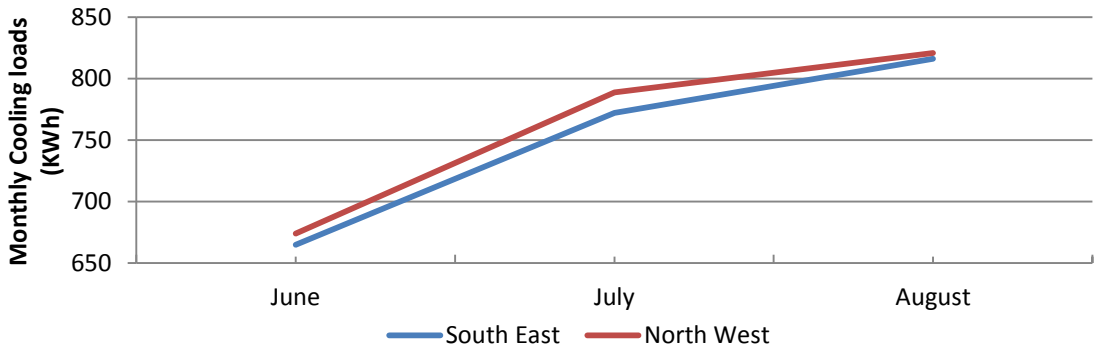

Figure 6.10: Simulations of cooling loads for the three hottest months of the year for the studied room of 40 m^2 of the B-19 building in both SE and NW orientations. Source: author.

6.2.6 Model validation

Annual thermal simulations also were made for the room in both SE and NW orientations as seen in Figure 6.11, which demonstrated that cooling loads in the SE orientation were a bit higher than the in NW which was an expected outcome as the SE orientation receives more solar radiation.

Results of annual cooling loads in SE and NW orientations predicted a consumption of 134 KWh/m^2 and 124.7 KWh/m^2 respectively demonstrated in Figure 6.11. Since these two orientations are the main ones of the building on which most spaces were located, then it can be assumed that the approximate annual cooling load per square meter is the average of these two values which results in *129 KWh/m^2*.

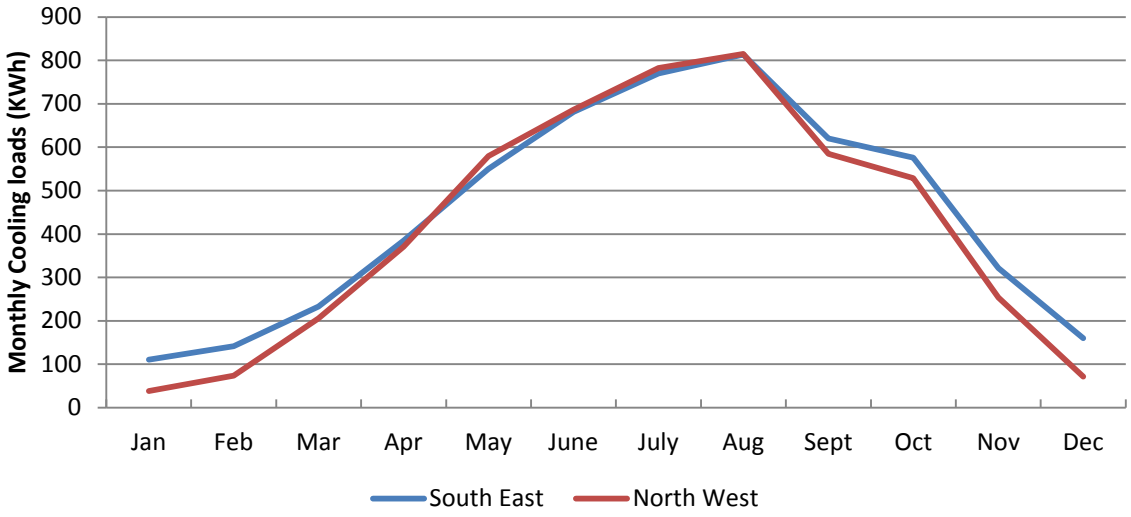

Figure 6.11: Simulated annual cooling loads of only the studied room of 40 m^2 of the B-19 building in South East and North West orientations. Source: author.

Simulation results were slightly over-estimated when compared with actual readings of the building which indicated that average annual consumption is *113 KWh/m^2*. However this over-estimation occurred mainly in the hot summer months, and was rather expected since the simulated models are rooms adjacent to external facades hence they were more subject to over-heating and require more cooling energy than other deep interior spaces in the building. The actual cooling loads however were for the entire building spaces, both interior and façade-adjacent ones. The comparison between annual simulated and actual cooling loads per square meter is presented in Figure 6.12.

This validated the digital model of the existing room since results were reassuring and the error between actual and simulated cooling loads was around 14%. This digital 'thermal' model of the existing room and its surroundings will be used as a base in the following sections to which the proposed DSF as well as the flat DSF will be added in order to see the resulting different performances in each case.

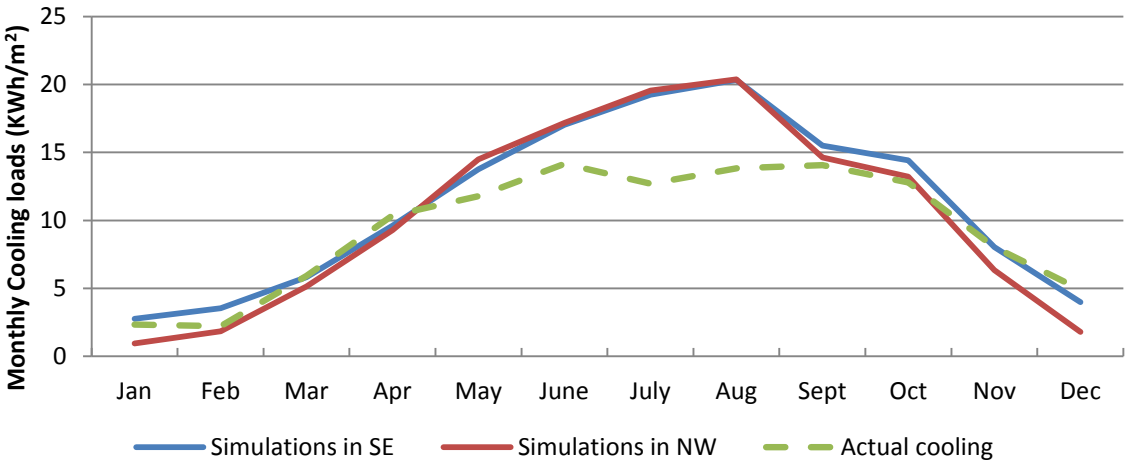

Figure 6.12: Comparison between annual simulated and actual cooling loads per square meter for the B-19 Building. The simulations are over-estimated in the summer months. However it was expected since the simulated spaces are always adjacent to an external façade subject to heat gain. While actual values are for the entire building include that of internal spaces as well that more 'sheltered' from external heat and hence require less energy. Source: author.

6.2.7 Daylight simulations (in SE/NW)

Simultaneously another digital model of the same existing room was prepared for daylight analyses that were performed in SE and NW orientations. Optical properties and specifications of the façade materials used were obtained from the building owner. Regarding the internal finishing materials, although the architect specified the type of materials used, their optical specifications were not available nor were the names of their providing companies. Hence the researcher depended on getting such information from technical data available in the literature of actual manufacturers of similar material types. The exact specifications of these materials along with other model setting are placed in Appendix A.

As mentioned in the previous chapter, the spatial Daylight Autonomy (sDA) metric was used to evaluate the existing room's performance. It is the first of a string of annual daylight metrics, now commonly referred to as 'dynamic daylight metrics'. It is represented as a percentage of annual daytime hours that a given point in a space is above a specified illumination level. It considers geographic location specific weather information on an annual basis. It also has power to relate to electric lighting energy savings if the user defined threshold is set based upon electric lighting criteria (Reinhart, 2011).

As seen in Figure 6.13, in the SE orientation, the Spatial Daylight Autonomy (sDA) of 300 lux, for half of occupied time, was barely achieved for 51% of the room area. However 37.5% of this area was over-lit, receiving more than 3000 lux in more than half of the occupied time. In the NE orientation the sDA reached only 46.3% of the room, and the over-lit area was 23.1% which is quite less than that in the SE.

Although no glare analyses were performed, the percentage of over-lit area indicated the probability of glare problems especially if this area exceeded 30% of the total room area (Sherif, et al., 2014). This would result in either occupants being located away from the over-lit area to avoid discomfort which reduces the efficiency of the office space, or simply using blinds as in most cases which increases the consumption of electrical lighting.

Another daylight metric was calculated as well which is the Daylight Factor (DF). It represents the ratio of internal light level to external light level. It is less accurate and thus faster to calculate than the sDA as it is calculated only on a specific point in time which is 21st of September at 12:00 PM based on a standard CIE overcast sky (CIE stands for *Commission Internationale de l'Éclairage:* the International Lighting Commission).

Daylight Factor minimum according to standards is a value of 2 for office spaces (British Standards Institution, 2008). This minimum was achieved in 36 nodes out of 104 in the room which represented just 34.6% of the room space. Despite not accurately reflecting the real daylight performance calculated by the sDA, this value was only important for later use during the comparison of optimisation results. The reason was because the Daylight Factor calculations are much faster so they are used in the evolutionary optimisation process of the deign proposal to be added. The sDA will be calculated again only for the selected results for accurate comparison with the existing room.

It is important to note that no actual measurements of daylighting were taken from the existing building due to the constraints of time and financial resources needed to buy the measurement tools. Nonetheless Radiance software which was used in daylight simulations was validated to be capable of modelling interior illuminances due to daylight for complex façade configurations (Reinhart & Andersen , 2006).

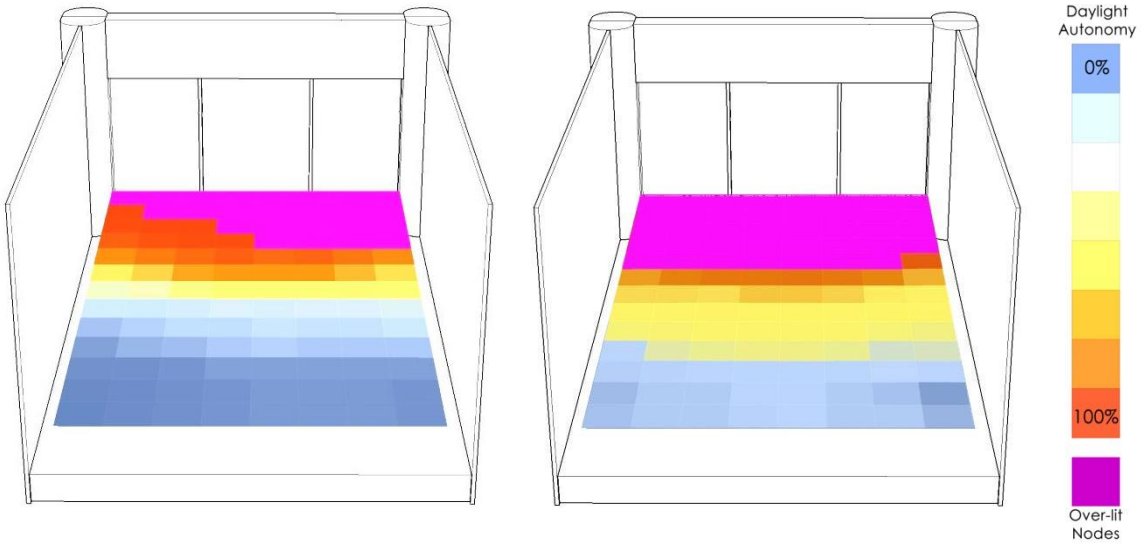

Figure 6.13: Daylight Autonomy simulations for the existing room in the B-19 building in the NW orientation (left): 46.3% and SE orientation: 51% (right). Source: author.

6.3 Typical Flat Double Skin Façade

6.3.1 Structure, components and materials

A flat double façade is proposed that is based on the main observations found after reviewing DSFs in hot climatic areas (Chapter 3). It is very similar to the one proposed by Hamza et al. (2007) which was also designed in Cairo.

It is added to the existing B-19 building model as a hypothetical proposal to see its effect on thermal and daylight performances compared to a more geometrically complex façade as the one presented in the next section. This is important in order to know whether or not building a geometrically-complex DSF is worth the effort and cost.

It is important to note that the glazing of the existing building model was changed because it is not suitable to use high-reflecting glazing as the inner glazing of a DSF. This is because of two reasons; firstly it is important to prevent heat from entering the cavity itself before reaching the rooms, secondly it will not be seen anyway from the exterior as it is covered by the outer glazing of the DSF.

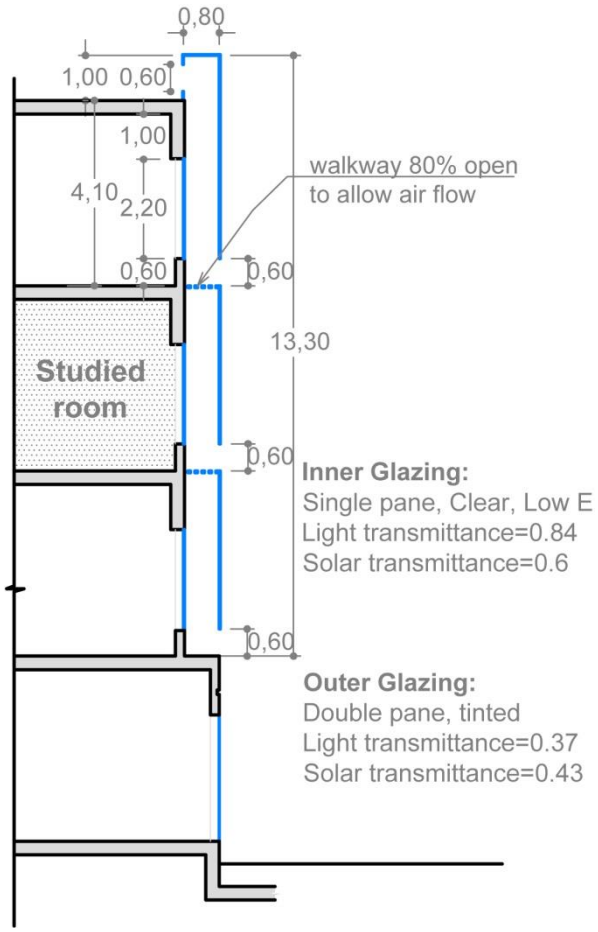

Figure 6.14: Schematic wall cross-section of the B-19 building with a flat DSF added to it. Source: author.

Figure 6.14 describes its geometrical configuration and the glazing materials used. It is a fully glazed double façade as follows:

- DSF type: corridor, separated at each floor with walkways that are 80% open to allow airflow and ventilation.
- Overall dimensions: 9 m wide, 13.3 m high (starting form first floor).
- Cavity width: 0.8 m.
- Air openings: 0.6 m at each floor level and at the top.
- Inner glazing: double pane, clear, Low E, light transmittance= 0.74, solar transmittance= 0.5.
- Outer glazing: double pane, blue tinted, light transmittance= 0.37, solar transmittance= 0.43 (same as that used in the existing building).

The technical specifications of these materials along with other settings of the thermal model are placed in Appendix A. The DSF is 9 m wide, extending 2 m from both sides of the studied room which is 5 m wide. The height of the DSF is 13.3 m as it covers three floors (starting the first not the ground) and extends 1 m after the ceiling of the last floor to include openings for ventilation.

6.3.2 Thermal simulations (in SE/NW)

After adding the flat DSF the thermal simulations were repeated in SE and NW orientations. Figure 6.15 shows the model used for the thermal simulations. They include the same four zones of the reference case in addition to zones 5, 6 and 7 that together represent the flat DSF. It was divided into three zones on top of each other instead of just one based on recommendations from existing literature (such as in Mateus et al., 2014) to increase the accuracy of the simulations.

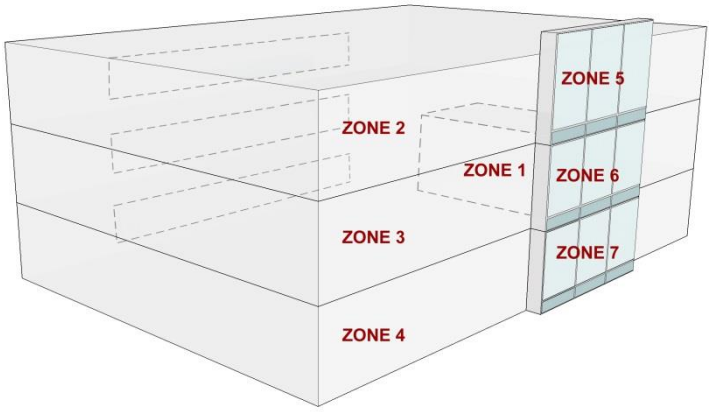

Figure 6.15: Diagram illustrating the zones of the thermal model of the Flat DSF to be simulated using EnergyPlus. The DSF is divided into 3 parts represented in zones 5, 6 and 7. Source: author.

Cooling loads for June, July and August were simulated and both orientations produced very similar results as seen in Figure 6.18. They resulted in a consumption of 2124.95 KWh and 2183 KWh for the SE and NW respectively which corresponds to a reduction of only 5.7% and 4.4% when compared with the existing reference case. These results confirm the argument that DSFs are not always suitable for hot climatic regions as they produce small energy savings and sometimes even an increase in energy consumption if not well designed. Cavity temperatures were also calculated.

The specific output selected from EnergyPlus to measure the cavity temperature is the Zone *Operative Temperature* (OT) which is the average of the Zone Mean Air Temperature[26] (MAT) and Zone Mean Radiant Temperature[27] (MRT). It is measured in degrees Celsius (EnergyPlus, 2014).

$$OT = 0.5*MAT + 0.5*MRT$$

Equation 6.1: The Zone Operative Temperature (OT) as calculated in EnergyPlus.

Cavity temperatures closely follow the ambient site temperature, being around 4˚C higher. The NW cavity temperature is usually higher than the SE orientation by 1˚C as seen in Figure 6.17. The cavity airflows follow the site wind speed pattern across the three months (Figure 6.16). They range between 80 and 240 ach which seem to be quite high, possibly indicating limitations in capability of EnergyPlus in simulating airflow in DSF.

[26] The zone mean air temperature is the average temperature of the air temperatures at the system timestep. The zone heat balance represents a "well stirred" model for a zone, therefore there is only one mean air temperature to represent the air temperature for the zone (EnergyPlus, 2014).

[27] The zone mean radiant temperature is a measure of the combined effects of temperatures of surfaces within that space. Specifically it is the surface area × emissivity weighted average of the zone inside surface temperatures, where emissivity is the Thermal Absorptance of the inside material layer of each surface (EnergyPlus, 2014).

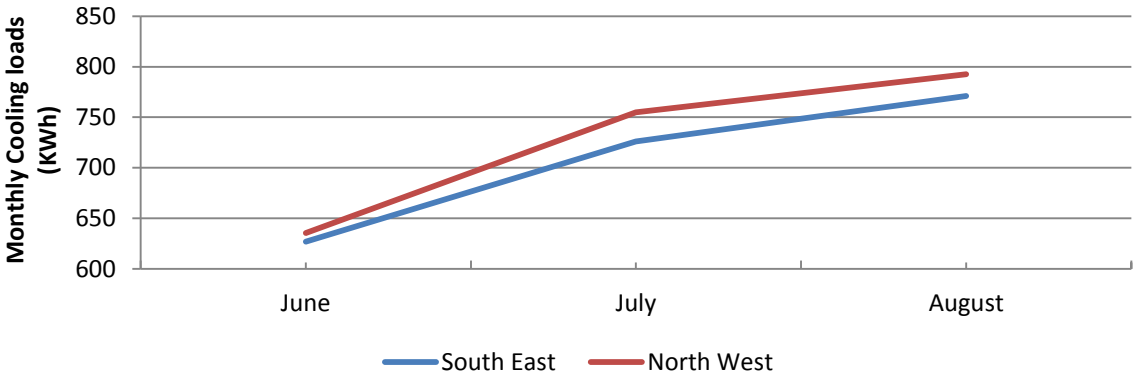

Figure 6.18: Simulated cooling loads for the months of June, July and August for the room with the added flat DSF and changed inner glazing material, for NW and SE orientations which turn out to be very similar. Source: author.

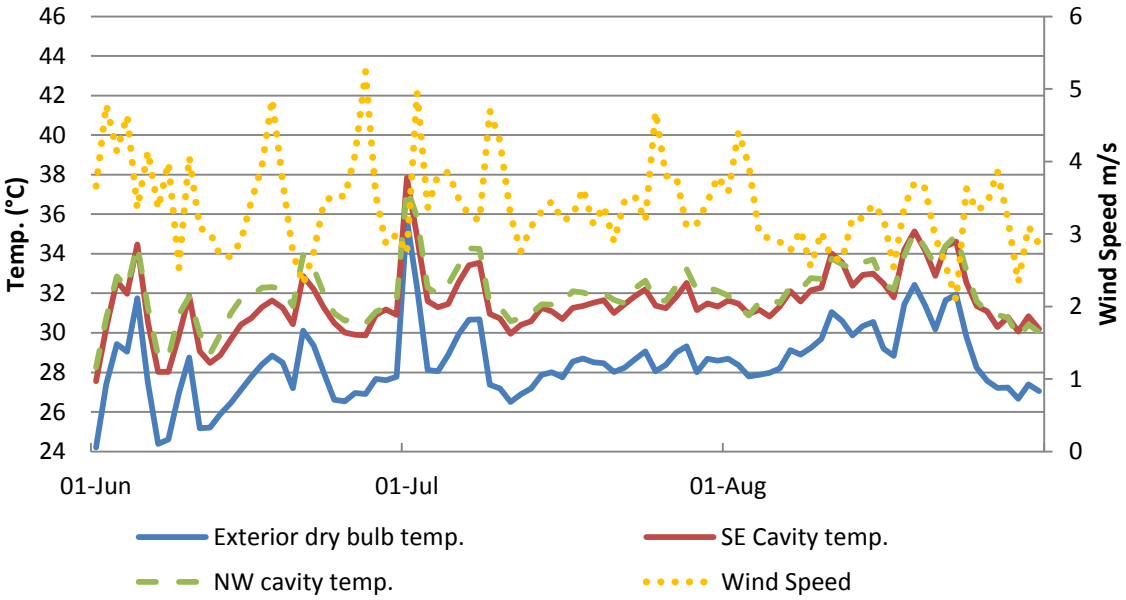

Figure 6.17: Cavity temperatures for the flat DSF in each orientation and the corresponding site wind speed and temperature in the 3 summer months. Source: author.

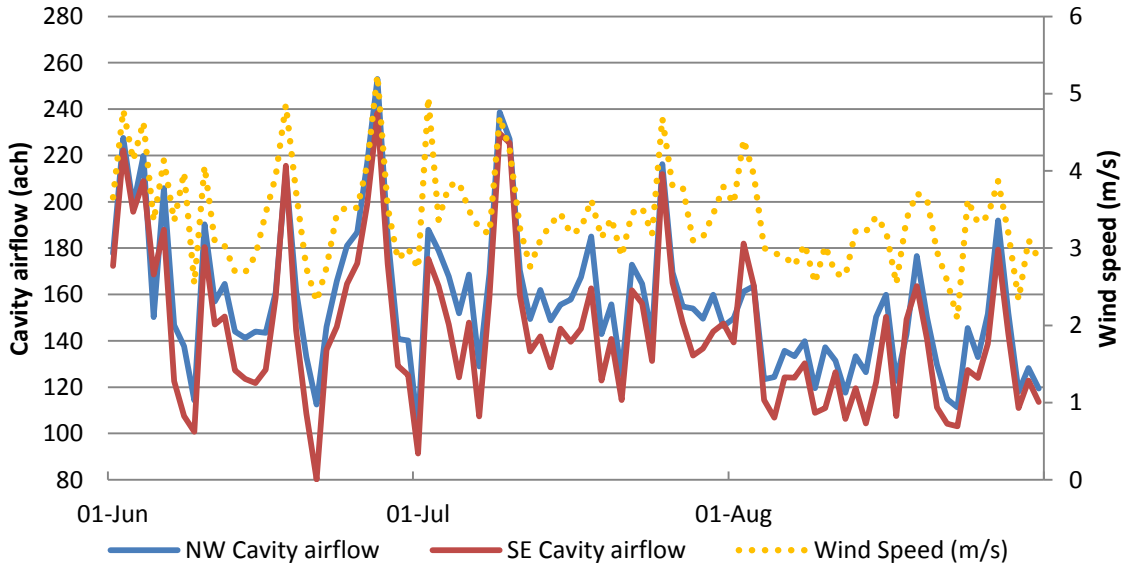

Figure 6.16: Cavity airflow in each orientation and the corresponding site wind speed in the 3 summer months. Source: author.

6.3.3 Daylight simulations (in SE/NW)

Similarly, sDA simulations were performed in both orientations. As shown in Figure 6.19, for the SW orientation, the sDA decreased to 46.2% compared to 51% in the reference case. And in the NE orientation it decreased to 38.5% compared to 46.2%. These results show that there is slight difference between the performance of the flat DSF in these two orientations. They also show that the decrease in cooling loads (even if it is quite small) comes with the price of reducing daylight performance.

This is a typical problem with applying DSFs in hot climatic areas, and it encourages the motivation to find a solution that achieves a balance between cooling and daylighting needs.

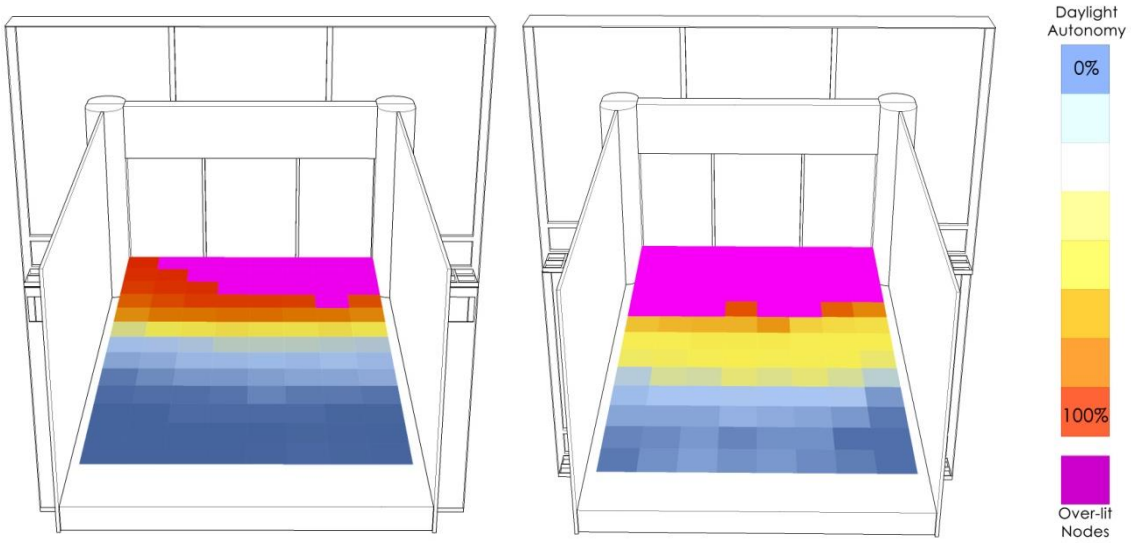

Figure 6.19: Spatial Daylight Autonomy simulations for the reference room in the B-19 building with the added flat DSF and changed inner glazing material, in the NW orientation: 38.5% (left) and SE orientation: 46.2% (right). Source: author.

6.4 Proposed Double Skin Façade

The proposed DSF discussed in the previous chapter is now applied in a real context to be tested and evaluated. As was done with the flat DSF, it is placed as a second layer to the studied reference case instead of the single façade alone.

6.4.1 Structure, components and materials

Figure 6.20 describes its general geometrical configuration and the glazing materials used:

- DSF type: multi-story (no vertical or horizontal partitioning in the cavity space).
- Overall dimensions: 9 m wide, 13.3 m high (starting form first floor)
- Inner glazing: double pane, blue tinted, light transmittance= 0.37, solar transmittance= 0.43 (same as that used in the existing building)
- Outer glazing (Pilkington, 2014): double pane, clear, Low E, light transmittance= 0.74, solar transmittance= 0.5
- Insulated Aluminum cladding panels (Alucobond, 2014): 14 mm in width:
  - Thermal resistance: 0.0172 m^2K/W
  - Thermal conductivity: 0.35 W/mK
  - Heat transfer coefficient[28]: 5.34 W/m^2K

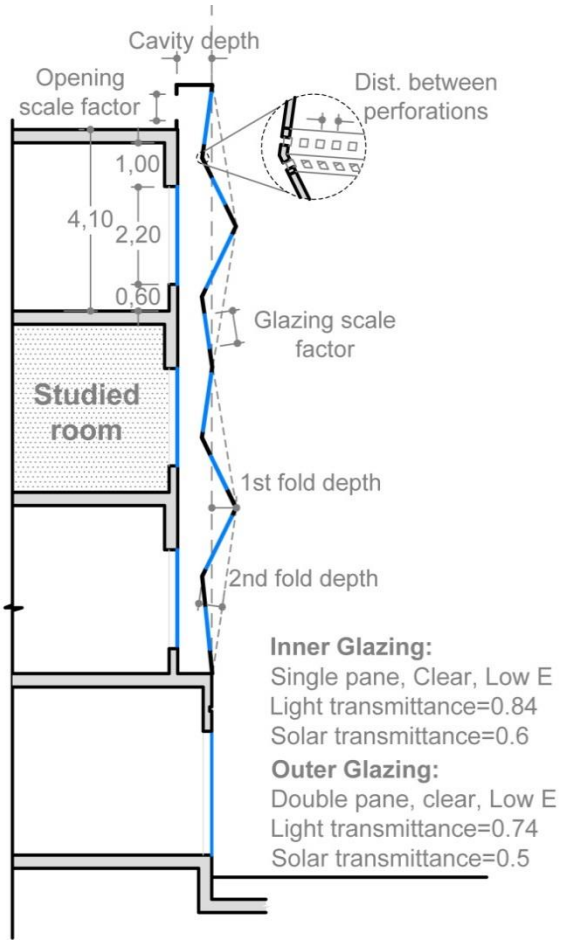

Figure 6.20: Schematic wall cross-section of the B-19 building with the folded DSF added to it. Source: author.

Figure 6.21 represents an exploded diagram of the studied room with the proposed DSF. The first fold iteration represents the main steel structural elements bearing the load of the DSF. It is a network of rectangular cross-sections with the dimensions of 15x8 cm. It serves another important function as it includes the small perforated openings that are 4x4 cm in dimensions and are responsible for the cavity ventilation preventing it from over-heating. Other openings are also included at the top of the cavity. The second and third fold iterations are smaller triangular panels made of insulated aluminium cladding and double low-E glazing. The height of the DSF is 13.3 m as it covers three floors (starting from the first not the ground) and extends 1 m after the ceiling of the last floor to include openings for ventilation. It exceeds the width of the room from both sides by 2 m, so its total width is 9 m.

[28] This is a measure of the general resistance of a heat exchanger to the flow of heat (Lienhard IV & Lienhard V, 2016).

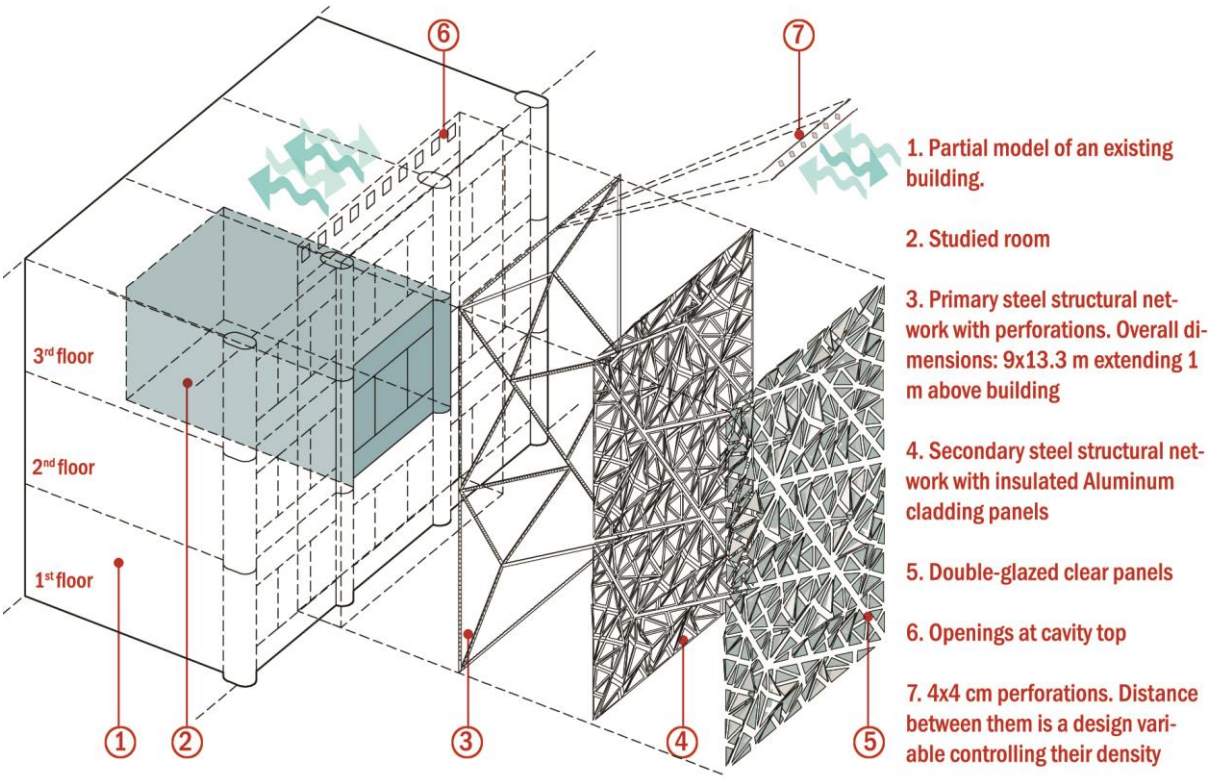

Figure 6.21: Diagram illustrating the structure and components of the proposed folded porous façade. Source: author.

The choice of the cladding and glazing materials of the DSF plays an important role in the thermal performance of the cavity and preventing it from over-heating. The technical characteristics of these materials were obtained from data sheets of existing suppliers (Pilkington, 2014; Alucobond, 2014) in order to be sure that they are realistic materials already existing in the market.

6.4.2 Preliminary testing of variables of folded DSF

For the preliminary testing of the variables, EnergyPlus simulations of the double façade facing the SE orientation take place on just one day that represents a typical hot summer day in Cairo (2nd of July) in which average ambient temperature is 32°C, average site wind speed is 4.9 m/s with an average direction of 287 degrees (North West). This was due to the large computation time needed to run annual energy simulations for this relatively complex model with a huge number of small air openings representing the intended perforations. When a solution is selected, cooling loads for the 3 hottest summer months will be compared to those of the existing room.

The variables are numerous and simultaneously affect performance criteria. At the beginning all variables were given a default fixed value, and then each one is manually tested individually (while others are fixed) to see its effect on performance criteria and assign a suitable search range accordingly. Table 6.1 shows the detailed description and default values of each variable. Figure 6.23 demonstrates a clarification of the variable of *folding depth* for each iteration.

The performance criteria are the cavity operative temperature (°C), cavity air flow measured in air changes per hour (ach), and Daylight Factor (DF) in the office space as explained in

section 5.6.3 in the previous chapter. The resulting Window-to-Wall Ratio (WWR) is also calculated to have a sense of the glazing area with respect to the whole façade as it is not clear from the glazing scale factor alone.

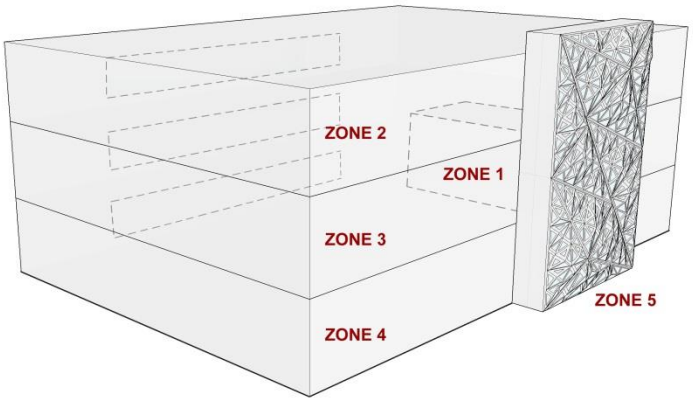

Figure 6.22: Diagram illustrating the zones of the thermal model of the folded DSF to be simulated using EnergyPlus. Source: author.

Figure 6.22 shows the thermal model used. It is composed of the same four zones of the reference case in addition to a fifth zone representing the proposed DSF. It is important to note that it was not possible to divide it into three zones on top of each other as was done with the flat DSF due to the nature of its geometry. The presence of the folded triangular surfaces made it very difficult to split the cavity into three parts.

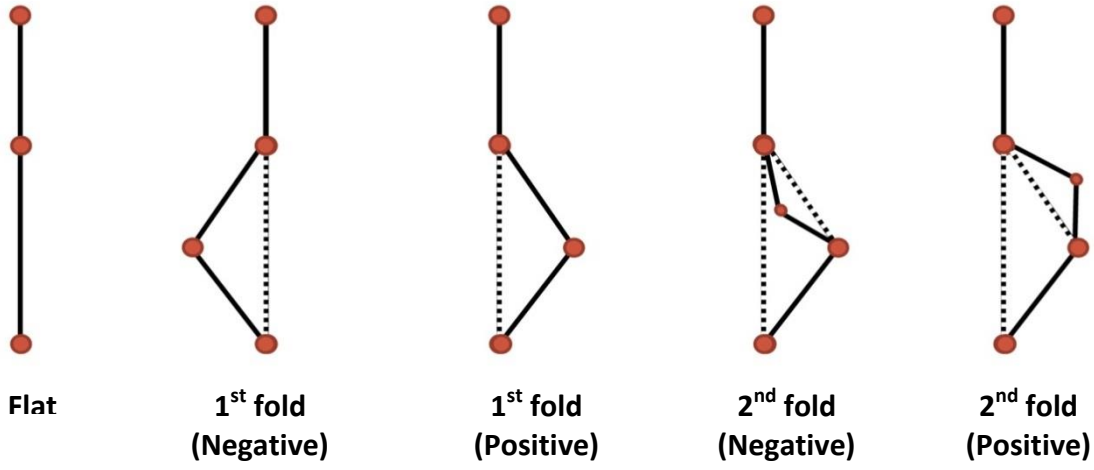

Figure 6.23: Diagram illustrating the fold depths of the first and second iterations, and that they can be either positive (folded outwards) or negative (folded inwards). The same applies for the third iteration as well but was not inserted in the diagram for simplification. Source: author.

Table 6.1: Description and default values of each variable for the preliminary testing phase.

Variable	Search range	Default value	Description
1st fold depth	-0.5 to 1.0 m	0	Distance measured from the cavity depth value (either added or subtracted). Minimum distance would leave 0.3 m clear space from the internal façade if minimum cavity depth (0.8 m) is set. Zero means no folding is done.
2nd fold depth	-0.5 to 0.6 m	0	Distance measured perpendicularly from the centre of each new the folded face. They are smaller in size than the 1st generation therefore the allowed range is smaller. Zero means no folding is done.
3rd fold depth	-0.4 to 0.4	0	Distance measured from the centre of each new the folded face. They are smaller in size than the 2nd generation therefore the allowed range is smaller. Zero means no folding is done.
Cavity depth	0.8 to 2.4 m	0.8 m	It is the distance between the base input surface used to create the fold and the inner building façade. The values are based on recommendations from literature and maintenance requirements. If the first fold depth is negative (inwards) then it should be subtracted from it to know the minimum clear depth of the cavity. If it is folded outwards, then the cavity depth represents the minimum clear depth.
Glazing Area scale factor	0.5 to 0.97	0.7	The insolation values on all triangular faces were calculated to be used as scale factors for these faces but in an inversely proportional manner; the bigger the insolation the smaller the scale factor. To use the list of insolation values as scale factors they had to be 'remapped' to a new list of numbers with a new domain. The start of the domain is fixed to 0.25% which is the smallest possible scale factor. The end of the domain is set a design variable to be optimised. It represents the biggest possible scale factor. A value of 0.5 will approximately result in a WWR= 0.1. A value of 0.97 will approximately result in a WWR=0.3. It is important to note that since the scaling factors depend on the amount of insolation on each face, then it also depends on the folding depth which changes the inclination of each face and thus the insolation it receives. These WWR values are in the case of no folding. They are quite low and increase with the presence of folding.
Spacing between air openings in ducts	0.16 cm to 0.9 cm	0	The spacing controls the distance between perforations hence controlling their density. The area of each opening is fixed to 4*4=16 cm^2. Zero means no perforations are present[29].
Area of openings at cavity top scale factor	0.5 to 0.9	0	The scale factor that controls the size of rectangular openings at the top of the cavity. Zero means no openings are present. A value of 0.5 corresponds to 2.25 m^2. A value of 0.9 corresponds to 7.3 m^2.

6.4.3 Effect of each variable on performance criteria

Table 6.2: Testing of each design variable independently to see its effect on performance criteria.

Design Variable		Cavity temp. (°C)	Cavity airflow (ach)	DF	WWR	Notes and brief observations
All default		**33.86**	**2.1**	**16**	0.24	
1st fold depth	-0.5	33.85	2.2	9	0.22	With increasing fold depth: -Slight increase in cavity temperature and ach. -DF increases then decreases again
	0	**33.86**	**2.1**	**16**	0.24	
	1.0	33.9	2.6	14	0.23	
2nd fold depth	-0.5	33.87	3.3	12	0.24	With increasing fold depth: -Slight increase in cavity temperature, ach decrease then increase again -DF increases then decreases again
	0	**33.86**	**2.1**	**16**	0.24	
	0.6	33.9	3.2	13	0.26	
3rd fold depth	-0.4	33.7	3.6	11	0.24	With increasing fold depth: -Slight increase in cavity temperature, ach decrease then increase again -DF increases then decreases again
	0	**33.86**	**2.1**	**16**	0.24	
	0.4	33.8	3.5	14	0.27	
Cavity depth	0.8	33.8	4.3	10	0.25	With increasing cavity depth: -Slight increase in cavity temperature, and ach decreases - DF increases then decreases again
	1.0	33.8	3.0	14	0.22	
	1.5	**33.86**	**2.1**	**16**	0.24	
	2.0	33.9	1.7	11	0.24	
	2.5	33.9	1.4	12	0.25	
Glazing Area scale factor	0.5	33.7	1.3	0	0.12	With increasing scale factor: - Increase in cavity temperature and ach - DF clearly increases
	0.75	**33.86**	**2.1**	**16**	0.24	
	0.97	34	2.8	25	0.35	
Spacing between air openings in ducts	**0**	**33.86**	**2.1**	-	-	0 m^2	The resulting total area of the perforations is presented in the column on the left. With increasing spacing: -Cavity temperature increases while ach decrease -no effect on DF
	0.3	33.5	9.3	-	-	1.1 m^2	
	0.6	33.6	6.1	-	-	0.62 m^2	
	0.9	33.7	4.9	-	-	0.42 m^2	
Area of openings at cavity top scale factor	**0**	**33.86**	**2.1**	-	-	0 m^2	The resulting total area of the openings is presented in the he column on the left. With increasing scale factor: -Cavity temperature slightly increases and ach clearly increases -no effect on DF
	0.3	33.4	14.1	-	-	0.8 m^2	
	0.6	33.4	18.9	-	-	3.2 m^2	
	0.9	33.5	19.5	-	-	7.3 m^2	

[29] It is important to note that although there are no air openings assigned in the default values of the variables, a certain amount of airflow exists in the cavity probably due to buoyancy and infiltration which is taken into account during the simulations in EnergyPlus.

Max. air openings (0.3 cm spacing & 0.9% upper openings)	33.2	52.1	-	-	With maximum openings areas, there is a clear decrease in temperature and increase in ach

Table 6.2 shows the effect of each variable on the performance criteria while others are fixed. The effect of some of them is clear. For example, increasing the glazing area increases cavity temperature (up to 34.0°C) and DF (up to 25 nodes in the office space) as expected, with slight increase in airflow. Air openings increase air changes per hour (up to 52 ach) as they increase, and generally decrease temperature (to 33.2°C).

Changing the depth of each iteration (1^{st}, 2^{nd} or 3^{rd}) alone shows very little effect on the cavity temperature. However, we could say that as they positively increase (as they fold outwards) they slightly increase cavity temperature. The DF also increases but decreases again after a certain point. Cavity airflow (ach) increases whether the folds increase positively or negatively when compared to a flat configuration (zero values).

Cavity depth had different effects on each criterion. As it increases, it slightly increases temperature, clearly decreases airflow, and increases daylight as it approached 1.5 m then after that value daylight decreases. For fold and cavity depths specifically, their effect changes a lot with different default values, and with different combinations of each other. This was seen in random trials that are not documented in Table 6.2.

It is observed that even with highest glazing scale factor (which had a WWR of 0.35), the Daylight Factor minimum value (2) was only reached in 25 nodes in the office space out of 104 nodes. This indicates that that the design proposal reduces the daylight performance of the room which had 36 nodes reaching the minimum Daylight Factor in its original existing state. Thus modifications are necessary to address this problem.

Another important observation is that an increase in airflow does not necessarily mean a decrease in temperature. When maximum air openings and perforations were assigned they had airflow of 52 ach which was associated with a decrease in temperature.

This means that the effect of airflow is somewhat confusing. This was important to know; as it implies that airflow should not be assigned as an objective in the evolutionary solver because it would just try to increase it as much as possible not understanding that it shouldn't try to increase it after that limit especially if this increase is at the expense of another objective (cavity temperature) being optimised in the same time.

Testing different combinations of variables for daylight and cavity temperature

Since the effect of fold depths and cavity depths was not clear, a single objective optimisation process was made for each of the DF and cavity temperature independently to see how they were affected by different combinations of variables. Best results for cavity temperature were obtained in many cases, but usually when first and second fold depths were at opposite extremes, and the third fold depth was always at maximum positive

(folded outwards*). Values near zero (complete flatness) for all three folds depths were always avoided.* There was no clear preferred range for the cavity depth.

Best results for daylight did not show a clear preferred variable range. It was noticed that only the first fold depth tended to have a positive value (folded outwards) rather than a negative one. This is due to the fact that the first iteration is the biggest in size in the façade, so when it is folded outwards it does not cause much shading and receives more insolation. Many different combinations produced the same results. This could be due to the big number of possible combinations between all variables.

6.4.4 Modifications to design variables and performance criteria

The search range for some variables was modified based on these preliminary results, to avoid wasting time in trying solutions that would not produce good results anyway. Table 6.3 shows the assigned variables and their new search ranges. The assigned performance criteria in the multi-objective optimisation process are minimising cavity temperature and maximising daylight.

Table 6.3: Modified search ranges of some of the design variables.

Design variable	Modified search range
3rd iteration fold depth	-0.3 to 0.4 m
Cavity Depth	0.8 to 1.5 m
Glazing scale factor	0.8 to 0.98%
Spacing between perforations	0.15 to 0.4 m
Top openings scale factor	0.6 to 0.9%

The modifications can be explained as follows:

- The lower limit of the 3rd fold depth changed from -0.4 m to -0.3 m as it was associated with low DF values.
- The upper limit of the cavity depth was reduced to 1.5 m instead of 2.5 m because it resulted in low DF and high cavity temperature.
- The lower limit of the glazing scale factor was increased to 0.8% instead of 0.5% because it caused extremely low DF values.
- The range of the spacing between the perforations was limited to '0.15 to 0.4' m so that we can always ensure a sufficient amount of airflow.
- The lower limit of the Top openings scale factor was increased from 0.3 to 0.6% to always ensure a sufficient amount of airflow.
- The minimum possible glazing scale factor was previously fixed to 0.25% (as explained in Table 6.1). It was increased to 0.4% to improve DF results.
- Cavity airflow was removed from the performance criteria due to its inconsistent effect on cavity temperature. Nonetheless, it was calculated to observe its influence on a bigger number of trials.

6.5 Evolutionary optimisation process

6.5.1 SE orientation: variables which produced best/worst results

The obtained results of the optimisation process were saved in an excel sheet. They were quite numerous (around 750 solutions in total) with varying performances. A specific tool was needed to visualise these results in order to analyse them. The tool is a web-based application called Pollination (Roudsari, et al., 2015) that is particularly designed to explore multi-dimensional data. It is dynamic as it allows the possibility of viewing only a desired range of values, such as best or worst results, which helps in understanding the effect of the design variables on them.

Effect of variables on cavity temperature:

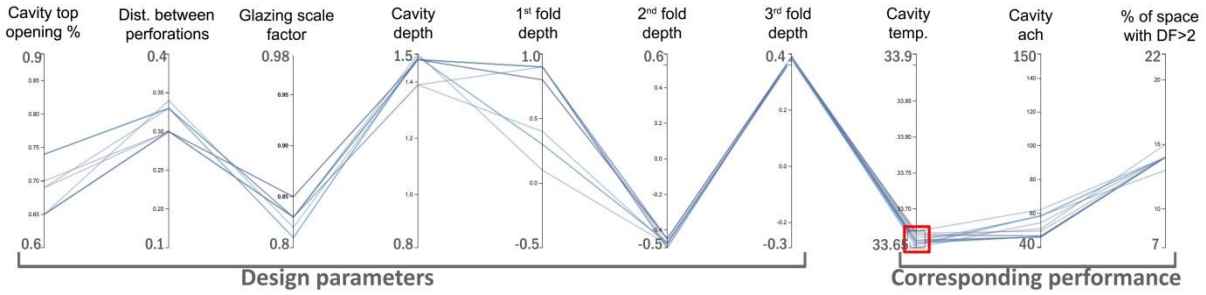

Figure 6.24: Results of optimisation process that achieved the minimum cavity temperature values highlighted in red. Results are visualised using Pollination web application (Roudsari, et al., 2015). The upper and lower limits for the design parameters represent their search ranges in the evolutionary solver. Source: author.

The lowest cavity temperatures reached were 33.64°C, corresponding with 14% of the space having a DF of 2 or more, and the air change rate was around 54 ach. The design parameters leading to these results are as follows:

- Folds: tended towards opposite extremes (folds in opposite directions); first and third fold depths had maximum positive values, while the second had maximum negative values.
- Cavity depth: tended towards higher values and ranged between 1.4 m and 1.5 m.
- Glazing area scale factor: tended towards minimum, which was an expected result.
- Air openings: tended to have mid-range values.

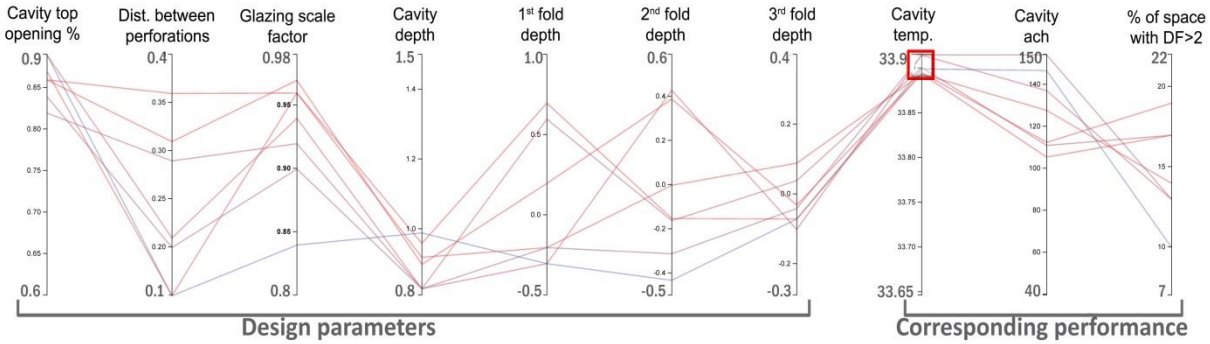

Figure 6.25: Results of optimisation process that achieved the maximum cavity temperature values highlighted in red. Results are visualised using Pollination web application (Roudsari, et al., 2015). Source: author.

The highest cavity temperatures reached were around 33.91°C corresponding with 10% to 19% of the space having a DF of 2 or more, and the air change rate was between 111 and 154 ach. The design parameters leading to these results are as follows:

- Folds: a wide range of combinations were observed. But generally there were fewer tendencies towards opposite extremes. The third fold depth specifically tended to have values near zero (being flat).
- Cavity depth: ranged between 0.83 m and 0.9 m.
- Glazing area scale factor: had a wide range but more results tended towards higher values.
- Air openings: unexpectedly top cavity openings were clearly in higher range of values (bigger openings), while the distance between perforations showed no particular tendency.

Effect on Daylight Performance:

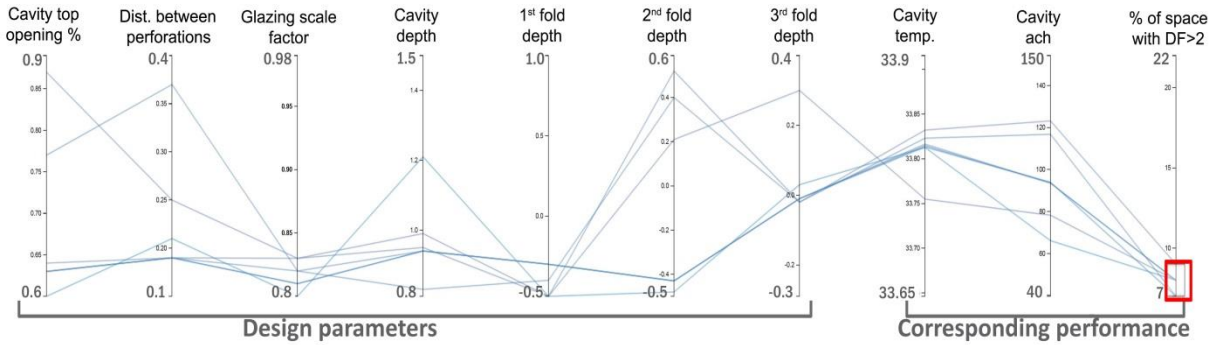

Figure 6.26: Results of optimisation process that achieved the minimum daylight performance highlighted in red. Results are visualised using Pollination web application (Roudsari, et al., 2015). Source: author.

The lowest daylight performance was 7% of the room area, corresponding with a temperature range of 33.75°C to 33.81°C, and the air change rate ranged from 66 ach to 116 ach. The design parameters leading to these results are as follows:

- Folds: the first fold depth clearly tended towards maximum negative values (folded inwards), the second fold depth had either extreme positive or negative values, and the third had positive or near zero values. In general, they tended towards opposite extremes to be folded in opposite directions.
- Cavity depth: tended towards lower values and ranged between 0.8 m and 1.2 m.
- Glazing area scale factor: tended towards minimum values and ranged between 0.8% and 0.83%.

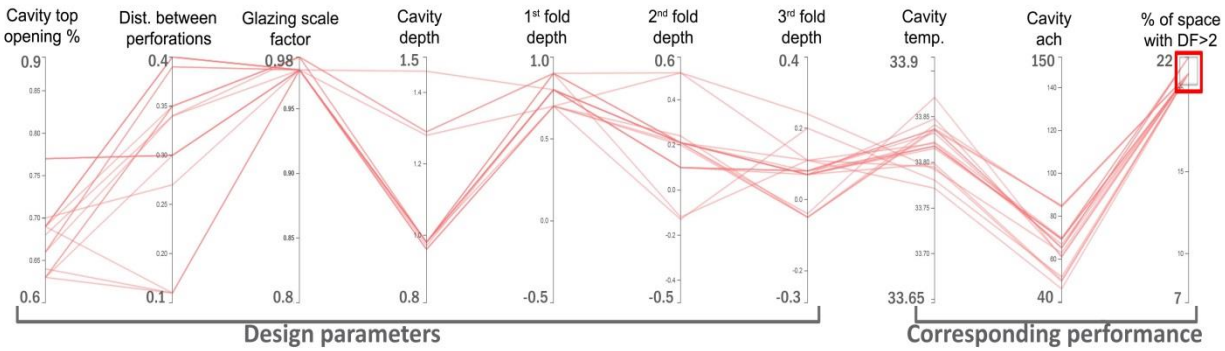

Figure 6.27: Results of optimisation process that achieved the maximum daylight performance highlighted in red. Results are visualised using Pollination web application (Roudsari, et al., 2015). Source: author.

The highest daylighting performance reached was 22% of the space, corresponding with a temperature range between 33.75°C and 33.9°C. The design parameters leading to these results are as follows:

- Folds: first fold depth clearly tended towards maximum positive values. The second and third fold depths did not show a clear value range but they were either near zero or positive values. In general, they tended not to be folded in opposite directions.
- Cavity depth: ranged between 0.97 m and 1.29 m.
- Glazing area scale factor: tended towards maximum values and ranged between 0.97% and 0.98%.

6.5.2 NW orientation: variables which produced best/worst results

Very similar tendencies were observed in the NW; the main differences were that the fold depths did not show the clear tendency towards opposite extremes, cavity temperatures were generally slightly less and there were more possible solutions achieving good trade-offs between daylight and temperature. In general, for both orientations, many different combinations of parameters produced very similar results. This gives the architect some freedom to choose according to other preferences (aesthetic, structural, etc.).

6.5.3 Effect of each variable on performance criteria

- The range of cavity temperature values was very narrow (33.64°C to 33.91°C) and air change rates were generally high (40 ach to 150 ach), this could be due to the search range of each variable that was narrowed down as explained in section 6.4.4. For example the range of air opening sizes was already high, and glazing area scale factor, even in its highest value (0.98) can correspond to WWR of up to 0.55 for the façade (depending on the fold depths and insolation). Therefore, a considerable amount of shading was still applied anyway which reduces cavity temperature.
- Bigger air opening areas were always associated with higher air changes per hour (ach). But higher ach does not necessarily mean a lower cavity temperature. In fact, they tended to increase with increasing air change rates after they exceed a certain limit which is quite strange.
- Despite the expected effects of glazing area on cavity temperatures and daylighting, the same glazing area could result in different performances if the rest of the variables are changed. For example, a high glazing scale factor of 0.98 produced a high DF performance of 22% of the area. The same glazing scale factor produced a DF performance as low as 13% of the area in some cases when different fold configurations were used. The main difference observed was that of the first fold depth which was 0.8 m and -0.4 m respectively. This shows the strong influence of folds on daylight performance, especially the first fold depth as it is the largest in the facade.
- A certain temperature value of the cavity does not necessarily have a fixed daylight performance. For example, a temperature of 33.74°C had a corresponding DF performance of 10% and in another solution 20%. The main difference between the two solutions was first fold depth, which was -0.5 m and 0.9 m respectively, and the glazing scale factor which was 0.8 and 0.98 respectively. This shows the importance of the first fold depth in particular as it is the largest in the façade. When it was folded outwards plus having a high glazing area, it resulted in a high DF performance.
- In general, the increase in cavity depth decreased its temperature.

- Fold depths strongly influence both thermal and daylight performances. The numerical value of each fold depth on its own does not count as much as the differences in directions among them.

6.6 Feedback and modifications

6.6.1 Design modifications to improve results

The best daylight performance reached in the optimisation process was around 22% of the space having a DF value of 2 or more. This is still much less than that of the existing room in which the DF standard was achieved in around 36% of the space. During the optimisation process, the glazing of the inner façade was initially left as that used in the reference case. This justifies the poor daylight performance.

In practical terms, if one would decide to build a double façade like this, then the choice for glazing specifications of the inner façade layer would not be a tinted one that only transmits 37% of light inside as that used in the reference case. This is because the inner façade layer has already become shaded by the added layer which reduces the amount of light entering the office spaces. Another reason is the unnecessary cost of this tinted reflective layer that would not be visible anyway. Consequently, it has been decided to use a different inner glazing which is double Low-E clear glazing, with light transmittance= 0.74 and solar transmittance= 0.5.

Other modifications were made; the minimum glazing scale factor was fixed to 0.5% instead of 0.4%. Also perforation sizes were increased to 5x5 cm instead of 4x4 cm to improve airflow and cavity temperature.

6.6.2 Selected results

One of the best performing results of the optimisation process was chosen for each orientation. The choice was mainly due to aesthetic preferences since their performances were very similar. And then the design modifications were applied to these two models and the simulations were performed again. Furthermore, the researcher manually edited some of the variables of these chosen results based on the understanding of their effect on the performance criteria as discussed in the previous section. This was considered as a final 'fine tuning' phase for further improvement of the performances of the selected results. The role of the architect is emphasised in this phase, as results generated by the evolutionary optimisation were not taken blindly. These modifications and fine tuning resulted in a considerable improvement of the façade daylight performance.

The chosen result shown in the SE orientation resulted in a cavity temperature of 33.4°C and airflow of 53.4 ach, and a DF of 2 in 39% of the space. The daylight performance in particular greatly improved and cavity airflow increased. This result has the following values for design variables:

- 1^{st} fold depth: 0.9 m
- 2^{nd} fold depth: -0.3 m
- 3^{rd} fold depth: 0.38 m
- Cavity depth: 1.25 m
- Glazing scale factor: 0.98 (corresponding to WWR of 0.55)
- Distance between perforations: 0.45 m (with a total surface area of 0.82 m^2)

- Air openings at cavity top scale factor: 0.9 (with a total surface area of 7.3 m^2)
- The resulting cavity volume is 175 m^3.

The chosen result shown in the NW resulted in a cavity temperature of 33.7°C and airflow of 63.9 ach and a DF of 2 in 40% of the space. It has the following values for design variables:

- 1st fold depth: 1.0 m
- 2nd fold depth: 0.4 m
- 3rd fold depth: 0.15 m
- Cavity depth: 1.4 m
- Glazing scale factor: 0.98% (corresponding to WWR of 0.54)
- Distance between perforations: 0.25 m (with a total surface area of 1.4 m^2)
- Air openings at cavity top scale factor: 0.9% (with a total surface area of 7.3 m^2)
- The resulting cavity volume is 200 m^3.

Figure 6.28: Rendered image of copies of the proposed DSF in the SE orientation. Source: author.

6.7 Evaluation and comparison of selected results

For more detailed evaluation of the selected results, the cooling loads are simulated in the 3 summer months of June, July and August instead of just a typical summer day, and the spatial Daylight Autonomy (sDA) is simulated instead of the DF. Then these results would be compared with those of the flat DSF and existing room.

6.7.1 Monthly Thermal & airflow simulations (in SE/NW)

The monthly cooling loads for each orientation are presented in Figure 6.29. They amount to 2045 KWh in the SE orientation and 1977 KWh in the NW orientation. This corresponds to a reduction of 9.3% and 13.4% respectively when compared to the existing room with the single façade. The cavity temperatures in both orientations are almost the same, and they follow the fluctuations of the ambient site temperature, being around 2˚C higher as seen in Figure 6.30. The air changes per hour in the cavities also follow the pattern of the site wind speed, and they are always higher in the NW than in the SE orientation as illustrated in Figure 6.31.

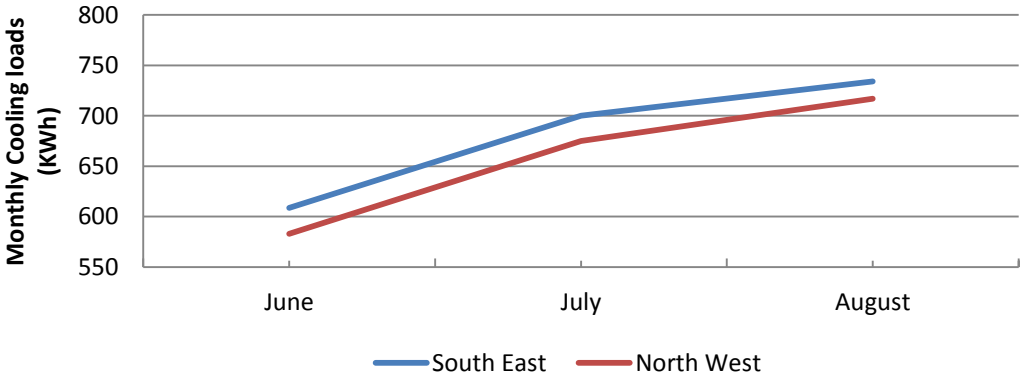

Figure 6.29: Cooling loads for the selected result in each orientation in the 3 summer months. Source: author.

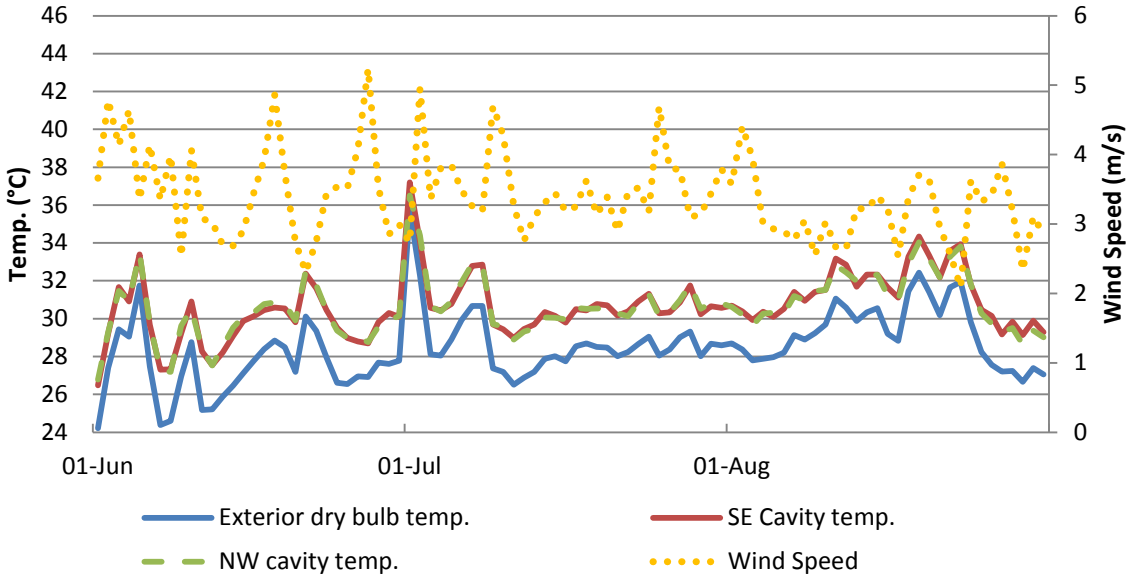

Figure 6.30: Cavity temperatures in each orientation and the corresponding site wind speed and temperature in the 3 summer months. Source: author.

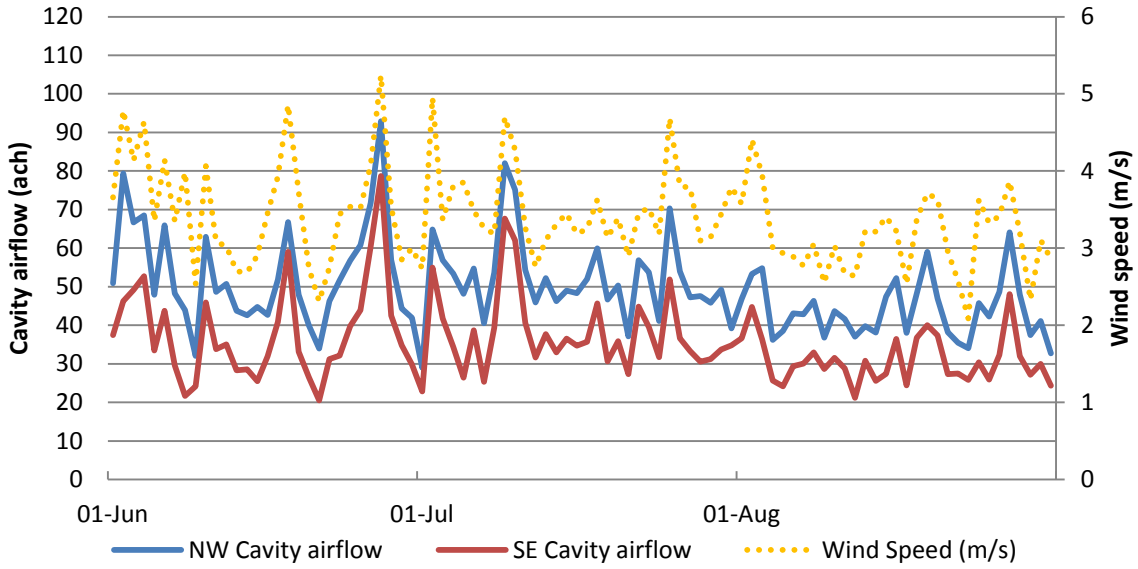

Figure 6.31: Cavity airflow in each orientation and the corresponding site wind speed in the 3 summer months.

6.7.2 Annual Daylight simulations (in SE/NW)

The sDA was simulated for both solutions. In the SE the sDA was 54.8% while in the NW it was 51%. The modifications of the glazing material used (described in section 6.6.1) had a strong effect on the improvement of the DSF's performance. The over-lit area in the NW was quite less than in the SE as seen in Figure 6.32. These values although they show small improvement than those of the existing room, they did achieve the LEED benchmark which is 50%. This represents the achievement of the main design objective since the reduction of the cooling loads was not at the expense of the reduction of daylight performance.

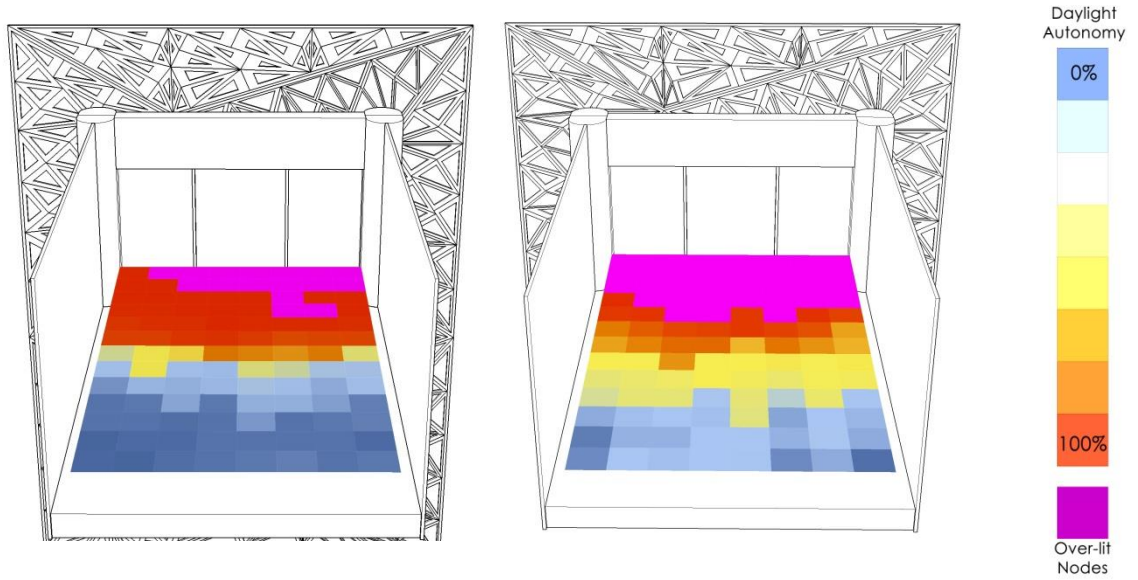

Figure 6.32: Daylight Autonomy simulations for the existing room with the added folded DSF and changed inner glazing material, in the NW orientation (left) and SE orientation (right). Source: author.

6.7.3 Comparison with the reference case and flat double façade

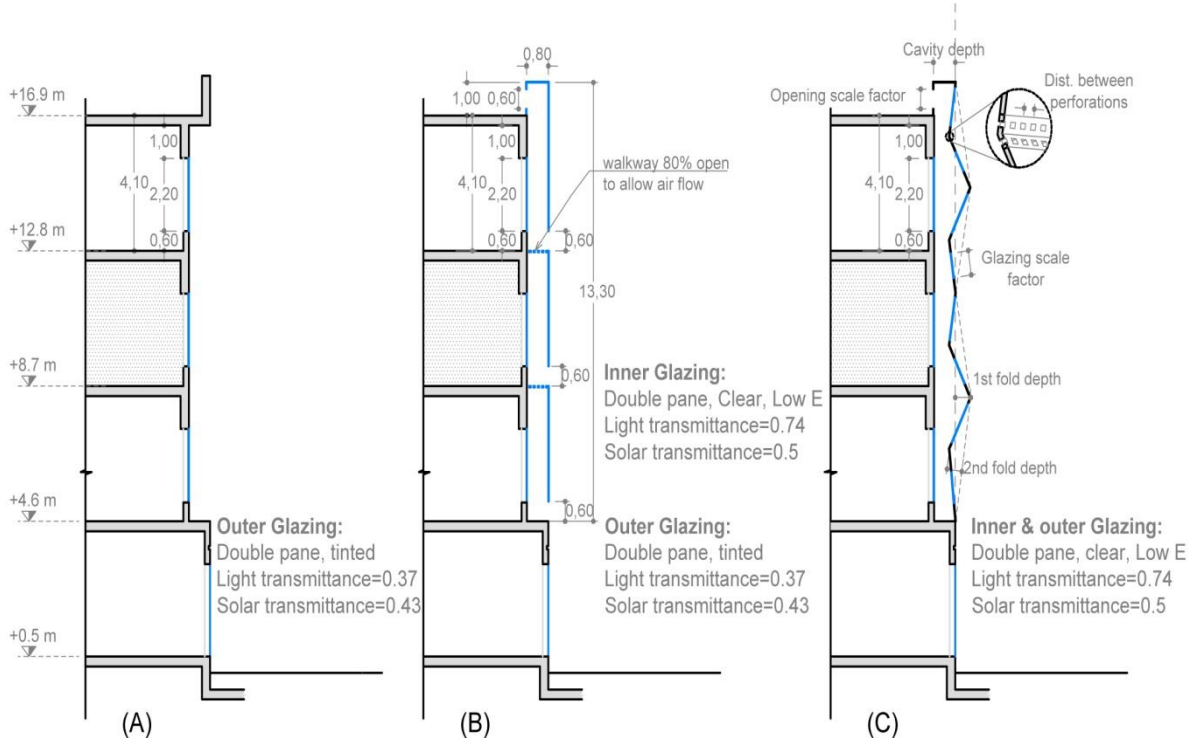

Figure 6.33: Geometric configuration and glazing properties of each façade type, (A) Existing reference case, (B) Flat double façade with air openings at each floor level and at top, (C) Folded façade showing the variables used in the optimisation process (the 3rd fold depth omitted for simplification). Source: author.

More accurate simulations of daily cooling loads and spatial Daylight Autonomy (sDA) were performed as seen in the previous section. Here the results of the proposed folded DSFs are compared with those of the reference case and the flat DSF. It is important to note that the flat DSF was assigned an outer glazing different from that of the folded one. It transmits less light and solar energy to compensate for the lack of shading devices. The folded one however is in itself a shading device, so it did not need the same glazing properties.

The cavity temperatures in the folded DSF were always around 2°C higher than ambient temperatures and around 1.7°C lower than the flat DSF (Figure 6.34). Consequently they showed better improvement to cooling loads as they were decreased by 9.3% and 13.4% in SE and NW orientations. This decrease was associated with slightly better sDA, in fact better performance was observed in both orientations with a little reduction in the over-lit area as light was better distributed reaching deeper into the space. The modified glazing properties of the inner façade layer were important to achieve this sDA performance; when the inner glazing was left as in the reference case, reduction in cooling loads reached 15% but was associated with a sDA of only 45% of the space.

The reference case in the SE barely achieved the sDA benchmark (LEED v.4), which is 50% of the space receiving at least 300 lux for half of the occupied time, and was slightly below it in the NW. In the reference and flat DSF cases a considerable amount of the space was over-lit near the windows, receiving more than 3000 lux for at least half of the occupied time. This requires the use of blinds and consequently more energy for artificial lighting. The flat DSF

slightly decreased the sDA, with slight improvement to the glare problem, and decreased cooling loads by only 5.7% and 4.4% in the SE and NW respectively. This means that shading devices or higher reflective glazing were required to improve the thermal performance, however it would be at the expense of even less DA. The use of light shelves could be a

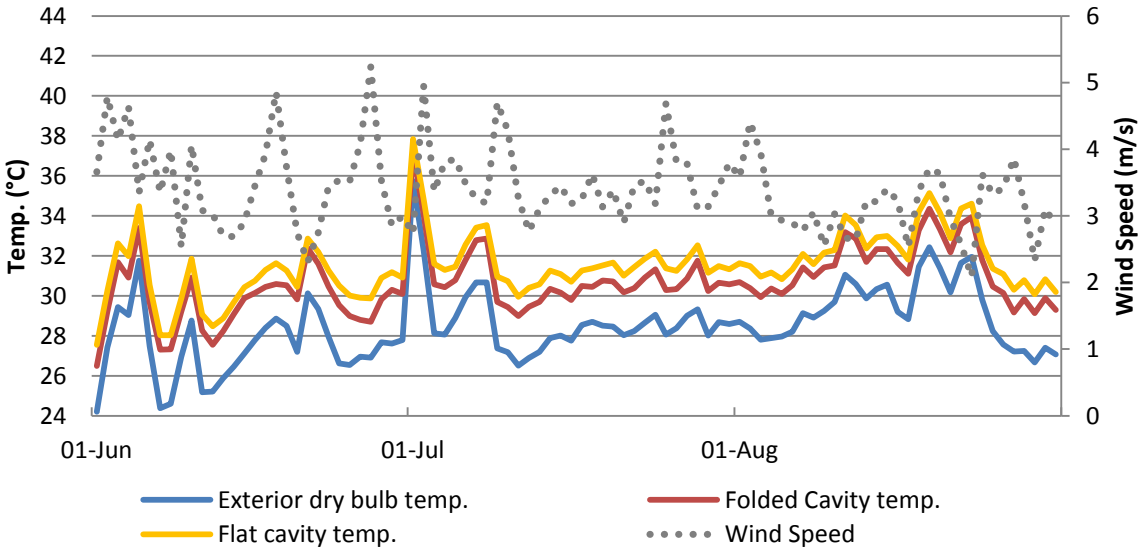

Figure 6.34: Cavity average temperatures for flat and folded DSFs in SE orientation, in June, July and August. The Wind direction is usually NW. Source: author.

solution.

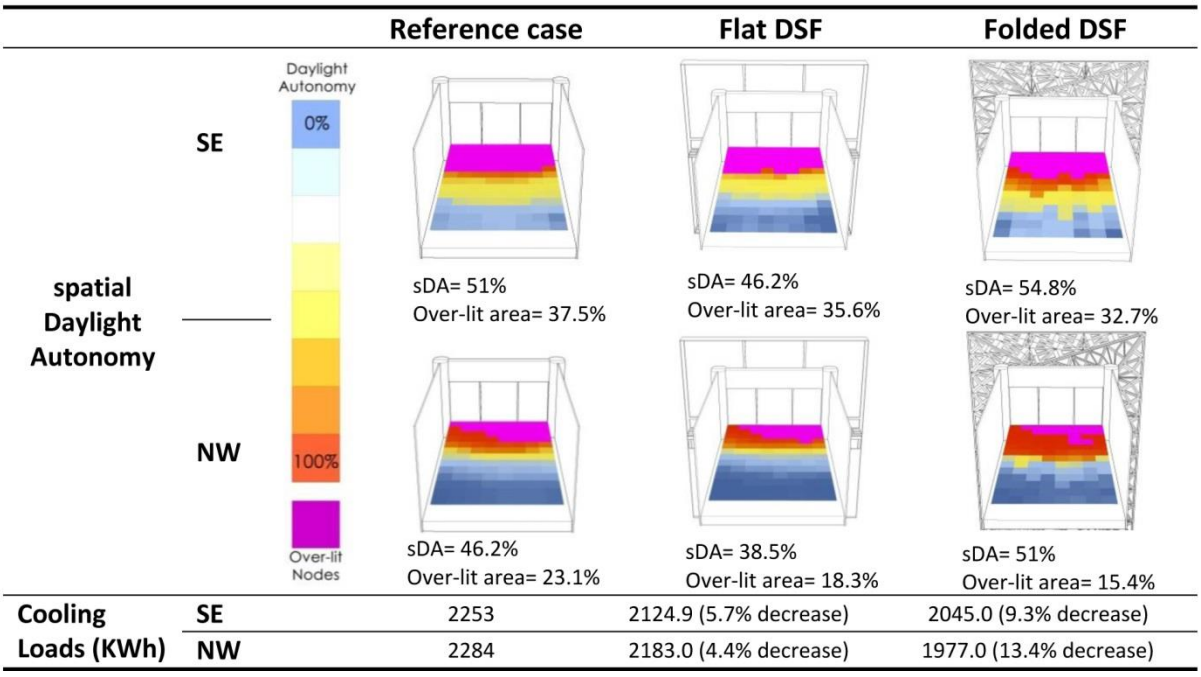

		Reference case	Flat DSF	Folded DSF
Cooling Loads (KWh)	SE	2253	2124.9 (5.7% decrease)	2045.0 (9.3% decrease)
	NW	2284	2183.0 (4.4% decrease)	1977.0 (13.4% decrease)

Figure 6.35: Daylight Autonomy (300 lux for 50% of occupied time) and cooling loads for the 40 m^2 room in the months of June, July and August for each case in SE and NW orientations for the 40 m^2 office room. Note that the folded DSFs are not the same since a different solution was chosen for each orientation. Source: author.

6.8 Summary and observations of results

6.8.1 Effect of biomimetic inspirations: Folds & perforations

The presence of the folded surface shaded both the inner façade layer as well as itself, achieving thermoregulation by reducing incident solar radiation. While the presence of the perforations together with openings at the top increased airflow inside the cavity, hence thermoregulation is further improved by increasing heat lost through convection. These two inspirations can decrease the cavity temperature by up to 2°C compared to that of a traditional flat DSF. Although this difference might not seem very big, it did lead to big reduction in the energy consumption for cooling.

6.8.2 Effect of orientation and wind

Cavity temperature is always around 1.7 to 2.0°C above ambient temperature even with changing wind speed and direction throughout the three months in which the simulations were performed. This is quite important so that the proposed design would not be always dependent on a specific wind direction, increasing its efficiency. Cavity airflow throughout the months closely followed wind speed and had a minimum of around 20 ach when wind speed was at its lowest (2.4 m/s).

The performance of the proposed skin changed with different orientations. In the NW orientation the thermal performance was better as it resulted in a reduction of 13.4% in the cooling loads compared to 9.3% in the SE. However, the daylight performance was slightly better in the SE, although it was associated with a bigger over-lit area.

6.8.3 Recommended range of values for each design variable in SE & NW

Table 6.4: Recommended values for each design variable for achieving a balance between thermal and daylighting performances.

Design variable	Range for best thermal performance	Range for best daylight performance	Range for possible balance
Folds	To have folds in opposite extremes	1st fold depth to be positive, 2nd and 3rd to have small differences	1st fold depth to be positive, 2nd and 3rd to be in opposite directions but with not great differences
Cavity Depth	1.4 m to 1.5 m	0.97 m to 1.29 m	1.3 m
WWR[30]	The smallest possible	The biggest possible	WWR= 0.56
Area of perforations	1.4 m^2 to 0.82 m^2	-	-
Area of air openings at cavity top	4.4 m^2 to 7.3 m^2	-	-

[30] The WWR is directly mentioned here as it has a more tangible meaning instead of the variable: glazing scale factor.

6.8.4 Consideration of software limitations

It is important to point out the limitation of EnergyPlus in modelling double facades, as the Airflow Network (AFN) model that it uses assumes that each thermal zone has a uniform temperature distribution, and it does not take into consideration the cavity airflow pattern (EnergyPlus, 2014). The only information it can give regarding the airflow in a thermal zone is the air changes per hour (ach), and in some results for the flat DSF for example it exceeded 220 ach, which is expected to be over-estimated. The AFN was discussed in more detail in section 3.4.

In addition, limitations regarding the geometry itself were also present since the AFN EnergyPlus v.8.2 was not capable of simulating airflow through horizontal and near-horizontal openings. This lead to the manual selection of all openings exceeding a certain angle of inclination and excluding them from the thermal model. However, this limitation was solved in later EnergyPlus versions that were issued after this work was finished.

Several studies (Zhang, et al., 2013; Sabooni, et al., 2012; Kim & Park, 2011) attempted to test the appropriateness of the AFN model for simulating double facades, and concluded with the recommendation of coupling EnergyPlus with a Computational Fluid Dynamics (CFD) tool to complement each other's limitations.

6.9 Summary

This chapter represents a critical empirical phase in the biomimetic-computational approach followed in this thesis, as it includes the actual *computing* and *evaluating* of the façade design that was proposed in the previous chapter. The thermal performance of DSFs is still not widely studied in hot climates as those in temperate ones, and their resulting daylight performance is rarely addressed. Simultaneously this chapter also represents an investigation of the application of an irregular DSF for the improvement of thermal and daylight performances of an office room in Cairo.

The proposal was compared to an existing reference case as well as a traditional flat DSF to know if it is worth the extra cost. The flat DSF showed very little reduction in cooling and a notable reduction in daylight performance. This shows the difficulty of using DSFs in hot climates as they do not guarantee improved performances. The design process presented in the introduction of this chapter is illustrated after applying it here once more in Figure 6.36 with more detailed explanation of the phases representing the scope of this chapter.

In the attempt to find a trade-off between conflicting daylight and thermal performances of the folded DSF, evolutionary search algorithms were used. The tools proved very useful in finding a suitable combination of the numerous design parameters, to achieve a balance among the performance criteria. The results also helped in understanding the combined effects of the design variables on the performances. However computational software alone were not enough, as the researcher needed to manually modify and *fine tune* the selected results to further improve their performance. This emphasises the role of the architect even in such a design approach that depends heavily on computation.

The main design objective intended in this thesis was successfully achieved. Results showed that the biomimetic inspirations represented in folded morphology which provides self-

shading, in addition to air openings and perforations that improve cavity airflow are important in reducing the cavity temperature. Cooling loads were reduced while slightly improving daylight performance. The selection of glazing properties was important to achieve these results. The capabilities of EnergyPlus are a limitation to the accuracy of the obtained results. Therefore the following chapter addresses this limitation by verifying the results using CFD simulations.

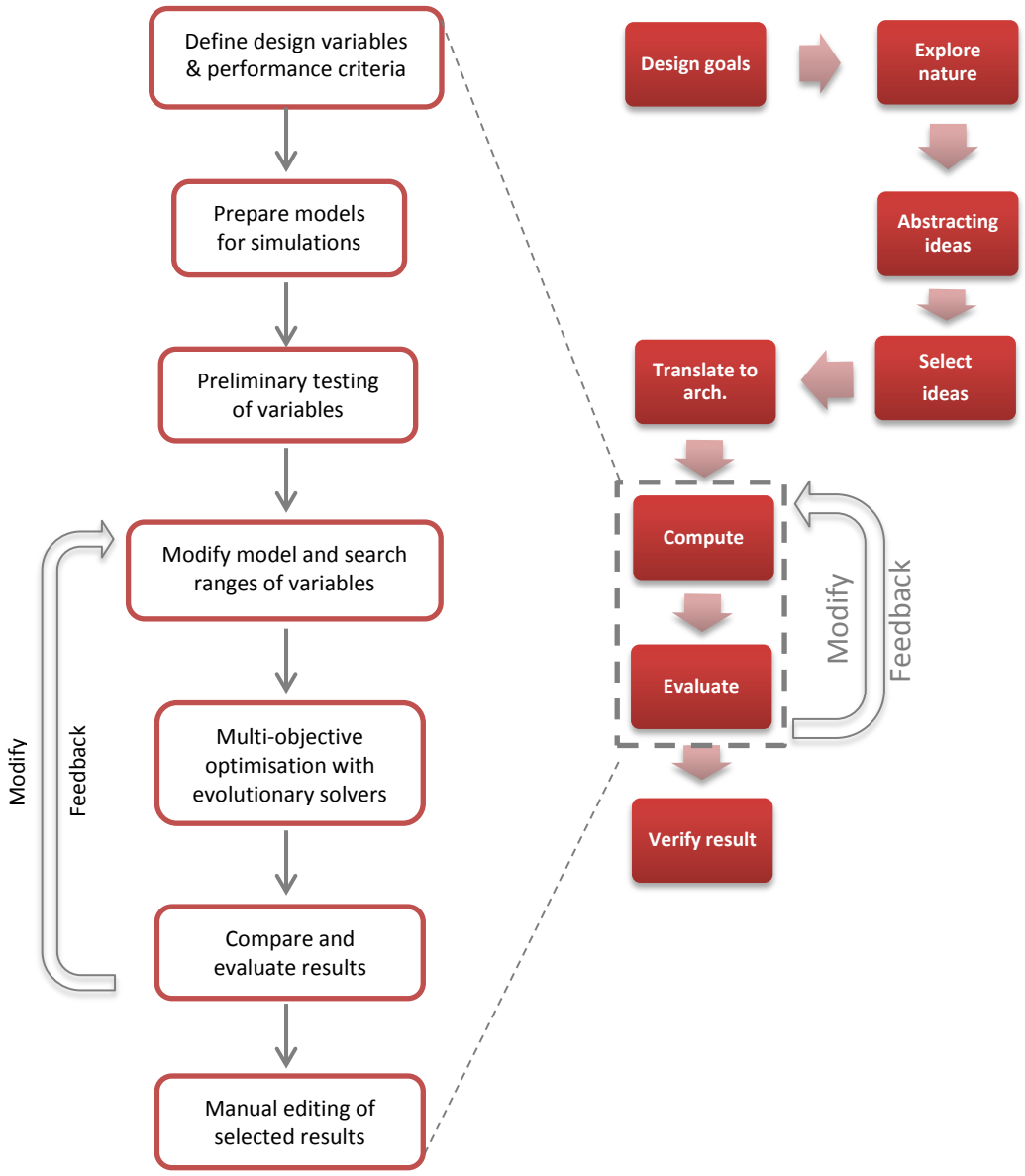

Figure 6.36: Detailed diagram of the design methodology that represented the scope of this chapter. Source: author.

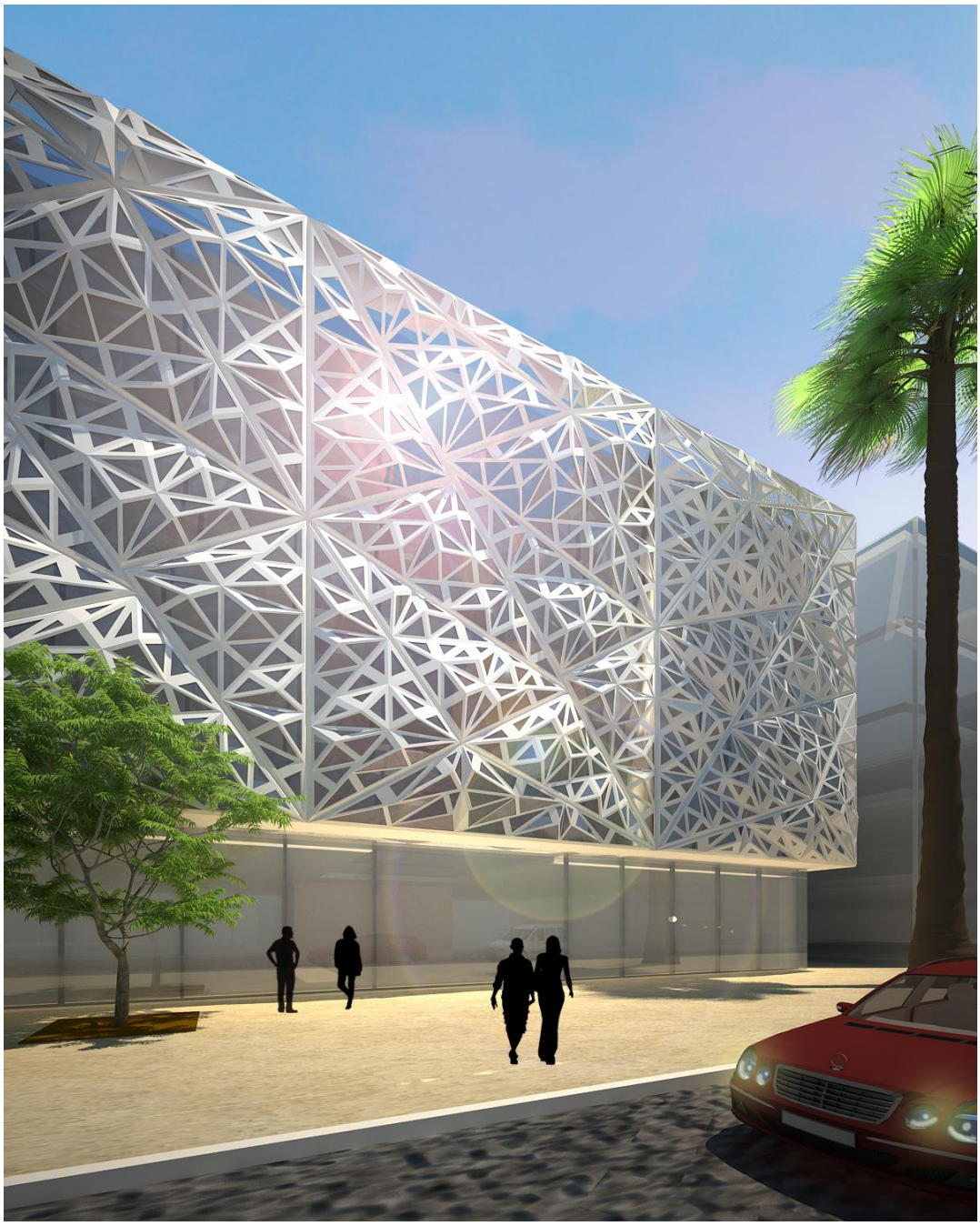

Figure 6.37: Rendered image of the proposed DSF. Source: author.

Chapter 7
CFD verification

7.1 Introduction

This chapter represents the final phase of the biomimetic-computational design approach followed in this thesis. It includes the verification of the results obtained in the previous chapter. The limitations of EnergyPlus in modelling DSFs were previously discussed and therefore inaccuracies are expected to be present.

The main objective of this chapter is to know the degree of inaccuracy of EnergyPlus and whether it can be relied on in simulating the temperature and airflow of a DSF that is considered geometrically complex.

This is quite important since the use of CFD is still not feasible in early design phases (due to need of time and expert knowledge), and building energy software like EnergyPlus is the most practical option for architects in the current time.

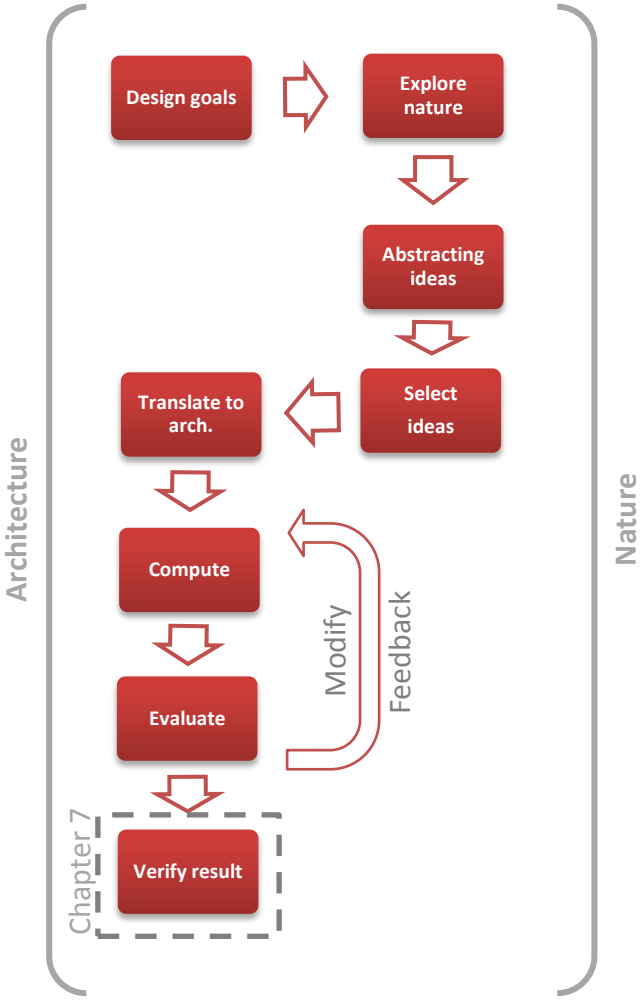

Figure 7.1: Scope of this chapter within the biomimetic-computational design process. Source: author.

The selected solution in the South East orientation that was demonstrated in the previous chapter is the chosen model for CFD verification. A new digital model is prepared for OpenFOAM CFD software. The temperature and airflow values inside the cavity are simulated and compared with those obtained earlier by EnergyPlus. The workflow in this chapter is divided into three general phases as with most CFD simulations;

- Pre-processing: in which the geometry is prepared, assumptions, simplifications and boundary conditions are defined.
- Solving: in which the simulation settings and running the solver itself are performed.
- Post-processing: for visualisation and analysis of the obtained results.

7.2 OpenFOAM software

OpenFOAM is an open-source C++ library used to create *applications* which are executable commands. The name stands for Open source Field Operation And Manipulation. There are two types of applications; *solvers*, that are used in order to solve a particular problem in continuum mechanics, and *utilities*, that are used in order to perform data manipulation. OpenFOAM contains a wide range of solvers and utilities that are able to solve various problems such complex fluid flows involving chemical reactions, turbulence and heat transfer, acoustics, solid mechanics and electromagnetics. One of the best advantages of OpenFOAM is that users can freely create their own new solvers and utilities according to the problem at hand. This however requires pre-requisite knowledge of the underlying method, physics and programming techniques involved. OpenFOAM utilities include pre- and post-processing environments which provides consistent data handling throughout the simulation process from beginning to end (OpenFOAM, 2015).The overall structure of OpenFOAM is shown in Figure 7.2.

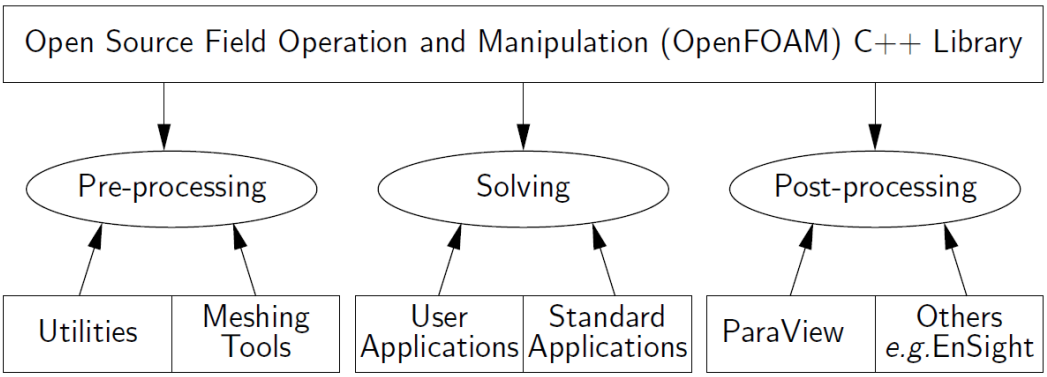

Figure 7.2: OpenFOAM software general structure (OpenFOAM, 2015).

Each solver in OpenFOAM is designed for a certain type of problem; hence it has its own set of equations and algorithms to solve. Therefore when a user selects a particular solver, he/she must be familiar with these equations and accordingly make certain choices, assumptions or simplifications while modelling the case.

OpenFOAM case directories all have the same general structure of folders and files (Figure 7.3) with some differences depending on the type of each solver. This structure includes the following:

- **A constant directory:** This contains a description of the mesh (grid of points representing the geometry) in a subdirectory called *polyMesh*. It also includes files that specify the physical properties of the case at hand such as thermo-physical or radiation properties.

- **A system directory:** This contains files regarding the settings of the solution procedure itself. At least 3 files are included: *controlDict* where 'run' control parameters are set including start/end time, time step and parameters for data output; *fvSchemes* where discretisation schemes used in the solution may be selected at run-time; and, *fvSolution* where the equation solvers, tolerances and other algorithm controls are set for the run.

- **The 'time' directories:** Those contain individual files of data for particular fields such as pressure, velocity, temperature, etc. The data can be: either, initial values and boundary conditions that the user must specify to define the problem; or, results written to files by OpenFOAM. The name of each time directory is based on the simulated time at which the data is written. Since we usually start our simulations at time t=0, the initial conditions are usually stored in a directory named 0.

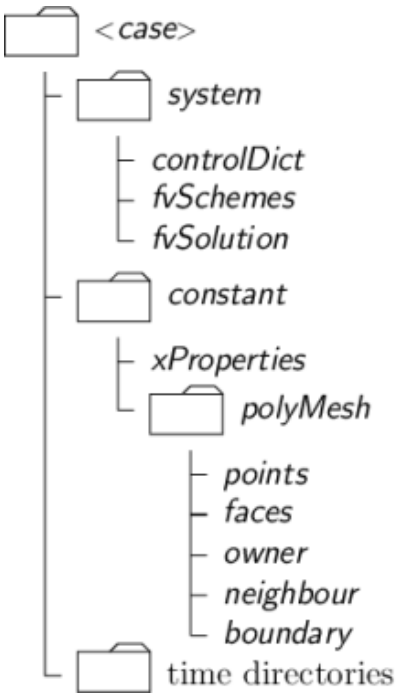

Figure 7.3: Typical case structure in OpenFOAM (OpenFOAM, 2015).

Various steps need to be undertaken when setting up a simulation in OpenFOAM: boundary conditions have to be set, fluid properties selected, numerical schemes and algorithms for the solution of systems of equations must be chosen, and finally general simulations settings must be fixed.

7.3 Pre-processing

7.3.1 Assumptions and simplifications

Based on the physics needed to be simulated, a suitable solver must be chosen. In the case of a DSF, there is heat transfer by free convection (buoyancy), forced convection (wind), radiation and conduction. To simulate all these phenomena in one single case in OpenFOAM was found to be a very difficult task after numerous trials and experimentations with different solvers, especially with complex geometrical configurations. This required expert knowledge and experience beyond the researcher's capabilities within the timeframe available for this research. Therefore certain simplifications had to be made in order to proceed.

It was decided to focus on airflow due to wind only, and heat transfer by convection and conduction. It was assumed that airflow due to buoyancy was weak compared to airflow due to wind since average wind speed was within the range of 5 m/s and also because the façade cavity was partially shaded from direct sunlight which reduced cavity heating. The contribution of buoyancy to overall airflow and heat transfer in the cavity could be neglected to simplify the simulation process.

Another simplification was made regarding the geometry itself. The original model had a series of 328 perforations distributed throughout the facade; each was 5x5 cm in size (0.0025 m^2) with a total surface area of 0.82 m^2. Given that the overall size of the DSF is 13 m in height and 9 m in width, an extremely high-resolution mesh would be needed in order to recognise these very small openings. This would increase the complexity of the problem and result in very long computation time which was not feasible. So a solution was to group these small openings into relatively larger ones with an average size of 9x12 cm having the same total surface area of 0.82 m^2. The total number of the bigger perforations is 96, each with an average area of 0.0086 m^2.

Regarding the required duration to simulate, CFD software are often used to simulate conditions in a specific moment in time rather than a range in time. This is in contrast with building energy software such as EnergyPlus which are often used to simulate durations ranging from days to a whole year. So a certain point in time was chosen which represents a typical hot summer day (2nd of July) at 16:00. The weather conditions at this specific time-step act as the initial boundary conditions needed to initiate the simulation in OpenFOAM. They include the outdoor dry bulb temperature, and the volume flow rate of the air at the inlet openings. Additionally, surface temperatures of the DSF calculated by EnergyPlus at this time were taken to act as boundary conditions as well. Table 7.1 summarises the assumptions of the model:

Table 7.1: Summary of assumptions and/or simplifications for the model prepared in OpenFOAM.

Model aspect	Assumption/simplification
Physics simulated	Airflow due to wind and heat transfer by convection and conduction
Geometry	Small perforations grouped into bigger ones with the same total surface area
Duration to simulate	Specific point in time: 2nd of July at 16:00

7.3.2 Geometry

A Stereo-lithography (stl) file format of the selected DSF in the South-East orientation was exported from the CAD software used which is Rhino 3d modeller. It was not exported all at once, as it was divided into different parts or *patches* which are surfaces with no thickness. This division enabled specifying different properties and boundary conditions to each patch. Otherwise they would all be assigned the same properties. Furthermore, this enables assigning different settings in the meshing process, such as refining (increasing mesh resolution) or adding more layers in certain patches when required. After exporting each patch individually they were all combined again in a single stl file in which each patch name is recognised. The DSF is divided into the following patches which are illustrated in Figure 7.4:

- Top
- Bottom
- Left
- Right
- Back1 (Back side exposed to outdoor environment)
- Back2 (Back side exposed to indoor environment)
- Front-solid
- Front-glazing
- Office windows
- Top openings (representing the inlets, with a total surface area of 7.3 m^2)
- Perforations (representing the outlets, with a total surface area of 0.82 m^2)

The overall dimensions are 13.3 m in height, 9 m in width, and 1.25 m in depth. The cavity volume of the DSF is 175 m^3.

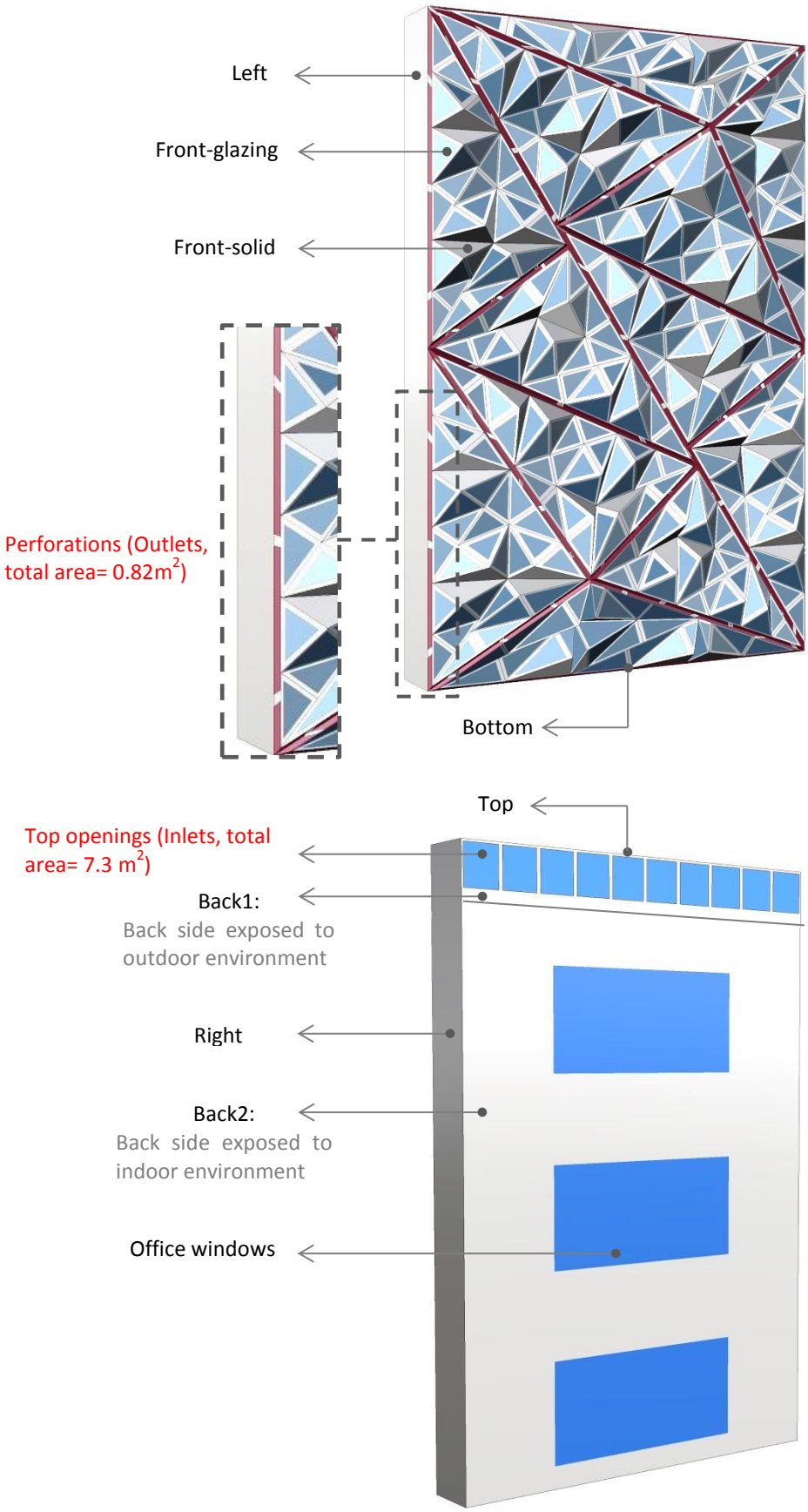

Figure 7.4: Diagram illustrating the different patches of the model in the front view (top) and back view (bottom), the inlets and outlets are written in red. Source: author.

7.3.3 Mesh

The mesh is a grid of points that represents the geometry. At each point, certain equations are solved (depending on the chosen solver) in order to simulate the physical phenomena which are fluid flow and heat transfer in this case. Certain criteria must be satisfied by the mesh to ensure a valid, accurate solution. This is why during any run, OpenFOAM will perform checks to see if these criteria are satisfied. These checks are quite strict and OpenFOAM will stop running if they are not satisfied. Otherwise the solution is inaccurate before the simulation has even begun. Mesh quality has a direct and crucial effect on the accuracy of the solution. The consequence of this strictness is that users often spend a lot of time correcting and improving the mesh before running a simulation. The mesh preparation phase could consume up to half of the time of the overall case preparation and solving.

Here the mesh is created through two main processes. First a background mesh is created using blockMesh utility. This basically creates a box surrounding the geometry. Secondly, the final refined mesh is created using snappyHexMesh utility. Both processes are explained in the following sections, and their detailed settings are placed in Appendix B.

Background Mesh using BlockMesh

BlockMesh is a built-in utility in OpenFOAM. It decomposes the domain of the geometry into one or more 3-dimensional hexahedral blocks. Each block is defined by its 8 vertices. The generated mesh is specified by the number of cells in each direction of these blocks (OpenFOAM, 2015). In this case only one block is needed for the cavity model. The dimensions of this block are slightly bigger than the overall dimensions of the cavity. The resolution of the block (number of cells) depends on the complexity of the geometry. Choosing a low resolution (and consequently large-sized cells) would not account for the folds of the facade and especially the small perforations in it. Yet choosing a high resolution greatly increases the computing time needed for mesh generation and simulations. Therefore after several trials, the following blockMesh settings were found to achieve a suitable balance:

- Bounding box corner to corner coordinates: (0 0 4), (3 10 19)
- Number of cells in X, Y, Z axes: (120 400 600)
- Total number of cells: 28,800,000
- Mesh grading in X, Y, Z axes: (0.5 1 1) this means that only in the X-axis the ratio between the first and last cell is 0.5. This increases the mesh resolution at the front side of the façade where there are small perforations that require a higher number of points to be recognised. While at the back side where it is flat, there will be a lower resolution as it is less complex.
- Cell sizes in X, Y, Z axes: 0.034 to 0.017 m, 0.025 m and 0.025 m respectively.

Final mesh using SnappyHexMesh

This utility creates 3-dimensional meshes containing hexahedra (hex) and split-hexahedra (split-hex) automatically from triangulated surface geometries, or tri-surfaces, in Stereolithography (STL) file format. Through an iterative process, the mesh approximately conforms to the STL surface by starting with a coarse mesh (created by the blockMesh utility earlier) then gradually refining it. Specifying the refinement level is flexible and can differ from one patch to another in the overall geometry depending on its complexity (OpenFOAM, 2015).

The STL geometry lies inside the block created by blockMesh as seen in Figure 7.5. The user must specify whether the desired final mesh is inside or outside the STL. In this case the desired mesh is inside. The meshing process takes place through three general stages as follows:

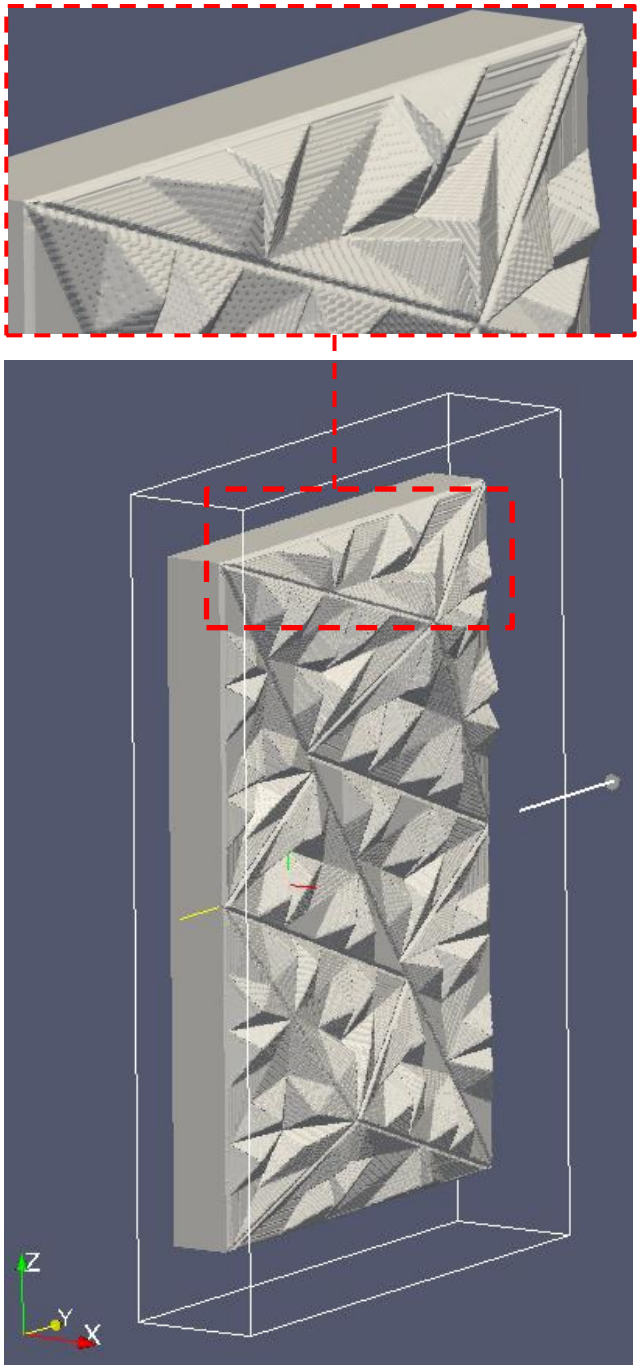

Figure 7.5: Final mesh created using SnappyHexMesh, placed within the bounding box created by blockMesh. The enlarged part is a close-up illustrating the quality of the final mesh. Source: author.

- Firstly, cells are split where the STL surface intersects with the background mesh leaving only the desired mesh inside. This results in a rough *castellated* mesh. Here the resolution of background mesh is critical, because if it is not sufficient, the resulting mesh may not be an accurate representation of the original geometry. The quality of the STL file is very important. All patches that form the STL surfaces must represent a closed water-tight geometry.

- Secondly, the castellated mesh will be snapped to match the geometry of the STL file. This process involves moving the vertices of the jagged castellated mesh onto the surface geometry to create a smoother mesh. It is important to note that this part of the meshing process was the most problematic. Many issues arose with the detection of skew faces and non-manifold points. This always caused the check that controls the mesh quality to fail (using checkMesh utility). Due to the limited time provided for the thesis and uncertainty of ever reaching a perfect setup, a set of parameters was chosen -

after numerous trials- that enabled the success of the mesh quality check but at the expense of the smoothness of the folded surface as seen in Figure 7.5.

- Thirdly, an optional final stage introduces additional layers of hexahedral cells aligned to the boundary surface. The process of mesh layer addition involves shrinking the existing mesh from the boundary and inserting layers of cells. This option was used in this model in generating the mesh, with extra layers added at the front-solid and front-glazing patches as they represent the folded surfaces which are more complex to mesh.

Meshing with snappyHexMesh utility has much potential and is particularly useful in the case of complex geometries. However numerous trials and errors in setting the appropriate parameters that control the meshing process are often required to be tested until a satisfactory result is reached. It is an extremely time-consuming phase especially if the user has no previous experience.

- Total number of mesh cells: 11,891,739
- Total number of mesh points: 11,711,751

7.3.4 Boundary conditions

In OpenFOAM, it is necessary to specify the initial field values and boundary conditions for each patch of the geometry. All the values for these fields are stored in the 0 folder as text files. They are briefly explained here, and are inserted in more detail in Appendix B.

- ***T***

Temperature is *fixed* at the inlet patches with a value of 308.82˚K (35.67˚C) which represents the outdoor dry bulb temperature. The *inletOutlet* type is specified for the outlet patch. All other patches representing the surfaces of the DSF have fixed values and are assigned temperatures obtained from EnergyPlus simulations for the assumed simulation time which is 2nd of July at 16:00.

Table 7.2: Boundary conditions of the Temperature field assigned to each patch of the model. The values are obtained from EnergyPlus results.

Patch name	T (˚C)	T (˚K)
Back	39.65	312.80
Left	40.17	313.32
Right	39.25	312.40
Top	48.96	322.11
Bottom	40.53	313.68
Front-solid	40.08	313.23
Front-glazing	39.24	312.39
office_windows	37.20	310.35
Upper_openings (T of inlet flow)	35.67	308.82

- ***U***

This is the velocity of the inlet air flow. This information was difficult to obtain from EnergyPlus in a direct manner as it is not an automatically generated output. At the beginning the outdoor wind speed at the inlets which is 4.39 m/s was used, as this can be generated by EnergyPlus. However preliminary results showed extremely high values of the airflow inside the cavity, which meant that something was wrong with this boundary condition. The comparison between EnergyPlus and OpenFOAM results would not be appropriate since the initial conditions of both models are not the same.

After communication with the EnergyPlus Help Service it was understood that the wind does not flow freely inside due to backward pressure in the cavity that is calculated by EnergyPlus. Therefore, the volume flow rate at the inlets was used to calculate the inlet flow velocity instead of the wind speed as it was the only output generated that gives information about the inlet airflow. Since all inlets have the same surface area, the total volume flow rate of all inlet openings was divided by their total surface area to calculate the velocity of air:

Total volume flow rate at the inlets (m^3/s) = total area of inlets x air velocity
0.374 *m^3/s = 0.73 m^2 x air velocity*

Therefore the air velocity at inlets = 0.374/0.73= **0.51 m/s**.

- ***P***

Pressure inside the cavity of the DSF is assigned to standard atmospheric pressure.

- ***Alphat***

Alphat describes the turbulent thermal diffusivity. The turbulent heat transfer is calculated using the equation:
$\alpha_t = \mu_t / Pr_t$
Here, α_t is turbulent thermal diffusivity. μ_t is mut, the turbulent viscosity. Lastly, Pr_t is turbulent Prandtl number[31] with a default value of 0.85. All patches are assigned the boundary condition *compressible::aplhatWallFunction*, except the inlets and outlets which are set to *calculated*.

- ***Epsilon***

The epsilon field allows for describing the turbulence dissipation rate at boundary inlets and walls. The wall entries are defined with compressible::*epsilonWallFunction* and inlet patches have type compressible::*turbulentMixingLengthDissipationRateInlet*. Note that the outlet patch is given the inletOutlet boundary condition. This fixes the outlet field to a given inletValue to prohibit instability in case of inward flow during simulation.

- ***K***

K represents the turbulence energy. The wall entries are defined with compressible::*kqRWallFunction* and inlet patches have type

[31] Prandtl number measures the ratio of the diffusivity of momentum and the diffusivity of heat (Fletcher, 1991).

turbulentIntensityKineticEnergyInlet. The outlet patch is given the *inletOutlet* boundary condition.

- ***Mut***

Mut is the turbulent kinematic viscosity and only needs to be defined at wall patches with *mutkWallFunction*. The remaining patches are *calculated*.

7.4 CFD solver

The solver used in this simulation process is called rhoSimpleFoam. It is a steady-state[32] solver used for simulating turbulent RANS (Reynolds Average Navier-Stokes equation) flow of compressible fluids. The effect of buoyancy on fluid flow is not included in this solver for simplification of the computation process. The standard k-ε turbulence model is used in this case. To have a better understanding of the underlying physics behind the fluid flow, it is important to point out the solved equations:

- Continuity equation

The continuity equation ensures that the simulation process obeys the law of conservation of mass. This means that no mass can be created or disappear in the flow medium.

- Momentum equations

Momentum equations or commonly referred to as Navier-Stokes equations state that the inertial forces acting on a fluid element are balanced by the surface and body forces.

- Energy equation

The energy transportation equation which states that the rate of change of energy inside the fluid element is equal to the net flux of heat into the element added to the rate of working done on the element due to body and surface forces.

Details about these equations and in-depth explanation of CFD are addressed abundantly in existing literature, such as Anderson Jr., (2009) and Fletcher, (1991).

rhoSimpleFoam, like any other flow solver in OpenFOAM, is largely procedural since it is a close representation of solution algorithms and equations, which are procedural in nature. Therefore, users do not necessarily need a deep knowledge of object-oriented paradigm and C++ programming to write a solver but should know the principles behind object-oriented paradigm and classes, and to have a basic knowledge of some C++ code syntax. As the name implies, the solution algorithm is based on the Semi-Implicit Pressure-Linked Equation (SIMPLE) algorithm (OpenFOAM, 2015).

When running a steady state solver in OpenFOAM, the time steps do not represent the elapsed time, but rather the number of iterations. Only the last converged results can be used for solution analysis. When running the rhoSimpleFoam solver there are a number of solvers settings and numerical schemes located in the system folder. These contain settings

[32] A steady flow is one in which the conditions (velocity, pressure and cross-section) may differ from point to point but *do not* change with time (Sleigh & Noakes, 2009).

for how the equations are to be solved. The settings are mentioned briefly in the following sections and are included in detail in Appendix B.

7.4.1 Solver settings and numeric model used

fvSchemes

Within the *fvSchemes* text file there are options to assign numerical schemes used for the terms to be solved. First, the time derivate scheme will be specified as *steady state* as it is not applicable for this case. Then the gradient schemes are all assigned *cellMDLimited Gauss linear* as method of discretization of the divergence. Next is the convection scheme, identified under divSchemes. Here the *bounded Gauss* is used, but the interpolation method is *upwind* for all values except for one. The exception is a part of the momentum equation, *div((muEff*dev2(T(grad(U))))),* which only works with *Gauss linear*. The upwind differencing is the most stable interpolation method available in OpenFOAM. The laplacian schemes are solved with *Gauss linear limited 0.777*. Lastly, the default interpolation schemes are *linear*, and the surface normal gradients set at *limited 0.777*.

fvSolution

In *fvSolution*, the settings specify how to solve the equations based on matrix inversions. Often the equations to be solved in OpenFOAM result in large matrices. These matrices are however mostly built by zero entries. Therefore, the traditional algebraic techniques become inefficient and iterative methods are adopted instead. There are three types of solvers to invert matrices in OpenFOAM. The first one is preconditioned (bi-) conjugate gradient, *PCG/PBiCG*, which distinguishes between symmetric and asymmetric matrices. The PCG solver is used for the pressure field. The second is geometric-agglomerated algebraic multigrid, *CAMG*. CAMG requires a positive definite, diagonally dominant matrix to operate. Lastly, there is the *smoothSolver*, which operates for both symmetric and asymmetric matrices. The *smoothSolver* is used for the velocity and epsilon fields.

7.4.2 Simulation

Parallel processing

The final created mesh requires a huge amount of computation power and time to be solved, despite efforts to try and keep it small in size as much as possible without compromising its accuracy. To speed up the simulation process, the mesh can be decomposed into several parts then assign them to different processing cores that run in parallel. This way, OpenFOAM utilises the available processing power with the maximum possible efficiency. The *decomposePar* command is used to perform this operation, and it requires a dictionary file in which we can specify the number of available processor cores. After running this command new folders, representing the number of cores, are created inside the case directory. These folders are combined again to reconstruct the final solution once the solver has finished.

Monitoring stability and convergence

As the simulation starts running, OpenFOAM writes information about the solving process of the different equations at each solved iteration. Through the observation of this

information it can be understood if the solution has converged[33]. The initial and final residuals written by the solver at each iteration can be observed. Residuals are the difference between a solution at a certain iteration and the following one. If the solution is converging, the initial residual should be approaching zero, while the final residual should be less than the initial one. Additionally, the number of iterations needed to solve the current equation for a particular field (such as pressure or velocity for example) can be monitored. These iterations should gradually decrease as the solution approaches convergence. The simulation reached a converged state after 1447 iterations.

Ideally, to double-check the convergence of the solution one would repeat the simulations using another mesh with a higher resolution. However, this proved to be very time consuming and therefore difficult to perform within the timeframe provided for this research.

Computation power and time

The simulation was performed using a cluster machine at the Department of Mechanics, Sapienza University. Four nodes of this cluster were used, each with 16 processors of 2,6 GHz and RAM of 64 GB. The running time of the simulation was approximately 81 hours.

7.5 Post-processing

Once the solver finishes running, results are written in text files in which field values for every single cell in the mesh are documented. Viewing and analysing the results in these text files is not useful and does not provide much insight without linking this information with an image of its location on the mesh.

OpenFOAM has a post-processing software called ParaView which is also open-source and can perform data visualisation and analysis. This is done by combining results of the field values with positional data and the mesh model to create a visual representation of the results. The field results can be coloured according to their magnitude, in addition to many other inspecting tools such as creating sections, isolating mesh parts, and graphing tools.

At the last simulated time step, the calculated results at all the mesh points were exported to a CSV (Comma-Separated Value) file to be viewed in Microsoft Excel for further inspection. Additionally, the results were visualised in ParaView as follows.

[33] Convergence means that the numerical solution obtained by the solver should approach the exact solution of the differential equation at any point in the domain, as Δx and Δt approach zero. Practically it is quite difficult to prove that a certain solution has converged since the exact solution is not known. The aim of the numerical approach to begin with is to get a solution that was not possible analytically.

7.5.1 Visualisation of results

To visualise the results of the 3-dimensional model, vertical cross-sections (Figure 7.6) were made at three different positions along the Y-axis:

- Section 1 at y=1.7 m
- Section 2 at y=5.2 m
- Section 3 at y=8 m

Additionally, three horizontal cross-sections were also made at different positions along the Z-axis:

- Section 4 at z= 17.55 m
- Section 5 at z= 12.2 m
- Section 6 at z= 5.6 m

The position of these sections was chosen to cut through the biggest possible number of outlets to have a better visualisation of the airflow. At each section the air temperatures and velocities are visualised.

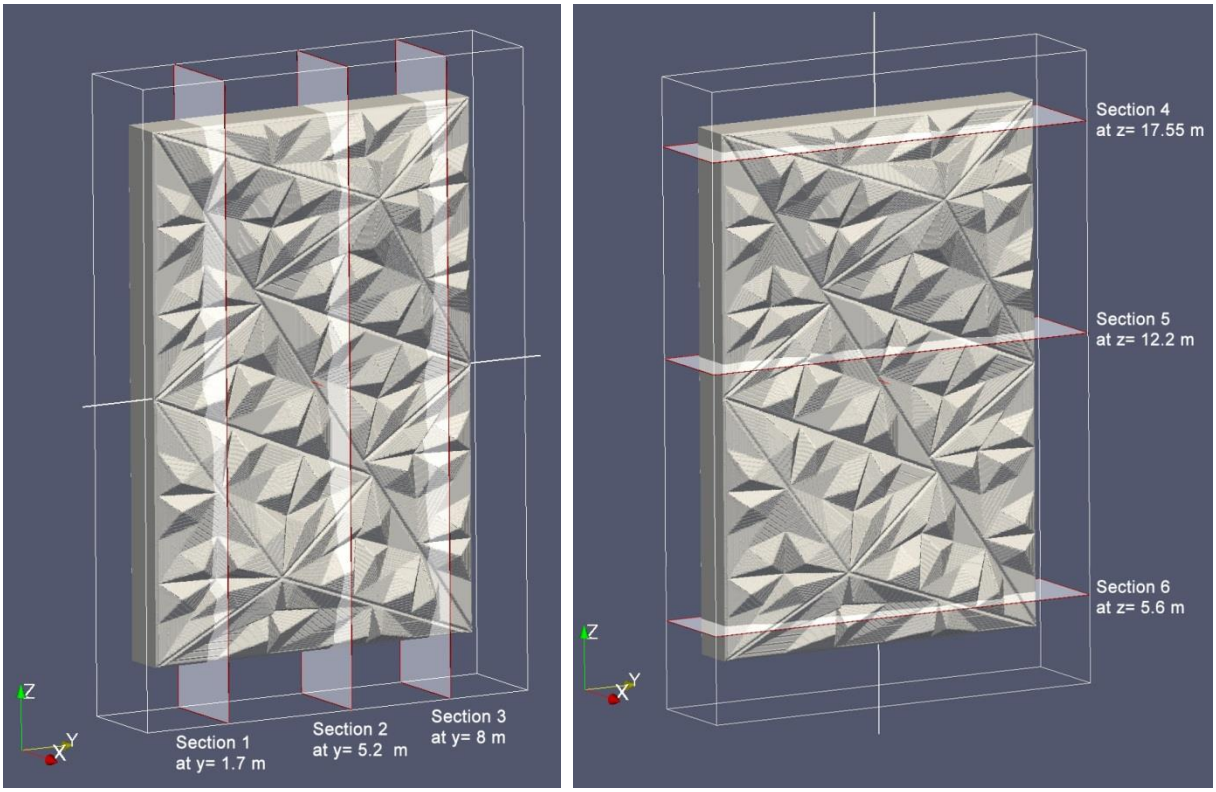

Figure 7.6: Location of vertical and horizontal cross-sections in the digital model. Source: author.

7.5.2 Observations

The temperature results in Figure 7.8 and Figure 7.10 show the dissipation of heat from the hot DSF surfaces to the inside of the cavity either by forced convection or by diffusion. In certain parts of the cavity the effect of convection is stronger when the velocity is relatively high, while in others diffusion has a greater effect when flow velocities are low.

Forced convection occurs due to the incoming air at the inlets cavity which is entering at a lower temperature than the surfaces and is equal to the ambient temperature of 308˚K (35.6˚C) which was assigned as a boundary condition. Cross-section 4 in Figure 7.10 shows that the incoming air pushes warmer air to the front folded faces of the DSF where it is trapped in some parts unless there is a perforation to act as an outlet and allow the warmer air to escape.

By comparing the visualised results of the temperature and velocity, it can be observed that, in general, the cavity temperature is often lower in areas with higher airflow velocity and therefore have more heat loss by convection. From Figure 7.7 and Figure 7.8 it can be seen that the velocity of the air in the lower half of the cavity is significantly less than the upper half, and therefore it is not well ventilated and heat gained by diffusion from the hot surfaces is higher. This implies the need for improvement of the DSF to direct air deeper into the cavity, possibly by using louvers at the inlets, adding openings at the sides or bottom of the DSF, or decreasing some perforations at the upper half of the cavity to allow a greater amount of cool air to reach down instead of escaping.

Inside the cavity, the temperature ranges from 322˚K to 308˚K, however in Figure 7.8 the top value of the scale bar is lowered to 312˚K for better visualisation of the temperature distribution. It is observed in cross-sections 5 and 6 in both Figure 7.10 and Figure 7.9 that the temperature in the middle of the cavity is higher than the bottom of the cavity despite having relatively higher airflow velocity. This is due to the thinner cross-section at the area so the heat transferred by diffusion has a strong effect and the flow velocity is not strong enough to ventilate it.

Regarding the airflow velocity magnitude, it mostly ranged between 0 and 5 m/s, with higher velocity in the cavity top near the inlets, and then it decreases gradually as the air moves downwards. It is observed that the velocity inside the cavity then starts increasing rapidly as air approaches the outlets. Since the outlets are very small in size (each of 0.0086 m^2) the velocity reaches its highest magnitude of about 5 m/s as the air exits the cavity. This behaviour is seen in the three cross-sections illustrated in Figure 7.7 and Figure 7.9.

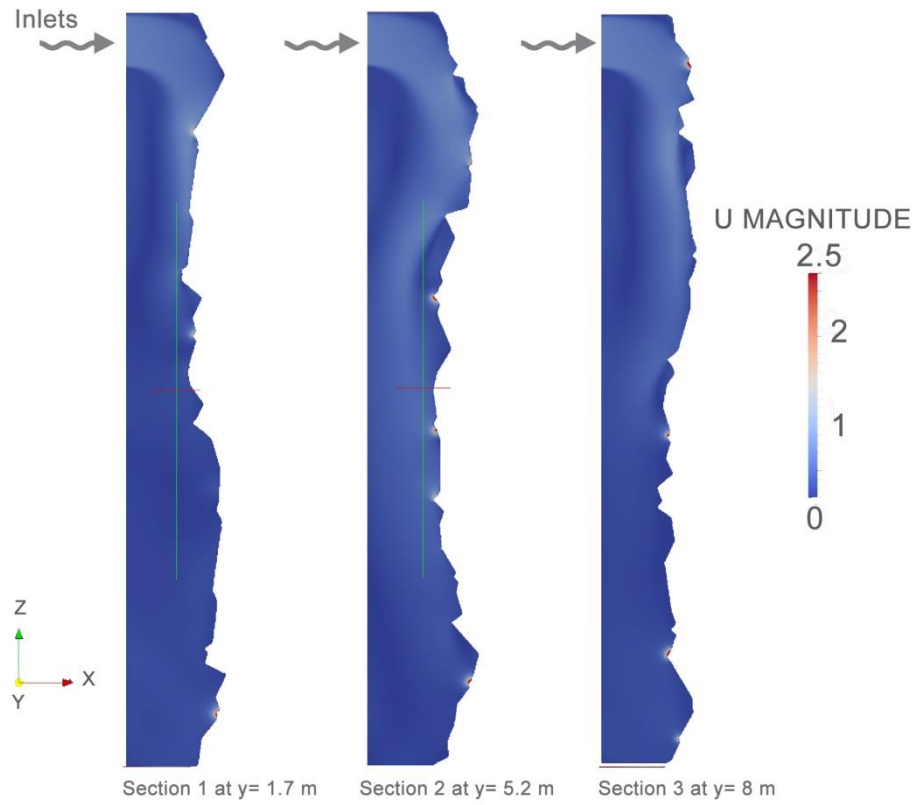

Figure 7.7: Vertical sections 1, 2 and 3 from left to right illustrating the magnitude of the airflow velocity (in m/s) throughout the DSF cavity at the last simulated time step at which a converged state of the flow is reached. Source: author.

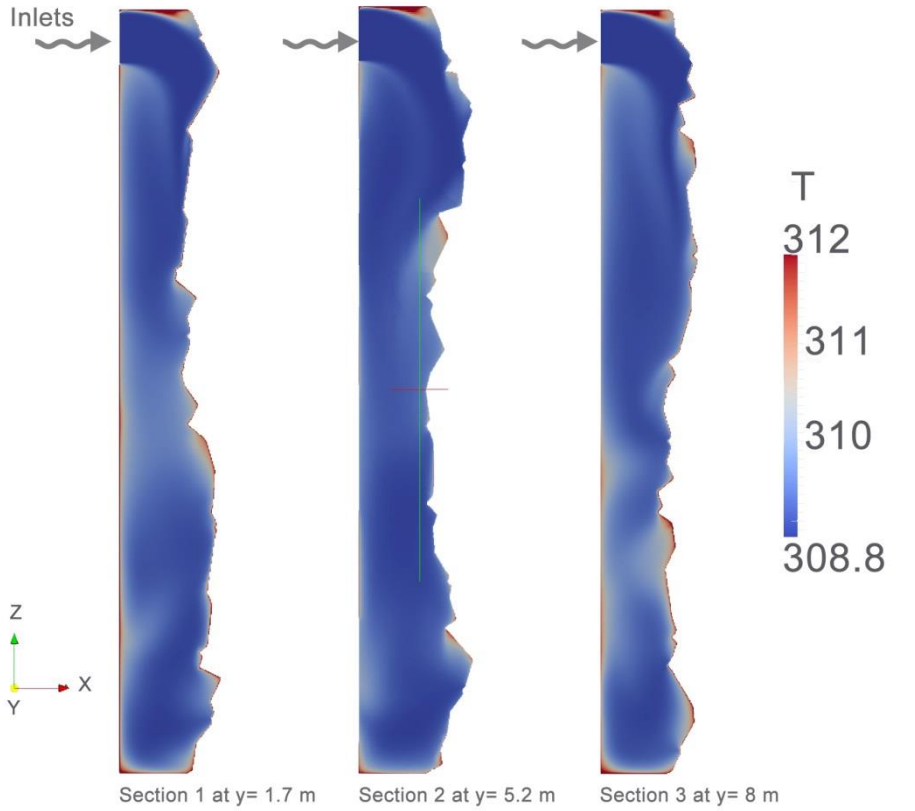

Figure 7.8: Vertical sections 1, 2 and 3 from left to right illustrating the temperature distribution (in Kelvin) throughout the DSF cavity at the last simulated time step at which a converged state of the flow is reached. Source: author.

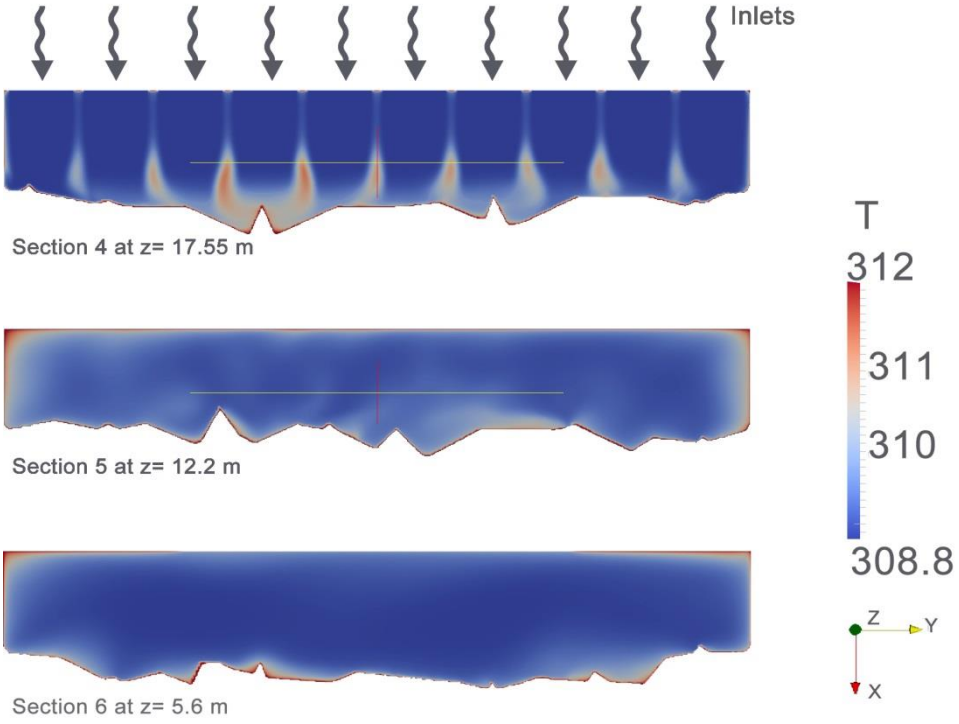

Figure 7.10: Horizontal sections 4, 5 and 6 from top to bottom illustrating the temperature distribution (in Kelvin) throughout the DSF cavity at the last simulated time step at which a converged state of the flow is reached. Source: author.

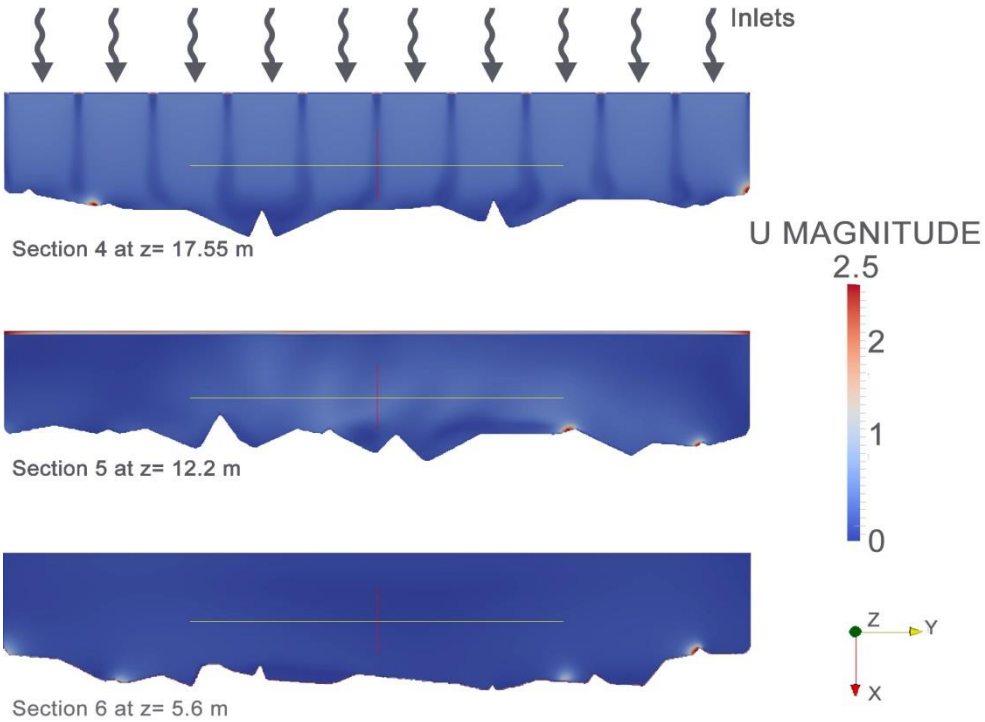

Figure 7.9: Horizontal sections 4, 5 and 6 from top to bottom illustrating the magnitude of the airflow velocity (in m/s) throughout the DSF cavity at the last simulated time step at which a converged state of the flow is reached. Source: author.

7.6 Comparison with EnergyPlus results

7.6.1 Cavity temperature

EnergyPlus calculates the temperature of a zone at only one point at its centroid. The selected output type is Zone Operative Temperature (OT) which is the average of the Zone Mean Air Temperature[34] (MAT) and Zone Mean Radiant Temperature[35] (MRT), OT = 0.5*MAT + 0.5*MRT. The calculated temperature by EnergyPlus was 37.6˚C for the selected time step.

In OpenFOAM the temperature is calculated at every single point of the mesh. Therefore in order to be able to compare it with the temperature output of EnergyPlus, an average value is calculated for all the points in the mesh. It resulted in an average value of 309.6˚K (36.46˚C).

7.6.2 Cavity airflow

Comparing results from EnergyPlus and OpenFOAM regarding airflow is not quite straightforward as they do not produce the same outputs. In the case of EnergyPlus, the available output data regarding airflow is the *air changes per hour* (ach) for the façade cavity, or the *volume flow rate* (in m^3/s) at each opening. While the output in OpenFOAM is the *velocity* (m/s) of the flow at all the mesh points of the entire geometry. It is possible to isolate only the outlets patch to know the velocities at these points specifically.

Since the openings in the OpenFOAM model have been grouped into bigger ones for approximation as explained in section 7.3.1, it would not be accurate to compare velocities as they should be different due to different opening sizes. However the total surface area of these openings is the same in both cases. Therefore it would be more accurate to compare the total volume flow rates at these openings rather than the flow velocities.

In EnergyPlus, calculating the total volume flow rate of all perforations is quite easy since it is already a generated output at each opening and a simple addition process is needed to calculate the total value of all perforations. Total volume flow rates of all perforations amounted to 3.74 m^3/s, which corresponded to 77 ach for the cavity volume of 175 m^3. In OpenFOAM, the velocity at the perforations ranged from 0 to 5 m/s, with an average of 4.36 m/s. The average velocity should be multiplied by their total surface area to calculate the total volume flow rate.

Total volume flow rate = total area of perforations (outlets) x average velocity at perforations

$= 0.82 \times 4.36 = 3.62\ m^3/s.$

[34] The zone mean air temperature is the average temperature of the air temperatures at the system timestep. The zone heat balance represents a “well stirred” model for a zone, therefore there is only one mean air temperature to represent the air temperature for the zone (EnergyPlus, 2014).

[35] The zone mean radiant temperature is a measure of the combined effects of temperatures of surfaces within that space. Specifically it is the surface area × emissivity weighted average of the zone inside surface temperatures, where emissivity is the Thermal Absorptance of the inside material layer of each surface (EnergyPlus, 2014).

7.6.3 Observations

The comparison between the results of EnergyPlus and OpenFOAM is summarised in the following table:

Table 7.3: Comparison between the results of each software and the difference in EnergyPlus results.

	EnergyPlus	OpenFOAM	Difference
Cavity temperature (˚C)	37.6	36.46	+3.1 %
Total volume flow rate at outlets (m^3/s)	3.74	3.62	+3.3 %

The comparison shows an unexpected similarity between the results. It was expected that there would be inaccuracies in EnergyPlus, especially in the results regarding the airflow. However, EnergyPlus only slightly overestimated both temperature and airflow values by only 3.1 % and 3.3 % respectively.

This shows that EnergyPlus can be reliable in giving a *general* estimation of the DSF behaviour. However, it cannot give us a detailed insight of the behaviour of the airflow and temperature distribution inside the cavity which is important for the evaluation of the proposed design solution. So even if it can more or less accurately predict the average velocity of the air, it is not capable of demonstrating that this air is not flowing evenly throughout the cavity and that only the upper half is considered well ventilated.

It is important here to point out once more that this OpenFOAM model has certain simplifications as explained in section 7.3.1. Therefore its results might (and probably will) contain inaccuracies. However, it is expected that these inaccuracies would be quite less than those of EnergyPlus due to huge differences in the calculation method of both software. What we can know for sure from the OpenFOAM model is *qualitative* information such as that regarding the flow pattern and behaviour, and temperature distribution. The *quantitative* information, such as the exact numerical values of the temperature and velocity, are subject to doubt.

7.7 Challenges and difficulties

As an architect with no previous studies regarding fluid dynamics, a number of issues were considered quite challenging and time consuming throughout the preparation of the OpenFOAM model and simulations:

- Learning the basics of CFD was critical in order to understand how the software works.
- Creating the mesh that represented the geometry of the DSF was also challenging due to the presence of the very small perforations that required a high resolution, as well as the folds themselves that produced many 'skew' faces and repeatedly caused the mesh check to fail. Countless trials were needed in the settings of SnappyHexMesh until a suitable balance was reached between accuracy and resolution of the mesh.
- Choosing an appropriate solver that can simulate the desired physical phenomena which are free and forced convection, in addition to heat transfer through radiation and conduction. This was the most time consuming phase as there wasn't a solver that readily simulates all these phenomena together, so a lot of effort was spent trying to 'combine' different solvers together. The complex nature of the geometry itself complicated this problem further. At the end, combining different solvers was not successful so we chose 'rhoSimpleFoam' that simulated only forced convection and conduction as explained earlier.
- Setting the correct boundary conditions, and knowing exactly which outputs from EnergyPlus that can be used as input data for OpenFOAM. Otherwise the comparison is not accurate before the simulation is even performed as the initial conditions of the two compared cases are not the same.
- Continuously addressing the errors that caused the solver to stop running. This was particularly exhausting since not all errors explicitly write their cause. Consequently numerous trial and error attempts were needed until we reached a successful configuration of the solver settings that enabled it to successfully work in the end.

7.8 Summary

This chapter concludes the biomimetic-computational approach presented in this thesis. It aimed at testing the reliability of EnergyPlus in simulating geometrically complex DSFs by comparing its results regarding cavity temperature and airflow with those simulated by OpenFOAM. This is particularly important since EnergyPlus (along with other similar building energy software) remain the most commonly used among architects who continuously seek new complex forms and better environmental performance at the same time.

The chosen DSF in the previous chapter in the South-East orientation was used for this verification. Another digital model for this DSF was prepared and simulated using OpenFOAM. The temperature and volume flow rates of the air of the two cases were compared. It was expected that EnergyPlus would show inaccuracies particularly regarding the airflow. However, EnergyPlus showed little variation between its results and those obtained in OpenFOAM as the values were only slightly over-estimated (by approximately 3 %) for both the cavity temperatures and volume flow rates.

Despite these positive results, EnergyPlus could not give more details about the airflow distribution inside the cavity which turned out to be inadequate in the lower half of the cavity and therefore requires design modification. It can be concluded that EnergyPlus can give a general idea of the DSF performance-even if it is geometrically complex- and is most suitable in early design phases. However, the airflow pattern and temperature distribution results by OpenFOAM are important in understanding the behaviour and improving the design accordingly. CFD simulations need expert knowledge and much more computing time, but are important in later more detailed design phases when final decisions must be taken.

It is important to note that it was intended to verify the results of three differently performing EnergyPlus models and not just one. If all models showed the same accuracy then it would have been more reassuring. However, due to time limitations only one model was verified. In all cases, simulating the behaviour of DSF is a very complex task even for CFD software and any simulation process will always be subject to inaccuracies. It must be noted that a real reliable verification of obtained results (from either software) requires comparing simulated data with data measured from physical models. Even physical models are subject to minor inaccuracies since the presence of the sensors and measurement tools themselves influence the fluid flow.

My sincere gratitude goes to my Tutor Dr. Francesco Battista from the Department of Mechanics at Sapienza University. This phase consumed the final year of this research, during which he spent much time and effort in teaching me about CFD and helping me prepare this model. Without his assistance and patience this phase would not have been possible.

Chapter 8
Discussion & Conclusion

8.1 Thesis summary

Biomimicry is an approach that derives inspiration for solutions to human problems through the study of natural designs, materials, structures and processes. This thesis attempted to apply this design approach in order to address the problem of building skin energy efficiency in sustainable design in the context of hot climates. In order to fully explore the potential of nature's inspirations in architectural design challenges and not just mimic shapes and forms, technological advances in parametric and computational design software in addition to environmental simulation means offer very useful tools. Hence, a *biomimetic-computational* approach was proposed and applied. The main aim of this research was to investigate solutions for building skins that would decrease cooling loads in hot climates. This was achieved by the proposal, application and criticism of a 'Biomimetic-Computational' design method.

A background and review of 'nature-inspired' design was presented in Chapter two where the origins of biomimicry, its pioneers throughout history, and the relationship between architecture and nature were addressed. A particular focus was made on the different levels and design methods applied in biomimetic design, in addition to its application using computational design tools. This review was particularly important in defining the main guidelines for the design approach to be followed in the subsequent chapters. Each chapter addressed a certain phase of this approach. And by actual application, the approach was gradually refined and better understood throughout the thesis.

The particular type of building skin chosen was the Double-Skin Façade (DSF). The different types and applications of DSFs were reviewed as well as the software commonly used for assessing their environmental performances. DSFs offer better acoustics, indoor environments and reduction in energy use during the operation of the building, and were mainly applied in cold and temperate climatic areas. However, there is a gap in the literature regarding their application in hot regions as they are perceived to cause over-heating and hence required particular attention in their design. Nonetheless, there are a number of case studies where DSFs were successfully applied in hot climates. These were analysed in order to define the main guidelines required for their successful application. A key observation was the importance of studying natural daylight alongside the thermal performance of the DSF. This can ensure that none is achieved at the expense of the other.

The beginning of the biomimetic-computational design approach started through investigating how natural organisms survive in hot climates and how to control heat gain/loss. Since the research deals with thermoregulation, the main methods of heat transfer which are radiation, conduction, convection and phase-change were defined. The output of the searching phase of living organisms was categorised depending on the means by which they regulate heat. This categorisation contributes to achieving a common ground between nature and architecture and facilitating the definition of the architectural feature corresponding to each idea explored. It included strategies used by trees, plants, animals, and humans regarding thermoregulation. It was then possible to assign building skin features corresponding to these strategies. The compiled list of strategies enabled the choice of two ideas to be applied in the development of the design proposal.

The design proposal applied the two selected ideas which were the folding skins that reduce heat gain by radiation, and the porosity of termite mounds which increase heat loss by convection. Architectural analogies for each idea were defined starting with the folding skins. The main parameters that describe this biomimetic idea were defined in order to interpret them into mathematical and geometrical terms and prepare the digital model for computational design. A preliminary design proposal for a shading screen for a typical office room in Cairo was studied and developed using parametric design software and evolutionary algorithms. The cooling loads in a typical July month and annual daylight performance of the room were compared before and after the presence of the shading screen. When the results were seen positive, the design developed into a DSF incorporating also the second biomimetic inspiration which is porosity.

The detailed study of the final design DSF proposal was evaluated by:

- Applying it to an existing building rather than a hypothetical one to act as a reference and compare its performance before and after its placement.
- Testing its performances in two orientations, South East (SE) and North West (NW). These were the two main orientations of the existing building.
- Comparing it to a typical flat DSF.
- Studying its thermal performance throughout the three hottest summer months instead of July only to have more indicative results.

Performance criteria and design variables of the proposed DSF were defined. Then the DSF was optimised using evolutionary algorithms with the fitness function set to minimise the façade cavity temperature while maximising the daylight inside the studied room. Preliminary results provided feedback and informed modifications to the model, and then the optimisation process was repeated. The final design proposals in the SE and NW orientations were successful in decreasing the cooling loads while maintaining the minimum daylight according to LEED standards. The effects of each biomimetic inspiration, orientation, wind, and software limitations on the final results were discussed.

The final phase of the design approach verified the obtained results using more accurate Computational Fluid Dynamics (CFD) software. The main objective was to know the degree of inaccuracy and whether EnergyPlus can be relied on in giving a general idea of the performance of geometrically-complex DSFs. This is quite important since the use of CFD is still not feasible in early design phases (due to need of more time, computation power and expert knowledge), and building energy software like EnergyPlus are the most practical option for architects in the current time.

8.2 Research contributions

8.2.1 Proposed DSF

The main aim of the thesis was to propose a building skin based on a biomimetic-computational design approach, which would decrease cooling loads for an office building in a hot climatic area. The proposed DSF achieved a reduction of 9.3% and 13.4% in the SE and NW orientations respectively when compared to the reference case with a single façade. Additionally, this reduction was not at the expense of daylight performance, which was improved and was able to meet the LEED daylight standards. Furthermore, the proposal performed better than a typical flat DSF that achieved a reduction on cooling loads of only 4.4% and 5.7%, at the expense of reducing daylight performance of the reference case and not meeting minimum daylight requirements. Finally, given the limited research and application of DSF in hot climatic areas, the proposal represents a successful attempt that encourages further investigations in this field of study.

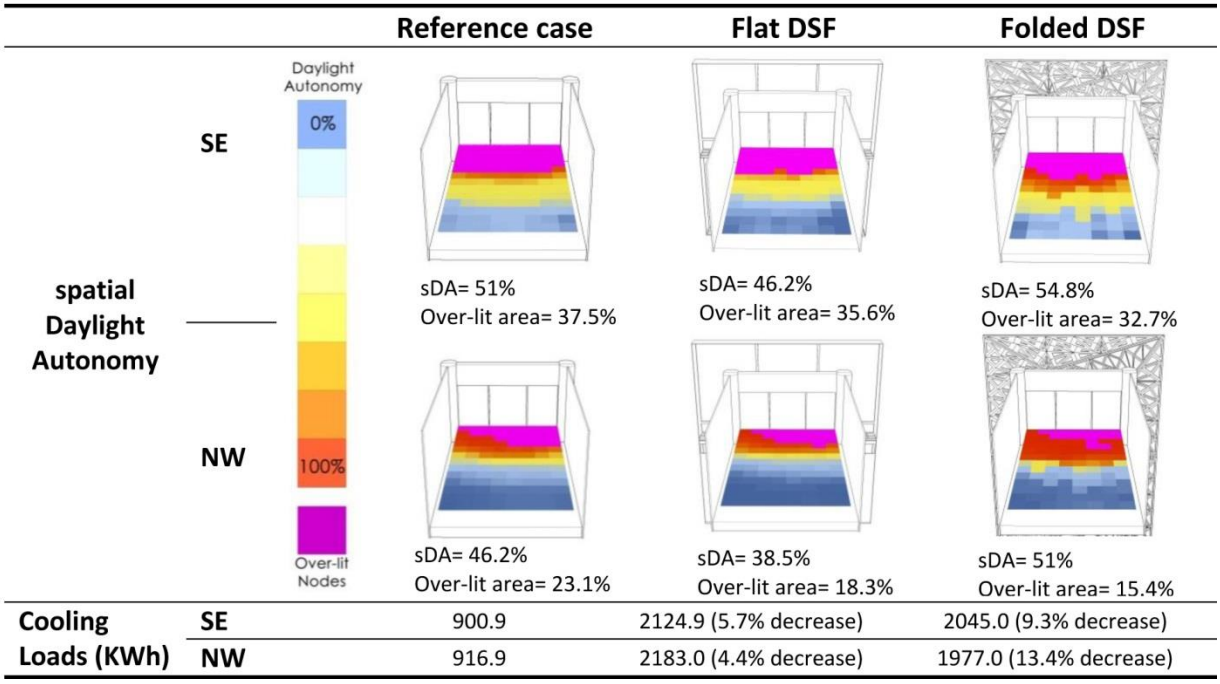

		Reference case	Flat DSF	Folded DSF
Cooling Loads (KWh)	SE	900.9	2124.9 (5.7% decrease)	2045.0 (9.3% decrease)
	NW	916.9	2183.0 (4.4% decrease)	1977.0 (13.4% decrease)

Figure 8.1: Daylight Autonomy (300lux for 50% of occupied time) and cooling loads for the months of June, July and August for each case in SE and NW orientations for the 40 m^2 office room. Note that the folded DSFs are not the same since a solution was chosen for each orientation. Source: author.

It is important to note that the specific shape or pattern is not of great importance but rather the fact that is it folded and was able to reduce insolation on itself hence decreasing heat gain. The proposed DSF represented a possible example just for the sake of applying the selected biomimetic ideas and testing them, in order to proceed with the design methodology as a whole. Other folding patterns might achieve the same design objectives, if properly designed and optimised as well, to be adapted to the context to which they are applied. This gives more freedom to the architect to choose among various shapes and patterns, taking into consideration aesthetic needs as well.

8.2.2 Detailed definition of the biomimetic-computational design approach

Biomimetic design approaches already exist in literature reviewed in Chapter Two. However, they are quite general in order to be applicable in a wide range of disciplines. Furthermore, although being already applied in the field of computational architectural design, a detailed explanation of the design methodology applied was not found in literature to the best of the researcher's knowledge up to this date. The design approach presented in the end of Chapter Two has been better understood and refined during its application in subsequent chapters throughout the thesis. Learning from actual experience enabled the detailed definition of this biomimetic-computational approach, especially regarding the computation phase. It included many steps to be taken that were not foreseen at the beginning before actually designing and applying first hand. Figure 8.2 represents the final definitive illustration of this design approach. Although it is quite detailed, nonetheless it is still general enough to be applied by other architects and designers interested in it and seeking new innovative solutions for their design problems. Each phase of this design approach was explained in its relevant chapter.

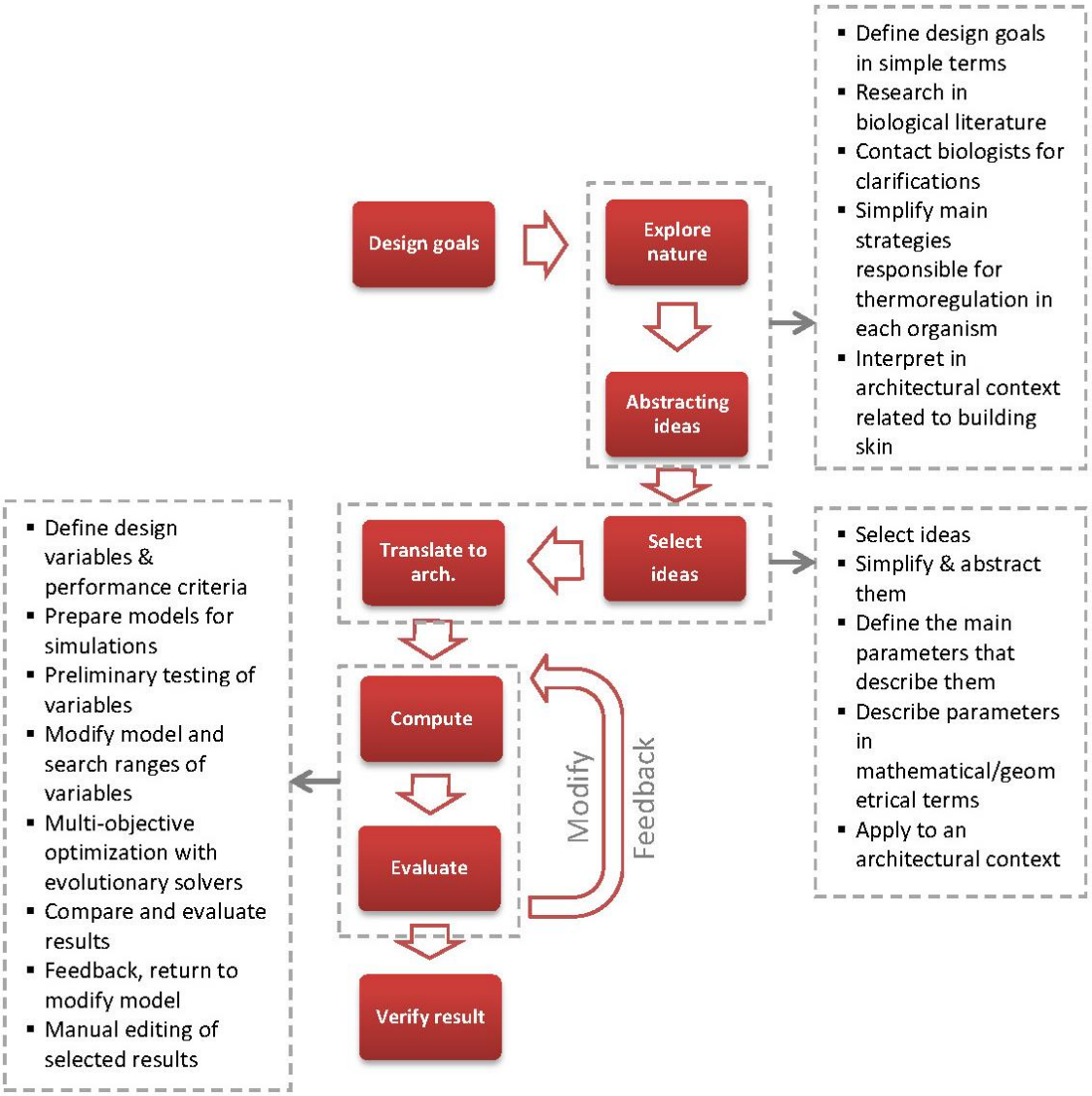

Figure 8.2: Detailed definition of the biomimetic-computational design approach as learned and understood from actual application throughout this thesis. Source: author.

8.2.3 General guidelines for DSFs in hot climates

As mentioned earlier, DSFs were developed mainly in cold climates and therefore most design guidelines available in literature were based on studies done in relatively cold climates. For the context of hot climates, after analysing a number of case studies in Chapter Three, it was concluded that DSFs could be used and the following design aspects were observed to be the most important for their successful use:

- Multiple openings in the outer layer to ensure sufficient ventilation of the cavity.
- Shading elements placed externally and not in the cavity.
- Use of shading devices with a high thermal mass.
- Recommended cavity depth range: 0.7 m to 1.2 m.
- Cavity should be higher than ground level and higher than roof level.
- Low Solar Heat Gain Coefficient of the outer glazing is very important.
- Double façade is preferably placed in the leeward side of the building where the highest pressure coefficients take place. Airflow in the cavity is lowest when the wind is parallel to the façade.

8.2.4 A small data-bank of biomimetic inspirations

Finding the appropriate inspirations and strategies in nature for a particular design problem was found to be quite challenging, in addition to actually understanding them and finding parallels in another context (which is architecture in this case) and applying them on a different scale. The biomimetic design strategies found and analysed in this thesis are compiled in a list of up to 37 possible ideas for thermoregulation (shown in Table 8.1). They can be useful for future work and other designers looking for inspirations in nature to solve heating or cooling related problems.

8.2.5 Verifying the accuracy of EnergyPlus in simulating complex geometries

The verification phase discussed in Chapter Seven aimed at testing the reliability of EnergyPlus in simulating geometrically complex DSFs by comparing its results regarding cavity temperature and airflow with those simulated by OpenFOAM. Despite expectations of inaccuracies in EnergyPlus results (as was seen in literature reviewed in Chapter Three), the comparison showed that EnergyPlus only slightly overestimated the cavity temperature and volume flow rate of the air. It does not give detailed information regarding the temperature distribution and airflow pattern, but it does give information that is sufficient for early design phases.

Table 8.1: Compiled list of all investigated strategies and the corresponding building skin features to study, categorised according to the four main heat transfer methods.

RADIATION			CONVECTION		
Organism	**Strategy**	**Arch. feature**	**Organism**	**Strategy**	**Arch. feature**
Leaves	Folds	Overall Morphology Shading elements	**Leaves**	Small narrow sizes	Shading elements
	Avoid horizontal position	Overall Morphology Shading elements		Lobes and dissections	Perforations
	Shiny surface	Cladding material		Holes and tears	Perforations
	Pubescence	Cladding material		Pubescence	Cladding material
Tree Barks	Round cross-section	Overall Morphology	**Tree Barks**	X	X
	Rough surface	Cladding material	**Succulents**	X	X
	Reflection of non-visible light spectrum	Cladding material	**Animals**	Respiratory counter current heat exchange	Ventilation system
Succulents	Ribs and grooves	Overall Morphology Shading elements		Tidal airflow	Ventilation system
	Spines and hairs	Cladding material		Porous termite mound surface	Ventilation system Cladding material
	Alternate curves	Overall Morphology Shading elements		Egress channels in termite mounds	Ventilation system Perforations
Animals	Vasodilation[36]	Ventilation system		Mound Ridges in termite mounds	Ventilation system Overall Morphology
Humans	Vasodilation	Ventilation system		Air suction at termite mound top	Ventilation system Overall Morphology
	Surface area to mass ratio	Overall Morphology		Colouration	Cladding material
			Humans	Anastomoses	Ventilation system
CONDUCTION			**EVAPORATION/CONDENSATION**		
Organism	**Strategy**	**Arch. feature**	**Organism**	**Strategy**	**Arch. feature**
Leaves	X	X	**Leaves**	More/bigger stomata	Ventilation system
Tree Barks	Thick outer layer	Insulation Cladding material		Closed, dense venation system	Ventilation system
	Peeling surface	Overall Morphology Cladding material	**Tree Barks**	Water transport through xylem	Ventilation system
Succulents	Surface area to mass ratio	Overall building design	**Succulents**	CAM	Ventilation system
				Spines and hairs	Cladding material
Animals	Vascular counter current heat exchange	Ventilation system	**Animals**	Respiratory evaporative cooling	Ventilation system
	Soil as thermal sink	Ventilation system		Respiratory counter current heat exchange	Ventilation system
	Colouration	Cladding material		Moisture harvesting	Ventilation system
Humans	X	X	**Humans**	Evaporative cooling by perspiration	Ventilation system

[36] All the strategies listed under the radiation section of the table aim at minimizing the heat gain caused by radiation. Vasodilation is the only strategy observed that aim at maximizing heat loss by radiation.

8.3 Research limitations

- The physical phenomena taking place within the façade cavity are too complex to be accurately simulated even with the best CFD tools available. Physical models must be made in order to verify and validate the accuracy of obtained results.
- Many biomimetic inspirations had direct applications in the development of new materials, which was not within the scope of this thesis.
- Only passive design strategies for thermoregulation are investigated in this thesis. The author acknowledges that best performances and results can be obtained by using both passive and active design means; however this would represent the scope of future research.

8.4 Criticism and discussion

A number of issues related to this research are important to be discussed and criticised as follows.

8.4.1 Applied methodology

The design methodology applied is based on the intention of learning from nature in order to solve challenges faced in architectural design, and not just imitating shapes or forms of natural organisms. Assessing a design methodology is not an easy task due to its qualitative nature. Nonetheless one can criticise the methodology based on its advantages, final output, tools used and challenges faced.

The advantages of this methodology include designing architecture that is more adapted to its local environment, and more sustainable in terms of energy consumption, as these were design goals from the outset. Other advantages include the fact that it is an interdisciplinary process in which architects interact with other fields of study in order to proceed with their designs, and finally the potential innovation and new ideas that arise from natural inspirations and from the exchange of knowledge between architecture and other fields of expertise in biology. It is a flexible methodology that can be adjusted based on the design problem at hand and the environmental context in which it is applied. The success of a methodology could be assessed from the success of its output. The proposed design output successfully met the required design goals. Additionally, it represented an innovative DSF that is different from the typical flat DSFs usually considered. The particular pattern applied in the DSF is not in itself important but rather it represents an example of a possible application of the biomimetic inspiration chosen.

The computational design software and environmental simulation tools played a critical role in the design development. Evolutionary algorithms enabled the optimisation of the proposal based on multiple conflicting design requirements which were improving the thermal and daylight behaviour in the same time. There were hundreds of possible combinations among the design parameters that were impossible to manually try. Environmental simulations provided real-time feedback along the design process enabling the architect to make informed decisions accordingly. However, the thermal simulation tool (EnergyPlus) in particular had certain limitations. The physical phenomena regarding heat transfer and airflow taking place in the DSF cavity are quite complex and hence were calculated in a simplified manner. In addition, handling complex geometries was another difficulty. Nonetheless the use of more accurate Computational Fluid Dynamics simulations

(CFD) is still not feasible in early design phases (due to need of time and expert knowledge), and building energy software like EnergyPlus remain the most practical option for architects in the current time.

Software tools continuously undergo rapid changes and developments that increase their capabilities and accuracies, so despite the current limitations of available software this does not affect the design methodology as a whole. Eventually, either building energy software will become more accurate and support complex geometries easily, or CFD software would become more 'user-friendly' for the non-experienced, and finally computers would become more powerful in terms of processing time.

Finally, a number of challenges were faced throughout the application of the proposed methodology that include:

- Understanding/analyzing biology-related literature, need of experts
- Translating the biomimetic idea to mathematical terms and relationships
- Managing conflicting performance criteria
- Limitations of the software used (EnergyPlus) in thermal simulations
- Requirement of advanced knowledge in fluid dynamics in order to run CFD simulations

8.4.2 Role of the designer

One of the criticisms regarding this design approach is the role of the designer. Some might claim that the increasing software development in computational design gradually diminishes the human role in the process. Although the presented design approach depends on computer software and technology, the architect's role remains significant and is summarised in the following points:

- Analysis of project requirements and constraints
- Description of the biomimetic inspiration as design parameters in the computational model
- Setting a suitable fitness function for the evolutionary solver
- Recurrently analysing and selecting best design solutions
- Continuous evaluation and feedback
- Manual adjustments of design solutions when necessary

8.4.3 Need of expert knowledge

After finding a number of relevant biomimetic strategies, an obstacle emerged which was actually to understand the strategy at hand due to terminology that seem unfamiliar to non-biologists. This required the assistance of experts on that particular organism or physical phenomena in order to provide further explanation or clarification.

8.4.4 Cost of construction

Complex geometries in architecture often raise the concern related to the manufacturing and assembly costs of buildings made from parts that are different in shape and size. However, by and large it is now accepted that feasible production is becoming gradually possible owing to contemporary computer-aided manufacturing (CAM) techniques. It is worth noting that the researcher along with colleagues at Sapienza University prepared a preliminary feasibility study of the proposed DSF as part of the documents submitted in an international competition on biomimetic design in 2015. The feasibility study is placed in Appendix C.

8.5 Future research and vision

There are a number of possible future investigations that could continue in this line of research such as:

- Address the limitations of EnergyPlus by coupling it with CFD software in order to complement each other's limitations. There is ongoing research in this area however often applied to simple geometrical configurations rather than complex ones.

- Verify the obtained results not only by using CFD software (as they too have their limitations) but also using physical prototypes to measure the simulated temperatures and airflow inside the façade cavity.

- Investigate possible passive solutions to cool the air in the façade cavity. This would enable its use for natural ventilation and further reduce energy consumed in cooling.

- Investigate the application of biomimetic inspiration on a material-level and not only morphological and geometrical level.

The research envisions the application of the presented design approach on a larger scale, so its benefits would reach more occupants and owners, more energy is saved, and more 'breathing' buildings are adapted to their local context. The strength of this system is the flexibility of the approach. It provides a framework that can be applied to different contexts using different inspirations. The research also envisions that the design approach would be applied in addressing other design goals and not just decreasing cooling loads. For example, ideas from nature could inspire the structural system, ventilation system, arrangement of spaces or the design of building as a whole, utilising the constantly developing computation tools, with the main aim of improving the building's performances.

References

Abere, S. A. & Oguzor, N. S., 2011. Adaptation of Animals to Arid Ecological Conditions. *World Journal of Zoology,* 6(2), pp. 209-214.

Abou-Houly, H. E., 2010. *PhD Thesis: Investigation of flow through and around the Macrotermes michaelseni termite mound skin,* Loughborough: Loughborough University.

Alexander, C., 1964. *A Much Asked Question About Computers and Design.* Boston, Architecture and the Computer.

Allen, E., 2005. *How Buildings Work: The Natural Order of Architecture.* 3rd ed. New York: Oxford University Press.

Alucobond, 2014. *Technical Data.* [Online]
Available at: http://www.alucobond.com/alucobond-technical-data.html?&L=9
[Accessed 29 June 2015].

Ander, G. D., 2014. *Windows and Glazing - Whole Building Design Guide (WBDG).* [Online]
Available at: http://www.wbdg.org/resources/windows.php
[Accessed 22 February 2016].

Anderson Jr., J. D., 2009. Chapter 2: Governing Equations of Fluid Dynamics. In: J. F. Wendt, ed. *Computational Fluid Dynamics Part 1.* Berlin: Springer Berlin Heidelberg, pp. 15-51.

ANSI/ASHRAE, 2004. *ANSI/ASHRAE Standard 55: Thermal Environmental Conditions for Human Occupancy,* Atlanta, GA: The American Society of Heating, Refrigerating and Air-Conditioning Engineers Inc..

ASHRAE, 2009. *ASHRAE Hanbook Fundamentals,* Atlanta, GA: American Society of Heating, Refrigerating and Air-Conditioning Engineers, Inc..

Attia, S., 2012. *PhD Thesis: A Tool for Design Decision Making-Zero Energy Residential Buildings in Hot Humid Climates,* Louvain: Universite Catholique de Louvain.

Attia, S., Evrard, A. & Gratia, E., 2012. Development of benchmark models for the Egyptian residential buildings sector. *Applied Energy,* Volume 94, pp. 279-284.

Attia, S., Hensen, J. L., Beltrán, L. & De Herde, A., 2012. Selection Criteria for Building Performance Simulation Tools: Contrasting Architects and Engineers Needs. *Journal of Building Performance Simulation,* 5(3), pp. 155-169.

Autodesk Ecotect Analysis, 2010. *Questions and Answers.* [Online]
Available at: http://images.autodesk.com/adsk/files/ecotectanalysis10_faq_customer_3.17.09.pdf
[Accessed 2014].

Autodesk Vasari, 2014. *Autodesk Sustainability Workshop.* [Online]
Available at: http://sustainabilityworkshop.autodesk.com/software/vasari
[Accessed 2014].

Baldinelli, G., 2009. Double skin façades for warm climate regions: Analysis of a solution with an integrated movable shading system. *Building and Environment,* Volume 44, p. 1107–1118.

Barbosa, S. & Ip, K., 2014. Perspectives of double skin façades for naturally ventilated buildings: A Review. *Renewable and Sustainable Energy Reviews,* Volume 40, p. 1019–1029.

Benyus, J., 1997. *Biomimicry: Innovation Inspired by Nature.* New York: William Morrow & Company.

Biology Online, 2009. *Xylem.* [Online]
Available at: http://www.biology-online.org/dictionary/Xylem
[Accessed September 2016].

Biomimicry 3.8, 2013. *Biomimicry Thinking.* [Online]
Available at: http://biomimicry.net/about/biomimicry/biomimicry-designlens/biomimicry-thinking/
[Accessed 9 June 2013].

Biomimicry 3.8, 2013b. *Life's Principles.* [Online]
Available at: http://biomimicry.net/about/biomimicry/biomimicry-designlens/lifes-principles/
[Accessed 4 April 2013].

British Standards Institution, 2008. *Lighting for buildings. Code of practice for daylighting.* 2nd ed. London: British Standards Institution (BSI).

Calsbeek, R., Knouft, J. H. & Smith, T. B., 2006. Variation in scale numbers is consistent with ecologically based natural selection acting within and between lizard species. *Evolutionary Ecology,* Volume 20, p. 377–394.

Castle, H., 2004. Geometry of Integration and Differentiation of Plant Stems. *Architectural Design,* 74(3), pp. 4-5.

Charkoudian, N., 2003. Skin Blood Flow in Adult Human Thermoregulation: How It Works, When It Does Not, and Why. *Mayo Clinic Proceedings,* pp. 603-612.

Chen, Q., 2009. Ventilation performance prediction for buildings: A method overview and recent applications. *Building and Environment,* 44(4), pp. 848-858.

Ching, F. D., 2007. *Architecture: Form, Space & Order.* 3rd ed. New Jersey: John Wiley & Sons.

Cole, L. C., 1943. Experiments on Toleration of High Temperature in Lizards with Reference to Adaptive Coloration. *Ecology,* 24(1), pp. 94-108.

Comanns, P. et al., 2011. Moisture harvesting and water transport through specialized micro-structures on the integument of lizards. *Beilstein journal of Nanotechnology,* Volume 2, p. 204–214..

Davis, D. & Peters, B., 2013. Customising the Architectural Design Environment with Software Plugins. *Architectural Design,* 83(2), pp. 124-131.

De Gracia, A. et al., 2013. Numerical modelling of ventilated facades: A review. *Renewable and Sustainable Energy Reviews,* Volume 22, p. 539–549.

Derix, C., Kimpian, J., Karanouh, . A. & Mason, J., 2011. Feedback Architecture. *Architectural Design,* Volume 81, p. 36–43.

DesignBuilder, 2014. *DesignBuilder Software For Architects.* [Online]
Available at: http://www.designbuilder.co.uk/software/for-architects
[Accessed 2014].

Dictionary.com, 2013. *autotrophic.* [Online]
Available at: http://www.dictionary.com/browse/autotrophic
[Accessed 22 July 2013].

Dictionary.com, 2013b. *heterotrophic.* [Online]
Available at: http://www.dictionary.com/browse/heterotrophic?s=t
[Accessed 22 July 2013].

Dogan, T., 2015. *Archsim.* [Online]
Available at: http://archsim.com/
[Accessed 5 March 2015].

Dollens, D., 2009. *Digital Bonatic Architecture 2.* Santa Fe, New Mexico: Lumen, Inc..

Dzialowski, E. M. & O'Connor, M. P., 1999. Utility of blood flow to the appendages in physiological control of heat exchange in reptiles. *Journal of Thermal Biology,* Volume 24, pp. 21-32.

Ehleringer, J., Bjorkman, O. & Mooney, H., 1976. Leaf Pubescence: Effects on Absorptance and Photosynthesis on a Desert Shrub. *Science,* 192(4237), pp. 376-377.

EIA, 2013. *U.S. Energy Information Administration.* [Online]
Available at: http://www.eia.gov/tools/faqs/faq.cfm?id=86&t=1
[Accessed 9 July 2013].

El Ahmar, S. & Fioravanti, A., 2014. *Botanics and Parametric Design Fusions for Performative Building Skins - An application in hot climates.* Newcastle upon Tyne, Proceedings of the 32nd eCAADe Conference, pp. 595-604 .

Encyclopædia Britannica, 2013. *Latent Heat.* [Online]
Available at: http://www.britannica.com/EBchecked/topic/331406/latent-heat
[Accessed November 2013].

Encyclopaedia Britannica, 2014. *Succulent.* [Online]
Available at: http://www.britannica.com/EBchecked/topic/571271/succulent
[Accessed 7 January 2014].

Encyclopædia Britannica, 2015. *Leonardo da Vinci's parachute.* [Online]
Available at: https://www.britannica.com/topic/Leonardo-da-Vincis-parachute-1704849#ref1092031
[Accessed October 2016].

EnergyPlus, 2014b. *Weather Data by Region.* [Online]
Available at: https://energyplus.net/weather-region/africa_wmo_region_1/EGY%20%20
[Accessed 2014].

EnergyPlus, 2014. *Input Output Reference: The Encyclopedic Reference to EnergyPlus Input and Output.* Illinois: US Department of Energy.

Farid, M., Khudhair, A., Razack, S. & Al-Hallaj, S., 2004. A review on phase change energy storage: materials and applications. *Energy Conversion and Management,* Volume 45, p. 1597–1615.

Fletcher, C. A. J., 1991. Fluid Dynamics: The Governing Equations. In: *Computational Techniques for Fluid Dynamics Volume 2: Specific Techniques for Different Flow Categories.* 2nd ed. Berlin: Springer Berlin Heidelberg, pp. 1-46.

Frazer, J., 1995. *An Evolutionary Architecture.* London: E.G. Bond Ltd.

Fuller, D. & Mcneil, A., 2016. *Radiance - A Validated Lighting Simulation Tool.* [Online]
Available at: http://www.radiance-online.org/author/AMcneil
[Accessed 1 September 2013].

Gillam, P., 2014. *PMG Biology, Vasodilation.* [Online]
Available at: https://pmgbiology.wordpress.com/tag/vasodilation/
[Accessed 15 August 2014].

Givnish, T. J., 1988. Adaptation to Sun and Shade: A Whole-plant Perspective. *Plant Physiology,* Volume 15, pp. 63-92.

Givnish, T. & Vermeij, G., 1976. Sizes and Shapes of Liane Leaves. *The American Naturalist,* 110(975), pp. 743-778.

Greenberg, R., Danner, R., Olsen, B. & Luther, D., 2011. High summer temperature explains bill size variation in salt marsh sparrows. *Ecography ,* Volume 34, p. 001–007.

Gruber, P., 2011. *Biomimetics in Architecture.* Vienna: Springer Vienna.

Gruber, P. et al. eds., 2011. *Biomimetics- Materials, Structures and Processes: Examples, Ideas and Case Studies.* Berlin: Springer.

Hadley, N. F., 1972. Society Desert Species and Adaptation: Plants and animals in arid environments show many strikin gsimilarities in their morphological and physiological adaptations. *American Scientist,* 60(3), pp. 338-347.

Hamza, N., 2008. Double versus single skin facades in hot arid areas. *Energy and Buildings ,* Volume 40 , p. 240–248.

Hamza, N. & Abohela, I., 2013. *Non-Uniform Double Skin Façade Cavities: An exploratory study on cavity heat stratification and daylight levels indoors.* Munich, Proceedings of Passive and Low Energy Architecture (PLEA) Conference.

Hamza, N., Cook, M. & Cropper, P., 2011. *Comparative Analysis of Natural Ventilation Performance in Non-Uniform Double Facades in Temperate Climates.* Sydney, Proceedings of the International Building Performance Simulation Association (IBPSA) Conference.

Hamza, N., Gomaa, A. & Underwood, C., 2007. *Daylighting and thermal analysis of an obstructed double skin façade in hot arid areas.* Helsinki, Proceedings of Clima 2007 WellBeing Indoors.

Harrington, E., 2012. *Gular Fluttering Dissipates Heat: Nightjars.* [Online]
Available at:
http://www.asknature.org/strategy/df479edb10713dec0097de25edf20b80#.VAigdU0cSUk
[Accessed June 2013].

Hashemi, N., Fayaz, R. & Sarshar, M., 2010. Thermal behaviour of a ventilated double skin facade in hot arid climate. *Energy and Buildings,* Volume 42, p. 1823–1832.

Helms, M., Swaroop, S. V. & Goel, A. K., 2009. Biologically inspired design: process and products. *Design Studies,* 30(5), pp. 606-622.

Hemberg, M. et al., 2008. Genr8: Architects' Experience with an Emergent Design Tool. In: . J. J. Romero & P. Machado, eds. *The Art of Artificial Evolution.* Berlin Heidelberg New York: Springer, pp. 167-188.

Henrion, W. & Tributsch, H., 2009. Optical solar energy adaptations and radiative temperature control of green leaves and tree barks. *Solar Energy Materials & Solar Cells,* Volume 93, p. 98–107.

Hensel, M., Menges, A. & Weinstock, M., 2004. Frei Otto in Conversation with the Emergence and Design Group. *AD: Emergence: Morphogenetic Design Strategies,* 74(3), pp. 18-25.

Hensel, M., Menges, A. & Weinstock, M., 2010. *Emergent Technologies & Design: Towards a biological paradigm for architecture.* New York: Routledge.
ICD Stuttgart University, 2013. *HygroSkin: Meteorosensitive Pavilion.* [Online]
Available at: http://icd.uni-stuttgart.de/?p=9869
[Accessed September 2013].
IDSC, 2012. *The Egyptian Cabinet: Information and Decision Support Center.* [Online]
Available at: http://www.idsc.gov.eg/Upload/Documents/304/electricity.pdf
[Accessed 4 July 2013].
Jones, H. G. & Rotenberg, E., 2011. Energy, Radiation and Temperature Regulation in Plants. In: A. M. Hetherington, ed. *Encyclopedia of Life Sciences (eLS).* s.l.:John Wiley & Sons.
Ju, J. et al., 2012. A multi-structural and multi-functional integrated fog collection system in cactus. *Nature Communications,* Volume 3, p. 1247.
Kalyanova, O. et al., 2009. *An emperical validation of building simulation software for modelling of double-skin facades (DSF).* Glasgow, Proceedings of the International Building Performance Simulation Association (IBPSA) Conference, pp. 1107-1114.
Kellogg Jr., D. L., 2006. In vivo mechanisms of cutaneous vasodilation and vasoconstriction in humans during thermoregulatory challenges. *Journal of Applied Physiology,* Volume 100, p. 1709–1718.
Keynes, R. D., 2001. *Charles Darwin's Beagle Diary.* 1st ed. Cambridge: Cambridge University Press.
Kim, D. W. & Park, C. S., 2011. Difficulties and limitations in performance simulation of a double skin facade. *Energy and Buildings,* Volume 43, p. 3635–3645.
Knippers, J., 2009. *Building and Construction as a Potential Field for the Application of Biomimetic Principles.* Stuttgart, International Biona Symposium, ITKE, Stuttgart University.
Knippers, J. & Speck, T., 2012. Design and construction principles in nature and architecture. *Bioinspiration and Biomimetics,* 7(1).
Knippers, J., Speck, T. & Milwich, M., 2012. *Bio-inspired Kinematics for Adaptive Shading Systems.* [Online]
Available at: http://www.itke.uni-stuttgart.de/forschung.php?id=61
[Accessed 5 October 2013].
Kobayashi, H., Kresling, B. & Vincent, J. F. V., 1998. The geometry of unfolding tree leaves. *The Royal Society, Proceedings B,* Volume 265, pp. 147-154.
Korb, J., 2003. Thermoregulation and ventilation of termite mounds. *Naturwissenschaften ,* Volume 90, p. 212–219.
Kull, U. & Herbig, A., 1994. *Leaf venation patterns and principles of evolution.* Stuttgart, Proceedings of the 3rd International Symposium of the Sonderforschungsbereich 230, pp. 167-175.
Lagios, K., 2016. *DIVA for Rhino.* [Online]
Available at: http://diva4rhino.com/
[Accessed 3 February 2014].
Langklide, T. & Boronow, K. E., 2012. Hot Boys Are Blue: Temperature-Dependent Color Change in Male Eastern Fence Lizards. *Journal of Herpetology,* 46(4), p. 461–465.
Lang, W., 2001. The Functional, energetic and structural aspects of the building skin. In: C. Schittich, ed. *In Detail: Building Skins.* Berlin: Birkhauser, pp. 9-28.
Leitão, A., Santos, L. & Lopes, J., 2012. Programming Languages For Generative Design: A Comparative Study. *International Journal of Architectural Computing,* 10(1), pp. 139-162.
Lienhard IV, J. H. & Lienhard V, J. H., 2016. *A Heat Transfer Textbook.* Fourth ed. Cambridge Massachusetts: Phlogiston Press.
Loonen, R., Trčka, M., Cóstola, D. & Hensen, J., 2013. Climate adaptive building shells: State-of-the-art and future challenges. *Renewable and Sustainable Energy Reviews,* Volume 25, p. 483–493.
Mateus, N. M., Pinto, A. & da Graca, G. C., 2014. Validation of EnergyPlus thermal simulation of a double skin naturallyand mechanically ventilated test cell. *Energy and Buildings ,* Volume 75, p. 511–522.
Mazzoleni, I. & Price, S., 2013. *Architecture Follows Nature: Biomimetic Principles For Innovative Design.* Boca Raton(Florida): CRC Press.
Mccafferty, D. J., 2007. The value of infrared thermography for research on mammals: previous applications and future directions. *Mammal Review,* Volume 37, p. 207–223.
McKeag, T., 2010. *Bringing Biomimicry To Cement, Offices and Daily Life.* [Online]
Available at: https://www.greenbiz.com/blog/2010/07/15/bringing-biomimicry-cement-offices-and-

daily-life
[Accessed April 2016].
Megahed, A. H., 2012. *Reality and the Future of Electricity in Egypt and the World.* [Online]
Available at: http://www.idsc.gov.eg/Upload/Documents/304/electricity.pdf
[Accessed 10 July 2013].
Menges, A. & Ahlquist, S., 2011. Computational Design Thinking. In: S. A. Achim Menges, ed. *Computational Design Thinking.* London: John Wiley and Sons, pp. 10-29.
Menges, A., Krieg , O. & Reichert, S., 2013. *HygroSkin: Meteorosensitive Pavilion.* [Online]
Available at: http://icd.uni-stuttgart.de/?p=9869
[Accessed 1 September 2013].
Menges, A. & Reichert, S., 2012. Material Capacity-Embodied Responsiveness. *Architectural Design,* 82(2), pp. 52-59.
Minner, K., 2011. *Moving Homeostatic Facade Preventing Solar Heat Gain.* [Online]
Available at: http://www.archdaily.com/?p=101578
[Accessed 11 December 2014].
Moloney, J., 2011. *Designing Kinetics for Architectural Facades- State Change.* New York: Routledge.
Nachtigall, W. & Wisser, A., 2015. *Bionics by Examples: 250 Scenarios from Classical to Modern Times.* London: Springer.
National Oceanic and Atmospheric Administration, 1990. *Cairo (A) Climate, World Meteorological Organization Normals.* [Online]
Available at: ftp://ftp.atdd.noaa.gov/pub/GCOS/WMO-Normals/TABLES/REG__I/UB/62366.TXT
[Accessed October 2016].
Nebelsick, A. R., Uhl, D., Mosbrugger, V. & Kerp, H., 2001. Evolution and Function of Leaf Venation Architecture: A Review. *Annals of Botany,* Volume 87, pp. 553-566.
Nobel, P. S., 1991. Light. In: P. S. Nobel, ed. *Physicochemical and Environmental Plant Physiolog.* San Diego: Academic Press, pp. 191-243.
Norgaard, T. & Dacke, M., 2010. Fog-basking behaviour and water collection efficiency in Namib Desert Darkling beetles. *Frontiers in Zoology,* 7(1), p. 23.
Nouidui, T., 2016. *Building Controls Virtual Test Bed.* [Online]
Available at: https://simulationresearch.lbl.gov/bcvtb
[Accessed September 2016].
OpenFOAM, 2015. *OpenFOAM The Open Source CFD toolbox.* [Online]
Available at: www.openfoam.com
[Accessed 4 April 2015].
Oxford Dictionaries, 2016b. *Metabolism.* [Online]
Available at: https://en.oxforddictionaries.com/definition/metabolism
[Accessed September 2016].
Oxford Dictionaries, 2016c. *Autopoiesis.* [Online]
Available at: https://en.oxforddictionaries.com/definition/autopoiesis
[Accessed September 2016].
Oxford Dictionaries, 2016d. *Evolution.* [Online]
Available at: https://en.oxforddictionaries.com/definition/evolution
[Accessed September 2016].
Oxford Dictionaries, 2016e. *Hydrophilic.* [Online]
Available at: https://en.oxforddictionaries.com/definition/hydrophilic
[Accessed October 2016].
Oxford Dictionaries, 2016f. *Elastomer.* [Online]
Available at: https://en.oxforddictionaries.com/definition/elastomer
[Accessed October 2016].
Oxford Dictionaries, 2016g. *Adiabatic.* [Online]
Available at: https://en.oxforddictionaries.com/definition/adiabatic
[Accessed October 2016].

Oxford Dictionaries, 2016. *homeostasis.* [Online]
Available at: https://en.oxforddictionaries.com/definition/homeostasis
[Accessed September 2016].

Panitz, K. & Garcia-Hansen, V. R., 2013. *Daylighting design and simulation : ease of use analysis of digital tools for architects.* Brisbane, Proceedings of the 19th CIB World Building Congress.

Papadaki, N., Papantoniou, S. & Kolokotsa, D., 2014. A parametric study of the energy performance of double-skin facades in climatic conditions of Crete, Greece. *International Journal of Low-Carbon Technologies,* 9(4), pp. 296-304.

Pappas, A. & Zhai, Z., 2008. Numerical investigation on thermal performance and correlations of double skin facade with buoyancy-driven airflow. *Energy and Buildings ,* Volume 40, p. 466–475.

Patil, H. S. & Vaijapurkar, S., 2007. Study of the Geometry and Folding Pattern of Leaves of Mimosa pudica. *Journal of Bionic Engineering,* Volume 4, pp. 19-23.

Pawlyn, M., 2011. *Biomimicry in Architecture.* London: RIBA Publishing.

Peters, B., 2013. The Building of Algorithmic Thought. *Architectural Design,* 83(2), pp. 8-15.

Pilkington, 2014. *Glass Range for Architects and Specifiers- Technical Information Datasheet.* [Online]
Available at:
https://www.google.it/url?sa=t&rct=j&q=&esrc=s&source=web&cd=3&cad=rja&uact=8&ved=0ahUKEwiY0Y68l5DLAhVFqA4KHVhfDogQFggmMAI&url=http%3A%2F%2Fassetmanager-ws.pilkington.com%2Ffileserver.aspx%3Fcmd%3Dget_file%26ref%3D3442%26cd%3Dcd&usg=AFQjCNEKtpqZmDzyY6ytWk
[Accessed 10 July 2014].

Poirazis, H., 2006. *Double Skin Facades: A literature review,* Lund: Lund University.

Radhi, H., Sharples, S. & Fikiry, F., 2013. Will multi-facade systems reduce cooling energy in fully glazed buildings? A scoping study of UAE buildings. *Energy and Buildings,* Volume 56, p. 179–188.

Raven, P. H., Evert, R. F. & Curtis, H., 1976. *Biology of Plants.* 2nd ed. New York: W.H. Freeman and Company.

Reichert, S., Menges, A. & Correa, D., 2015. Meteorosensitive architecture: Biomimetic building skins based on materially embedded and hygroscopically enabled responsiveness. *Computer-Aided Design,* March, Volume 60, pp. 50-69.

Reinhart, C. F., 2011. Daylight Performance Predictions. In: J. L. Hensen & R. Lamberts, eds. *Building Performance Simulation for Design and Operation.* New York: Spon Press, pp. 235-255.

Reinhart, C. F. & Andersen , M., 2006. Development and validation of a Radiance model. *Energy and Buildings,* 38(7), pp. 890-904.

Reinhart, C. F. & Walkenhorst, O., 2001. Dynamic RADIANCE-based Daylight Simulations for a full-scale Test Office with outer Venetian Blinds. *Energy & Buildings,* 33(7), pp. 683-697.

Rosenman, M. A., 1996. The Generation of Form Using Evolutionary Algorithms. *Artificial Intelligence in Design,* Volume 96, pp. 643-662.

Roudsari, M. S. et al., 2015. *Pollination.* [Online]
Available at: http://mostapharoudsari.github.io/Honeybee/Pollination
[Accessed 20 June 2015].

Sabooni, M. A., Vaseti, H. M., Maerefat, M. & Azimi, A., 2012. *Development of the capability of Energyplus software to simulation of building double-skin facade.* Kusadasi, International Symposium on Sustainable Energy in Buildings and Urban Areas (ICHMT).

Sack, L. et al., 2012. Developmentally based scaling of leaf venation architecture explains global ecological patterns. *Nature Communications,* Volume 3, p. 837.

Sanchez, R. U., 2010. Parametric Performative Systems: Designing a Bioclimatic Responsive Skin. *International journal of architectural computing,* 8(3), pp. 273-300.

Schittich, C., 2001. Shell, Skin, Materials. In: C. Schittich, ed. *In Detail: Building Skins.* Berlin: Birkhauser, pp. 8-27.

Schuepp, P. H., 1993. Leaf Boundary Layers. *New Phytologist, Tansley Review,* 125(3), pp. 477-507.

Sherbrooke, W. C., Scardino, A. J., de Nys, R. & Schwarzkopf, L., 2007. Functional morphology of scale hinges used to transport water: convergent drinking adaptations in desert lizards. *Zoomorphology,* Volume 126, p. 89–102.

Sherif, A., Sabry, H. & Wagdy, A., 2014. *Hospital Patient Room Design for Desert Climates: Effect of Room Shape on Window Design for Daylighting.* Riyadh, The Saudi Umran Society, pp. 200-213.

Sherif, S., 2010. *The Confluence of Digital Design/Fabrication & Biological Principles,* Massachusetts : Massachusetts Institute of Technology.

Shibasaki, M., Wilson, T. E. & Crandall, C. G., 2006. Neural control and mechanisms of eccrine sweating during heat stress and exercise. *Journal of applied physiology,* Volume 100, p. 1692–1701.

Simon, H. A., 1996. *The Sciences Of The Arificial.* 3rd ed. Cambridge, Massachusetts: MIT Press.

Sleigh, A. & Noakes, C., 2009. *An Introduction To Fluid Mechanics, Unit 3: Fluid Dynamics.* [Online] Available at: http://www.efm.leeds.ac.uk/CIVE/FluidsLevel1/Unit03/T1.html [Accessed September 2016].

Soma, 2012. *Theme Pavilion Expo, Yeosu.* [Online] Available at: http://www.soma-architecture.com/index.php?page=theme_pavilion&parent=2# [Accessed October 2016].

Steadman, P., 2008. *The Evolution of Designs-Biological Analogy in Architecture & Applied Arts.* Oxon: Routledge.

StoCorp, 2015. *StoCoat Lotusan.* [Online] Available at: http://www.stocorp.com/building-solutions/new-build/coatings/#lotusan [Accessed September 2016].

Sullivan, L., 1896. The Tall Office Building Artistically Considered. *Lippincott's*, March, pp. 403-408.

Tattersall, G. J., Andrade, D. . V. & Abe, A. S., 2009. Heat Exchange from the Toucan Bill Reveals a Controllable Vascular Thermal Radiator. *Science,* Volume 325, pp. 468 -470.

Tattersall, G. . J. & Cadena, V., 2010. Insights into animal temperature adaptations revealed through thermal imaging. *The Imaging Science Journal ,* Volume 58, pp. 261-268.

Tattersall, G. J., Cadena, V. & Skinner, M. C., 2006. Respiratory cooling and thermoregulatory coupling in reptiles. *Respiratory Physiology & Neurobiology,* Volume 154, p. 302–318.

Taylor, N. A. S., Moreira, C. A. M., van den Heuvel, A. M. J. & Caldwell, J. N., 2014. Hands and feet: physiological insulators, radiators and evaporators. *European Journal of Applied Physiology,* 114(10), pp. 2037-2060.

The Biomimicry Institute, 2015. *About.* [Online] Available at: https://biomimicry.org/history/#.VwevKnrm6zQ [Accessed 8 4 2016].

Thompson, D. W., 1945. *On growth and form.* 1st ed. Cambridge : Cambridge University Press.

Toe, D. & Kubota, T., 2013. Development of an adaptive thermal comfort equation for naturally ventilated buildings in hot–humid climate susing ASHRAERP-884 database. *Frontiers of Architectural Research,* Volume 2, p. 278–291.

Turner, J. S., 2001. On the Mound of Macrotermes michaelseni as an Organ of Respiratory Gas Exchange. *Physiological and Biochemical Zoology,* 74(6), pp. 798-822.

Turner, J. S. & Soar, R. C., 2008. *Beyond biomimicry: What termites can tell us about realizing the living building.* Loughborough , Loughborough University.

USGBC, 2013. *LEED Reference Guide for Building Design and Construction.* 4th ed. Washington: USGBC.

Vangimalla, P. R., Olbina, S. J., Issa, R. R. & Hinze, J., 2011. *Validation of Autodesk Ecotect Accuracy for Thermal and Daylight Simulations.* Phoenix, WSC, pp. 3388-3399.

Vierling, R., 2014. *Octopus.* [Online] Available at: http://www.food4rhino.com/project/octopus?etx [Accessed 8 March 2015].

Vogel, S., 2009. Leaves in the lowest and highest winds: temperature, force and shape. *New Phytologist, Transley Review,* Volume 183, pp. 13-26.

Weissenböck, N., 2010. *PhD Dissertation: Thermoregulation of African (Loxodonta africana) and Asian (Elephas maximus) Elephants,* Vienna: University of Vienna.

Wide Screen Wallpapers, 2016. *Succulent Plant Wallpaper.* [Online] Available at: http://wide-wallpapers.net/succulent-plant-wide-wallpaper/ [Accessed May 2016].

Wigginton, M. & Harris , J., 2002. *Intelligent Skins.* Oxford: Butterworth-Heinemann.

Wikipedia, 2016. *Glossary of leaf morphology.* [Online]
Available at: https://en.wikipedia.org/wiki/Glossary_of_leaf_morphology#lanceolate
[Accessed September 2016].

WilkinsonEyre, 2014. *Royal Botanic Gardens, Kew: Davies Alpine House.* [Online]
Available at: http://www.wilkinsoneyre.com/projects/royal-botanic-gardens-kew-davies-alpine-house.aspx?category=cultural

Wilson, H. D., 2016. *Taxonomy of Flowering Plants -Lecture Notes- Vegetative Morphology II, The Leaf.* [Online]
Available at: http://botany.csdl.tamu.edu/FLORA/Wilson/tfp/veg/tfplec3s01.htm
[Accessed September 2016].

Yiatros, S., Wadee, M. A. & Hunt, G. R., 2007. The load-bearing duct: biomimicry in structural design. *Proceedings of the Institution of Civil Engineers Engineering Sustainability,* Volume 160, p. 179–188.

You, W., Qin, M. & Ding, W., 2013. Improving building facade design using integrated simulation of daylighting, thermal performance and natural ventilation. *Building Simulation,* Volume 6, p. 269–282.

Yowell, J., 2011. *Master of Architecture Thesis: Biomimetic Building Skin, A Phenomenological Approach Using Tree Bark as Model,* Oklahoma: University of Oklahoma.

Zähr, M. et al., 2010. Bionic Photovoltaic Panels Bio-Inspired by Green Leaves. *Journal of Bionic Engineering,* Volume 7, p. 284–293.

Zang, H., Zhang, S. & Hapeshi, K., 2010. A Review of Nature-Inspired Algorithms. *Journal of Bionic Engineering,* Volume 7 Suppl., p. S232–S237.

Zari, M. P., 2007. *Biomimetic Approaches to Architectural Design for Increased Sustainability.* Auckland, Sustainable Building Conference.

Zari, M. P. & Storey, J., 2007. *An ecosystem based biomimetic theory for a regenrative built environment.* Lisbon, Lisbon Sustainable Building Conference 07.

Zhang, R., Lam, K., Yao, S.-C. & Zhang, Y., 2013. Coupled Energyplus and computational fluid dynamics natural ventilation simulation. *Building and Environment,* Volume 68, pp. 100-113.

Research Activities

Publications

El Ahmar, S. & Fioravanti, A., 2015. Simulating the thermal and daylight performances of a folded porous double façade for an office building in Cairo. Melbourne, 49th International Conference of the Architectural Science Association (ASA).

El Ahmar, S. & Fioravanti, A., 2015. Biomimetic-Computational Design for Double Facades in Hot Climates - A Porous Folded Façade for Office Buildings. Vienna, Proceedings of the 33rd Conference of The Association for Education and Research in Computer Aided Architectural Design in Europe (eCAADe), pp. 687-696.

El Ahmar, S. & Fioravanti, A., 2014. Botanics and Parametric Design Fusions for Performative Building Skins, An Application in Hot Climates. Newcatsle Upon Tyne, Proceedings of the 32nd conference of the Association for Education and research in Computer Aided Architectural Design in Europe (eCAADe), pp. 595-604.

El Ahmar, S. & Fioravanti, A., 2014. How Plants Regulate Heat: Biomimetic Inspirations for Building Skins. Genoa, 48th International Conference of the Architectural Science Association (ASA), p. 343–354.

El Ahmar, S., Fioravanti, A. & Hanafi, M., 2013. A Methodology for Computational Architectural Design Based on Biological Principles. Delft, Proceedings of the 31st conference of The Association for Education and Research in Computer Aided Architectural Design in Europe (eCAADe), pp. 539-548.

International competitions

- VisionArtech international competition: “Biomorphic design in the project of a regenerative global society” 1st edition 2015-2016.
  Honourable mention
  http://visionartech.eu/

- DIVA Day international student competition, Seattle, Washington, 2014.
  First prize winner
  http://diva4rhino.com/photo/diva-day-competition-winner-salma-el-ahmar?context=latest

Workshops

- **Robotic Woodcraft, 16 hours, Vienna, 2015**

Tutors and affiliation:
-Johannes Braumann, Association for Robots in Architecture and University for Arts and Design Linz.
-Sigrid Brell-Cokcan, Association for Robots in Architecture and RWTH University.

- **Translate-Structural Design in Material Fabrication, 40 hours, Rome, 2014.**

Tutor and affiliation:
-Manja van de Worp, NOUS Engineering, Institute for Advanced Architecture of Catalonia.

- **Daylight Simulations using DIVA, 16 hours, Cairo, 2014.**

Tutors and affiliation:
-Shady Attia, LEED AP, PhD Catholic University of Louvain.
-Mohamed Amer Hegazy, MSc Stuttgart University.

- **Parametric Passive Design 32 hours, Cairo, 2014.**

Tutors and affiliation:
-Ayman Wagdy, MSc Politecnico di Milano, Researcher at the American University of Cairo.
-Mohamed Amer Hegazy, MSc Stuttgart University.

Appendices

Appendix A: Thermal and daylight model settings

Thermal model settings

The following settings are those used for the thermal models of the reference case, flat DSF and proposed DSF that were explained in Chapter Six. These are the settings available in ArchSim Plugin for Grasshopper that runs on EnergyPlus (v.8.2). Any other EnergyPlus settings not mentioned here are left as default values.

Table 0.1: General simulation settings.

	Zones of reference case	Zones of Flat DSF	Proposed DSF zone
General simulation settings			
Run period	1st of June till 31st of August	1st of June till 31st of August	1st of June till 31st of August
Monthly ground temperature (˚C)	20 ˚C for all months	20 ˚C for all months	20 ˚C for all months
Airflow simulation	Airflow Network	Airflow Network	Airflow Network
Solar distribution	Full interior & exterior with reflections	Full interior & exterior with reflections	Full Exterior
Shadow calculation frequency	20	20	20
Shadow calculation overlap	15000	15000	15000
Heat balance settings			
Time steps per hour	20	20	20
Algorithm	Conduction Transfer Function	Conduction Transfer Function	Conduction Transfer Function
Space discretization	3	3	3

Table 0.2: Thermal zone settings. Specifications of construction materials and availability schedules are placed in separate tables.

	Zones of reference case	Zones of Flat DSF	Proposed DSF zone
Loads			
People (p/m^2)	0.2	Off	Off
Occupancy schedule	Egy_OpenOfficeOcc	Off	Off
Equipment (W/m^2)	12	Off	Off
Equipment schedule	Egy_OpenOfficeOcc	Off	Off
Power density (W/m^2)	12	Off	Off
Target illumination (Lux)	300	Off	Off
Dimming	Continuous	Off	Off
Availability schedule	Egy_OpenOfficeOcc	Off	Off
Domestic hot water	Off	Off	Off
Conditioning			
Heating	Off	Off	Off
Cooling	On	Off	Off
Set point (˚C)	25	Off	Off
Availability schedule	Egy_OpenOfficeOcc	Off	Off
Limit (Watt/ floor area)	No limit	Off	Off
Mechanical ventilation	Off	Off	Off
Ventilation (SV)	Off	Off	Off
Materials			
Roof construction	Egy_roof	DSF_AlumClad	DSF_AlumClad4
Partition construction	Egy_wall1	Egy_wall1	Egy_wall1
Slab/ceiling construction	Egy_roof	DSF_walkway	DSF_AlumClad4
Ground/exterior floor construction	BASE_ground_base	DSF_AlumClad	DSF_AlumClad4
Façade construction	Egy_wall1	DSF_AlumClad	DSF_AlumClad4
Internal mass	Default construction	Default construction	Default construction
Partition assembly order	1	1	1
Inside convention algorithm	TARP	TARP	TARP
Outside convection algorithm	DOE-2	DOE-2	DOE-2

Table 0.3: Window settings.

	Window type	Glazing construction	Shading	Zone mixing	Operable area	Discharge coefficient	Temp. set point (˚C)	Ventilation Availability schedule
Zones of reference case	External glazing	Egy_Dbl_tinted	Off	Off	0.01	0.5	20	BASE_AllOff
	Internal doors	defaultGlazing	Off	Off	0.01	0.5	20	BASE_AllOff
Zones of Flat DSF	External glazing	Egy_Dbl_tinted	Off	Off	0.01	0.5	20	BASE_AllOff
	External air openings & walk-ways	AirWall	Off	Off	0.99	0.65	20	AllOn
	Internal glazing	Egy_BASE_Dbl_Clear_6_6_6_Air_LoE	Off	Off	0.01	0.5	20	BASE_AllOff
Proposed DSF zone	External glazing	BASE_Dbl_Clear_6_6_6_Air_LoE	Off	Off	0.01	0.5	20	BASE_AllOff
	External air openings	AirWall	Off	Off	0.99	0.65	20	AllOn
	Internal glazing	BASE_Dbl_Clear_6_6_6_Air_LoE	Off	Off	0.01	0.5	20	BASE_AllOff

Table 0.4: Building material properties.

Construction name	Construction type	Material layers (outside to inside)	Thickness (m)	Conductivity (W/mK)	Density (kg/m^3)	Specific heat (J/kgK)	Thermal emittance (0-1)	Solar absorptance (0-1)	Visible absorptance (0-1)
BASE_Ground_base	Ground floor	Carpet	0.015	0.0452	110	840	0.9	0.7	0.7
		Concrete	0.2	2.15	2400	900	0.9	0.6	0.6
		Insulation	0.03	0.029	29	1210	0.9	0.5	0.5
defaultConstruction	Façade	Concrete-default	0.25	2.3	2400	900	0.9	0.6	0.6
DSF_AlumClad	Metal Cladding	Aluminium sheet	0.001	0.35	1460	904	0.9	0.7	0.7
		polyethylene	0.005	0.35	1840	2400	0.9	0.7	0.7
		Aluminium sheet	0.001	0.35	1460	904	0.9	0.7	0.7
DSF_AlumClad4	Façade Cladding	Aluminium sheet	0.002	0.35	1460	904	0.9	0.7	0.7
		polyethylene	0.01	0.35	1840	2400	0.9	0.7	0.7
		Aluminium sheet	0.002	0.35	1460	904	0.9	0.7	0.7
DSF_walkway	Perforated walkway	Aluminium	0.005	0.35	1460	904	0.9	0.7	0.7
Egy_Roof	Roof	Cement Plaster	0.1	0.72	1860	840	0.9	0.6	0.6
		Concrete	0.3	2.15	2400	900	0.9	0.6	0.6
		Gypsum board	0.02	0.58	800	1090	0.9	0.4	0.4
Egy_wall1	Façade	Cement Plaster	0.025	0.72	1860	840	0.9	0.6	0.6
		Masonry	0.35	0.675	1600	790	0.9	0.6	0.6
		Cement Plaster	0.025	0.72	1860	840	0.9	0.6	0.6

Table 0.5: Glazing material properties.

	Material layer name	Thickness (m)	Conductivity (W/mK)	Density (kg/m^3)	Solar transmittance (0-1)	Solar reflectance front (0-1)	Solar reflectance back (0-1)	Visible transmittance (0-1)	Visible reflectance front (0-1)	Visible reflectance back (0-1)	IR transmittance (0-1)	IR emissivity front (0-1)	IR emissivity back (0-1)
Airwall	Air	-	5	0.0001	0.99	0.005	0.005	0.99	0.005	0.005	0.99	0.005	0.005
BASE_Dbl_Clear_6_6_Air_LowE	Clear Low E glass	0.006	0.9	160	0.6	0.17	0.22	0.84	0.055	0.078	0.01	0.84	0.84
	Air	0.006	5	0.0001	0.99	0.005	0.005	0.99	0.005	0.005	0.99	0.005	0.005
	Clear glass	0.006	0.9	160	0.775	0.071	0.071	0.881	0.08	0.08	0.01	0.84	0.84
Default Glazing	default glass	0.006	0.9	2500	0.68	0.09	0.1	0.81	0.11	0.12	0	0.84	0.2
Egy_BASE_Dbl_Clear_6_6_6_Air_LowE	Clear Low E glass	0.006	0.9	160	0.6	0.17	0.22	0.84	0.055	0.078	0.01	0.84	0.84
	Air	0.02	5	0.0001	0.99	0.005	0.005	0.99	0.005	0.005	0.99	0.005	0.005
	Clear glass	0.006	0.9	160	0.775	0.071	0.071	0.881	0.08	0.08	0.01	0.84	0.84
Egy_Dbl_tinted	Tinted glass	0.006	0.672	160	0.43	0.17	0.22	0.37	0.055	0.078	0.02	0.84	0.84
	Air	0.012	5	0.0001	0.99	0.005	0.005	0.99	0.005	0.005	0.99	0.005	0.005
	Clear glass	0.006	0.9	160	0.775	0.071	0.071	0.881	0.08	0.08	0.01	0.84	0.84

Availability schedules:

a) BASE_AllOff: always off.

b) AllOn: always on.

c) Egy_OpenOfficeOcc: based on the working hours in the B-19 office building. The information was obtained from the building owner. It is explained as follows:
   - Working days: from Sunday till Thursday.
   - Working hours: from 9:00 until 17:00. Air conditioning starts before employees arrive and is switched off after they leave. The figure below shows the daily occupancy over a 24 hour period. 0 means no occupancy, 1 means fully occupied.
   - Weekend days: Friday and Saturday, air conditioning is always off.

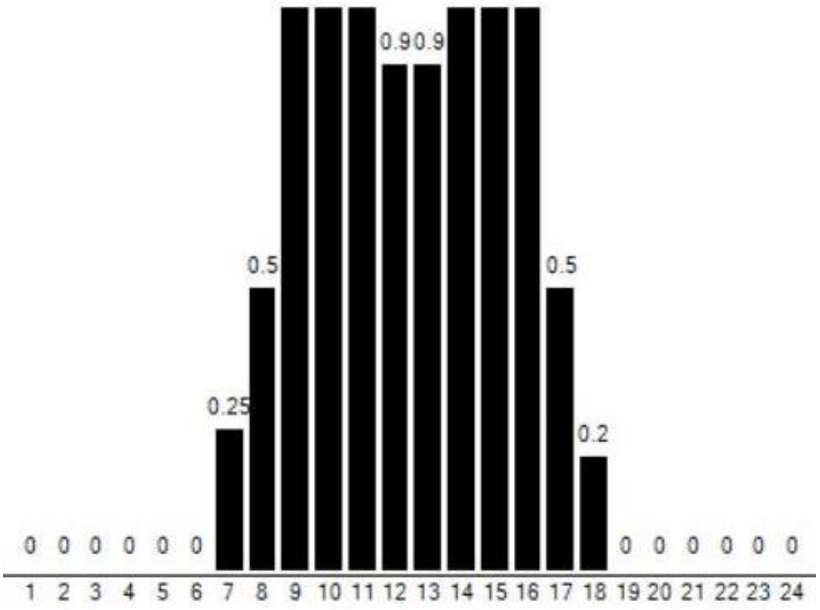

Figure 0.1: Daily availability schedule for working days in the B-19 office building. 0 means no occupancy, 1 means fully occupied.

Daylight model settings

The following settings are those used for the daylight models of the reference case, flat DSF and proposed DSF that were presented in Chapter Six. They were prepared using DIVA plug-in for Grasshopper that runs using Radiance.

Opaque Materials

The following materials were the same for the reference case, flat DSF and proposed DSF.

Table 0.6: Opaque geometrical components of the daylight models and their material settings in Radiance.

Geometry	Material name	Radiance settings
Room interior walls	GenericInteriorWall_50	# material type: opaque # comment: This is a purely diffuse reflector with a standard wall reflectivity of 60%. void plastic GenericInteriorWall_50 0 0 5 0.5 0.5 0.5 0 0
Room exterior walls	HighReflectanceCeiling_90	# material type: opaque # comment: This is a purely diffuse reflector with a standard ceiling reflectivity of 90%. void plastic HighReflectanceCeiling_90 0 0 5 0.9 0.9 0.9 0 0
Room ceiling	GenericCeiling_80	# material type: opaque # comment: This is a purely diffuse reflector with a standard ceiling reflectance of 80%. void plastic GenericCeiling_80 0 0 5 0.8 0.8 0.8 0 0
Room floor	Egy_CarpetFloor_15	#Bluish grey carpet floor similar to B19 office building flooring #reflectance= 15% void plastic Egy_CarpetFloor_15 0 0 5 0.15 0.15 0.15 0 0
Window framing and opaque geometry of flat and proposed DSFs	matte_silver	# material type: reflective # comment: default material for standard external venetian blind slats and curtain wall frames # author: Christoph Reinhart void plastic matte_silver 0 0 5 0.52 0.52 0.52 0.15 0.05

Glazing Materials

Table 0.7: Glazing geometrical components of the daylight models and their material settings in Radiance.

	Material name	RADIANCE settings
Glazing of reference case	Egy_DoublePane_tinted_37	#Double glazed curtain wall in B19 office building: U-value= 2.8 W/m2k # visual transmittance: 37% # visual transmissivity: 40.3% void glass Egy_DoublePane_tinted_37 0 0 3 0.403 0.403 0.403
Flat DSF interior glazing	Egy_SinglePane_clearLowE_84	# visual transmittance: 84% # visual transmissivity: 91.4% void glass Egy_SinglePane_clearLowE_84 0 0 3 0.914 0.914 0.914
Flat DSF exterior glazing	Egy_DoublePane_tinted_37	#Double glazed curtain wall in B19 office building: U-value= 2.8 W/m2k # visual transmittance: 37% # visual transmissivity: 40.3% void glass Egy_DoublePane_tinted_37 0 0 3 0.403 0.403 0.403
Proposed DSF interior and exterior glazing	Glazing_DoublePane_Clear_80	# Glazing_DoublePane_Clear: Tau_vis = 0.80; SHGC= 0.72 ; U-Value= 2.71W/m2K # visual transmittance: 80% # visual transmissivity: 87% void glass Glazing_DoublePane_Clear_80 0 0 3 0.87 0.87 0.87

DIVA simulation settings

The following settings were the same for the reference case, flat DSF and proposed DSF models.

Table 0.8: General simulation settings in DIVA for all daylight models.

Parameter	Setting
Simulation type	climate based
Occupancy schedule	weekdays 9 to 5 with DST 60min
Minimum illuminance	300 lux
Lighting control	photosensor controlled dimming
Lighting parameters	-W 250.0 -Set 300 -Loss 20 -Standby 0.0
RADIANCE parameters	-ab 7 -ad 1000 -as 20 -ar 300 -aa 0.1

Appendix B: CFD model settings

```
/*--------------------------------*- C++ -*----------------------------------*\
| =========                 |                                                 |
| \\      /  F ield         | OpenFOAM: The Open Source CFD Toolbox           |
|  \\    /   O peration     | Version:  2.3.0                                 |
|   \\  /    A nd           | Web:      www.OpenFOAM.org                      |
|    \\/     M anipulation  |                                                 |
\*---------------------------------------------------------------------------*/
FoamFile
{
    version     2.0;
    format      ascii;
    class       volScalarField;
    object      T;
}
// * * * * * * * * * * * * * * * * * * * * * * * * * * * * * * * * * * * * * //

dimensions      [0 0 0 1 0 0 0];

internalField   uniform 308.82; // 35.67 degC

boundaryField
{
    topOpenings //inlets
    {
        type            fixedValue;
        value           $internalField;
    }

     perforations //outlets
    {
        type            inletOutlet;
        value           $internalField;
        inletValue      $internalField;
    }

    air_to_top
    {
        type            fixedValue;
        value           uniform 322.11; // 48.96 degC
    }

    air_to_bottom
    {
        type            fixedValue;
        value           uniform 313.68; // 40.53 degC
    }

    air_to_left
    {
        type            fixedValue;
        value           uniform 313.32; // 40.17 degC
    }

    air_to_right
    {
        type            fixedValue;
        value           uniform 312.40; // 39.25 degC
    }

    air_to_back1
    {
        type            fixedValue;
        value           uniform 312.8; // 39.65 degC
    }

    air_to_back2
    {
        type            fixedValue;
        value           uniform 312.8; // 39.65  degC
    }

    air_to_officeWindows
    {
        type            fixedValue;
        value           uniform 310.35; // 37.2 degC
    }

    air_to_frontSolid
    {
        type            fixedValue;
        value           uniform 313.23; // 40.08 degC
    }

    air_to_frontGlazing
    {
        type            fixedValue;
        value           uniform 312.39; // 39.24 degC
    }
}


// ************************************************************************* //

```

```
/*--------------------------------*- C++ -*----------------------------------*\
| =========                 |                                                 |
| \\      /  F ield         | OpenFOAM: The Open Source CFD Toolbox           |
|  \\    /   O peration     | Version:  2.3.0                                 |
|   \\  /    A nd           | Web:      www.OpenFOAM.org                      |
|    \\/     M anipulation  |                                                 |
\*---------------------------------------------------------------------------*/
FoamFile
{
    version     2.0;
    format      ascii;
    class       volVectorField;
    object      U;
}
// * * * * * * * * * * * * * * * * * * * * * * * * * * * * * * * * * * * * //

dimensions      [0 1 -1 0 0 0 0];

internalField   uniform (0 0 0);

boundaryField
{
    topOpenings //inlets
    {
        type            fixedValue;
        value           uniform (0.51 0 0);
    }

   perforations //outlets
    {
        type            zeroGradient;
//        type            inletOutlet;
//        value           uniform (0 0 0);
//        inletValue      uniform (0 0 0);
    }

    air_to_top
    {
        type            fixedValue;
        value           uniform (0 0 0);
    }
    air_to_bottom
    {
        type            fixedValue;
        value           uniform (0 0 0);
    }
    air_to_left
    {
        type            fixedValue;
        value           uniform (0 0 0);
    }
    air_to_right
    {
        type            fixedValue;
        value           uniform (0 0 0);
    }

    air_to_back1
    {
        type            fixedValue;
        value           uniform (0 0 0);
    }

    air_to_back2
    {
        type            fixedValue;
        value           uniform (0 0 0);
    }

    air_to_officeWindows
    {
        type            fixedValue;
        value           uniform (0 0 0);
    }

    air_to_frontSolid
    {
        type            fixedValue;
        value           uniform (0 0 0);
    }

    air_to_frontGlazing
    {
        type            fixedValue;
        value           uniform (0 0 0);
    }
}


// ************************************************************************* //

```

```
/*--------------------------------*- C++ -*----------------------------------*\
| =========                 |                                                 |
| \\      /  F ield         | OpenFOAM: The Open Source CFD Toolbox           |
|  \\    /   O peration     | Version:  2.3.0                                 |
|   \\  /    A nd           | Web:      www.OpenFOAM.org                      |
|    \\/     M anipulation  |                                                 |
\*---------------------------------------------------------------------------*/
FoamFile
{
    version     2.0;
    format      ascii;
    class       volScalarField;
    object      p;
}
// * * * * * * * * * * * * * * * * * * * * * * * * * * * * * * * * * * * * * //

dimensions      [1 -1 -2 0 0 0 0];

internalField   uniform 1.0e5;

boundaryField
{
    topOpenings //inlets
    {
        type            zeroGradient;
    }

    perforations //outlets
    {
        type            fixedValue;
        value           $internalField;
        //value           1.0e5;
    }

    air_to_top
    {
        type            zeroGradient;
    }

    air_to_bottom
    {
        type            zeroGradient;
    }

    air_to_left
    {
        type            zeroGradient;
    }

    air_to_right
    {
        type            zeroGradient;
    }

    air_to_back1
    {
        type            zeroGradient;
    }

    air_to_back2
    {
        type            zeroGradient;
    }

    air_to_officeWindows
    {
        type            zeroGradient;
    }

    air_to_frontSolid
    {
        type            zeroGradient;
    }

    air_to_frontGlazing
    {
        type            zeroGradient;
    }
}

// ************************************************************************* //
```

```
/*--------------------------------*- C++ -*----------------------------------*\
| =========                 |                                                 |
| \\      /  F ield         | OpenFOAM: The Open Source CFD Toolbox           |
|  \\    /   O peration     | Version:  2.3.0                                 |
|   \\  /    A nd           | Web:      www.OpenFOAM.org                      |
|    \\/     M anipulation  |                                                 |
\*---------------------------------------------------------------------------*/
FoamFile
{
    version     2.0;
    format      ascii;
    class       volScalarField;
    object      k;
}
// * * * * * * * * * * * * * * * * * * * * * * * * * * * * * * * * * * * * * //

dimensions      [0 2 -2 0 0 0 0];

internalField   uniform 1;

boundaryField
{
    topOpenings //inlets
    {
        type            turbulentIntensityKineticEnergyInlet;
        intensity       0.05;
        value           uniform 1;
    }

    perforations //outlets
    {
        type            inletOutlet;
        inletValue      $internalField;
        value           $internalField;
    }

    air_to_top
    {
        type            compressible::kqRWallFunction;
        value           uniform 1;
    }

    air_to_bottom
    {
        type            compressible::kqRWallFunction;
        value           uniform 1;
    }

    air_to_left
    {
        type            compressible::kqRWallFunction;
        value           uniform 1;
    }

    air_to_right
    {
        type            compressible::kqRWallFunction;
        value           uniform 1;
    }

    air_to_back1
    {
        type            compressible::kqRWallFunction;
        value           uniform 1;
    }

    air_to_back2
    {
        type            compressible::kqRWallFunction;
        value           uniform 1;
    }

    air_to_officeWindows
    {
        type            compressible::kqRWallFunction;
        value           uniform 1;
    }

    air_to_frontSolid
    {
        type            compressible::kqRWallFunction;
        value           uniform 1;
    }

    air_to_frontGlazing
    {
        type            compressible::kqRWallFunction;
        value           uniform 1;
    }
}


// ************************************************************************* //

```

```
/*--------------------------------*- C++ -*----------------------------------*\
| =========                 |                                                 |
| \\      /  F ield         | OpenFOAM: The Open Source CFD Toolbox           |
|  \\    /   O peration     | Version:  2.3.0                                 |
|   \\  /    A nd           | Web:      www.OpenFOAM.org                      |
|    \\/     M anipulation  |                                                 |
\*---------------------------------------------------------------------------*/
FoamFile
{
    version     2.0;
    format      ascii;
    class       volScalarField;
    location    "0";
    object      epsilon;
}
// * * * * * * * * * * * * * * * * * * * * * * * * * * * * * * * * * * * * * //

dimensions      [ 0 2 -3 0 0 0 0 ];

internalField   uniform 200;

boundaryField
{
    topOpenings //inlets
    {
        type            compressible::turbulentMixingLengthDissipationRateInlet;
        mixingLength    0.005;
        value           uniform 200;
    }

    perforations //outlets
    {
        type            inletOutlet;
        inletValue      uniform 200;
        value           uniform 200;
    }

    air_to_top
    {
        type            compressible::epsilonWallFunction;
        value           uniform 200;
    }

    air_to_bottom
    {
        type            compressible::epsilonWallFunction;
        value           uniform 200;
    }

    air_to_left
    {
        type            compressible::epsilonWallFunction;
        value           uniform 200;
    }

    air_to_right
    {
        type            compressible::epsilonWallFunction;
        value           uniform 200;
    }

    air_to_back1
    {
        type            compressible::epsilonWallFunction;
        value           uniform 200;
    }

    air_to_back2
    {
        type            compressible::epsilonWallFunction;
        value           uniform 200;
    }

    air_to_officeWindows
    {
        type            compressible::epsilonWallFunction;
        value           uniform 200;
    }

    air_to_frontSolid
    {
        type            compressible::epsilonWallFunction;
        value           uniform 200;
    }

    air_to_frontGlazing
    {
        type            compressible::epsilonWallFunction;
        value           uniform 200;
    }
}


// ************************************************************************* //

```

```
/*--------------------------------*- C++ -*----------------------------------*\
| =========                 |                                                 |
| \\      /  F ield         | OpenFOAM: The Open Source CFD Toolbox           |
|  \\    /   O peration     | Version:  2.3.0                                 |
|   \\  /    A nd           | Web:      www.OpenFOAM.org                      |
|    \\/     M anipulation  |                                                 |
\*---------------------------------------------------------------------------*/
FoamFile
{
    version     2.0;
    format      ascii;
    class       volScalarField;
    location    "0";
    object      alphat;
}
// * * * * * * * * * * * * * * * * * * * * * * * * * * * * * * * * * * * * * //

dimensions      [1 -1 -1 0 0 0 0];

internalField   uniform 0;

boundaryField
{
    topOpenings //inlets
    {
        type            calculated;
        value           uniform 0;
    }
    perforations //outlets
    {
        type            calculated;
        value           uniform 0;
    }
    air_to_top
    {
        type            compressible::alphatWallFunction;
        value           uniform 0;
    }
    air_to_bottom
    {
        type            compressible::alphatWallFunction;
        value           uniform 0;
    }
    air_to_left
    {
        type            compressible::alphatWallFunction;
        value           uniform 0;
    }
    air_to_right
    {
        type            compressible::alphatWallFunction;
        value           uniform 0;
    }
    air_to_back1
    {
        type            compressible::alphatWallFunction;
        value           uniform 0;
    }
    air_to_back2
    {
        type            compressible::alphatWallFunction;
        value           uniform 0;
    }
    air_to_officeWindows
    {
        type            compressible::alphatWallFunction;
        value           uniform 0;
    }
    air_to_frontSolid
    {
        type            compressible::alphatWallFunction;
        value           uniform 0;
    }
    air_to_frontGlazing
    {
        type            compressible::alphatWallFunction;
        value           uniform 0;
    }
}


// ************************************************************************* //

```

```
/*--------------------------------*- C++ -*----------------------------------*\
| =========                 |                                                 |
| \\      /  F ield         | OpenFOAM: The Open Source CFD Toolbox           |
|  \\    /   O peration     | Version:  2.3.0                                 |
|   \\  /    A nd           | Web:      www.OpenFOAM.org                      |
|    \\/     M anipulation  |                                                 |
\*---------------------------------------------------------------------------*/
FoamFile
{
    version     2.0;
    format      binary;
    class       volScalarField;
    location    "3";
    object      mut;
}
// * * * * * * * * * * * * * * * * * * * * * * * * * * * * * * * * * * * * * //

dimensions      [1 -1 -1 0 0 0 0];

internalField   uniform 0;

boundaryField
{
    topOpenings //inlets
    {
        type            calculated;
        value           uniform 0;
    }
    perforations //outlets
    {
        type            calculated;
        value           uniform 0;
    }

    air_to_top
    {
        type            mutkWallFunction;
        value           uniform 0;
    }
    air_to_bottom
    {
        type            mutkWallFunction;
        value           uniform 0;
    }
    air_to_left
    {
        type            mutkWallFunction;
        value           uniform 0;
    }
    air_to_right
    {
        type            mutkWallFunction;
        value           uniform 0;
    }
    air_to_back1
    {
        type            mutkWallFunction;
        value           uniform 0;
    }
    air_to_back2
    {
        type            mutkWallFunction;
        value           uniform 0;
    }
    air_to_officeWindows
    {
        type            mutkWallFunction;
        value           uniform 0;
    }
    air_to_frontSolid
    {
        type            mutkWallFunction;
        value           uniform 0;
    }
    air_to_frontGlazing
    {
        type            mutkWallFunction;
        value           uniform 0;
    }
}


// ************************************************************************* //

```

```
/*--------------------------------*- C++ -*----------------------------------*\
| =========                 |                                                 |
| \\      /  F ield         | OpenFOAM: The Open Source CFD Toolbox           |
|  \\    /   O peration     | Version:  2.3.0                                 |
|   \\  /    A nd           | Web:      www.OpenFOAM.org                      |
|    \\/     M anipulation  |                                                 |
\*---------------------------------------------------------------------------*/
FoamFile
{
    version     2.0;
    format      ascii;
    class       dictionary;
    object      blockMeshDict;
}

// * * * * * * * * * * * * * * * * * * * * * * * * * * * * * * * * * * * * * //

convertToMeters 1;

vertices
(
    (0 0 4)
    (3 0 4)
    (3 10 4)
    (0 10 4)
    (0 0 19)
    (3 0 19)
    (3 10 19)
    (0 10 19)
);

blocks
(
    hex (0 1 2 3 4 5 6 7) (120 400 600) simpleGrading (0.5 1 1)
);

edges
(
);

boundary
(
    frontAndBack
    {
        type patch;
        faces
        (
            (3 7 6 2)
            (1 5 4 0)
        );
    }
    left_ext
    {
        type patch;
        faces
        (
            (0 4 7 3)
        );
    }
    right_ext
    {
        type patch;
        faces
        (
            (2 6 5 1)
        );
    }
    lowerWall
    {
        type wall;
        faces
        (
            (0 3 2 1)
        );
    }
    upperWall
    {
        type patch;
        faces
        (
            (4 5 6 7)
        );
    }
);

// ************************************************************************* //

```

```
/*--------------------------------*- C++ -*----------------------------------*\
| =========                 |                                                 |
| \\      /  F ield         | OpenFOAM: The Open Source CFD Toolbox           |
|  \\    /   O peration     | Version:  2.3.0                                 |
|   \\  /    A nd           | Web:      www.OpenFOAM.org                      |
|    \\/     M anipulation  |                                                 |
\*---------------------------------------------------------------------------*/
FoamFile
{
    version     2.0;
    format      ascii;
    class       dictionary;
    object      snappyHexMeshDict;
}
// * * * * * * * * * * * * * * * * * * * * * * * * * * * * * * * * * * * * * //

// Which of the steps to run
castellatedMesh true;
snap            true;
addLayers       true;


// Geometry. Definition of all surfaces. All surfaces are of class
// searchableSurface.
// Surfaces are used
// - to specify refinement for any mesh cell intersecting it
// - to specify refinement for any mesh cell inside/outside/near
// - to 'snap' the mesh boundary to the surface
geometry
{
    air.stl
    {
        type triSurfaceMesh;
        regions
        {
             air_to_top     {name air_to_top;}
             air_to_bottom    {name air_to_bottom;}
             air_to_left      {name air_to_left;}
             air_to_right    {name air_to_right;}
             air_to_back1       {name air_to_back1;}
             air_to_back2  {name air_to_back2;}
             air_to_officeWindows  {name air_to_officeWindows;}
             air_to_frontSolid  {name air_to_frontSolid;}
             air_to_frontGlazing  {name air_to_frontGlazing;}
             topOpenings  {name topOpenings;}
             perforations  {name perforations;}

        }
    }

};



// Settings for the castellatedMesh generation.
castellatedMeshControls
{

    // Refinement parameters
    // ~~~~~~~~~~~~~~~~~~~~

    // If local number of cells is >= maxLocalCells on any processor
    // switches from from refinement followed by balancing
    // (current method) to (weighted) balancing before refinement.
    maxLocalCells 100000;

    // Overall cell limit (approximately). Refinement will stop immediately
    // upon reaching this number so a refinement level might not complete.
    // Note that this is the number of cells before removing the part which
    // is not 'visible' from the keepPoint. The final number of cells might
    // actually be a lot less.
    maxGlobalCells 2000000;

    // The surface refinement loop might spend lots of iterations refining just a
    // few cells. This setting will cause refinement to stop if <= minimumRefine
    // are selected for refinement. Note: it will at least do one iteration
    // (unless the number of cells to refine is 0)
    minRefinementCells 10;

    // Allow a certain level of imbalance during refining
    // (since balancing is quite expensive)
    // Expressed as fraction of perfect balance (= overall number of cells /
    // nProcs). 0=balance always.
    maxLoadUnbalance 0.10;


    // Number of buffer layers between different levels.
    // 1 means normal 2:1 refinement restriction, larger means slower
    // refinement.
    nCellsBetweenLevels 3;



    // Explicit feature edge refinement
    // ~~~~~~~~~~~~~~~~~~~~~~~~~~~~~~~~

    // Specifies a level for any cell intersected by its edges.
    // This is a featureEdgeMesh, read from constant/triSurface for now.
    features
    (
        {
            file "air.eMesh";
            level 7;
        }
    );



    // Surface based refinement
    // ~~~~~~~~~~~~~~~~~~~~~~~~

    // Specifies two levels for every surface. The first is the minimum level,
    // every cell intersecting a surface gets refined up to the minimum level.
    // The second level is the maximum level. Cells that 'see' multiple
    // intersections where the intersections make an
    // angle > resolveFeatureAngle get refined up to the maximum level.

    refinementSurfaces
    {
        air.stl
        {  //general refinement
           // Surface-wise min and max refinement level
           level (5 6);

```

```
            regions
            {

             topOpenings        {level (6 7);}
             perforations       {level (10 11);}
            }
        }
    }

    // Resolve sharp angles
    resolveFeatureAngle 10;


    // Region-wise refinement
    // ~~~~~~~~~~~~~~~~~~~~~~

    // Specifies refinement level for cells in relation to a surface. One of
    // three modes
    // - distance. 'levels' specifies per distance to the surface the
    //   wanted refinement level. The distances need to be specified in
    //   descending order.
    // - inside. 'levels' is only one entry and only the level is used. All
    //   cells inside the surface get refined up to the level. The surface
    //   needs to be closed for this to be possible.
    // - outside. Same but cells outside.

    refinementRegions
    {

    }

    // Mesh selection
    // ~~~~~~~~~~~~~~

    // After refinement patches get added for all refinementSurfaces and
    // all cells intersecting the surfaces get put into these patches. The
    // section reachable from the locationInMesh is kept.
    // NOTE: This point should never be on a face, always inside a cell, even
    // after refinement.
    locationInMesh (1.5 5 7);


    // Whether any faceZones (as specified in the refinementSurfaces)
    // are only on the boundary of corresponding cellZones or also allow
    // free-standing zone faces. Not used if there are no faceZones.
    allowFreeStandingZoneFaces true;
}



// Settings for the snapping.
snapControls
{
    //- Number of patch smoothing iterations before finding correspondence
    //  to surface
    nSmoothPatch 8;

    //- Relative distance for points to be attracted by surface feature point
    //  or edge. True distance is this factor times local
    //  maximum edge length.
    tolerance 2.0;

    //- Number of mesh displacement relaxation iterations.
    nSolveIter 40;

    //- Maximum number of snapping relaxation iterations. Should stop
    //  before upon reaching a correct mesh.
    nRelaxIter 6;

    // Feature snapping

        //- Number of feature edge snapping iterations.
        //  Leave out altogether to disable.
        nFeatureSnapIter 10;

        //- Detect (geometric only) features by sampling the surface
        //  (default=false).
        implicitFeatureSnap false;

        //- Use castellatedMeshControls::features (default = true)
        explicitFeatureSnap true;

        //- Detect points on multiple surfaces (only for explicitFeatureSnap)
        multiRegionFeatureSnap false;
}



// Settings for the layer addition.
addLayersControls
{
    // Are the thickness parameters below relative to the undistorted
    // size of the refined cell outside layer (true) or absolute sizes (false).
    relativeSizes true;

    // Per final patch (so not geometry!) the layer information
    layers
    {
        air_to_top       {nSurfaceLayers 2;}
        air_to_bottom     {nSurfaceLayers 2;}
        air_to_left        {nSurfaceLayers 2;}
        air_to_right   {nSurfaceLayers 2;}
        air_to_back1   {nSurfaceLayers 3;}
        air_to_back2   {nSurfaceLayers 3;}
        air_to_officeWindows   {nSurfaceLayers 3;}
        air_to_frontSolid   {nSurfaceLayers 4;}
        air_to_frontGlazing   {nSurfaceLayers 4;}
    }

    // Expansion factor for layer mesh
    expansionRatio 1.0;

    // Wanted thickness of final added cell layer. If multiple layers
    // is the
    // thickness of the layer furthest away from the wall.
    // Relative to undistorted size of cell outside layer.
    // is the thickness of the layer furthest away from the wall.
    // See relativeSizes parameter.
    finalLayerThickness 0.3;

    // Minimum thickness of cell layer. If for any reason layer
    // cannot be above minThickness do not add layer.
    // Relative to undistorted size of cell outside layer.
    minThickness 0.1;
```

```
249
250     // If points get not extruded do nGrow layers of connected faces that are
251     // also not grown. This helps convergence of the layer addition process
252     // close to features.
253     // Note: changed(corrected) w.r.t 17x! (didn't do anything in 17x)
254     nGrow 0;
255
256     // Advanced settings
257
258     // When not to extrude surface. 0 is flat surface, 90 is when two faces
259     // are perpendicular
260     featureAngle 60;
261
262     // At non-patched sides allow mesh to slip if extrusion direction makes
263     // angle larger than slipFeatureAngle.
264     slipFeatureAngle 30;
265
266     // Maximum number of snapping relaxation iterations. Should stop
267     // before upon reaching a correct mesh.
268     nRelaxIter 3;
269
270     // Number of smoothing iterations of surface normals
271     nSmoothSurfaceNormals 1;
272
273     // Number of smoothing iterations of interior mesh movement direction
274     nSmoothNormals 3;
275
276     // Smooth layer thickness over surface patches
277     nSmoothThickness 10;
278
279     // Stop layer growth on highly warped cells
280     maxFaceThicknessRatio 0.5;
281
282     // Reduce layer growth where ratio thickness to medial
283     // distance is large
284     maxThicknessToMedialRatio 0.3;
285
286     // Angle used to pick up medial axis points
287     // Note: changed(corrected) w.r.t 17x! 90 degrees corresponds to 130 in 17x.
288     minMedianAxisAngle 90;
289
290
291     // Create buffer region for new layer terminations
292     nBufferCellsNoExtrude 0;
293
294
295     // Overall max number of layer addition iterations. The mesher will exit
296     // if it reaches this number of iterations; possibly with an illegal
297     // mesh.
298     nLayerIter 100;
299 }
300
301
302
303 // Generic mesh quality settings. At any undoable phase these determine
304 // where to undo.
305 meshQualityControls
306 {
307
308 //- Maximum non-orthogonality allowed. Set to 180 to disable.
309 maxNonOrtho 65;
310
311 //- Max skewness allowed. Set to <0 to disable.
312 maxBoundarySkewness 1;
313 maxInternalSkewness 1;
314
315 //- Max concaveness allowed. Is angle (in degrees) below which concavity
316 //  is allowed. 0 is straight face, <0 would be convex face.
317 //  Set to 180 to disable.
318 maxConcave 80;
319
320 //- Minimum pyramid volume. Is absolute volume of cell pyramid.
321 //  Set to a sensible fraction of the smallest cell volume expected.
322 //  Set to very negative number (e.g. -1E30) to disable.
323 minVol 1e-13;
324
325 //- Minimum quality of the tet formed by the face-centre
326 //  and variable base point minimum decomposition triangles and
327 //  the cell centre. This has to be a positive number for tracking
328 //  to work. Set to very negative number (e.g. -1E30) to
329 //  disable.
330 //     <0 = inside out tet,
331 //      0 = flat tet
332 //      1 = regular tet
333 minTetQuality 1e-15;
334
335 //- Minimum face area. Set to <0 to disable.
336 minArea -1;
337
338 //- Minimum face twist. Set to <-1 to disable. dot product of face normal
339 // and face centre triangles normal
340 minTwist 0.02;
341
342 //- Minimum normalised cell determinant. This is the determinant of all
343 //  the areas of internal faces. It is a measure of how much of the
344 //  outside area of the cell is to other cells. The idea is that if all
345 //  outside faces of the cell are 'floating' (zeroGradient) the
346 //  'fixedness' of the cell is determined by the area of the internal faces.
347 //  1 = hex, <= 0 = folded or flattened illegal cell
348 minDeterminant 0.001;
349
350 //- Relative position of face in relation to cell centres (0.5 for orthogonal
351 //  mesh) (0 -> 0.5)
352 minFaceWeight 0.05;
353
354 //- Volume ratio of neighbouring cells (0 -> 1)
355 minVolRatio 0.01;
356
357 //- Per triangle normal compared to average normal. Like face twist
358 //  but now per (face-centre decomposition) triangle. Must be >0 for Fluent
359 //  compatibility
360 minTriangleTwist -1;
361
362
363 //- if >0 : preserve cells with all points on the surface if the
364 //  resulting volume after snapping (by approximation) is larger than
365 //  minVolCollapseRatio times old volume (i.e. not collapsed to flat cell).
366 //  If <0 : delete always.
367 //minVolCollapseRatio 0.1;
368
369     // Advanced
370
371     //- Number of error distribution iterations
372     nSmoothScale 4;
```

```
    //- amount to scale back displacement at error points
    errorReduction 0.75;

}


// Advanced

// Write flags
writeFlags
(
    layerFields     // write volScalarField for layer coverage
);


// Merge tolerance. Is fraction of overall bounding box of initial mesh.
// Note: the write tolerance needs to be higher than this.
mergeTolerance 1e-6;


// ************************************************************************* //
```



```
/*--------------------------------*- C++ -*----------------------------------*\
| =========                 |                                                 |
| \\      /  F ield         | OpenFOAM: The Open Source CFD Toolbox           |
|  \\    /   O peration     | Version:  2.3.0                                 |
|   \\  /    A nd           | Web:      www.OpenFOAM.org                      |
|    \\/     M anipulation  |                                                 |
\*---------------------------------------------------------------------------*/
FoamFile
{
    version     2.0;
    format      ascii;
    class       dictionary;
    object      meshQualityDict;
}
// * * * * * * * * * * * * * * * * * * * * * * * * * * * * * * * * * * * * * //

// Include defaults parameters from master dictionary
#include "$WM_PROJECT_DIR/etc/caseDicts/meshQualityDict"

//- minFaceWeight (0 -> 0.5)
minFaceWeight 0.02;


// ************************************************************************* //

```

```
/*--------------------------------*- C++ -*----------------------------------*\
| =========                 |                                                 |
| \\      /  F ield         | OpenFOAM: The Open Source CFD Toolbox           |
|  \\    /   O peration     | Version:  2.3.0                                 |
|   \\  /    A nd           | Web:      www.OpenFOAM.org                      |
|    \\/     M anipulation  |                                                 |
\*---------------------------------------------------------------------------*/
FoamFile
{
    version     2.0;
    format      ascii;
    class       dictionary;
    location    "constant";
    object      radiationProperties;
}
// * * * * * * * * * * * * * * * * * * * * * * * * * * * * * * * * * * * * * //

radiation on;

radiationModel  P1;

// Number of flow iterations per radiation iteration
solverFreq 1;

absorptionEmissionModel constantAbsorptionEmission;

constantAbsorptionEmissionCoeffs
{
    absorptivity    absorptivity    [ 0 -1 0 0 0 0 0 ] 0.5;
    emissivity      emissivity      [ 0 -1 0 0 0 0 0 ] 0.5;
    E               E               [ 1 -1 -3 0 0 0 0 ] 0;
}

scatterModel    none;

sootModel       none;


// ************************************************************************* //

```



```
/*--------------------------------*- C++ -*----------------------------------*\
| =========                 |                                                 |
| \\      /  F ield         | OpenFOAM: The Open Source CFD Toolbox           |
|  \\    /   O peration     | Version:  2.3.0                                 |
|   \\  /    A nd           | Web:      www.OpenFOAM.org                      |
|    \\/     M anipulation  |                                                 |
\*---------------------------------------------------------------------------*/
FoamFile
{
    version     2.0;
    format      ascii;
    class       dictionary;
    location    "constant";
    object      RASProperties;
}
// * * * * * * * * * * * * * * * * * * * * * * * * * * * * * * * * * * * * * //

RASModel        kEpsilon;

turbulence      on;

printCoeffs     on;


// ************************************************************************* //

```

```
/*--------------------------------*- C++ -*----------------------------------*\
| =========                 |                                                 |
| \\      /  F ield         | OpenFOAM: The Open Source CFD Toolbox           |
|  \\    /   O peration     | Version:  2.3.0                                 |
|   \\  /    A nd           | Web:      www.OpenFOAM.org                      |
|    \\/     M anipulation  |                                                 |
\*---------------------------------------------------------------------------*/
FoamFile
{
    version     2.0;
    format      ascii;
    class       dictionary;
    object      surfaceFeatureExtractDict;
}
// * * * * * * * * * * * * * * * * * * * * * * * * * * * * * * * * * * * * * //

air.stl
{
    // How to obtain raw features (extractFromFile || extractFromSurface)
    extractionMethod    extractFromSurface;

    extractFromSurfaceCoeffs
    {
        // Mark edges whose adjacent surface normals are at an angle less
        // than includedAngle as features
        // - 0  : selects no edges
        // - 180: selects all edges
        includedAngle   150;
    }

    subsetFeatures
    {
        // Keep nonManifold edges (edges with >2 connected faces)
        nonManifoldEdges       no;

        // Keep open edges (edges with 1 connected face)
        openEdges       yes;
    }


    // Write options

        // Write features to obj format for postprocessing
        writeObj                yes;
}


// ************************************************************************* //

```



```
/*--------------------------------*- C++ -*----------------------------------*\
| =========                 |                                                 |
| \\      /  F ield         | OpenFOAM: The Open Source CFD Toolbox           |
|  \\    /   O peration     | Version:  2.3.0                                 |
|   \\  /    A nd           | Web:      www.OpenFOAM.org                      |
|    \\/     M anipulation  |                                                 |
\*---------------------------------------------------------------------------*/
FoamFile
{
    version     2.0;
    format      ascii;
    class       dictionary;
    location    "constant";
    object      thermophysicalProperties;
}
// * * * * * * * * * * * * * * * * * * * * * * * * * * * * * * * * * * * * * //

thermoType
{
    type            hePsiThermo;
    mixture         pureMixture;
    transport       sutherland;
    thermo          hConst;
    equationOfState perfectGas;
    specie          specie;
    energy          sensibleInternalEnergy;
}

mixture
{
    specie
    {
        nMoles      1;
        molWeight   28.9;
    }
    thermodynamics
    {
        Cp          1005;
        Hf          0;
    }
    transport
    {
        As          1.4792e-06;
        Ts          116;
    }
}


// ************************************************************************* //

```

```
/*--------------------------------*- C++ -*----------------------------------*\
| =========                 |                                                 |
| \\      /  F ield         | OpenFOAM: The Open Source CFD Toolbox           |
|  \\    /   O peration     | Version:  2.3.0                                 |
|   \\  /    A nd           | Web:      www.OpenFOAM.org                      |
|    \\/     M anipulation  |                                                 |
\*---------------------------------------------------------------------------*/
FoamFile
{
    version     2.0;
    format      ascii;
    class       dictionary;
    location    "system";
    object      fvSchemes;
}
// * * * * * * * * * * * * * * * * * * * * * * * * * * * * * * * * * * * * //

ddtSchemes
{
    default         steadyState;
}

gradSchemes
{
    default         cellMDLimited Gauss linear 0.5;
//    default         Gauss linear;
}

divSchemes
{
    div(phi,U)      bounded Gauss upwind;
    div(phi,e)      bounded Gauss upwind;
    div(phi,k)      bounded Gauss upwind;
    div(phi,Ekp)    bounded Gauss upwind;
    div(phi,epsilon) bounded Gauss upwind;
    div((muEff*dev2(T(grad(U))))) Gauss linear;
}

laplacianSchemes
{
    default         Gauss linear limited 0.777;
//    default         Gauss linear corrected;
}

interpolationSchemes
{
    default         linear;
}

snGradSchemes
{
    default         limited 0.777;
//    default         corrected;
}

fluxRequired
{
    default         no;
    p_rgh;
    p;
}

// ************************************************************************* //
```

```
/*--------------------------------*- C++ -*----------------------------------*\
| =========                 |                                                 |
| \\      /  F ield         | OpenFOAM: The Open Source CFD Toolbox           |
|  \\    /   O peration     | Version:  2.3.0                                 |
|   \\  /    A nd           | Web:      www.OpenFOAM.org                      |
|    \\/     M anipulation  |                                                 |
\*---------------------------------------------------------------------------*/
FoamFile
{
    version     2.0;
    format      ascii;
    class       dictionary;
    location    "system";
    object      fvSolution;
}
// * * * * * * * * * * * * * * * * * * * * * * * * * * * * * * * * * * * * //

solvers
{
    p_rgh
    {
        solver          PCG;
        preconditioner  DIC;
        tolerance       1e-06;
        relTol          0.001;
    }


    p
    {
        solver          PCG;
        preconditioner  DIC;
        tolerance       1e-06;
        relTol          0.001;
    }
//    p
//    {
//        solver                GAMG;
////        tolerance             1e-05;
////        relTol                0.01;
//        tolerance             1e-03;
//        relTol                0.5;
//        smoother              GaussSeidel;
//        nCellsInCoarsestLevel 1000;
//        cacheAgglomeration    on;
//        agglomerator          faceAreaPair;
//        mergeLevels           1;
//        nPreSweeps            0;
//        nPostSweeps           2;
//    }

    U
    {
        solver          smoothSolver;
        smoother        GaussSeidel;
        nSweeps         2;
        tolerance       1e-06;
        relTol          0.01;
    }

    e
    {
        solver          smoothSolver;
        smoother        symGaussSeidel;
//        tolerance       1e-06;
//        relTol          0.01;
        tolerance            1e-03;
        relTol               0.5;
    }

    "(k|epsilon)"
    {
        $U;
        tolerance       1e-07;
        relTol          0.01;
    }

    G
    {
        $p_rgh;
        tolerance       1e-05;
        relTol          0.01;
    }
}

SIMPLE
{
    nNonOrthogonalCorrectors 2;
    rhoMin          rhoMin [ 1 -3 0 0 0 ] 0.5;
    rhoMax          rhoMax [ 1 -3 0 0 0 ] 1.5;

    residualControl
    {
        p_rgh           1e-2;
        p               1e-2;
        U               1e-4;
        e               1e-3;
        G               1e-3;

        // possibly check turbulence fields
        "(k|epsilon)" 1e-4;
    }
}

relaxationFactors
{
    fields
    {
        p_rgh           0.3;
        p               0.3;
        rho             0.1;
    }
    equations
    {
        U               0.7;
        "(k|epsilon)"   0.7;
        e               0.5;
        G               0.7;
    }
}

potentialFlow
{
    nNonOrthogonalCorrectors 10;
```

```
}


// ************************************************************************* //

```



```
/*--------------------------------*- C++ -*----------------------------------*\
| =========                 |                                                 |
| \\      /  F ield         | OpenFOAM: The Open Source CFD Toolbox           |
|  \\    /   O peration     | Version:  2.3.0                                 |
|   \\  /    A nd           | Web:      www.OpenFOAM.org                      |
|    \\/     M anipulation  |                                                 |
\*---------------------------------------------------------------------------*/
FoamFile
{
    version     2.0;
    format      ascii;
    class       dictionary;
    location    "system";
    object      controlDict;
}
// * * * * * * * * * * * * * * * * * * * * * * * * * * * * * * * * * * * * * //

application     rhoSimpleFoam;
//application     potentialFoam;

//startFrom       startTime;
startFrom       latestTime;

startTime       0;

stopAt          endTime;

endTime         1001.5;

deltaT          0.5;

writeControl    timeStep;

writeInterval   50;

purgeWrite      0;

writeFormat     ascii;

writePrecision  7;

writeCompression off;

timeFormat      general;

timePrecision   6;

graphFormat     raw;

runTimeModifiable true;


// ************************************************************************* //

```

Appendix C: Preliminary Feasibility Study

FEASIBILITY STUDY

PROJECT'S TITLE AND SUBTITLE:

Biomimetic-Computational Design for Double-Skin Facades in Hot Climates

A porous folded façade for office buildings

ALPHANUMERIC CODE:

VARTCH 037

DATE:

11/09/2015

1. INTRODUCTION

The influence of ideas derived from nature has always been pervasive throughout the history of architecture. Through a deep exploration into how nature solves problems that are experienced today, beneficial solutions could be extracted and new directions for our built environments could be explored. Through a 3.8 billion-year history of brilliant designs and development, nature provides an inspirational source of possible innovation that could enhance the performance and create a more sustainable built environment. Digital modeling and simulation tools together with computational design processes are facilitating the realization of complex forms and materials of many contemporary buildings. They also represent an opportunity to fully explore the potential benefits of biological principles found in nature through deeper understanding of nature's systems and processes.

Through a research-based biomimetic computational design approach, this project investigated inspirations in nature that deal with thermoregulation. A number of potential organisms were analysed and categorised based on main heat transfer method by which thermoregulation was achieved (i.e. radiation, conduction, convection and phase change). Two of these organisms then were chosen as inspirations for the design of a building skin as shown in the poster. These two inspirations are: folding strategies seen in leaveas and cacti which reduce heat gained by radiation, and the porosity of termite mound surfaces that reduce heat gain by convection.

This report presents a general overview of the feasiblity of a folded porous Double-Skin Facade (DSF), highlighting it potential benefits that are financial as well as social. Energy savings are of central importance to the development of the proposal but definetly are coupled with many other benefits discussed through the report.

2. PROJECT'S DESCRIPTION

This project addresses the design of a building skin that deals with the challenge of reducing cooling loads while trying to maintain daylight needs of office buildings in hot climatic regions. Following a biomimetic-computational design process a folded, porous double skin façade was proposed that is adapted to its local environmental context and aims at enhancing community and environmental welfare when applied on an urban scale.

Design goals where defined as parameters from the outset which can be dynamically changed. If the initial inputs change, then the exact amounts of energy savings would change accordingly. As a proof of concept, simulations were done on an existing building in a hot climatic zone. An energy saving up to 12% was achieved through the application of the proposed double façade system. This number represents a positive indicator for the savings that could be achieved in other case specific scenarios.

Benefits for consumers:

Building occupants would benefit from the thermal and visual comfort resulting from the proposed skin. Building owners would also benefit from the reduction in energy consumed for cooling and artificial lighting, and from the wellbeing and increased productivity of his/her employees. The designed system also improves the aesthetics of the buildings to which they are applied, whether new constructions or refurbishment of existing buildings.

Benefits for society:

When the proposed skin is applied on an urban scale then its benefits would reach more occupants and owners, more energy is saved, and more 'breathing' buildings are adapted to their local context. The strength of this system is the flexibility of the approach. It provides a framework that can be applied to different contexts using different patterns, tools and inspirations. The project respects the individuality of people while maintaining a common language that connects and bonds, an invisible bond of being part of a global caring society. The ultimate goal is always generating a more sustainable built environment and increasing the welfare of society.

Benefits for market and companies:

Mass production (One size fits all) concept contradicts with the very nature of architecture as a practice relating to context, culture and environment. Façade construction companies and investors would benefit from offering a different façade system to emerging markets that competes with traditional double facades and curtain walls. Existing systems tend to mass produce typical profiles and details with minimal variation. These markets already have a rising number of office buildings with massive curtain walls reflecting their desire for

power and modernism, but not as much desire for energy saving. The proposed façade system would provide these potential clients with a building skin that is modern, innovative and energy saving as well. It's a big market opportunity that needs to be addressed.

3. TECHNOLOGY INNOVATION

Daylight and thermal performances of the double façade are rarely studied together in hot climates, and most attempts to improve the thermal performance of the building skin are often at the expense of natural daylight entering the space which means more energy consumption for artificial lighting. So the idea is to decrease cooling loads while maintain daylighting needs to ensure both the maximum possible reduction in energy consumption and the occupants' visual comfort.

In the attempt of finding a range of solutions that reduce cooling loads while maintaining daylight needs, the skin is modelled parametrically. Parametric design is a process based on algorithmic thinking that enables explicit expression of parameters and rules that define and clarify the relationship between design intent and design response. This proposal used Grasshopper Visual Programming Language for Rhino 3D Modeller, and it is optimized using multi-objective evolutionary algorithms which were particularly important for finding the required trade-off between conflicting factors. This project serves as a proof of concept; the same design methodology can be applied using different modelling tools, different inputs such as changing the folding pattern, project location and other requirements so that it would be a flexible process that can produce a variety of possible solutions.

Simulations regarding the thermal performance were performed using ArchSim plug-in which runs on EnergyPlus building energy simulation engine, and those regarding day lighting were performed using DIVA plug-in for daylight simulations which runs on Radiance and Daysim daylighting simulation engines.

The use of EnergyPlus in simulating double façades is debatable. One of the most important reasons is because it uses the Airflow Network model which assumes that each thermal zone has a uniform temperature distribution, and it does not take into consideration the cavity airflow pattern (EnergyPlus, 2014). Several studies (Zhang, et al., 2013; Sabooni, et al., 2012; Kim and Park, 2011) recommend coupling EnergyPlus with a Computational Fluid Dynamics (CFD) tool to complement each other's limitations. The authors are currently undertaking a detailed verification process using CFD as a part of their ongoing research initiative.

As for physical construction; digital fabrication provides a flexible mode of manufacturing that can accommodate for the complexity of designed patterns, panelling systems and joints. Flexible manufacturing systems are already being adopted by many big scale

manufacturers around the world replacing the old one-machine-per-operation to multi-operation machinery. Through the possibility of choice, personalization and expression that digital fabrication promises to offer, the real sense of mass-customization starts to evolve.

4. MARKET PLACE AND CONSUMERS' TARGET

Double skin façades are widely applied and studied in the context of temperate climates. Their application in hot climates however is not fully explored and their potential benefits are under investigation, which opens a new window of opportunity for investment.

In this century, global markets are demanding choice, expression, individuality and the ability to change decisions at the last minute. This new practice is already being provided by companies working in the industrial production. Examples like shoes, watches and Automobile manufacturers. They provide real time choice for lower price and higher quality. Through supply chain management achieved by electronic software they can tailor to your need the exact product of your choice.

Moreover, sustainability and the reduction of energy consumption are growing global trends specifically due to the decline of natural world resources. Clients and investors in building construction are becoming more aware of energy problems and potential economic savings gained with the application of energy saving design strategies. Architectural Studios and companies involved in façade design/construction are expected to provide such solutions through design activities. One of which is this proposal that addresses buildings in hot climates with a focus on office buildings.

Target markets for this double façade system basically exist in the Arabian Gulf region, North Africa, Southern Mediterranean Europe and parts of Asia; a very promising market with growing economies that require infrastructures as well as big scale constructions in the short and medium range future.
A recent announcement made by the Egyptian government in March 2015, is the construction of the new capital Cairo, which is a massive scale development with hundreds of new institutional and office buildings to be built over an area of 700 square kilometres east of Cairo.

5. SCHEDULE

This section provides a tentative time frame for the development of the prototype. It gives a broad plan to the expected evolution towards a finalized market oriented product. A more elaborate time frame shall be developed later by means of an implementation plan.

(8 weeks): Computational Fluid Dynamics CFD verification

The tools used for thermal analysis of the proposal had limitations as described in section 3, a detailed CFD analysis will be performed in order to have more accurate results and improve the proposal accordingly.

(4 weeks): Design Feedback and modification

Iterative feedback loops are expected to take around one month to implement through the parametric setting and re-run simulations which need computational power and time to execute.

(3 weeks): Contact manufacturers and suppliers

During this period, potential manufacturers and suppliers are contacted to establish a network of interested stakeholders that can take the proposal forward.

(4 weeks): Final feasibility study

In parallel to the previous step, a final feasibility study would be performed that is multi-disciplinary and covers financial, economic, market feasibility along other scopes shall be performed with the aid of interested professionals.

(2 weeks): Structural analyses

In parallel with the process of creating the network of interested manufacturers and suppliers, structural analyses shall be performed in order to verify the structural performance of the proposal. Wind loads, seismic behaviour and other factors are to be considered at this stage.

(8 weeks): Scaled prototype

Several physical scaled prototypes are to be built in order to double check the behaviour regarding its constructability, and environmental performance. This would validate the results previously obtained by the simulations. Digital fabrication and rapid prototyping will be used at this point.

(4 weeks): Modifications

Based on feedback from scaled models, some design modifications are expected.

(4 weeks): Construction drawings

At this stage of the proposal development, detailed construction documents will be developed for final full-scale fabrication.

(8 weeks): Full-scale final prototype

The application of a full-scale prototype to an existing building would represent a great opportunity to evaluate and test the actual performance of the skin. Physical

tests of cavity temperature, air flows and energy consumption can be thoroughly verified.

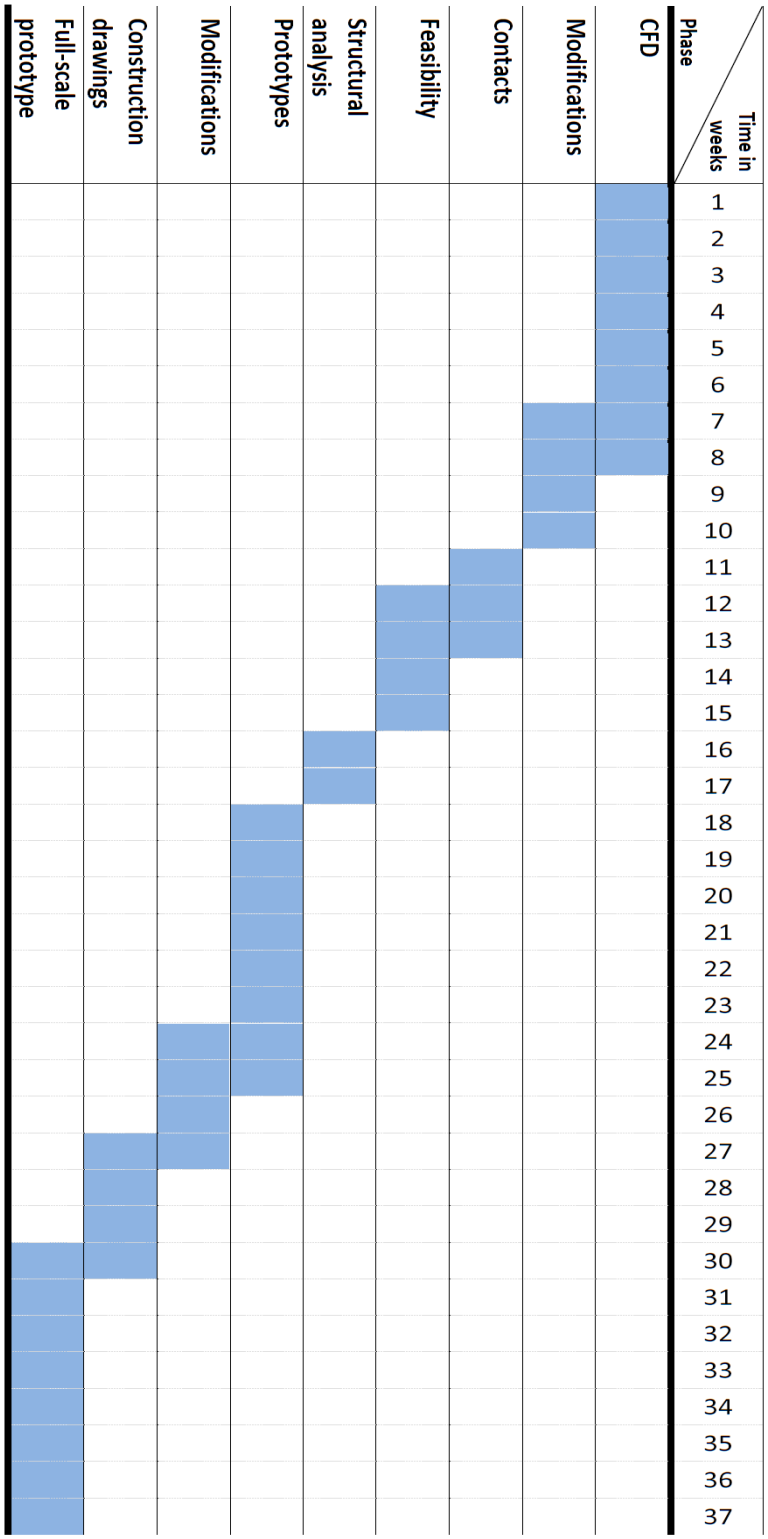

Figure 1: Proposed schedule for the development of the double-skin façade.

6. FINANCIAL PROJECTIONS

For all types of projects, understanding the economics of the situation and including them in the decision making process is of crucial importance. The classical approach used in assessing high performance building economics is LCC (Life Cycle Cost), which includes a consideration of both first cost (sometimes referred to as construction cost or capital cost) and operating costs (utilities and maintenance). These two major cost factors are combined in a cost model that takes into account the time value of money, the cost of borrowed money, inflation and other financial factors.

Two distinctly different cost categories can be identified:

Hard Costs: are those that are easily documented because the owner receives periodic billing for them – for example, electricity, natural gas, water, waste-water, and solid waste.

Soft costs: are those that are less easy to document and for which assumptions must be made for their quantification. Examples of soft costs are maintenance, employee comfort/health/productivity attributable to building, improved indoor environmental air quality and reduced emissions.

An LCC analysis using only hard costs is generally acceptable as justification for alternative strategies that include a trade-off of operational costs versus capital costs. Including soft costs in an LCC is far more difficult to justify because the data cannot be verified with the same degree of rigor as for hard costs.

Within the scope of our study, it is quite challenging to include all these possible factors in an early conceptual phase. Hence our team performed a break-down of the capital costs of the outer layer of the proposed double façade, then a calculation of the operational energy savings in cooling loads in order to calculate the potential pay back period.

The proposed DSF is divided into an inner layer, which a typical single façade for office buildings, and a second outer layer which is the folded porous layer. To estimate the cost of the outer layer it is broken down into its constituting elements and their prices are calculated in the following table:

Outer façade layer				
Façade Element	Description	Quantity	Unit price (in US dollars)	Total price (in US dollars)
Primary structure	Steel structural network with a box cross-section of 150x80 mm, thickness= 4 mm and 2.5x2.5 cm perforations 40 cm apart	1.672 ton	798 $/ton	1335
Secondary structure	Steel structural network with a box cross-section of 70x70 mm, thickness= 4 mm	1.218 ton	798 $/ton	973
Aluminium cladding	Insulated aluminium cladding panels, thickness=14 mm 10 mm Polyethylene sandwiched between 2mm Aluminium sheets. Used for the triangular panels and sides and top of the DSF	150 m^2	20 $/$m^2$	3000
Glazing units	Double glazing: -6mm clear low-E pane -2cm Argon gap -6mm clear pane -light transmittance=0.74 -solar transmittance=0.5	43.2m^2	10 $/$m^2$	432
Steel joints	Joints connecting the steel structural elements	60	40 $	2400
Connecting structure	Steel beams with a box cross-section of 150x150 mm , 4 mm thickness and a length of 1.4 m (which is the cavity depth) connecting the outer façade layer with the inner one	0.3 ton	798 $/ton	246
Construction material prices for a façade of area of 117m^2				8,386
Add 40% for labour, energy, transportation and other services				3,354
Façade cost				**11,740**
Add 6% interest rate and 1% unexpected expenses				821
TOTAL FAÇADE COST (of area of 117m^2)				**12,561 USD**
TOTAL PRICE PER SQUARED METER				**107 USD**

Table 1: Cost Estimate for the DSF

Notes:

- Since the proposal was studied in Cairo, the steel prices were based on those available in the Egyptian market: 6250 EGP/ton which is equal to approximately 798 USD/ton.
- Price of electricity consumption for commercial buildings that consume more than 1000 KWh per month in Egypt= 0.86 EGP/KWh which is equal to approximately 0.11 USD/KWh.
- Prices of aluminium cladding and glazing were based on average prices provided by international suppliers as they are not locally produced.
- Daylight simulations showed an improved performance after the presence of the proposed DSF however the exact savings in electricity consumption due to this improvement were not calculated.

Payback:

To calculate the energy savings in cooling loads, we will consider the studied office room shown in the poster that has South-East orientation and is 5 m wide, 8 m deep and 3 m high, therefore it has a façade area of 5x3= 15 m^2. The cost of a folded porous DSF with an area of 15 m^2 is equal to 15x107 USD = **1,605 USD**.

	Single Facade	**Proposed DSF**	**Savings (12%)**
Cooling loads in July for a 40 m^2 room	900 KWh	818 KWh	82 KWh
Cooling loads in July per square meter of office space	22.5 KWh/m^2	20.45 KWh/m^2	2.05 KWh/m^2
Cost of cooling loads in July for a 40 m^2 room	99 USD	90 USD	9 USD
Cost of cooling loads in July per square meter of office space	2.47 USD/m^2	2.25 USD/m^2	0.225 USD/m^2

Table 2: Comparison of the cooling loads and their corresponding cost between a single and a double façade.

This room has a monthly energy saving due to reduced cooling loads of **9 USD** per summer month (April to September). So to calculate the payback period needed= 1605/9= 178 summer months as only 6 months per year (mpy) save energy, it takes 178 months/ 6 mpy =29,8 years. It is clear that the payback period is relatively long.

But following the incremental increase in oil prices that took place within last decades, we can project a shorter period due to that increase. With the projection of doubling the energy prices in the following years we can estimate a payback period of **20 years** only instead of 30 years. It is crucial to emphasise that the overall payback has to be seen in light with other benefits provided by this idea:

Direct benefits include:

- Reduction in energy consumption in cooling and artificial lighting.
- Noise reduction.
- Improved daylight distribution and reduction of glare which increases the efficiency of the used office area.
- Improving aesthetics of built environment if applied to new constructions and in refurbishment projects.

Indirect benefits:

- Improving the wellbeing of building occupants which increases productivity. For example, the worth of 1 percent improvement in employee productivity translates to 14.0 USD to 30.0 USD per square meter (Kibert, 2010). Although these savings are quite high compared to other savings, it is difficult to justify their inclusion in a Life Cycle Cost.
- Establishing a sense of belonging to a global community that cares and acts responsibly. Businesses opting for high-performance and environmental awareness also gain reputation as a consequence of their efforts.
- Increasing property value. When the building has lower energy demand, higher performance and better indoor environmental quality it implies a superior operational and health performance hence buyers will be willing to pay more for these features.
- Achieving more predictable results. The design process and delivery system includes improved decision-making processes, integrated design, computer modelling of energy and lighting which ensures that the owner will receive a final product that is of a predictable high quality.

7. CONCLUSION

This report presented a brief description of the feasibility of a biomimetic building skin that aims at decreasing cooling loads while improving daylight performance. It is a preliminary feasibility study aiming to highlight the flexibility of the applied method, the direct and indirect benefits of the proposed double-skin façade and the potential applications of biomimicry in sustainable architectural design and computation. The indications are surely positive; however a detailed feasibility study has to be performed with interested partners in construction and manufacturing industry in order to have a broader multi-disciplinary, multi-criteria analysis.

References:

EnergyPlus (2014) Input Output Reference: The Encyclopedic Reference to EnergyPlus Input and Output, Department of Energy, Illinois.

Kim, D. W. and Park, C. S. (2011) Difficulties and limitations in performance simulation of a double skin facade. Energy and Buildings, 43, 3635–3645.

Sabooni, M. A., Vaseti, H. M., Maerefat, M. and Azimi, A. (2012) Development of the capability of Energyplus software to simulation of building double-skin facade, International Symposium on Sustainable Energy in Buildings and Urban Areas (ICHMT), Kusadasi.

Zhang, R., Lam, K., Yao, S.-C. and Zhang, Y. (2013) Coupled Energyplus and computational fluid dynamics natural ventilation simulation. Building and Environment, 68, 100-113.

Kibert, C. J., (2008) Economic Analysis of Green Buildings. In: *Sustainable Construction: Green Building Design and Delivery.* New Jersey: Wiley and Sons, pp. 327-344.